

George W. S. Hou

SPRINGER TRACTS IN MODERN PHYSICS 233

Flavor Physics and the TeV Scale



Springer

Springer Tracts in Modern Physics

Volume 233

Managing Editor: G. Höhler, Karlsruhe

Editors: A. Fujimori, Chiba
J. Kühn, Karlsruhe
Th. Müller, Karlsruhe
F. Steiner, Ulm
J. Trümper, Garching
P. Wölfe, Karlsruhe

Available  online at
SpringerLink.com

Starting with Volume 165, Springer Tracts in Modern Physics is part of the [SpringerLink] service. For all customers with standing orders for Springer Tracts in Modern Physics we offer the full text in electronic form via [SpringerLink] free of charge. Please contact your librarian who can receive a password for free access to the full articles by registration at:

springerlink.com

If you do not have a standing order you can nevertheless browse online through the table of contents of the volumes and the abstracts of each article and perform a full text search.

There you will also find more information about the series.

Springer Tracts in Modern Physics

Springer Tracts in Modern Physics provides comprehensive and critical reviews of topics of current interest in physics. The following fields are emphasized: elementary particle physics, solid-state physics, complex systems, and fundamental astrophysics.

Suitable reviews of other fields can also be accepted. The editors encourage prospective authors to correspond with them in advance of submitting an article. For reviews of topics belonging to the above mentioned fields, they should address the responsible editor, otherwise the managing editor.

See also springer.com

Managing Editor

Gerhard Höhler

Institut für Theoretische Teilchenphysik
Universität Karlsruhe
Postfach 69 80
76128 Karlsruhe, Germany
Phone: +49 (7 21) 6 08 33 75
Fax: +49 (7 21) 37 07 26
Email: gerhard.hoehler@physik.uni-karlsruhe.de
www.ttp.physik.uni-karlsruhe.de/

Elementary Particle Physics, Editors

Johann H. Kühn

Institut für Theoretische Teilchenphysik
Universität Karlsruhe
Postfach 69 80
76128 Karlsruhe, Germany
Phone: +49 (7 21) 6 08 33 72
Fax: +49 (7 21) 37 07 26
Email: johann.kuehn@physik.uni-karlsruhe.de
www.ttp.physik.uni-karlsruhe.de/~jk

Thomas Müller

Institut für Experimentelle Kernphysik
Fakultät für Physik
Universität Karlsruhe
Postfach 69 80
76128 Karlsruhe, Germany
Phone: +49 (7 21) 6 08 35 24
Fax: +49 (7 21) 6 07 26 21
Email: thomas.muller@physik.uni-karlsruhe.de
www.ekp.physik.uni-karlsruhe.de

Fundamental Astrophysics, Editor

Joachim Trümper

Max-Planck-Institut für Extraterrestrische Physik
Postfach 13 12
85741 Garching, Germany
Phone: +49 (89) 30 00 35 59
Fax: +49 (89) 30 00 33 15
Email: jtrumper@mpe.mpg.de
www.mpe-garching.mpg.de/index.html

Solid-State Physics, Editors

Atsushi Fujimori

Editor for The Pacific Rim

Department of Physics
University of Tokyo
7-3-1 Hongo, Bunkyo-ku
Tokyo 113-0033, Japan
Email: fujimori@wyvern.phys.s.u-tokyo.ac.jp
http://wyvern.phys.s.u-tokyo.ac.jp/welcome_en.html

Peter Wölflé

Institut für Theorie der Kondensierten Materie
Universität Karlsruhe
Postfach 69 80
76128 Karlsruhe, Germany
Phone: +49 (7 21) 6 08 35 90
Fax: +49 (7 21) 6 08 77 79
Email: woelfle@tkm.physik.uni-karlsruhe.de
www-tkm.physik.uni-karlsruhe.de

Complex Systems, Editor

Frank Steiner

Institut für Theoretische Physik
Universität Ulm
Albert-Einstein-Allee 11
89069 Ulm, Germany
Phone: +49 (7 31) 5 02 29 10
Fax: +49 (7 31) 5 02 29 24
Email: frank.steiner@uni-ulm.de
www.physik.uni-ulm.de/theo/qc/group.html

George W. S. Hou

Flavor Physics and the TeV Scale

 Springer

Prof. George W. S. Hou
National Taiwan University
Dept. Physics
Taipei 106
Taiwan R.O.C.
wshou@phys.ntu.edu.tw

G. W. S. Hou, *Flavor Physics and the TeV Scale*, STMP 233 (Springer, Berlin Heidelberg 2009), DOI 10.1007/978-3-540-92792-1

ISBN 978-3-540-92791-4

e-ISBN 978-3-540-92792-1

DOI 10.1007/978-3-540-92792-1

Springer Dordrecht Heidelberg London New York

Springer Tracts in Modern Physics ISSN 0081-3869

e-ISSN 1615-0430

Physics and Astronomy Classification Scheme (PACS):

12.15.Ff, 12.15.Hh, 12.15.Ji, 12.60.-I, 13.20.-v

Library of Congress Control Number: 2009920055

© Springer-Verlag Berlin Heidelberg 2009

This work is subject to copyright. All rights are reserved, whether the whole or part of the material is concerned, specifically the rights of translation, reprinting, reuse of illustrations, recitation, broadcasting, reproduction on microfilm or in any other way, and storage in data banks. Duplication of this publication or parts thereof is permitted only under the provisions of the German Copyright Law of September 9, 1965, in its current version, and permission for use must always be obtained from Springer. Violations are liable to prosecution under the German Copyright Law.

The use of general descriptive names, registered names, trademarks, etc. in this publication does not imply, even in the absence of a specific statement, that such names are exempt from the relevant protective laws and regulations and therefore free for general use.

Cover design: Integra Software Services Pvt. Ltd.

Printed on acid-free paper

Springer is part of Springer Science+Business Media (springer.com)

*To the memories of
Prof. Chia-Chu Hou and Mr. Chiao-Shen Lu,
beloved father and father in-law.*

Preface

The flavor sector carries the largest number of parameters in the Standard Model of particle physics. With no evident symmetry principle behind its existence, it is not as well understood as the $SU(3) \times SU(2) \times U(1)$ gauge interactions. Yet it tends to be underrated, sometimes even ignored, by the erudite. This is especially so on the verge of the LHC era, where the exploration of the physics of electroweak symmetry breaking at the high energy frontier would soon be the main thrust of the field.

Yet, the question of “Who ordered the muon?” by I.I. Rabi lingers.

We do not understand why there is “family” (or generation) replication. That three generations are needed to have CP violation is a partial answer. We do not understand why there are only three generations, but Nature insists on (just about) only three active neutrinos. But then the CP violation with three generations fall far short of what is needed to generate the baryon asymmetry of the Universe. We do not understand why most fermions are so light on the weak symmetry breaking scale (v.e.v.), yet the third-generation top quark is a v.e.v. scale particle. We do not understand why quarks and leptons look so different, in particular, why neutrinos are rather close to being massless, but then have (at least two) near maximal mixing angles. We shall not, however, concern ourselves with the neutrino sector. It has a life of its own.

This monograph is on the usefulness of flavor physics as probes of the TeV scale to provide a timely interface for the emerging LHC era. Historically, the kaon system has been a major wellspring for the emergence of the Standard Model. It gave us the Cabibbo angle, hence quark mixings, $K^0-\bar{K}^0$ oscillations, CP violation, absence of FCNC and, the GIM mechanism, prediction of charm (mass), and ultimately the Kobayashi–Maskawa model and the prediction of the third generation. The torch, however, has largely passed on to the B meson system, the elucidation of which forms the bulk of this book. Following, and expanding on, the successful paths of the CLEO and ARGUS experiments, the B factories have dominated the scene for the past decade.

The B factories have produced a vast amount of knowledge. Fortunately, by concerning ourselves only with the TeV scale connection, a large part of the B factory output can be bypassed. We do not concern ourselves with rather indirect links to physics beyond the Standard Model, such as the measurement of CKM sides or the consistency of the unitary phases with three generations. The advantage is that we

do not need to go into the details of “precision measurement” studies, as they are now rather involved. Our emphasis is on loop-induced processes, which allow us to probe virtual TeV scale physics through quantum processes, in the good traditions of muon $g - 2$ and rare kaon processes. In this sense, flavor physics is quite complementary to the LHC collider physics that would soon unfold before us. If New Physics is discovered by the LHC, flavor probes would provide extra information to help pin down parameters. If no New Physics emerges from the LHC, then flavor physics still provides multiple probes to physics above the TeV scale. Either way, the construction of the so-called Super B factories, to go far beyond the successful B factories in luminosity, is called for.

A glance at the Table of Contents shows that two thirds of the book is concerned with $b \rightarrow s$ or $b\bar{s} \leftrightarrow s\bar{b}$ transitions. The B factories have not uncovered strong hints for New Physics in $b\bar{d} \leftrightarrow d\bar{b}$ or $b \rightarrow d$ transitions. It is remarkable that all evidence supports the three generation Kobayashi–Maskawa model in the so-called $b \rightarrow d$ CKM triangle, $V_{ud}V_{ub}^* + V_{cd}V_{cb}^* + V_{td}V_{tb}^* = 0$ (and the Nobel prize has been awarded). Further probes in $b \rightarrow d$ transitions tend to be marred by hadronic or Standard Model effects and at best are part of the long road of three generation Standard Model consistency tests that we have decided to sidestep. In contrast, $b \rightarrow s$ transitions are not only the current frontier of flavor physics, it actually offers good hope that New Physics may soon be uncovered, maybe even before the first physics is repeated at the LHC. On the one hand, this is because the $V_{us}V_{ub}^* + V_{cs}V_{cb}^* + V_{ts}V_{tb}^* = 0$ CKM triangle is so squashed and hardly a triangle in the Standard Model, so the expected CP violation in loop-dominated $b \rightarrow s$ transitions is tiny. This means that any clear observation could indicate New Physics. On the other hand, $b \rightarrow s$ transitions offer multiple probes into physics beyond the Standard Model that have come of age only recently. As we advocate, the measurement of $\sin 2\Phi_{B_s}$ in $B_s \rightarrow J/\psi\phi$, analogous to $\sin 2\phi_1/\beta$ measurement in $B_d \rightarrow J/\psi K_S$ at the B factories, holds the best promise for an unequivocal discovery of New Physics, if its measured value at the Tevatron or LHC turn out to be sizable. It is exciting that we seem to be heading that way.

A common thread that links the several hints of New Physics in $b \rightarrow s$ transitions, to our prediction of large and negative $\sin 2\Phi_{B_s}$, is the existence of a fourth generation. Of course, there are strong arguments against the existence of a fourth generation, by the aforementioned “neutrino counting” and by electroweak precision tests. However, these objections arise from outside of flavor physics. While these should be taken seriously, one should not throw the fourth generation away when considering flavor physics, since the richness of flavor physics rests on the existence of three generations and extending to four generations provide considerable enrichment, particularly in $b \rightarrow s$ transitions. It also provides multiple links between different flavor processes, through the unitarity of the 4×4 CKM matrix. As emphasized in this book, a fourth generation could most easily enter box and electroweak penguin diagrams. Accounts of these are scattered throughout the book, as we touch upon different processes. These are effects due to large Yukawa couplings, which link flavor physics to the Higgs, or electroweak symmetry breaking sector.

While writing this book, we observed that *adding a fourth quark generation could enhance the so-called Jarlskog invariant for CP violation by a factor of 10^{+13} or more*, and the (fourth generation) KM model could provide the source of CP violation for the baryon asymmetry of the Universe. A sketch of this insight is given in the final discussion chapter, which also serves as justification for our frequent mentioning of the fourth generation throughout the book. *Flavor physics could provide CP violation for the Heaven and the Earth.*

Two other chapters, on D^0 mixing and $K \rightarrow \pi \nu \nu$ and on lepton number violating τ decays, are loop-induced probes of New Physics that are analogous to the emphasis of our main text on B physics. Interestingly, there are still tree-level processes that can probe New Physics, such as the probe of charged Higgs boson H^+ through $B^+ \rightarrow \tau^+ \nu_\tau$, or light dark matter or pseudoscalar Higgs boson search in $Y(nS)$ decays.

We have taken an experimental perspective in writing this book. This means selecting *processes*, rather than the theories or models, as the basis to explore flavor physics as probe of the TeV scale. In the first few chapters, emphasis is on CP violation measurables in $b \rightarrow s$ transitions. We then switch to using a particular process to illustrate the probe of a special kind of physics. We therefore also spend some time in elucidating what it takes to measure these processes. However, this is not a worker's manual for experimental analysis, but on bringing out the physics. For the same reason, we do not go into any detail on theoretical models. Our guiding principle has been: unless it can be identified as the smoking gun, it is better to stick to the simplest (rather than elaborate) explanation of an effect that requires New Physics.

The origins of this monograph is the plenary talk I gave at the SUSY 2007 conference held in Karlsruhe, Germany. It was interesting to attend the SUSY conference for the first time, while giving an *experimental* plenary talk. I thank the Belle spokespersons, Masa Yamauchi in particular, for nominating me as "that special physicist" to give this talk. I also thank my old friend and former colleague, Hans Kühn, for encouraging and inviting me to expand the talk into a monograph for Springer Tracts of Modern Physics. It is impossible to thank the numerous colleagues in the field of flavor physics for benefits of discussion and insight. I thank Yeong-jyi Lei for help on figures. Last, and above all, I thank my family for the understanding and support throughout the period of writing this book.

Les Houches, Geneva, and Taipei
September 2008

George W.S. Hou

Contents

1	Introduction	1
1.1	Outline, Strategy, and Apologies	2
1.2	A Parable: What if?	4
1.3	The Template: Δm_{B_d} , Heavy Top, and V_{td}	6
	References	9
2	CP Violation in Charmless $b \rightarrow s\bar{q}q$ Transitions	11
2.1	The $\Delta\mathcal{S}$ Problem	11
2.1.1	Measurement of TCPV at the B Factories	12
2.1.2	TCPV in Charmless $b \rightarrow s\bar{q}q$ Modes	15
2.2	The $\Delta\mathcal{A}_{K\pi}$ Problem	18
2.2.1	Measurement of DCPV in $B^0 \rightarrow K^+\pi^-$ Decay	18
2.2.2	$\Delta\mathcal{A}_{K\pi}$ and New Physics	21
2.3	$\mathcal{A}_{CP}(B^+ \rightarrow J/\psi K^+)$	26
2.4	An Appraisal	29
	References	30
3	B_s Mixing and $\sin 2\Phi_{B_s}$	33
3.1	B_s Mixing Measurement	34
3.1.1	Standard Model Expectations	34
3.1.2	DØ Measurement of Δm_{B_s}	38
3.1.3	CDF Observation of $B_s^0-\bar{B}_s^0$ Oscillations	40
3.2	Search for TCPV in B_s System	42
3.2.1	$\Delta\Gamma_{B_s}$ Approach to $\phi_{B_s}: \cos 2\Phi_{B_s}$	43
3.2.2	Prospects for $\sin 2\Phi_{B_s}$ Measurement	44
3.2.3	Can $ \sin 2\Phi_{B_s} > 0.5$?	46
3.2.4	Hints at Tevatron in 2008	50
	References	54
4	H^+ Probes: $b \rightarrow s\gamma$ and $B \rightarrow \tau\nu$	57
4.1	$b \rightarrow s\gamma$	57
4.1.1	QCD Enhancement and the CLEO Observation	57

4.1.2	Measurement of $b \rightarrow s\gamma$ at the B Factories	59
4.1.3	Implications	61
4.2	$B \rightarrow \tau\nu$ and $D^{(*)}\tau\nu$	63
4.2.1	Enhanced H^+ Effect in $b \rightarrow c\tau\nu$ and $B^+ \rightarrow \tau^+\nu_\tau$	64
4.2.2	$B \rightarrow \tau\nu$ and $B \rightarrow D^{(*)}\tau\nu$ Measurement	66
	References	71
5	Electroweak Penguin: bsZ Vertex, Z', Dark Matter	73
5.1	$A_{\text{FB}}(B \rightarrow K^*\ell^+\ell^-)$	73
5.1.1	Observation of m_t Enhancement of $b \rightarrow s\ell^+\ell^-$	73
5.1.2	B Factory Measurements of $A_{\text{FB}}(B \rightarrow K^*\ell^+\ell^-)$	77
5.1.3	Interpretation and Future Prospects	79
5.2	$B \rightarrow K^{(*)}\nu\nu$	82
5.2.1	Experimental Search	83
5.2.2	Constraint on Light Dark Matter	84
	References	86
6	Right-Handed Currents and Scalar Interactions	87
6.1	TCPV in $B \rightarrow K_S^0\pi^0\gamma, X^0\gamma$	87
6.2	$B_s \rightarrow \mu^+\mu^-$	90
	References	92
7	Bottomonium Decay and New Physics	93
7.1	$\Upsilon(3S) \rightarrow \pi^+\pi^-\Upsilon(1S) \rightarrow \pi^+\pi^- + \text{Nothing}$	93
7.2	$\Upsilon(1S) \rightarrow \gamma a_1^0$ Search	96
	References	99
8	D and K Systems: Box and EWP Redux	101
8.1	D^0 Mixing	101
8.1.1	SM Expectations and Observation at B Factories	102
8.1.2	Interpretation and Prospects	107
8.2	$K \rightarrow \pi\nu\bar{\nu}$ Decays	109
8.2.1	Current Status	110
8.2.2	Future Prospects	112
	References	114
9	Lepton Number Violating μ and τ Decay	115
9.1	$\mu \rightarrow e\gamma$	115
9.2	$\tau \rightarrow \ell\gamma, \ell\ell\ell'$	117
9.3	$\tau \rightarrow \tilde{\Lambda}\pi, \tilde{p}\pi^0$	119
	References	121
10	Discussion and Conclusion	123
10.1	From Unparticles to Extending the Standard Model	123

10.2	Fourth Generation—CPV for Heaven and Earth ?	125
10.2.1	New Physics CPV on Earth: from $\Delta A_{K\pi}$ to $\sin 2\Phi_{B_s}$. . .	125
10.2.2	Jarlskog Invariant for Three Generations	128
10.2.3	New Physics CPV for the Heavens: Fourth Generation for BAU !?	129
10.2.4	Litmus Test on Earth: Search for t' and b'	130
10.3	Summary and Conclusion	132
	References	133
A	A CP Violation Primer	135
A.1	Generalities	135
A.2	Illustration: Direct CP Violation	138
A.3	Time-Dependent CP Violation	139
	References	140
Index	141

Chapter 1

Introduction

As humans, we aspire to reach up to the heavens. It is our unquenchable human nature. An old fable illustrates the point: Jack and the Beanstalk. It is simply impossible for Jack not to climb the Beanstalk, when it stands in front of him, extending all the way up, to beyond the clouds.

Let us elaborate. We illustrate Jack and the Beanstalk as an allegory in Fig. 1.1. In particle physics, we are now truly at the threshold of reaching beyond the veiling clouds of the “v.e.v. scale.” We know firmly that some vacuum expectation value, of order 246 GeV, has developed in the early Universe, which breaks the ElectroWeak Symmetry (EWSB) down to electromagnetism. This is the scale for all fundamental masses¹ in the Standard Model (SM). The conventional high-energy approach, such as with the Large Hadron Collider (LHC) that is finally entering operation at CERN, is like Jack climbing straight up the Beanstalk. Current impressions are that the Higgs boson may be nearby in its mass, i.e., around 120 GeV or so, just like the Castle floating on a low cloud in Fig. 1.1. But then maybe not ... It could all be a mirage. We don’t really know where the Higgs boson is. It, or the something, may lie up above the darker clouds of the v.e.v.! And, in fact, the “nearby cloud” of 120 GeV in this case turns out to be just about the most difficult to reach.

In this direct ascent approach, Jack has to be fearful of the giant, which in this case could even be the projects like LHC and ILC (International Linear Collider) themselves. The cost of machines is becoming so prohibitive, Jack may not be able to survive or return, whatever the riches he may or may not uncover. However, “Jack” may *not* have to actually climb the Beanstalk: quantum physics allows him to stay on Earth and let virtual “loops” do the work. The virtual Jack has no fear of getting eaten by the Giant.

This parable illustrates how flavor physics offers probes of the TeV scale, at much reduced costs. The flavor connection to TeV scale physics is typically through loops.

¹ The mass of the proton (hence all masses on earth) arises actually predominantly from a similar phenomena of chiral symmetry breaking induced by QCD.

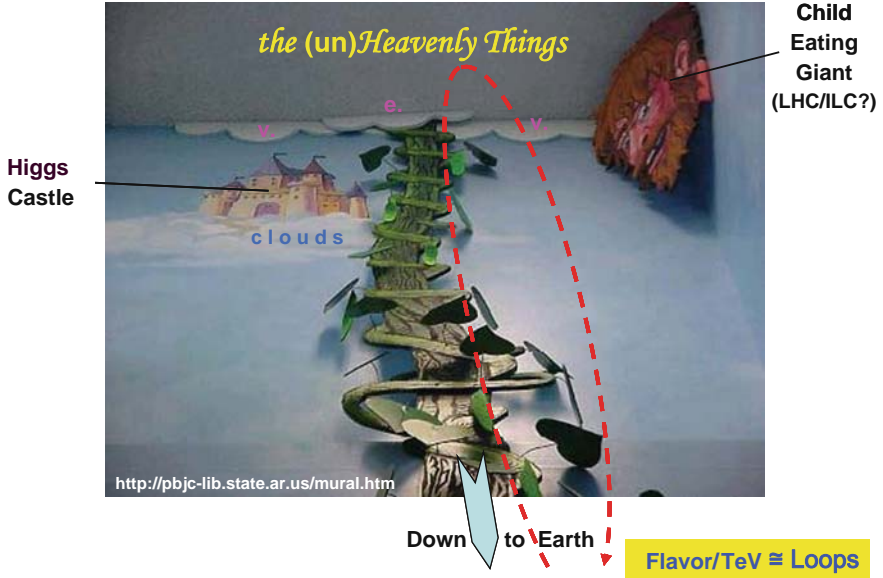


Fig. 1.1 Parable of Jack and the Beanstalk (adapted from the mural by Henri Linton and Ariston Jacks, located at the Main Library of the Pine Bluff/Jefferson County Library, Pine Bluff, Arkansas, USA; used with permission)

1.1 Outline, Strategy, and Apologies

The outline of this book is as follows.

We take an experimental view on the physics of flavor and the TeV scale connection. In the remainder of this chapter, we entertain a “What if?” question to elucidate the possible surprises from flavor physics, then use B^0 – \bar{B}^0 mixing as a template to illustrate loop physics. In the next chapter, we cover the main subject of New Physics (NP) CP Violation (CPV) search in loop-induced $b \rightarrow s$ transitions: the mixing-dependent CPV difference $\Delta\mathcal{S}$ between $b \rightarrow c\bar{c}s$ and $s\bar{q}q$ processes, and the direct CPV difference $\Delta\mathcal{A}_{K\pi}$ between B^+ and B^0 decay to $K^+\pi$. We also cover briefly direct CPV in $B^+ \rightarrow J/\psi K^+$ decay. In Chap. 3, we continue with the main subject of New Physics CPV search in loop-induced $b \leftrightarrow s$ transitions, namely the status and prospects for measuring the CPV phase $\sin 2\Phi_{B_s}$ involving B_s mixing, discussing in particular *whether it could be large*. This is the current focus of flavor physics. In Chap. 4, we turn to the forefront probes of charged Higgs boson (H^+) effects, namely $b \rightarrow s\gamma$ and $B^+ \rightarrow \tau^+\nu$, where the latter is in fact a tree diagram probe. In Chap. 5, we use the forward–backward asymmetry in $B \rightarrow K^*\ell^+\ell^-$ to show how such electroweak penguin observables can probe the weak phase of the bsZ vertex, without detecting CPV. In discussing the analogous $B \rightarrow K^{(*)}\nu\nu$ mode, we illustrate how it provides a window on light dark matter. In Chap. 6, we use time-dependent CPV in $B^0 \rightarrow K_S\pi^0\gamma$ to illustrate the probes of right-handed dynamics and $B_s \rightarrow \mu^+\mu^-$ search as probe of the extended Higgs sector. This

brings us to a detour from loop physics in Chap. 7 to a discussion of the usefulness of the bottomonium system as probes of light dark matter, as well as exotic light Higgs bosons. We then return to loop effects in D^0 mixing and rare $K \rightarrow \pi \nu \nu$ decays in Chap. 8 and lepton flavor violation in τ decays in Chap. 9. We close with some discussions and insight and offer our conclusions in Chap. 10. In Appendix A, we elucidate and demystify the mechanism of CPV.

Flavor physics is a very vast subject, and many topics are rather elaborate and very specialized. Our selection of experimental topics is simplified drastically by choosing only those that are *pertinent* to physics Beyond the Standard Model (BSM), while avoiding those that are too intricate, or too long and winding, to present. The emphasis is on *bringing out the physics*, rather than on the experimental or theoretical details. As the (Chinese) saying goes, one should avoid “Seeing the trees but miss the forest,” which is often the case for experts that get lost in the details.

Another criteria for selection of topics is our emphasis on the short- or near-term impact. We are at the juncture where the B factory era is coming to a close. The unprecedented luminosities have plateaued; another leap forward (upward) on the luminosity frontier (see Fig. 1.2) is needed to make further progress. We are entering a phase for the “Super B factory,” or preparations for upgrades. We will not be able to see far beyond what we have already seen, until we get of order 50 times or more data than present. On the other hand, LHC data have not yet arrived, and unless things work out exceedingly well, one should not expect it to arrive so quickly. LHC is an unprecedented effort, where the accelerator, the detectors, even the computing all provide daunting challenges. Fortunately, the Tevatron Run-II is now going about very smoothly, and there are a few key measurements that could

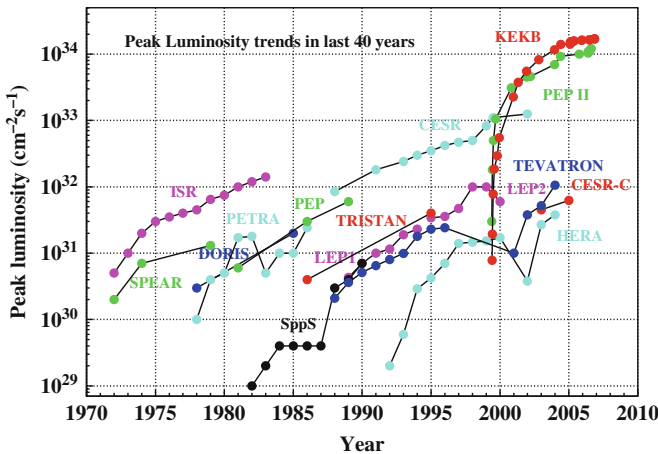


Fig. 1.2 The B factories led the luminosity frontier in the past decade. (Source: <http://www-kekb.kek.jp/Commissioning/lumi/>, by Samo Stanič, used with permission.)

reveal surprises before the actual dawn of the LHC era. We aim at preparing the stage for this dawning. Hence, we have elaborated a little more on the details here.

We have largely picked traditional theoretical models for Beyond the Standard Model “New Physics.” Most new theoretical ideas of the past decade are motivated by ElectroWeak Symmetry Breaking (EWSB) physics, in some good measure because of the long wait for LHC construction and commissioning. For flavor physics, thanks to the B factories, it has experienced a tremendous leap forward from the CLEO era of the 1990s, and the frontier has been pushed back considerably (see Fig. 1.2). No smoking gun New Physics (NP) signal has yet emerged in an unequivocal way. We believe the signature of many of the more extravagant or fascinating ideas motivated by EWSB are either better probed at the energy frontier of the LHC (or future ILC) or they can be illustrated already by the traditional NP models on our list. After all, EWSB physics and flavor physics are orthogonal and complementary directions. It is then important that the world keeps this complementarity by having a Super B factory facility in the near future to enhance the synergies with the LHC.

Having said all this, we apologize for incomplete citations of theoretical work. We cite what we deem to be of key importance, again, to illustrate the physics. However, we are not impartial in promoting our own phenomenological work. Besides illustrating key data, some of the reasons would become clear only in the discussion section of Chap. 10.

1.2 A Parable: What if?

Another “parable” illustrates the potential of heavy flavor physics to make impact. Let us entertain a hypothetical “What if?” question.

Forwarding to the recent past, on July 31, 2000, at the ICHEP conference in Osaka, the BaBar experiment announced the low value of $\sin 2\beta \sim 0.12$ [1],

$$\sin 2\beta = 0.12 \pm 0.37 (\text{stat}) \pm 0.09 (\text{syst}) \quad (\text{BaBar, ICHEP 2000}). \quad (1.1)$$

We will gradually define what $\sin 2\beta$ means. The result of (1.1) was analyzed with a data set of 9 fb^{-1} integrated luminosity on the $Y(4S)$ resonance, corresponding to about 10M $B\bar{B}$ meson pairs produced in the clean e^+e^- collider environment. The value for the equivalent $\sin 2\phi_1 = 0.45^{+0.43+0.07}_{-0.44-0.09}$ [2] measurement from the Belle experiment (using 6.2 fb^{-1} data, or almost 7M $B\bar{B}$ pairs) was slightly higher, but also consistent with zero. Note that the errors are quite large. Within the same day, however, a theory paper appeared on the arXiv [3], entertaining the implications of the low $\sin 2\beta$ value for the strategy of exploring New Physics. It seems that² some

² This parable was meant as a joke, but as I was preparing for my SUSY2007 talk (the starting point of this volume), the paper “Search for Future Influence from L.H.C.” appeared [4]. So it was not a joke after all. The future can wormhole back !? It seems to have received preliminary confirmation with the magnet quench right after the successful first beam at LHC in September 2008.

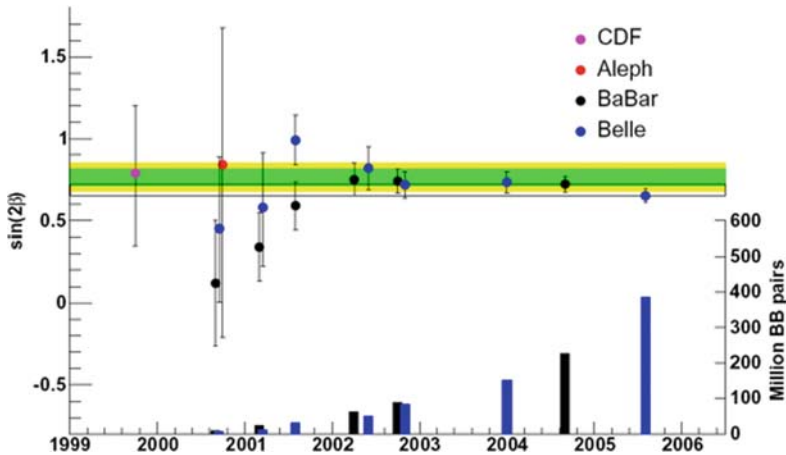


Fig. 1.3 Measurement of $\sin 2\beta/\phi_1$, 2000–2005, illustrating how the combined result of Belle and BaBar settled already in 2001. (Source: talk by R. Cahn [8] given at 2006 SLAC Summer Institute, used with permission.)

theorists have the power to “wormhole” into the future ! A year later, however, both BaBar and Belle claimed the observation [5, 6] of $\sin 2\beta/\phi_1 \sim 1$, which turned out to be consistent with Standard Model (SM) expectations, i.e., confirming the Kobayashi–Maskawa [7] source of CPV.

In Fig. 1.3, we illustrate how the summer 2001 measurements by Belle and BaBar “settled” the value for $\sin 2\beta/\phi_1$. The band is some mean value, roughly of 2002. With impressive accumulation of data, as seen in the bars at the bottom of the figure, the measured mean remains more or less the same. We note that since 2005 there is some indication, from Belle mostly (the last entry in Fig. 1.3), that the measured $\sin 2\phi_1$ value may be dropping again.

What if $\sin 2\beta/\phi_1$ stayed close to zero ? Well, as stated already, it certainly didn’t. Otherwise, you would have heard much more about it—a definite large deviation from the SM has been found! For even in the last century, one expected from indirect data that $\sin 2\beta/\phi_1$ had to be nonzero within SM (see Fig. 1.4). Note that within SM, with the standard phase convention of taking V_{cb} to be real, and placing the unique CPV phase in V_{ub} , one has $\beta/\phi_1 = -\arg V_{td}$ [10, 11]. The awkward notation of β/ϕ_1 (like the original J/ψ) is just to respect the friendly competition across the Pacific Ocean.

The measurement of $\sin 2\beta/\phi_1$ is the measurement of the CPV phase in the $B_d^0-\bar{B}_d^0$ mixing matrix element M_{12}^d . We recall that the discovery of $B^0-\bar{B}^0$ mixing itself by the ARGUS experiment [12] more than 20 years ago was the first clear indication that the *top* is heavy, that it is a *v.e.v. scale quark*, a decade before the top quark was actually discovered at the Tevatron. The ARGUS discovery caused a Gestalt switch, and to this day we do not yet quite understand why the top is so heavy compared to other fermions.

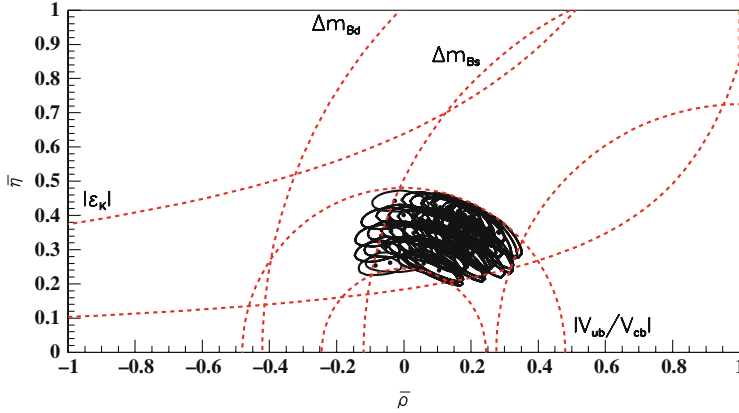


Fig. 1.4 Expectation for $\sin 2\beta/\phi_1$ measurement ca. 1998. (Source: BaBar Physics Book, SLAC Report R-504, Ref. [9]; used with permission.) This figure should be compared with Fig. 1.6; for definition of $\bar{\rho}$ and $\bar{\eta}$, as well as a discussion of CPV in SM, see Appendix A

Such is the impact of loop effects and the power of the flavor and TeV link. With the $B^0-\bar{B}^0$ mixing frequency Δm_{B_d} proportional to $|V_{td}|^2 m_t^2$, it is *the template* for flavor loops as probes into high energy scales. So let us learn from it.

1.3 The Template: Δm_{B_d} , Heavy Top, and V_{td}

As shown in Fig. 1.5, the $B_d^0-\bar{B}_d^0$ mixing amplitude M_{12}^d is generated by the box diagram involving two internal W bosons and top quarks in the loop.

Normally, heavy particles such as the top quark would decouple from the loop, in the heavy $m_t \rightarrow \infty$ limit. After all, our daily experience does not seem to depend on yet-unknown heavy particles. This is the case for QED and QCD. However, for chiral gauge theories, such as the electroweak theory, the longitudinal component of the W boson, which is a charged Higgs scalar that got eaten by the W through spontaneous symmetry breaking, couples to the top quark *mass*. This gives rise to the phenomenon of *nondecoupling* of the top quark effect from the box diagram, i.e., $M_{12}^d \propto (V_{td}^* V_{tb})^2 m_t^2$ to first approximation. It illustrates the *Higgs affinity* of heavy SM-like (chiral) quarks, namely $\lambda_t \sim 1$ for the top quark Yukawa coupling.

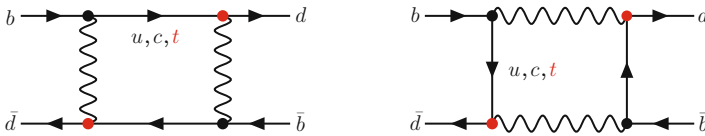


Fig. 1.5 The box diagrams for $B_d^0-\bar{B}_d^0$ mixing. The top quark dominates the loop and brings in the CPV phase in $(V_{td}^* V_{tb})^2$

It is the Yukawa coupling to the Higgs boson that links the left- and right-handed chiral quarks, which are in different representations of the $SU(2) \times U(1)$ electroweak gauge group that generates quark masses. The rather large Yukawa coupling of the top quark compensates for the suppression of V_{td}^{*2} ($\sim 10^{-4}$ in strength), bringing forth the CPV phase $\sin 2\beta/\phi_1$ that was measured by the B factories in 2001.

The formula for M_{12}^d is very well known. Since the top quark dominates, one has

$$M_{12}^d \simeq -\frac{G_F^2 m_B}{12\pi^2} \times \eta_B m_W^2 S_0(m_t^2/m_W^2) \times f_{B_d}^2 B_{B_d} \times (V_{td}^* V_{tb})^2. \quad (1.2)$$

From this formula, we can get a feeling of what a loop calculation involves. The first factor with G_F^2 counts the number of W propagators. The second factor is from short distance physics and calculable, with $\eta_B \approx 0.6$ a QCD correction factor and

$$S_0(m_t^2/m_W^2) \approx 0.55 m_t^2/m_W^2, \quad (1.3)$$

for our purpose, which is proportional to m_t^2 as stated before. For the third factor, the decay constant f_{B_d} accounts for the probability for the b and \bar{d} quarks to meet and annihilate, and the “bag” parameter B_{B_d} is to compensate for the so-called vacuum insertion approximation, of separating the $[\bar{b}d][\bar{d}b]$ four-quark operator into a product of two currents, then taking the matrix element of $[\bar{b}d]$ between the $|B_d\rangle$ and $|0\rangle$ states. The decay constant f_{B_u} is accessible in B^+ decay, the measurement of which can help infer f_{B_d} . But in general, we rely on nonperturbative calculational methods like lattice QCD for information on $f_{B_d}^2 B_{B_d}$. Finally, $(V_{td}^* V_{tb})^2$ is just the product of the four CKM factors from the weak interaction vertices.

We recall that K^0 – \bar{K}^0 mixing, or Δm_K , provided the basic source of insight for the Glashow Iliopoulos Maiani (GIM) mechanism [13], which lead to the prediction of the charm quark before it was actually discovered, even an estimation of the charm mass (using a formula similar to (1.2)). With three generations, as suggested by Kobayashi and Maskawa [7] (KM), the top quark in the box diagram provided the SM explanation for the origin of CPV in $K_L \rightarrow 2\pi$ decay [14], the ε_K parameter.

None of this, however, prepared people for the B_d system. It is curious to note that the charm contribution to K^0 – \bar{K}^0 mixing gives the correct order of magnitude for Δm_K , i.e., $x_K \equiv \Delta m_K/\Gamma_{K_S} \sim 0.5$. This lead people to expect that $x_{B_d} \equiv \Delta m_{B_d}/\Gamma_B < 1\%$, even when the B lifetime was found to be greatly prolonged [15, 16]. This is because the B meson decay width is still so much larger than that of the kaon and since people tacitly assumed that the top quark was “just around the corner,” meaning of order 20–30 GeV or less (remember the march of the e^+e^- colliders PEP, PETRA, and Tristan, even SLC and LEP). Thus, when Δm_{B_d} was found to be comparable to Γ_B , it was quite a shock to realize that the top quark is actually a special, v.e.v. scale particle.

So B physics provided insight into the TeV scale. But that was just the beginning. It is truly remarkable that the measured $x_{B_d} \sim 0.8$ was just right to allow the beautiful, but originally somewhat esoteric (because of the $x_{B_d} \ll 1$ mindset), method for measuring [17] mixing-dependent CPV, to suddenly appear realistic in the late

1980s. This paved the way for the construction of the B factories, but not without the key experimental insight, i.e., to boost the $Y(4S)$, hence the produced $B\bar{B}$ pair. This allowed one to capitalize on vertex detector development by going to an asymmetric energy collider [18]. After intense studies, two B factories, one at SLAC in California and one at KEK in Japan, were constructed in the 1990s.

All this impact was stimulated by the observation of the nondecoupled loop effect of the heavy top quark in Fig. 1.5, at the tiny DORIS e^+e^- collider, rather cost-effective indeed. Providing diverse probes of flavor physics, often using loop effects, the B factories themselves are quite cost-effective, as we shall see.

As we will only be interested in New Physics (NP), we note that extensive studies at the B factories (and elsewhere) indicate that $b \rightarrow d$ transitions are consistent with the SM [19]. As illustrated in Fig. 1.6, no discrepancy is apparent with the CKM (Cabibbo–Kobayashi–Maskawa) unitarity triangle³

$$V_{ud}^* V_{ub} + V_{cd}^* V_{cb} + V_{td}^* V_{tb} = 0, \quad (1.4)$$

which is the db element of $V^\dagger V = I$, where V is the quark mixing matrix. An enormous amount of information and effort has gone into this figure (compare Fig. 1.4), the phase of $V_{td}^* V_{tb}$ being only one of the prominent entries that emerged through the B factory studies. Although there are some tensions here and there, e.g., in the value of $|V_{ub}|$, in general, we see remarkable consistency with CKM expectations.

What about $b \rightarrow s$ transitions? This is the current frontier for heavy flavor physics, offering a window into a multitude of possible TeV scale physics. It will therefore be our starting point and main theme.

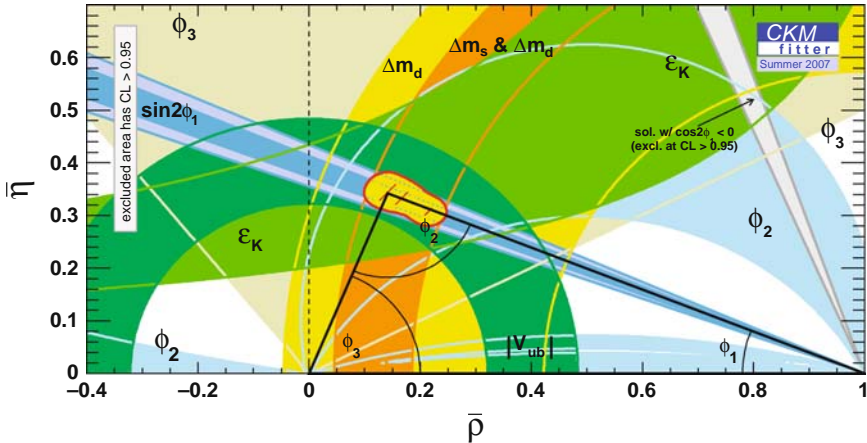


Fig. 1.6 CKM unitarity fit to all data as of summer 2007 (from the CKMfitter group [20], used with permission). The triangle corresponds to $V_{ud}^* V_{ub} + V_{cd}^* V_{cb} + V_{td}^* V_{tb} = 0$

³ We will often refer to the Particle Data Group [10] for many useful discussions.

References

1. Hitlin, D.: Plenary talk at the XXXth International Conference on High Energy Physics (ICHEP2000), Osaka, Japan, 31 July 2000 4
2. Aihara, H.: Plenary talk at the XXXth International Conference on High Energy Physics (ICHEP2000), Osaka, Japan, 31 July 2000 4
3. Kagan, A.L., Neubert, M.: Phys. Lett. B **492**, 115 (2000) (arXiv:hep-ph/0007360) 4
4. Nielsen, H.B., Ninomiya, M.: Int. J. Mod. Phys. A **23**, 919 (2008) (arXiv:0707.1919 [hep-ph]) 4
5. Aubert, B., et al. [BaBar Collaboration]: Phys. Rev. Lett. **87**, 091801 (2001) 5
6. Abe, K., et al. [Belle Collaboration]: Phys. Rev. Lett. **87**, 091802 (2001) 5
7. Kobayashi, M., Maskawa, T.: Prog. Theor. Phys. **49**, 652 (1973) 5, 7
8. Cahn, R.: Talk at SLAC Summer Institute 2006, Stanford, 25 July 2006 5
9. BaBar Physics Book. <http://www.slac.stanford.edu/pubs/slacreports/slac-r-504.html> 6
10. Yao, W.M., et al. [Particle Data Group]: J. Phys. G **33**, 1 (2006) 5, 8
11. Amsler, C., et al.: Phys. Lett. B **667**, 1 (2008); and <http://pdg.lbl.gov/> 5
12. Albrecht, H., et al. [ARGUS Collaboration]: Phys. Lett. B **192**, 245 (1987) 5
13. Glashow, S.L., Iliopoulos, J., Maiani, L.: Phys. Rev. D **2**, 1285 (1970) 7
14. Christenson, J.H., Cronin, J.W., Fitch, V.L., Turlay, R.: Phys. Rev. Lett. **13**, 138 (1964) 7
15. Fernandez, E., et al. [MAC Collaboration]: Phys. Rev. Lett. **51**, 1022 (1983) 7
16. Lockyer, N.S., et al. [MARK II Collaboration]: Phys. Rev. Lett. **51**, 1316 (1983) 7
17. Bigi, I.I.Y., Sanda, A.I.: Nucl. Phys. B **193**, 85 (1981) 7
18. Oddone, P.: At UCLA Workshop on Linear Collider $B\bar{B}$ Factory Conceptual Design, Los Angeles, California, January 1987 8
19. See the webpage of the Heavy Flavor Averaging Group (HFAG). <http://www.slac.stanford.edu/xorg/hfag>. We usually, but not always, take the Lepton-Photon 2007 (LP2007) numbers as reference 8
20. See the webpage of the CKMfitter group. <http://ckmfitter.in2p3.fr> 8

Chapter 2

CP Violation in Charmless $b \rightarrow s\bar{q}q$ Transitions

With the study of CP violation in $b \rightarrow d$ transitions seemingly in good agreement with Standard Model (SM) expectations, the subject of CPV studies in charmless $b \rightarrow s$ transitions (including $b\bar{s} \leftrightarrow s\bar{b}$) is the current frontier of heavy flavor research. Because there is little CPV weak phase in the controlling product of CKM matrix elements for loop-induced $b \rightarrow s$ transitions, $V_{ts}^* V_{tb}$, any observed deviation could indicate New Physics. As transitions between $3 \rightarrow 2$ generation quarks, the subject also has $\tau \rightarrow \mu$ transition echoes in the lepton sector, an interesting subject covered in Chap. 9. More generally, with the Sakharov conditions [1] that link CPV with the Baryon Asymmetry of the Universe (BAU), i.e., why there is no trace of antimatter in our Universe, we do expect NP sources for CPV. It is well known that the three generation SM falls short by *many orders of magnitude* from the CPV that is needed to generate the observed BAU, a point that we will elaborate in Chap. 10. This certainly has been one of the strongest motivations to search for New Physics in CP violation.

In this chapter, we focus on three topics: the ΔS problem for mixing- or time-dependent CPV (TCPV) in charmless $b \rightarrow s\bar{q}q$ modes vs. $b \rightarrow c\bar{c}s$ modes, where we elucidate also how TCPV studies are conducted; the $\Delta\mathcal{A}_{K\pi}$ problem between direct CPV (DCPV) in $B^+ \rightarrow K^+\pi^0$ and $B^0 \rightarrow K^+\pi^-$ decays; and the DCPV asymmetry $\mathcal{A}_{B^+ \rightarrow J/\psi K^+}$. We close with an appraisal of New Physics search in hadronic $b \rightarrow s$ transitions. The status and prospects for $\sin 2\Phi_{B_s}$ measurement (analogous to $\sin 2\phi_1/\beta$ for B_d system) at the Tevatron and LHC, which is the new forefront, will be discussed in the Chap. 3. Further charmless $b \rightarrow s$ probes of different New Physics are covered in subsequent chapters.

2.1 The ΔS Problem

The B factories were built to measure mixing- or time-dependent CPV (TCPV) in the $B^0 \rightarrow J/\psi K_S$ mode [2]. This is the billion dollar question that started with the ARGUS discovery of large $B^0-\bar{B}^0$ mixing [3]. With the suggestion by Oddone [4] of boosting the $\Upsilon(4S)$, thereby boosting the B^0 and \bar{B}^0 mesons, by the late 1980s, both SLAC and KEK initiated feasibility studies for e^+e^- colliders with asymmetric

beam energies. The push toward asymmetric beam energies also contributed partly to the demise, in 1989, of the proposed machine at Paul Scherrer Institute (PSI), which had a symmetric double ring design. By 1994 or so, both the PEP-II/BaBar and the KEKB/Belle accelerator and detector complexes entered construction phase.

Several miraculous points that aid B factory studies are worthy of note. First, m_B is so close to $m_{\Upsilon(4S)}/2$, such that not only the $\Upsilon(4S)$ decays practically 100% to $B^0\bar{B}^0$ and B^+B^- pairs, the B mesons are produced with rather small momenta. Second, m_{B^+} and m_{B^0} are rather close in mass, such that charged and neutral B mesons are almost equally produced. Their production ratio is of course measured. Third point, which will be immediately discussed in the following, is the “EPR” coherence (or entanglement) of the $B^0\bar{B}^0$ meson pair from $\Upsilon(4S)$ decay. That is, although each meson starts to oscillate between B^0 and \bar{B}^0 after being produced, the pair remains in coherence, such that the determination of the B^0 (or \bar{B}^0) nature of one meson at time t in the $\Upsilon(4S)$ frame, the other meson starts to oscillate from a \bar{B}^0 (or B^0) from time t onward. This quantum coherence has in fact been tested at Belle [5]. Of course, Quantum Mechanics is again affirmed. The fraction of produced B^0 and \bar{B}^0 pairs (out of 76M) that disentangle and decay incoherently is measured to be 0.029 ± 0.057 , which is consistent with zero.

2.1.1 Measurement of TCPV at the B Factories

At B factories, TCPV measurement utilizes the coherent production of $B^0\bar{B}^0$ pairs from $\Upsilon(4S)$ decay. That is, as the produced B^0 (and vice versa the \bar{B}^0) undergoes oscillations back and forth from B^0 to \bar{B}^0 , the pair remains coherent. As the original B^0 and \bar{B}^0 are produced at the same time, if one measures at time t the decay of one B meson, and found that it decays as, say, B^0 , we then know from quantum coherence that the other B meson is a \bar{B}^0 meson at time t . From then on, this \bar{B}^0 meson again oscillates back and forth from \bar{B}^0 to B^0 , until time Δt later, where it also decays.

Having this picture visualized, we can go further and discuss what is done experimentally to measure TCPV. We repeat (A.9) of Appendix A.3 for TCPV asymmetry,

$$\begin{aligned} A_{CP}(\Delta t) &\equiv \frac{\Gamma(\bar{B}^0(\Delta t) \rightarrow f) - \Gamma(B^0(\Delta t) \rightarrow f)}{\Gamma(\bar{B}^0(\Delta t) \rightarrow f) + \Gamma(B^0(\Delta t) \rightarrow f)} \\ &= -\xi_f(\mathcal{S}_f \sin \Delta m \Delta t + \mathcal{A}_f \cos \Delta m \Delta t), \end{aligned} \quad (2.1)$$

where ξ_f is the CP eigenvalue of final state f and $\Delta m \equiv \Delta m_{B_d}$. This asymmetry measures, at time Δt , the difference in rate between a state tagged at $t = 0$ as \bar{B}^0 vs. B^0 . Thus, the Γ 's are really shorthands for differential decay rates. With the Δt distribution of $A_{CP}(\Delta t)$, which are actually done by fitting $\Gamma(\bar{B}^0(\Delta t) \rightarrow f)$ and $\Gamma(B^0(\Delta t) \rightarrow f)$ distributions, the CPV parameters \mathcal{S}_f and \mathcal{A}_f are just the Fourier coefficients of the sine and cosine Δt oscillation terms. Of course, experimentally

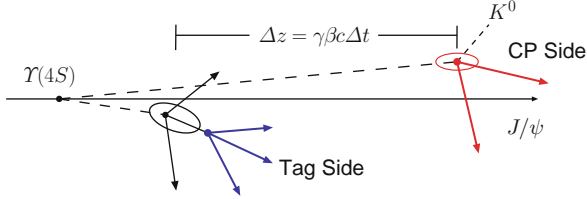


Fig. 2.1 Figure illustrating TCPV measurement. The $\Upsilon(4S)$, which decays into a $B^0-\bar{B}^0$ pair, is boosted in the z -direction. After one B is tagged by its decay, quantum coherence dictates the other B would start evolving from the conjugate of the tagged state. At time $\Delta t = \gamma\beta c\Delta z$ (can be negative), where Δz is the measured difference between the decay vertices, the other B decays into a CP eigenstate such as $J/\psi K_S$. See text for further discussion

one has to correct for inefficiencies and dilution factors, which we do not go into. As discussed in Chap. 1 and Appendix A, $\mathcal{S}_{J/\psi K^0}$ is just $\sin 2\beta/\phi_1$, the CPV phase of $B^0-\bar{B}^0$ mixing amplitude, while $\mathcal{A}_{J/\psi K^0}$ is the direct CPV for this mode.

To conduct $A_{CP}(\Delta t)$ measurement, as illustrated in Fig. 2.1, one needs to

- (1) tag the flavor of one B decay (B^0 or \bar{B}^0) at “ $t = 0$,”
- (2) reconstruct the other B in a CP eigenstate (cannot tell B^0 vs. \bar{B}^0), and
- (3) measure decay vertices for both B decays.

For the last point, one utilizes the boost along the z - or beam direction, and $\Delta z \cong \gamma\beta c\Delta t$ is the measured difference between the two B decay vertices. The $\gamma\beta$ factor is 0.56 and 0.43 for PEP-II and KEKB, respectively. With B lifetime of order picosecond, $\gamma\beta c\tau_B$ is of order $200\text{ }\mu\text{m}$ or so. For the CP side, one therefore demands a σ_z resolution of less than $100\text{ }\mu\text{m}$.

The BaBar and Belle detectors are rather similar to each other. A side view of the Belle detector is given in Fig. 2.2 showing subdetectors. The subdetectors of BaBar and Belle consist of a Silicon Vertex Detector (SVT/SVD), a Central Drift Chamber (DCH/CDC), an Electromagnetic Calorimeter (EMC/ECL) based on CsI(Tl), a Particle Identification Detector (PID) system, superconducting solenoid magnet, and an Iron Flux Return that is instrumented (IFR for BaBar) for K_L and muon detection (hence KLM for Belle).

The difference between the two detectors is basically only in the PID system that is crucial for flavor tagging, in particular the task of charged K/π separation at various energies. Note that, even for $B \rightarrow J/\psi K$ decay, p_K is almost $1.7\text{ GeV}/c$ and rather relativistic, and in addition one has the boost. The Belle PID system consists of Aerogel Cherenkov Counters (ACC), a threshold device with several indices of refraction n for the silica aerogel for different angular coverage, plus a Time of Flight (TOF) counter system. BaBar uses the DIRC, basically a system of quartz bars that generate and guide the Cherenkov photons (by internal reflection) and project them into a water tank at the back end (called the Stand-Off-Box, or SOB) of the detector. It provides more dynamical information, but the large SOB is a little

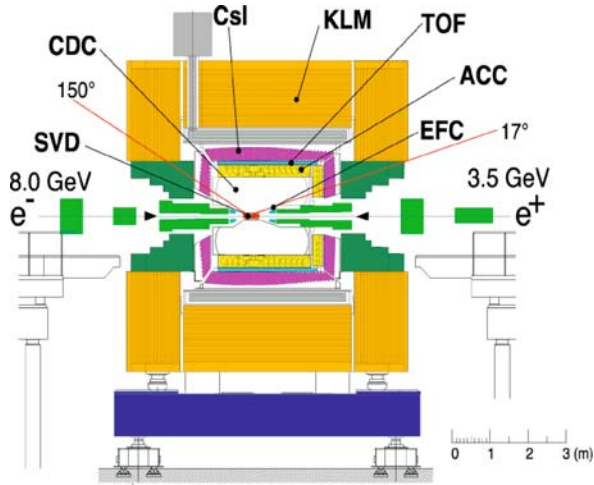


Fig. 2.2 Schematic side view of the Belle detector, with markings of the subdetector systems. (Source: <http://belle.kek.jp/belle/transparency/detector1.html>.)

unwieldy.¹ One other difference between Belle and BaBar is the Interaction Region (IR), which is at the intersection between detector and accelerator. PEP-II made the conservative choice of zero angle crossing (electrostatic beam separation by permanent magnets), while KEKB used finite angle crossing. This eventually became a main limiting factor for the luminosity reach of PEP-II, although it ensured faster accelerator turn on. In any case, it is truly impressive that both accelerators reached beyond design luminosities, especially since the asymmetric energy design was a new challenge.

The real novelty of the B factories, of course, is the asymmetric beam energies. The $\gamma\beta$ factor for the produced $\Upsilon(4S)$ is 0.56 and 0.43, respectively, for PEP-II and KEKB. Boosting the B^0 and \bar{B}^0 mesons allowed the time difference $\Delta t \cong \Delta z/\beta\gamma c$ used in (2.1) to be inferred from the decay vertex difference Δz in the boost direction, while the proximity of $2m_{B^0}$ to $m_{\Upsilon(4S)}$ means rather minimal lateral motion. Both the PEP-II and KEKB accelerators were commissioned in 1999 with a roaring start. By 2001, KEKB outran PEP-II in the instantaneous luminosity and in integrated luminosity as well by the following year (see Fig. 2.3). In April 2008, PEP-II dumped its beam for the last time.

With the good performance of the accelerators and with relatively standard detectors, by 2001, the measurement of the gold-plated mode of $B^0 \rightarrow J/\psi K^0$ (including K_L^0) was settled. As can be seen from Fig. 1.3, the mean value between

¹ The aerogel technique was originally developed at BaBar and adopted by Belle when there was insufficient confidence in the original design of a RICH detector system. When BaBar adopted the innovative DIRC, the extra space available, together with budget pressures, led to a slight compromise of the EMC system.

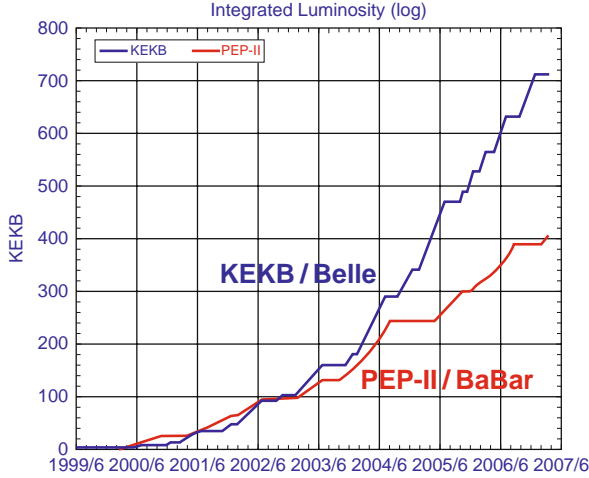


Fig. 2.3 Comparison of integrated luminosities achieved by KEKB/Belle and PEP-II/BaBar, up to early summer 2007

Belle and BaBar remained largely unchanged since then. It would seem that the *raison d'être* of the B factories was accomplished just 2 years after commissioning!

2.1.2 TCPV in Charmless $b \rightarrow s\bar{q}q$ Modes

With the measurement of TCPV in $B^0 \rightarrow J/\psi K_S$ settled in summer 2001, attention quickly turned to the $b \rightarrow s$ penguin modes, where a virtual gluon is emitted from the virtual top quark in the vertex loop.

Let us take $B^0 \rightarrow \phi K_S$ as example [6], where, as shown in Fig. 2.4(a), the virtual gluon pops out an $s\bar{s}$ pair. The $b \rightarrow s$ penguin amplitude is practically real within SM, just like the tree level $B^0 \rightarrow J/\psi K_S$. This is because $V_{us}^* V_{ub}$ is very suppressed, so the c and t contributions carry equal and opposite CKM coefficients $V_{ts}^* V_{tb} \cong -V_{cs}^* V_{cb}$, which is practically real, as can be seen from (A.3). Thus, one has the SM prediction,

$$S_{\phi K_S} \cong \sin 2\phi_1 / \beta \quad (\text{SM}), \quad (2.2)$$

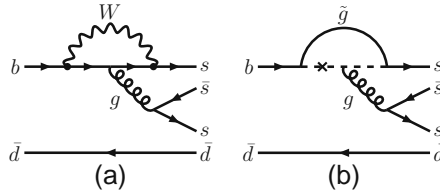


Fig. 2.4 (a) Strong penguin (P) diagram for $\bar{B}^0 \rightarrow \phi \bar{K}^0$ in SM, and (b) a possible diagram in SUSY with \tilde{b} - \tilde{s} squark mixing, which is illustrated by the cross on the squark line inside the loop

where $\mathcal{S}_{\phi K_S}$ is the analogous TCPV measure in the $B^0 \rightarrow \phi K_S$ mode, following the \mathcal{S}_f notation of (2.1). New physics-induced Flavor-Changing Neutral Current (FCNC) and CPV effects, such as having supersymmetric (SUSY) particles in the loop (for example, \tilde{b} - \tilde{s} squark mixing, Fig. 2.4(b)), could break this equality. That is, deviations from (2.2) would indicate New Physics. This prospect prompted the experiments to search vigorously.

The first ever TCPV study in charmless $b \rightarrow s\bar{q}q$ modes was performed for $B^0 \rightarrow \eta' K_S$ [7] by Belle in 2002 with 45M $B\bar{B}$ pairs [8]. Part of the motivation is the large enhanced rate, which is still not fully understood. But many might remember better the big splash made by Belle in summer 2003, where $\mathcal{S}_{\phi K_S}$ was found to be opposite in sign [9] to $\sin 2\phi_1/\beta$, where the significance of deviation was more than 3σ . But the situation softened by 2004 and is now far less dramatic. What happened was that the Belle value for $\mathcal{S}_{\phi K_S}$ changed by 2.2σ , shifting from ~ -1 in 2003 to ~ 0 in 2004. 123M $B\bar{B}$ pairs were added to the analysis in 2004, but they gave the results with sign opposite to the earlier data of 152M $B\bar{B}$ pairs. The new data was taken with the upgraded SVD2 silicon detector, which was installed in summer 2003. The SVD2 resolution was studied with B lifetime and mixing and was well understood, while $\sin 2\phi_1$ measured in $J/\psi K_S$ and $J/\psi K_L$ modes showed good consistency between SVD2 and SVD1. Many other systematics checks were also done. By Monte Carlo study of pseudoexperiments, Belle concluded [10] that there is 4.1% probability for the 2.2σ shift. This is a sobering and useful reminder, especially when one is conducting New Physics search, that large fluctuations do happen.

The study at Belle and BaBar has expanded to include many charmless $b \rightarrow s\bar{q}q$ modes. After several years of vigorous pursuit, some deviation has persisted in an interesting if not nagging kind of way. Let us not dwell on analysis details, except stressing that this is one of the major, concerted efforts at the B factories. Comparing to the average of $\mathcal{S}_{c\bar{c}s} = 0.681 \pm 0.025$ [11] over $b \rightarrow c\bar{c}s$ transitions, \mathcal{S}_f is smaller in practically all $b \rightarrow s\bar{q}q$ modes measured so far (see Fig. 2.5), with the naive mean² of $\mathcal{S}_{s\bar{q}q} = 0.56 \pm 0.05$ [11]. That is,

$$\mathcal{S}_{s\bar{q}q} = 0.56 \pm 0.05 \quad \text{vs.} \quad \mathcal{S}_{c\bar{c}s} = 0.681 \pm 0.025. \quad (2.3)$$

The deviation $\Delta\mathcal{S} \equiv \mathcal{S}_{s\bar{q}q} - \mathcal{S}_{c\bar{c}s} < 0$ is only 2.2σ from zero, and the significance has been slowly diminishing. However, it is worthwhile to stress that the persistence over several years, and in multiple modes, taken together make this “ $\Delta\mathcal{S}$ problem” a potential indication for New Physics from the B factories. Despite the lack in significance, it should not be taken lightly. After all, the experiments were not able to “make it go away.”³

² We use the LP2007 update by Heavy Flavor Averaging Group (HFAG) that excludes the new $\mathcal{S}_{f_0(980)K_S}$ result from BaBar. The HFAG itself warns “treat with extreme caution” when using this BaBar result [11]. The value is larger than $\mathcal{S}_{c\bar{c}s}$ and is very precise, with errors three times smaller than the ϕK_S mode. But $f_0(980)K_S$ actually has smaller branching ratio than ϕK_S ! The BaBar result needs confirmation from Belle in $B^0 \rightarrow \pi^+\pi^-K_S$ mode.

³ The Summer 2008 update by HFAG seems to indicate that there is no deviation and the $\Delta\mathcal{S}$ problem now rests in the errors.

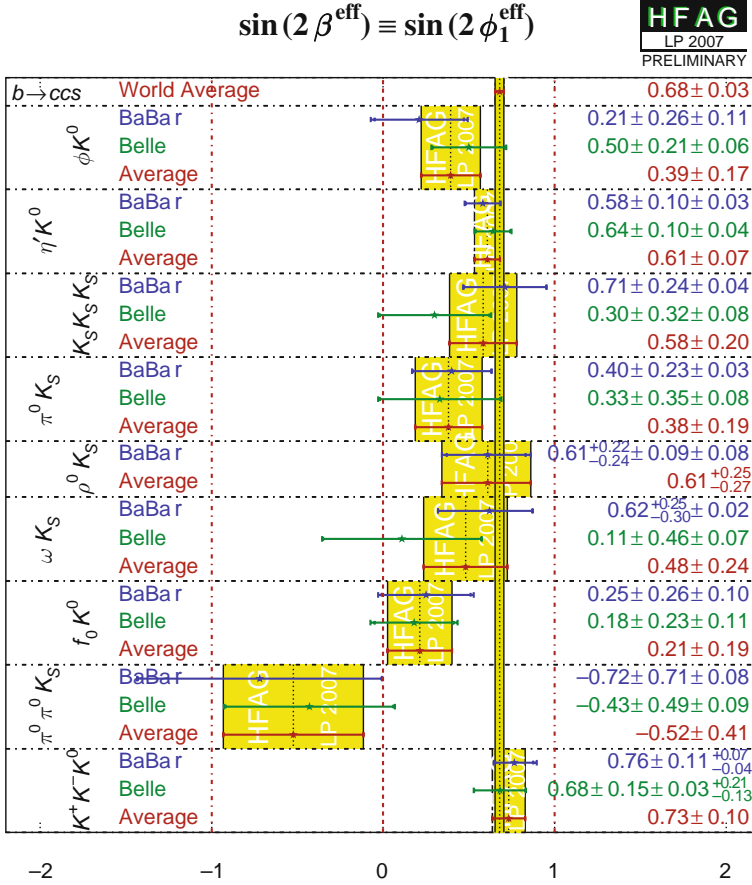


Fig. 2.5 Measurements of S_f in $b \rightarrow s\bar{q}q$ penguin modes [11]. (Summer 2007 results from HFAG, used with permission.) See Footnote 2 for comment on the $B^0 \rightarrow f_0(980)K_S$ mode

The point is that theoretical studies, although troubled by hadronic effects, all give $S_{s\bar{q}q}$ values that are *above* [12–15] $S_{c\bar{c}s}$, or

$$\Delta S|^{\text{TH}} > 0. \quad (2.4)$$

This elevates the tension that is already present with the experimental situation, i.e., what lies behind the apparent $\Delta S|^{\text{EXP}} < 0$.

Is this New Physics? We remark that there are limitations for what one can interpret from deviations in penguin-dominant $b \rightarrow s$ hadronic modes. While a large, *definite* effect in a single mode, such as the relatively clean ϕK_S mode, (pure $b \rightarrow s\bar{s}s$ penguin) would clearly indicate NP, many of these modes, as well as theoretical approaches, suffer from large hadronic uncertainties, such that the NP effect would vary from mode to mode. So, whether ϕK_S or $\eta' K_S$, or the combined effect in $b \rightarrow s\bar{q}q$, one may not gain much more information by averaging over

modes. We also note that the mode with the largest branching fraction, and the first mode to be studied [8], i.e. $\eta' K_S$, is now in very good agreement with $b \rightarrow c\bar{c}s$. This is not surprising, for it is now believed that the enhancement of $B^0 \rightarrow \eta' K^0$ is not due so much to New Physics, but some combination of “hadronic” effects.

It is a bit frustrating for the B factory worker that, after many years of work, this deviation is not much more than 2σ . Clearly, we need more data ! But BaBar has ended its data taking, while Belle would stop for (hopeful) upgrade after reaching 1 ab^{-1} , so the data set for analysis can only double within the present B factory era, which is drawing to an end. As B factory data can at best double, it seems that one would probably need a Super B factory to resolve the issue of ΔS . In this context, we need a clear litmus test.

One promising development is a model-independent geometric approach, which suggests [16] that, once one has enough experimental precision, a deviation as little as a couple of degrees would indicate New Physics. It would be splendid if there is no loophole in this argument, for this is what is needed when we reach the precision of the Super B factory era. However, this approach needs better elucidation, before the commissioning of the upgraded B factory, for people to grasp and appreciate the insight. Other approaches to ascertain at what level a $\Delta S_{(f)}$ deviation can be called an indication for New Physics should also be developed.

One may think that the LHC, which started first beam in September 2008 (but immediately started facing turn-on pains), and the LHCb experiment in particular should be able to make great progress on the ΔS problem. Curiously, because of lack of good vertices or the presence of neutral (π^0 , γ) particles (a weakness for LHCb) in the leading channels of $\eta' K_S$, ϕK_S , and $K_S \pi^0$, the situation may not improve greatly with LHCb data. An improved LHCb detector (i.e., after an upgrade), or some different approach, needs to be developed.

The ΔS problem seems to demand a Super B Factory for its clarification.

2.2 The $\Delta\mathcal{A}_{K\pi}$ Problem

There is a second possible indication for BSM physics in $b \rightarrow s\bar{q}q$ decays. It became widely known through the Belle paper published in *Nature* [17] in March 2008. Unlike the situation with ΔS , experimentally it is very firm. But for interpretation, opinions still differ.

2.2.1 Measurement of DCPV in $B^0 \rightarrow K^+ \pi^-$ Decay

Just 3 years after the observation of TCPV in $B^0 \rightarrow J/\psi K^0$, Direct CPV (DCPV) in the B system was claimed in 2004 between BaBar and Belle [18, 19]. This attests to the prowess of the B factories, as it took 35 years for the same evolution in the K system [18, 19].

Unlike mixing-dependent CPV, where one needs decay time information and tagging, the experimental study of DCPV is just a counting experiment, hence much simpler. In the self-tagging modes such as $K^\mp\pi^\pm$, one simply counts the difference between the number of events in $K^-\pi^+$ vs. $K^+\pi^-$. Self-tagging means that a $K^-\pi^+$ would be decaying from a \bar{B}^0 , while $K^+\pi^-$ comes from a B^0 .

Of course, there is the standard rare B reconstruction techniques to reject continuum (from $e^+e^- \rightarrow q\bar{q}$, where q is a u, d, s , or c quark) and other backgrounds by some multivariate “filter” methods. We do not go into these technical details. But it is worthwhile to mention a special technique at the B factories that utilizes the kinematics of the $\Upsilon(4S)$ production environment. One reconstructs m_B of a potential candidate, by replacing the measured energy sum with the known center-of-mass beam energy. This trick utilizes the fact that for $\Upsilon(4S) \rightarrow B\bar{B}$ two-body production (which has 100% branching fraction), the B meson would carry exactly the CMS beam energy, $E_{\text{CM}}/2$. One then checks the signal region around $\Delta E \sim 0$, where the energy difference between the measured energy sum and $E_{\text{CM}}/2$ should vanish for a genuine B candidate, but for a background event it would not vanish.

Thus, the two standard variables are the *beam-constrained mass* M_{bc} (called “beam energy-substituted mass” by BaBar, m_{ES}) and the *energy difference* ΔE ,

$$M_{\text{bc}} = \sqrt{(E_{\text{CM}}/2)^2 - \sum (\mathbf{p}_i)^2}, \quad \Delta E = \sum E_i - E_{\text{CM}}/2, \quad (2.5)$$

where E_i and \mathbf{p}_i are the measured energy and momentum for particle i , and $E_{\text{CM}} = \sqrt{s}$ is precisely known from the accelerator. A correctly reconstructed B meson event would peak in M_{bc} and ΔE , as can be visualized by 1D projection plots illustrated in Fig. 2.6, while background events would not. Note that the K^\pm and π^\pm in $B \rightarrow K^\pm\pi^\mp, \pi^\pm\pi^\mp$ decays are rather highly boosted, hence PID performance is very critical for the separation of $K^\pm\pi^\mp$ vs. $\pi^+\pi^-$ events.

With these relatively standard techniques, it was a matter of time and providence (which specific mode) for one to eventually catch the first DCPV measurement, which happened to be the $B^0 \rightarrow K^+\pi^-$ mode.

Indications for a negative DCPV in this mode, defined as

$$\mathcal{A}_{K^+\pi^-} \equiv \mathcal{A}_{\text{CP}}(B^0 \rightarrow K^+\pi^-) = \frac{\Gamma(\bar{B}^0 \rightarrow K^-\pi^+) - \Gamma(B^0 \rightarrow K^+\pi^-)}{\Gamma(\bar{B}^0 \rightarrow K^-\pi^+) + \Gamma(B^0 \rightarrow K^+\pi^-)}, \quad (2.6)$$

(basically the same definition as in (A.2)) had been emerging for a couple of years. BaBar announced (using 227M $B\bar{B}$ pairs) a value [20] with 4.2σ significance just before ICHEP 2004, while at that conference, the Belle measurement [21] (using 275M $B\bar{B}$ pairs) was reported with 3.9σ significance. The M_{bc} and ΔE results from Belle are plotted in Fig. 2.6. It is clear by inspection that the number of $\bar{B}^0 \rightarrow K^-\pi^+$ events are fewer than $B^0 \rightarrow K^+\pi^-$. The combined Belle and BaBar result that year was $\mathcal{A}_{K^+\pi^-} = -0.114 \pm 0.020$, with 5.7σ significance, which established DCPV in the B system. The QCD Factorization (QCDF) approach had predicted the opposite sign [22], while the Perturbative QCD Factorization (PQCD)

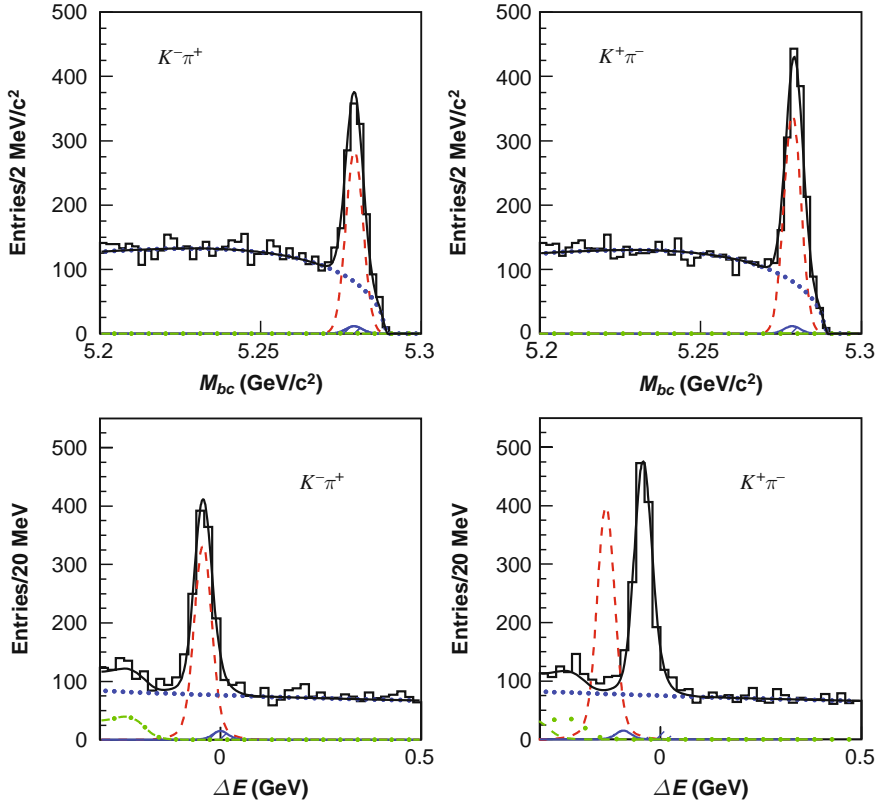


Fig. 2.6 M_{bc} and ΔE projection plots for $B^0 \rightarrow K^-\pi^+$ vs. $\bar{B}^0 \rightarrow K^+\pi^-$ from Belle [21] based on 275M $B\bar{B}$ pairs. [Copyright (2004) by The American Physical Society.] The CPV asymmetry is apparent, with more $K^+\pi^-$ events than $K^-\pi^+$

approach [23, 24] predicted the correct sign and magnitude. Thus, the measurement has implications for the theory of hadronic B decays.

The CDF experiment at the Tevatron has also measured $\mathcal{A}_{K^+\pi^-}$ with 1 fb^{-1} data [25] at 3.5σ significance, and the result is consistent with the B factories. Let us give a very brief account of the CDF study. Two opposite-charged track events from a common displaced vertex were selected. But there is not enough invariant mass resolution to separate different contributions clearly. Nor does CDF have sufficient PID capability to separate K^\pm from π^\pm in B decay (which is more boosted than at B factories). Using tagged $D^{*\pm}$ decays, charged K, π separation with dE/dx from tracker response is only at 1.4σ . But by combining kinematic and PID information into an unbinned maximum likelihood fit, CDF obtained $\mathcal{A}_{K^+\pi^-} = -0.086 \pm 0.023 \pm 0.029$, based on 1 fb^{-1} data. This should be compared with the latest values from BaBar [26], $-0.107 \pm 0.018^{+0.007}_{-0.004}$ (383M $B\bar{B}$), and Belle [17], $-0.094 \pm 0.018 \pm 0.008$ (535M $B\bar{B}$).

Comparing the BaBar and Belle studies, one can see that the analysis philosophy is slightly different, and in any case, the 5.5σ significance for BaBar vs. 4.8σ for Belle largely reflects a stronger central value for BaBar. Comparing CDF vs. the B factory results, one can see the effect of lack of PID on the systematic error. A statistical power of 1.6 fb^{-1} at CDF could already be comparable to current B factories. However, without improvement in systematic error, which is not likely to happen, CDF cannot be competitive in this study. The advent of LHCb should change the situation, since it has active RICH systems.

We have spent some effort describing how DCPV studies are done, at B factory vs. hadronic environment, largely for sake of comparison. Incorporating even the CLEO measurement [18, 19] done in 2000 (with just $9.7\text{M } B\bar{B}$), the current world average [11] is

$$\mathcal{A}_{B^0 \rightarrow K^+\pi^-} = -9.7 \pm 1.2 \%. \quad (2.7)$$

This by itself does not suggest New Physics, but rather, it indicates the presence of a finite strong phase δ between the strong penguin (P) and tree (T) amplitudes, where the latter provides the weak phase via $V_{us}^* V_{ub}$. See Appendix A for a discussion. Most QCD-based factorization approaches failed to predict $\mathcal{A}_{K^+\pi^-}$, largely because of lack of control over how to properly generate δ .

Even in 2004, however, there was a whiff of a puzzle [21]. With large errors, $\mathcal{A}_{\text{CP}}(B^+ \rightarrow K^+\pi^0)$ was found to be consistent with zero for both Belle and BaBar, and the mean was $\mathcal{A}_{K^+\pi^0} = +0.049 \pm 0.040$. We plot the M_{bc} and ΔE results from Belle in Fig. 2.7. Comparing with the 2004 mean value of -0.114 ± 0.020 for $\mathcal{A}_{K^+\pi^-}$ (see Fig. 2.6 for the corresponding Belle plot), there seemed to be a difference⁴ between DCPV in $B^+ \rightarrow K^+\pi^0$ and $B^0 \rightarrow K^+\pi^-$, a point which was emphasized already in the Belle paper [21].

The difference between the charged and neutral mode has steadily strengthened since 2004, and the current [11] average of

$$\mathcal{A}_{B^+ \rightarrow K^+\pi^0} = +5.0 \pm 2.5 \% \quad (2.8)$$

shows some significance for the sign being *positive*, i.e., opposite to the sign of $\mathcal{A}_{K^+\pi^-}$ in (2.7).

2.2.2 $\Delta\mathcal{A}_{K\pi}$ and New Physics

In a recent paper published in *Nature*, the Belle collaboration used 535M $B\bar{B}$ pairs to demonstrate the difference [17]

⁴ Actually, the 2003 value by BaBar, with 88M $B\bar{B}$ pairs, was $\mathcal{A}_{K^+\pi^0} = -0.09 \pm 0.09 \pm 0.01$. But with 227M $B\bar{B}$ pairs, the 2004 value by BaBar changed sign [27], becoming $\mathcal{A}_{K^+\pi^0} = +0.06 \pm 0.06 \pm 0.01$. Combining with the positive value of Belle, $\mathcal{A}_{K^+\pi^0} = +0.04 \pm 0.05 \pm 0.02$ (based on 275M $B\bar{B}$), this made the difference between $\mathcal{A}_{K^+\pi^0}$ and $\mathcal{A}_{K^+\pi^-}$ stand out already in 2004.

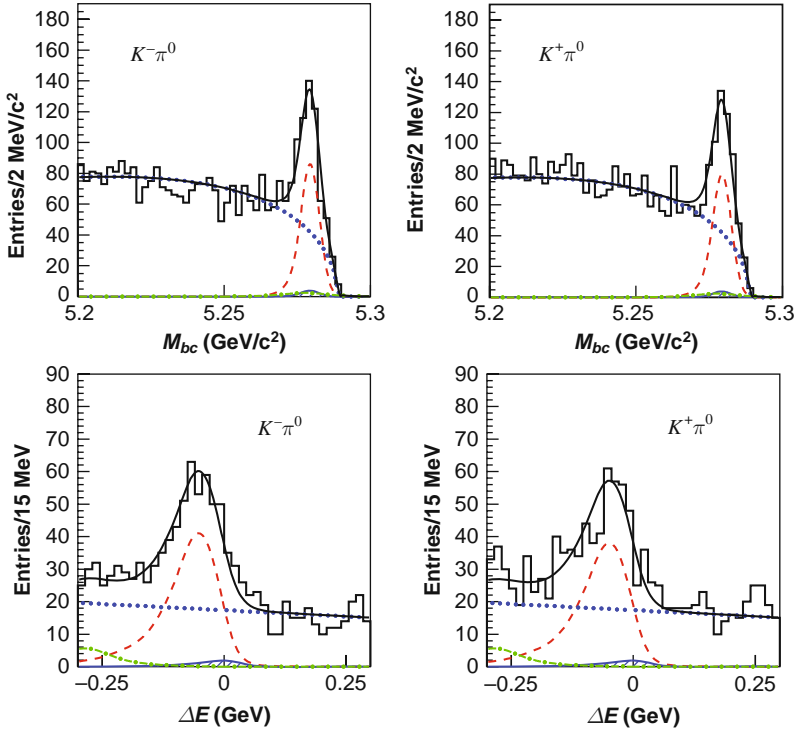


Fig. 2.7 M_{bc} and ΔE projection plots for $B^+ \rightarrow K^+\pi^0$ vs. $B^- \rightarrow K^-\pi^0$ from Belle [21], based on 275M $B\bar{B}$ pairs. [Copyright (2004) by The American Physical Society.] The CPV asymmetry is consistent with zero, with a slight hint for more $K^-\pi^0$ events

$$\Delta\mathcal{A}_{K\pi} \equiv \mathcal{A}_{K^+\pi^0} - \mathcal{A}_{K^-\pi^0} = +0.164 \pm 0.037, \quad (2.9)$$

with 4.4σ significance by a single experiment, and emphasized the possible indication for New Physics. As mentioned, the Belle effort traces back to the 2004 paper [21], where the difference was already noted. One difference with BaBar is that, even in 2004, the Belle paper covered both $B^+ \rightarrow K^+\pi^0$ and $B^0 \rightarrow K^+\pi^-$ studies. The comparison, and potential implications of a difference, was already emphasized. Noticing the curiosity, Belle conducted a meticulous study with a data set that is twice as large, which resulted in the *Nature* paper. BaBar, however, published the $B^+ \rightarrow K^+\pi^0$ mode [28] separately from the $B^0 \rightarrow K^+\pi^-$ [26], bundling it together with the $\pi\pi^0$ modes. The approach and physics emphasis was therefore very different from those of Belle's.

The world average [11] for the direct CPV difference is

$$\Delta\mathcal{A}_{K\pi} = 0.147 \pm 0.027, \quad (2.10)$$

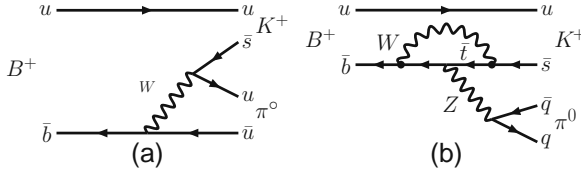


Fig. 2.9 (a) Color-suppressed tree diagram (C) and (b) electroweak penguin diagram (P_{EW}) for $B^+ \rightarrow K^+ \pi^0$

to predict. Although DCPV is one of the simplest things to measure experimentally, the strong phase difference in a decay amplitude is usually hard to extract.

The $B^+ \rightarrow K^+ \pi^0$ decay amplitude is similar to the $B^0 \rightarrow K^+ \pi^-$ one, up to subleading corrections, that is

$$\sqrt{2}\mathcal{M}_{K^+\pi^0} - \mathcal{M}_{K^+\pi^-} = C + P_{EW}, \quad (2.12)$$

where C is the color-suppressed tree amplitude, while P_{EW} is the electroweak penguin (replacing the virtual gluon in P by Z or γ) amplitude. These diagrams are illustrated in Fig. 2.9. In the limit that these subleading terms vanish, one expects $\Delta\mathcal{A}_{K\pi} \sim 0$. For a very long time before the experimental advent, this was broadly expected to be the case. But, eventually, it turned out contrary to the experimental result of (2.10). We therefore understand why something like this was not predicted by any calculations.

Large C ? Need Large “Finesse”!

Could C be greatly enhanced? This is certainly an option, and it is the attitude taken by many [30]. Indeed, fitting with data, one finds $|C/T| > 1$ is needed [31], in strong contrast to the very tiny value for C suggested 10 years ago [32]. Note that from the usual nonperturbative large N_C expansion perspective, one expects color suppression to be stronger than $1/N_C$. There is further difficulty for an enhanced C amplitude. As this amplitude has the same weak phase ϕ_3 as T , the enhancement of C has to contrive in its strong phase structure to cancel the effect of the strong phase difference δ between T and P that helped induce the sizable $\mathcal{A}_{K^+\pi^-}$ of (2.7) in the first place. The amount of “finesse” needed is therefore quite considerable. This point seems to have been deemphasized by the casual attitude taken by many across the Atlantic Ocean.

It should be stressed that the difference $\Delta\mathcal{A}_{K\pi}$ was *not* anticipated by any calculations beforehand, and theories that do possess calculational capabilities⁵ have

⁵ For the noncalculational approaches of fitting data with T , P , C , and P_{EW} , etc., we stress that they are just that, fitting to data. Without being able to compute these contributions, they are saying nothing more than “Data implies a large C ,” which is a tautological statement in essence, or a mere translation of data. For example, in the pre-B factory era, by *assuming* $|C| \ll |T|$, there was the suggestion [33] to combine $\mathcal{A}_{CP}(K^+\pi^0)$ with $\mathcal{A}_{CP}(K^+\pi^-)$ for sake of increasing statistics. With

only played catching up, after the experimental fact. In Perturbative QCD (PQCD) Factorization calculations at Next to Leading Order (NLO) [34], taking cue from data, C does move in the right direction. But the central value is insufficient to account for experiment, and the claim to consistency with data is actually hiding behind large errors. For QCD Factorization (QCDF), it has been declared [35] that $\Delta\mathcal{A}_{K\pi}$ is difficult to explain, that it would need very large and *imaginary* C (or electroweak penguin) compared to T , which is “Not possible in SM plus factorization [approach].” In the Soft Colinear Effective Theory (SCET) approach [36], which is rather sophisticated, $\mathcal{A}_{K^+\pi^0}$ is actually predicted, in 2005, to be even more negative than $\mathcal{A}_{K^+\pi^-}$, where the latter has been taken as input. In a way, the SCET proponents were wishing the $\Delta\mathcal{A}_{K\pi}$ to go away. But the $\Delta\mathcal{A}_{K\pi}$ problem has persisted, and SCET people have now admitted to the problem [37]. On whether it could be New Physics, SCET needs to “see a coherent pattern of deviations,” before it can be convinced about the need for New Physics. Perhaps we will have more convincing information emerging (soon), as discussed in the next section. In any case, the problem appears to be with SCET itself, rather than with experiment.

Large P_{EW} ? Then New Physics!

The other option is to have a large CPV contribution from the electroweak penguin [29, 31, 38] amplitude, P_{EW} . The interesting point is that *this calls for a New Physics CPV phase*, as it is known that P_{EW} carries practically no weak phase within SM ($V_{ts}^* V_{tb}$ is practically real, see (A.4)) and has almost the same strong phase as T [39].

— So, what New Physics can this be? —

Note that this would not so easily arise from SUSY, since SUSY effects tend to be of the “decoupling” kind, compared to the *nondecoupling* of the top quark effect already present, in fact dominating, in the Z penguin loop.⁶ The latter is very analogous to what happens in box diagrams.

So, can there be more *nondecoupled* quarks beyond the top in the Z penguin loop? This is the so-called (sequential) fourth generation. It would naturally bring into the $b \rightarrow s\bar{q}q$ electroweak penguin amplitude P_{EW} (but not so much in the strong penguin amplitude P) a new CPV phase, in the new CKM product $V_{ts}^* V_{tb}$.

experimental indication that $|C/T|$ is finite, the same mentality flips over [30] to allow C/T , both in strength and (strong) phase, to be free parameters.

⁶ In Fig. 2.4, we compared the gluonic penguin P for $b \rightarrow s\bar{s}s$ in SM with a possible SUSY effect through $\bar{b}-\bar{s}$ mixing. This is possible in SUSY. Unlike the Z penguin, the top quark mass effect in the gluonic penguin largely decouples, as it is weaker than logarithmic dependence [40]. The usual image of top dominance in the strong penguin loop is somewhat misplaced. It really is just due to operator running from W scale, rather than a genuine heavy top mass effect. It does rely on m_t being heavier than M_W , but QCD running between m_t and M_W is rather mild.

It was shown [38] that (2.9) can be accounted for in this extension of SM. We will look further into this, after we discuss NP prospects in B_s mixing.

With the two hints for New Physics in $b \rightarrow s$ penguin modes, i.e., the ΔS (TCPV) and $\Delta A_{K\pi}$ (DCPV) problems, one might expect possible NP in B_s mixing. Note that recent results for Δm_{B_s} and $\Delta \Gamma_{B_s}$ are SM-like. However, the real test clearly should be in the CPV measurables, $\sin 2\Phi_{B_s}$ and $\cos 2\Phi_{B_s}$, as the NP hints all involve CPV. This is the subject of the next section.

2.3 $\mathcal{A}_{CP}(B^+ \rightarrow J/\psi K^+)$

If the $\Delta A_{K\pi}$ problem is genuinely rooted in the electroweak penguin amplitude P_{EW} , one can infer a corollary to be checked relatively quickly as a confirmation. Rather than becoming a π^0 , the Z^* from the effective $b s Z^*$ vertex could produce a J/ψ . If there is New Physics in the $B^+ \rightarrow K^+ \pi^0$ electroweak penguin, one can then contemplate DCPV in $B^+ \rightarrow J/\psi K^+$ as a probe of NP.

$B^+ \rightarrow J/\psi K^+$ decay is of course dominated by the color-suppressed $b \rightarrow c\bar{c}s$ amplitude (Fig. 2.10(a)), which is proportional to the CKM element product $V_{cs}^* V_{cb}$ that is real to very good approximation. At the loop level, the penguin amplitudes are proportional to $V_{ts}^* V_{tb}$ in the SM. Because $V_{us}^* V_{ub}$ is very suppressed, $V_{ts}^* V_{tb} \cong -V_{cs}^* V_{cb}$ is not only practically real (see (3.5) in Chap. 3), it has the same phase as the tree amplitude and can be absorbed into it, as far as the CKM factor is concerned. Hence, it is commonly argued that DCPV is less than 10^{-3} in this mode, and $B^+ \rightarrow J/\psi K^+$ has often been viewed as a calibration mode in search for DCPV. However, because of possible hadronic effects, there is no firm prediction that can stand scrutiny. A recent calculation [41] of $B^0 \rightarrow J/\psi K_S$ that combines QCDF-improved factorization and the PQCD approach confirms the three generation SM expectation that $\mathcal{A}_{CP}(B^+ \rightarrow J/\psi K^+)$ should be at the 10^{-3} level. Thus, if % level asymmetry is observed in the next few years, it would support the scenario of New Physics in $b \rightarrow s$ transitions, in particular, stimulating theoretical efforts to compute the strong phase difference between C and P_{EW} .

We shall argue that, in the fourth-generation scenario, DCPV in $B^+ \rightarrow J/\psi K^+$ decay could be at the % level. We give the electroweak penguin amplitude in SM in Fig. 2.10(b). Within SM, the same remark as before holds, and little CPV is generated. But, as we have seen for $B \rightarrow K\pi$ decay, if P_{EW} picks up a sizable New

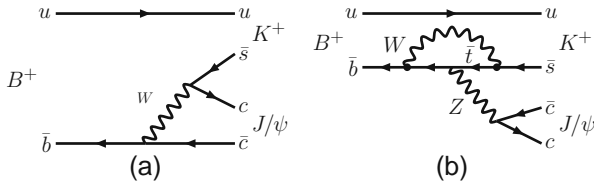


Fig. 2.10 (a) Color-suppressed tree diagram (C) and (b) electroweak penguin diagram (P_{EW}) for $B^+ \rightarrow K^+ J/\psi$

Physics CPV phase, then it can interfere with the C amplitude and generate DCPV, if there is a strong phase difference. More generally, one can view the $P_{\text{EW}}(b \rightarrow s\bar{c}c)$ amplitude as a four-quark operator (e.g., Z' models). Then the CPV phase of this amplitude is not constrained by the effect in $B \rightarrow K^+\pi^0$.

The experiment so far is consistent with zero, but has a somewhat checkered history [18]. Belle has not updated from their 2003 study based on a mere 32M $B\bar{B}$ pairs, although they now have more than $25\times$ the data. BaBar's study flipped sign from the 2004 study based on 89M to the 2005 study based on 124M, which seemed dubious at best. However, the sign was flipped back in PDG 2007, simply because it was found that the 2005 paper used the opposite convention to the (standard) one used for 2004. The opposite sign between Belle and BaBar suppresses the central value, but the error is at 2% level. This already rules out, for example, the suggestion [42] of enhanced H^+ effect at 10% level.

One impediment to the further study of the available higher statistics at the B factories is the control of the systematic error. It seems formidable to break the 1% barrier. Recent progress has been made, however, by the DØ experiment at the Tevatron. Based on 2.8 fb^{-1} data, DØ reconstructed around 40000 $B^\pm \rightarrow J/\psi K^\pm$ events, together with $\sim 1600 B^\pm \rightarrow J/\psi \pi^\pm$. The $M(J/\psi K)$ distribution is shown in Fig. 2.11. Of course, the more important issue is systematics control. DØ measures [43]

$$\mathcal{A}_{B^+ \rightarrow J/\psi K^+} = 0.75 \pm 0.61 \pm 0.27 \% \quad (\text{DØ}). \quad (2.13)$$

We should note that there is a correction twice as large as the central value in (2.13) for the K^\pm asymmetry due to detector effects, because the detector is made of *matter*. This is because the K^-N cross section is different from K^+N cross section, especially for lower p_K , because of the \bar{u} quark. This leads to lower reconstruction

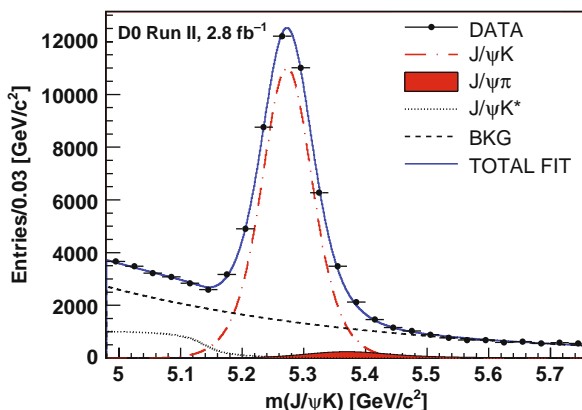


Fig. 2.11 $M(J/\psi K)$ distribution for $B^\pm \rightarrow J/\psi K^\pm$ events by DØ [43] with 2.8 fb^{-1} data [Copyright (2008) by The American Physical Society], where there is a rather small component for $B^\pm \rightarrow J/\psi \pi^\pm$

efficiency for K^- . This “kaon asymmetry” from detector effect is directly measured in the same data. One enjoys a larger control sample in hadronic production, as compared with B factories. DØ compares $D^* \rightarrow D^0\pi^+$ ($D^0 \rightarrow \mu^+\nu K^-$) with the charge conjugate process, and the kaon asymmetry is measured for different kaon momentum and convoluted with $B \rightarrow J/\psi K$ decay. It was found that the detector-matter-induced asymmetry for $B \rightarrow J/\psi K$ is of order -0.0145 . Correcting the measured one at order -0.007 gives (2.13). One other crucial aspect of the DØ analysis is the cancellation of reconstruction efficiency differences between positive and negative particles. For these purposes, DØ periodically reverses the magnet polarity for equivalent periods.

Overall, in comparison to the challenge at the B factories, of special note is the rather small (roughly a quarter %!) systematic error of the DØ measurement. Thus, even scaling up to $6\text{--}8\text{ fb}^{-1}$, one is still statistics limited, and 2σ sensitivity for % level asymmetries could be attainable. CDF should have similar sensitivity (except the issue of magnet polarity flip), and the situation can drastically improve with LHCb data once it becomes available.

The Tevatron measurement was in fact inspired by a theoretical fourth-generation study [44], which followed the lines that have already been presented in the previous sections. The fourth-generation parameters are taken from the $\Delta\mathcal{A}_{K\pi}$ study [38]. By making analogy with what is observed in $B \rightarrow D\pi$ modes, and especially between different helicity components in $B \rightarrow J/\psi K^*$ decay, the dominant color-suppressed amplitude C for $B^+ \rightarrow J/\psi K^+$ would likely possess a strong phase of order 30° . The P_{EW} amplitude is assumed to factorize and hence does not pick up a strong phase. Heuristically, this is because the Z^* produces a small, color singlet $c\bar{c}$ that penetrates and leaves the hadronic “muck” without much interaction, subsequently projecting into a J/ψ meson. With a strong phase in C and a weak phase in P_{EW} , one then finds $\mathcal{A}_{B^+ \rightarrow J/\psi K^+} \simeq \pm 1\%$.

We plot $\mathcal{A}_{B^+ \rightarrow J/\psi K^+}$ vs. strong phase difference δ in Fig. 2.12, with weak phase ϕ_{sb} fixed to the range corresponding to (3.25), and the notation is as in Fig. 3.11 (we refrain until Chap. 3, when the motivation is further strengthened, for a more

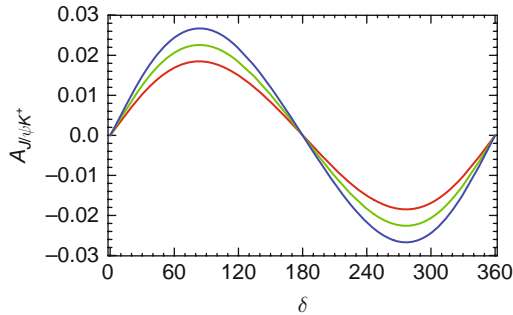


Fig. 2.12 $\mathcal{A}_{B^+ \rightarrow J/\psi K^+}$ vs. strong phase difference δ between C and P_{EW} in the fourth-generation model [44]. A nominal $\delta \sim 30^\circ$ is expected from strong phases in $J/\psi K^*$ mode. Negative asymmetries are ruled out by the DØ result given in (2.13)

detailed discussion of the fourth-generation scenario). The negative sign is ruled out by the $D\bar{0}$ result (2.13). But, of course, DCPV is directly proportional to the strong phase difference, which is not predicted, so $\mathcal{A}_{B^+ \rightarrow J/\psi K^+} \sim +1\%$ is consistent with the $D\bar{0}$ result and can be probed further.

We remark that other exotic models like Z' with FCNC couplings could also generate various effects we have discussed. For example, with $\delta \sim 30^\circ$, $\mathcal{A}_{B^+ \rightarrow J/\psi K^+}$ could be considerably larger than a percent. With the $D\bar{0}$ result of (2.13), however, only % level asymmetries are allowed, ruling out a large (and in any case quite arbitrary) region of parameter space for possible Z' effects.

2.4 An Appraisal

In Chap. 1, we teased with the earlier possible hint that $\sin 2\phi_1/\beta$ could be much smaller than expected. However, the SM expectation was subsequently rather quickly affirmed. It is remarkable that the studies so far confirm the three-generation CKM unitarity triangle for $b \rightarrow d$ transitions (1.6).

With unprecedented luminosities (see Fig. 1.2), there were high hopes for the B factories to uncover some Beyond the Standard Model physics, in particular in CPV in $b \rightarrow s\bar{q}q$ decays. There were indeed ups and downs, excitements and disappointments. The $B^0 \rightarrow \phi K_S$ TCPV splash, gradually faded with more data and more modes, though it has never fully gone away. The $\Delta\mathcal{S}$ problem is indeed a nagging one: experimentally it is not even established, while theoretically it is hampered by hadronic uncertainties, which further vary from mode to mode, making the combination of modes dubious.

For the $\mathcal{A}_{B^+ \rightarrow K^+\pi^0}$ vs. $\mathcal{A}_{B^0 \rightarrow K^+\pi^-}$ DCPV difference, experimentally it is genuine. But the presence of a possible C amplitude, though rather demanding on factorization calculations, has seemingly made the majority so far carry the doubt that this $\Delta\mathcal{A}_{K\pi}$ problem is yet another hadronic effect. Perhaps people suffer from the “cry wolf” syndrome due to the long-suffering $\Delta\mathcal{S}$ saga. But *remember, the wolf did come eventually.*

Personally, we believe there is a rather good possibility that the $\Delta\mathcal{A}_{K\pi}$ problem is a genuine harbinger for New Physics in CPV $b \rightarrow s\bar{q}q$ transitions. We will continue to discuss this in the Chap. 3, on the implications for $\sin 2\Phi_{B_s}$ measurement. However, the problem of hadronic uncertainties for hadronic $b \rightarrow s\bar{q}q$ transitions cannot be taken lightly. Even for DCPV in $B^+ \rightarrow J/\psi K^+$, although it has often been used as a calibration mode, if it emerges experimentally at the 1% level, as discussed in the previous section, people would still question what is the genuine value within SM, whether it cannot reach subpercent level, i.e., again attributing it to “hadronic uncertainty.”

To top it off, and in comparison, we mention briefly the surprisingly large transverse polarization in several charmless $B \rightarrow VV$ final states that emerged around 2004. When this emerged experimentally [18], e.g., f_L or the longitudinal polarization fraction, in $B \rightarrow \phi K^*$ was only 50%, it was suggested [45] that this could be

due to New Physics. However, this is now widely believed to be due to hadronic physics, maybe due to [46] our unfamiliarity with the $B \rightarrow K^*$ form factor A_0 . What convinced us that this is likely not New Physics is from the polarization and triple-product correlation measurements [47].

References

1. Sakharov, A.D.: Pisma Zh. Eksp. Teor. Fiz. **5**, 32 (1967) [JETP Lett. **5**, 24 (1967)] 11
2. Bigi, I.I.Y., Sanda, A.I.: Nucl. Phys. B **193**, 85 (1981) 11, 23
3. Albrecht, H., et al. [ARGUS Collaboration]: Phys. Lett. B **192**, 245 (1987) 11
4. Oddone, P.: At UCLA workshop on Linear Collider $B\bar{B}$ Factory Conceptual Design, Los Angeles, California, January 1987 11
5. Go, A., Bay, A., et al. [Belle Collaboration]: Phys. Rev. Lett. **99**, 131802 (2007) [arXiv:quant-ph/0702267] 12
6. Grossman, Y., Worah, M.P.: Phys. Lett. B **395**, 241 (1997) 15
7. London, D., Soni, A.: Phys. Lett. B **407**, 61 (1997) 16
8. Chen, K.F., Hara, K., et al. [Belle Collaboration]: Phys. Lett. B **546**, 196 (2002) 16, 18
9. Abe, A., et al. [Belle Collaboration]: Phys. Rev. Lett. **91**, 261602 (2003) 16
10. Chen, K.F., et al. [Belle Collaboration]: Phys. Rev. D **72**, 012004 (2005) 16
11. See the webpage of the Heavy Flavor Averaging Group (HFAG). <http://www.slac.stanford.edu/xorg/hfag>. We usually, but not always, take the Lepton-Photon 2007 (LP2007) numbers as reference 16, 17, 21, 22
12. See e.g. Beneke, M.: Phys. Lett. B **620**, 143 (2005) 17
13. Cheng, H.Y., Chua, C.K., Soni, A.: Phys. Rev. D **72**, 014006 (2005) 17
14. Li, H.n., Mishima, S., Sanda, A.I.: Phys. Rev. D **72**, 114005 (2005) 17
15. Williamson, A.R., Zupan, J.: Phys. Rev. D **74**, 014003 (2006) 17
16. Sinha, R., Misra, B., Hou, W.S.: Phys. Rev. Lett. **97**, 131802 (2006) 18
17. Lin, S.W., Unno, Y., Hou, W.S., Chang, P., et al. [Belle Collaboration]: Nature **452**, 332 (2008) 18, 20, 21, 23
18. Yao, W.M., et al. [Particle Data Group]: J. Phys. G **33**, 1 (2006) 18, 21, 27, 29
19. Amsler, C., et al.: Phys. Lett. B **667**, 1 (2008); and <http://pdg.lbl.gov/> 18, 21
20. Aubert, B., et al. [BaBar Collaboration]: Phys. Rev. Lett. **93**, 131801 (2004) 19
21. Chao, Y., Chang, P., et al. [Belle Collaboration]: Phys. Rev. Lett. **93**, 191802 (2004) 19, 20, 21, 22
22. Beneke, M., Buchalla, G., Neubert, M., Sachrajda, C.T.: Nucl. Phys. B **606**, 245 (2001) 19
23. Keum, Y.Y., Li, H.n., Sanda, A.I.: Phys. Rev. D **63**, 054008 (2001) 20
24. Keum, Y.Y., Sanda, A.I.: Phys. Rev. D **67**, 054009 (2003) 20
25. Morello, M. (for the CDF Collaboration): Talk at B-Physics at Hadron Machines (Beauty 2006), Oxford, England, September 2006, appeared as Nucl. Phys. Proc. Suppl. **170**, 39 (2007); and CDF Public Note 8579 20
26. Aubert, B., et al. [BaBar Collaboration]: Phys. Rev. Lett. **99**, 021603 (2007) 20, 22
27. Aubert, B., et al. [BaBar Collaboration]: Phys. Rev. Lett. **94**, 181802 (2005) 21
28. Aubert, B., et al. [BaBar Collaboration]: Phys. Rev. D **76**, 091102 (2007) 22
29. Peskin, M.E.: Nature **452**, 293 (2008), companion paper to Ref. [17] 23, 25
30. See, e.g., Gronau, M.: Talk at Flavour Physics and CP Violation Conference (FPCP2007), Bled, Slovenia, May 2007 24, 25
31. Baek, S., London, D.: Phys. Lett. B **653**, 249 (2007) 24, 25
32. See, for example, Neubert, M., Stech, B.: In: Buras, A.J., Lindner, M. (eds.) Heavy Flavours II. World Scientific, Singapore (1998) 24
33. Gronau, M., Rosner, J.L.: Phys. Rev. D **59**, 113002 (1999) 24
34. Li, H.n., Mishima, S., Sanda, A.I.: Phys. Rev. D **72**, 114005 (2005) 25
35. Beneke, M.: Talk at Flavor Physics and CP Violation Conference (FPCP2008), Taipei, Taiwan, May 2008 25

- 36. Bauer, C.W., Rothstein, I.Z., Stewart, I.W.: Phys. Rev. D **74**, 034010 (2006) 25
- 37. Rothstein, I.: Talk at Flavor Physics and CP Violation Conference (FPCP2008), Taipei, Taiwan, May 2008 25
- 38. Hou, W.S., Nagashima, M., Soddu, A.: Phys. Rev. Lett. **95**, 141601 (2005) 25, 26, 28
- 39. Neubert, M., Rosner, J.L.: Phys. Rev. Lett. **81**, 5076 (1998) 25
- 40. Hou, W.S.: Nucl. Phys. B **308**, 561 (1988) 25
- 41. Li, H.n., Mishima, S.: JHEP **0703**, 009 (2007) 26
- 42. Wu, G.H., Soni, A.: Phys. Rev. D **62**, 056005 (2000) 27
- 43. Abazov, V.M., et al. [D; Collaboration]: Phys. Rev. Lett. **100**, 211802 (2008) 27
- 44. Hou, W.S., Nagashima, M., Soddu, A.: hep-ph/0605080 28
- 45. Kagan, A.L.: Phys. Lett. B **601**, 151 (2004) 29
- 46. Li, H.n.: Phys. Lett. B **622**, 63 (2005) 30
- 47. Chen, K.F., et al. [Belle Collaboration]: Phys. Rev. Lett. **94**, 221804 (2005) 30

Chapter 3

B_s Mixing and $\sin 2\Phi_{B_s}$

It is clear from Chap. 2 that the study of CP violation phenomena in $b \rightarrow s$ transitions is the current frontier for New Physics search in flavor physics. We have two intriguing hints from the B factories. One is the ΔS problem, a difference in time-dependent CPV measurement between charmless $b \rightarrow s\bar{q}q$ modes and the established $\sin 2\phi_1/\beta$ in $b \rightarrow c\bar{c}s$ modes. But this effect is not experimentally established, and we need to wait for the Super B factory upgrade to clarify the situation. The other hint is the $\Delta A_{K\pi}$ problem, the difference in direct CPV asymmetries in $B^+ \rightarrow K^+\pi^0$ vs. $B^0 \rightarrow K^+\pi^-$ decays. Here, the effect is an experimental fact, and indeed it could arise from New Physics CPV through the electroweak penguin amplitude. However, despite the immense challenge it poses to calculational approaches, it is not impossible that the color-suppressed amplitude is enhanced in Nature, in a rather special and major way, to generate $\Delta A_{K\pi}$ in (2.10).

In this chapter, we turn to a new focus on New Physics search, in the B_s^0 - \bar{B}_s^0 mixing amplitude, which are $b \leftrightarrow s$ transitions. The oscillation between B_s^0 and \bar{B}_s^0 mesons is too rapid for the B factories to resolve. This brings us to the hadron colliders, which enjoy a large boost for the produced B mesons. But one then faces the much higher background levels typical in a hadronic environment. B_s^0 mixing was finally measured in 2006 by the Collider Detector at Fermilab (CDF) experiment [1] at the Tevatron, and the measured value is not inconsistent with Standard Model expectations. However, the real interest is in the CPV phase $\sin 2\Phi_{B_s}$ of the B_s^0 - \bar{B}_s^0 mixing amplitude, analogous to $\sin 2\phi_1/\beta$ for B_d^0 - \bar{B}_d^0 mixing case (which could have been called $\sin 2\Phi_{B_d}$). After all, the ΔS and $\Delta A_{K\pi}$ problems are all CPV measures. The SM expectation for $\sin 2\Phi_{B_s}$ is almost zero, hence this offers a great window for effects. As we will show, any evidence for finite $\sin 2\Phi_{B_s}$, before the arrival of LHC data, would amount to an indication for New Physics. From the current trends at the Tevatron, this could well be the case, and we illustrate the growing tension between Tevatron and LHC in the period 2008–2010. If no convincing indication emerges from the Tevatron, then of course this would be the dominion of the LHC, in particular the LHCb experiment.

Unlike the ΔS problem, the measurement of $\sin 2\Phi_{B_s}$ should already be settled before the arrival of the Super B factory. Unlike the $\Delta A_{K\pi}$ problem, which is marred by potential hadronic effects, once $\sin 2\Phi_{B_s}$ is measured, and it is demonstrated that it differs from SM expectation, there will be no doubt of its BSM origins.

3.1 B_s Mixing Measurement

The measurement of B_s mixing has been pursued since the Large Electron-Positron Collider (LEP) (and SLAC Linear Collider (SLC)) era, as well as at the Tevatron Run I. By 2005, the world limit had been hovering around $\Delta m_{B_s} > 14.5 \text{ ps}^{-1}$ [2, 3] for several years, in wait for Tevatron Run II. In fact, LEP data showed a 2σ indication for Δm_{B_s} around 17.2 ps^{-1} .

It had been advertised that Δm_{B_s} measurement would be easy for CDF in Tevatron Run II, that a SM value could be measured with several hundred pb^{-1} . But, things did not work out as planned, and, as can be seen from Fig. 3.1, the Tevatron Run II had a rather slow start. Only by 2004 or so did the accelerator performance finally start to pick up. By summer 2005 or so, each experiment had collected 1 fb^{-1} data, and interesting results started to come out. The CDF and DØ experiments have recently reached $\sim 4 \text{ fb}^{-1}$ integrated luminosity per experiment and expect to accumulate an overall of 6–8 fb^{-1} per experiment throughout the Tevatron Run II lifetime, where it is crucial to run beyond 2009. The physics output cannot be ignored.

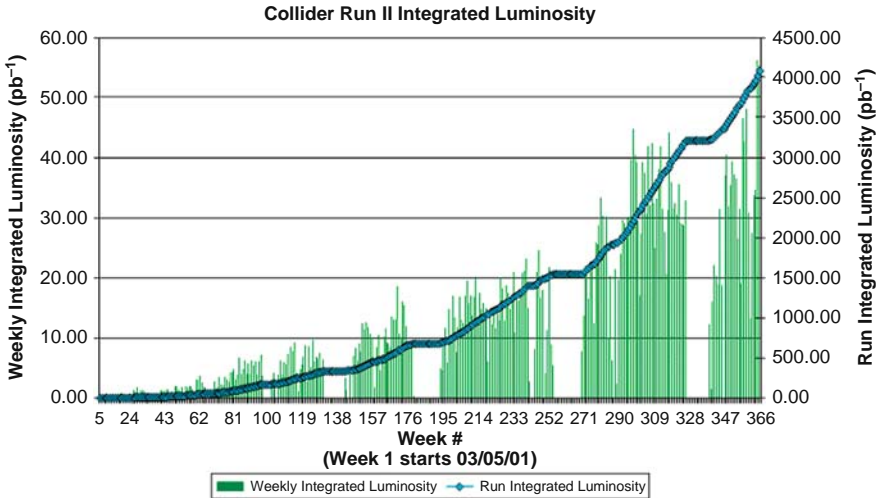


Fig. 3.1 Integrated luminosity for Tevatron Run II, up to early May 2008. (Source: <http://www.fnal.gov/pub/now/tevlum.html>, by the Fermilab Accelerator Division, used with permission.)

3.1.1 Standard Model Expectations

As shown in Fig. 3.2(a), analogous to the case for B_d oscillations, the amplitude for B_s mixing in SM behaves as $M_{12}^s \propto (V_{tb}V_{ts}^*)^2 m_t^2$ to first approximation, i.e.,

$$M_{12}^s \simeq -\frac{G_F^2 m_W^2 S_0(m_t^2/m_W^2) \eta_{B_s}}{12\pi^2} m_{B_s} f_{B_s}^2 B_{B_s} (V_{ts}^* V_{tb})^2 \quad (\text{SM}). \quad (3.1)$$

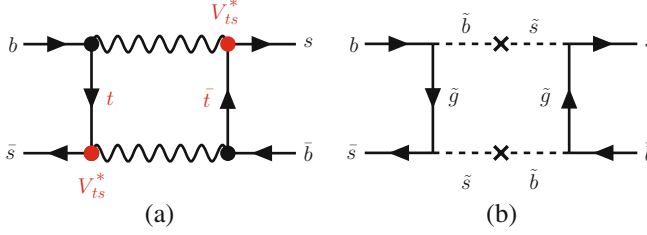


Fig. 3.2 For $B_s^0 - \bar{B}_s^0$ mixing, (a) one of the box diagrams in SM, where the CPV phase, is brought in through $(V_{ts}^* V_{tb})^2$ from top quark dominance; (b) a possible SUSY contribution through $\tilde{s} - \tilde{b}$ squark mixing. The $c\bar{c}$ contribution in the SM box diagram, though negligible for M_{12}^s , generates Γ_{12}^s , since $b \rightarrow c\bar{c}s$ is a major component of b decay

This is of the same form as (1.2), with simple replacement of $d \rightarrow s$. With top quark dominance, to very good approximation, one therefore has

$$\frac{\Delta m_{B_s}}{\Delta m_{B_d}} = \frac{f_{B_s}^2 B_{B_s} m_{B_s}}{f_{B_d}^2 B_{B_d} m_{B_d}} \frac{|V_{ts}|^2}{|V_{td}|^2} \equiv \xi^2 \frac{m_{B_s}}{m_{B_d}} \frac{|V_{ts}|^2}{|V_{td}|^2} \quad (\text{SM}), \quad (3.2)$$

where $\Delta m \equiv 2|M_{12}|$ is the oscillation frequency. With $\xi > 1$, one immediately sees that Δm_{B_s} is much larger than $\Delta m_{B_d} \simeq 0.5 \text{ ps}^{-1}$ in the SM. We note that $f_{B_s}^2 B_{B_s}$ in (3.1) needs to be computed in lattice QCD, which at present carry large errors. But with (3.2), like in experimental errors, many lattice errors cancel in the ratio $\xi^2 = f_{B_s}^2 B_{B_s} m_{B_s} / f_{B_d}^2 B_{B_d} m_{B_d}$. This is why in Fig. 1.6 the constraint from “ Δm_s & Δm_d ” is considerably better than from the experimentally well measured $\Delta m_d \equiv \Delta m_{B_d}$ alone. Thus, from the SM perspective, the measurement of Δm_{B_s} , together with Δm_{B_d} , provides a constraint on $|V_{ts}|^2 / |V_{td}|^2$, modulo the lattice errors on ξ , or¹

$$\frac{1}{\lambda} \frac{|V_{td}|}{|V_{ts}|} = \frac{\xi}{\lambda} \sqrt{\frac{\Delta m_{B_d} m_{B_s}}{\Delta m_{B_s} m_{B_d}}} \simeq \sqrt{(1 - \rho)^2 + \eta^2} \quad (\text{SM}), \quad (3.3)$$

where $\lambda \equiv V_{us}$.

Implications of Three-Generation Unitarity

Assuming three-generation CKM unitarity, gathering all information, including that on ξ , the CKM unitarity fitter groups gave the predictions of $\Delta m_{B_s} = 20.9_{-4.2}^{+4.5} \text{ ps}^{-1}$ (CKMfitter [4, 5]) and $21.2 \pm 3.2 \text{ ps}^{-1}$ (UTfit [6]), respectively, before the CDF announcement [7] of evidence for Δm_{B_s} at the FPCP 2006 conference in Vancouver, Canada. We show in Fig. 3.3 the results of CKM fitter group using all data other than

¹ For our purpose of New Physics search, we will not distinguish between ρ, η and $\bar{\rho}, \bar{\eta}$. See [2, 3] and Appendix A.

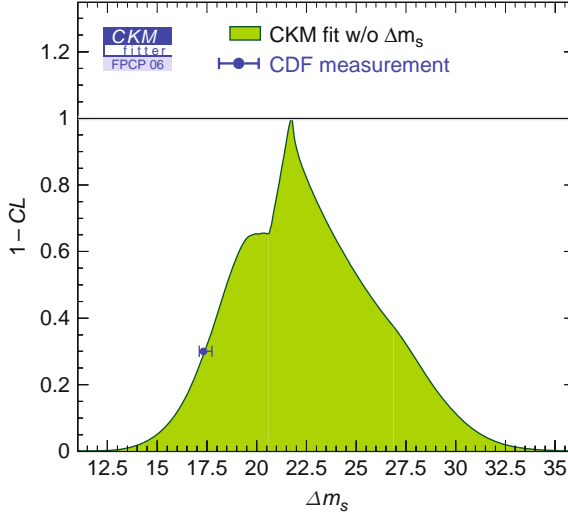


Fig. 3.3 SM expectation for Δm_{B_s} at FPCP 2006 conference, combining all information other than B_s mixing itself, just before the CDF announcement [7] of evidence for Δm_{B_s} , which is also shown in the figure (from the CKMfitter group [4], used with permission)

Δm_{B_s} , plotted together with the CDF result. This illustrates the power and impact of the Δm_{B_s} measurement. It also indicates how the CDF result is slightly on the low side. But, of course, the errors from the unitarity fits were very forgiving to make this point somewhat mute. We will discuss the experimental measurement in the following section.

CPV in B_s mixing is controlled by the phase of V_{ts} in SM. Since $|V_{us}^* V_{ub}|$ is rather small, unlike the analogous case for $b \rightarrow d$ transitions (1.4), the triangle relation

$$V_{us}^* V_{ub} + V_{cs}^* V_{cb} + V_{ts}^* V_{tb} = 0 \quad (3.4)$$

$$\Rightarrow V_{ts}^* V_{tb} \simeq -V_{cb} \quad (3.5)$$

collapses to approximately a line and $V_{ts}^* V_{tb}$ is practically real (in the standard phase convention [2, 3] that V_{cb} is real; see Appendix A.1). In practice, defining

$$\Phi_{B_s} \equiv \arg M_{12} \quad (3.6)$$

$$\simeq \arg V_{ts}^* V_{tb} \simeq -\lambda^2 \eta \sim -0.02 \text{ rad} \quad (\text{SM}), \quad (3.7)$$

which is tiny² compared to the well-measured $\Phi_{B_d}|^{\text{SM}} \simeq \arg V_{td}^* V_{tb} = \beta/\phi_1 \sim 0.37 \text{ rad}$.

² See (A.6) of Appendix A.1 for a discussion on phase of V_{ts} in the Wolfenstein parameterization of V_{CKM} to order λ^5 .

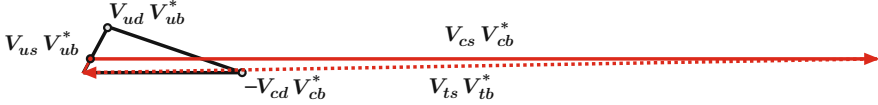


Fig. 3.4 Geometric representations of the three-generation unitarity relations (1.4) and (3.4), the latter being the long, *squashed triangle*. This picture is identical to Fig. A.2 in Appendix A.

At this point, it is instructive to give a geometric picture of the discussion above. The “ $b \rightarrow d$ triangle” corresponding to the db element of $V^\dagger V = I$, i.e., $V_{ud}^* V_{ub} + V_{cd}^* V_{cb} + V_{td}^* V_{tb} = 0$ or (1.4), is the normal looking triangle in Fig. 3.4. This is the same triangle that is now suitably well measured, as shown in Fig. 1.6. For the “ $b \rightarrow s$ triangle” corresponding to the sb element of $V^\dagger V = I$, i.e., $V_{us}^* V_{ub} + V_{cs}^* V_{cb} + V_{ts}^* V_{tb} = 0$ or (3.4), one has a rather squashed triangle. This can be easily seen: $|V_{us}^* V_{ub}| \sim \lambda |V_{ud}^* V_{ub}|$, so this side is 1/4 the length of $b \rightarrow d$ case; on the other hand, $|V_{cs}^* V_{cb}| \sim \lambda^{-1} |V_{cd}^* V_{cb}|$, so this side is about four times as long. This results in the squashedness, or elongation, of the $b \rightarrow s$ triangle. One thus sees that the angle on the far right, Φ_{B_s} , becomes rather diminished with respect to Φ_{B_d} of the $b \rightarrow d$ case. Note also that the orientation of the $b \rightarrow s$ triangle is opposite to the $b \rightarrow d$ triangle, hence the sign difference between the phase angles Φ_{B_s} vs. Φ_{B_d} .

Thus, not only $B_s^0 - \bar{B}_s^0$ oscillation is much faster than B_d case because of $\sim \lambda^{-2}$ enhancement (plus hadronic factors), the associated CPV phase is so small in SM, it is very challenging to measure. If Φ_{B_s} is at the SM expectation of a few percent level, then only the LHCb experiment, which is designed for B physics studies at the LHC, would have enough sensitivity to probe it. Thus, it is well known that $\sin 2\Phi_{B_s}$ is an excellent window on BSM [8]. Any observation that deviates from

$$\sin 2\Phi_{B_s}|^{\text{SM}} \cong -0.04 \quad (3.8)$$

would be an indication for New Physics. In SUSY, this could arise from squark-gluino loops with \tilde{s} - \tilde{b} mixing, which is illustrated in Fig. 3.2(b).

Mass Vs. Width Mixing

Unlike the $B_d^0 - \bar{B}_d^0$ situation, the $B_s^0 - \bar{B}_s^0$ system is in fact richer than just oscillations. Recall the $K^0 - \bar{K}^0$ system. Besides the mass difference Δm_K , or oscillations, it was well known beforehand that the two states K_S^0 and K_L^0 differ very much in lifetime, since by CP symmetry the former decays via 2π while the latter by 3π (CP violation was discovered through the observation of $K_L^0 \rightarrow \pi^+ \pi^-$ [9]). For the present case of the box diagram of Fig. 3.2(a), if one replaces the t quark by the c quark and cuts on both the c quark lines, the amplitude is that of the $b \rightarrow c\bar{c}s$ decay amplitude interfering with the antiquark process, which is just the decay rate for this subprocess. As the $b \rightarrow c\bar{c}s$ subprocess is a major component for b decay, i.e., there is no additional CKM suppression, this generates the absorptive Γ_{12}^s (a width), namely

$$H_{12}^s = M_{12}^s - i \frac{\Gamma_{12}^s}{2}, \quad (3.9)$$

for the full Hamiltonian that mediates $B_s^0 - \bar{B}_s^0$ transitions. Γ_{12}^s leads to a width difference³ $\Delta\Gamma_{B_s}$ or mixing in width. Both M_{12}^s and Γ_{12}^s are complex in the presence of CPV. We remark that this bears only formal resemblance to the $K^0 - \bar{K}^0$ system. For $B_s^0 - \bar{B}_s^0$ system, not only $|\Gamma_{12}^s/M_{12}^s|$ is quite different from the kaon case, we have far richer final states for B_s to decay to, allowing for interference effects in many channels.

We do not wish to get too deep into formalism. We just note that it is difficult for New Physics to affect tree level $b \rightarrow c\bar{c}s$ transitions, where the CKM coefficient $V_{cs}^* V_{cb}$ have been chosen to be real by convention. Also, since one already knows by experiment that $\Delta m_{B_s} \gg \Gamma_{B_s}$, we know that $|M_{12}^s| \gg |\Gamma_{12}^s|$. With these understandings, we therefore just quote the formula [8],

$$\Delta\Gamma_{B_s} = \Delta\Gamma_{B_s}^{\text{SM}} \cos 2\Phi_{B_s}. \quad (3.10)$$

A finite $\sin 2\Phi_{B_s}$ deviating from zero (or (3.8)) would lead to a dilution of the width difference in flavor-specific final states. In (3.10), $\Delta\Gamma_{B_s}^{\text{SM}}$ is calculated within SM, where the current value is [10]

$$\Delta\Gamma_{B_s}^{\text{SM}} = 0.096 \pm 0.039 \text{ ps}^{-1} \quad (3.11)$$

and can be measured via decay to a CP eigenstate. That is, one could measure $\Delta\Gamma_{B_s}^{\text{CP}}$ via $B_s^0 \rightarrow D_s^+ D_s^-$, which in principle can also be measured using $\Upsilon(5S) \rightarrow B_s^0 \bar{B}_s^0$ at B factories. From a general study of say $B_s \rightarrow J/\psi \phi$ to explore width difference effects, one can infer $\cos 2\Phi_{B_s}$, offering a different route to New Physics CPV phase, *without* necessarily resolving the rapid $B_s^0 - \bar{B}_s^0$ oscillations.

3.1.2 $D\bar{D}$ Measurement of Δm_{B_s}

Based on $\sim 1 \text{ fb}^{-1}$ data, the $D\bar{D}$ experiment made a study [11] of $B_s^0 - \bar{B}_s^0$ oscillations using semileptonic $B_s^0 \rightarrow \mu^+ D_s^- X$ decays. The D_s^- is reconstructed in the $\phi\pi^-$ final state, with $\phi \rightarrow K^+ K^-$. Assuming that both the width difference and CPV are small, one measures the so-called no-oscillation and oscillation probability, i.e., the probability density P^+ or P^- for a \bar{B}_s^0 meson produced at $t = 0$ to decay as a \bar{B}_s^0 or a B_s^0 at time t ,

$$P_{B_s}^{\pm}(t) = \frac{\Gamma_{B_s}}{2} e^{-\Gamma_{B_s} t} (1 \pm \cos \Delta m_{B_s} t), \quad (3.12)$$

³ The usual definition is $\Delta m_{B_s} = 2|M_{12}^s| = M_H - M_L$, and $\Delta\Gamma_{B_s} = 2|\Gamma_{12}^s| = \Gamma_L - \Gamma_H$, where H (L) stands for the heavier (lighter) mass eigenstate from mixing.

where Γ_{B_s} is the mean width. Note that, just like in (2.1), the notation of $P_{B_s}^{\pm}(t)$ used by experiments are shorthand for differential probability densities.

Compared to studying $B_d^0-\bar{B}_d^0$ oscillations at the B factories, there are several additional difficulties or loss of information. For this semileptonic B_s^0 decay, by requiring just a μ^+ to form a common B_s^0 vertex with the reconstructed D_s^- , the missing neutrino and other particles lead to a smearing of the proper decay time, because of insufficient knowledge of the B_s^0 momentum (hence boost). One does not have the advantage of knowing the “beam profile” (and boost) at the B factories. The effect of this smearing is studied by Monte Carlo (MC). Also, unlike the coherent $B_d^0-\bar{B}_d^0$ production from $Y(4S)$ decay, the $B_q-\bar{B}_{q'}$ pairs are produced incoherently at a hadron collider. To determine the B_s^0 or \bar{B}_s^0 flavor at $t = 0$, DØ uses Opposite Side Tagging (OST). The purity was studied with $B^+ \rightarrow \mu^+ \bar{D}^0 X$ and $B_d^0 \rightarrow \mu^+ D^{*-} X$ decays, where the former has no oscillations, while the latter has some oscillations from B_d^0 . The determined effectiveness of flavor tagging, $\epsilon \mathcal{D}^2$, is about 2.5%, where ϵ is the tagging efficiency (fraction of signal candidates with a flavor tag), and $\mathcal{D} = 1 - 2w$ is the dilution, with w the probability of wrong tag (hence $\mathcal{D} = 0$ when w is 50%).

The traditional amplitude scan method [12] is to include an additional oscillation amplitude coefficient \mathcal{A} for $\cos \Delta m_{B_s} t$ in (3.12). One fixes the oscillation frequency Δm_{B_s} and fit for \mathcal{A} , which should give $\mathcal{A} \sim 1$ when this Δm_{B_s} value is the true value but yield $\mathcal{A} \sim 0$ when the chosen Δm_{B_s} value is far from the true oscillation frequency. From this method, DØ finds that $\Delta m_{B_s} > 14.8 \text{ ps}^{-1}$ at 95% C.L., which is better than previous studies, and the preferred value is $\sim 19 \text{ ps}^{-1}$. To quantify further, DØ used an unbinned likelihood (\mathcal{L}) fit. We show the $-\Delta \log \mathcal{L}$ plot, i.e., change in $-\Delta \log \mathcal{L}$ vs. Δm_{B_s} , in Fig. 3.5. The maximum likelihood is indeed at 19 ps^{-1} , and the confidence interval around this value is well behaved. Assuming the uncertainties are Gaussian, DØ obtained the 90% C.L. interval of $17 \text{ ps}^{-1} < \Delta m_{B_s} < 21 \text{ ps}^{-1}$, the first two-sided experimental bound for $B_s^0-\bar{B}_s^0$ oscillations.

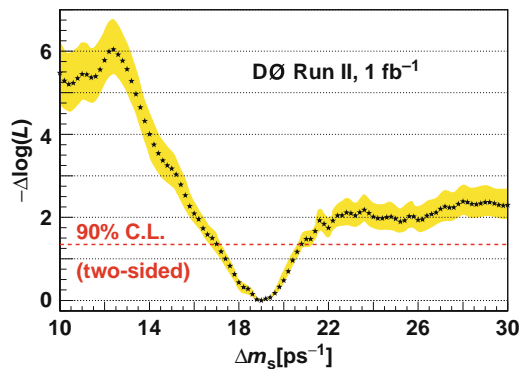


Fig. 3.5 Change in $-\Delta \log \mathcal{L}$ vs. Δm_{B_s} in the DØ measurement [11] of B_s mixing. [Copyright (2006) by The American Physical Society]. The shaded band reflects systematic uncertainties. The plateauing out for large Δm_{B_s} means loss of sensitivity beyond $\Delta m_{B_s} > 22 \text{ ps}^{-1}$

3.1.3 CDF Observation of $B_s^0-\bar{B}_s^0$ Oscillations

Despite the earlier announcement made by DØ in Winter 2006, the CDF experiment quickly surpassed the DØ result, first by showing evidence [7] at FPCP 2006, then by actual observation, all within a matter of months. By Summer 2006, based on 1 fb^{-1} data, B_s mixing became a precision measurement [1],

$$\Delta m_{B_s} = 17.77 \pm 0.10 \pm 0.07\text{ ps}^{-1}, \quad (3.13)$$

which is a rather dramatic change.

But it should be remembered that CDF had advertised that measurement of Δm_{B_s} in the SM-predicted range should be achievable with just a few hundred pb^{-1} of Run II data. This was based on several improvements special to CDF: (1) increased signal sample: Silicon Vertex Trigger (SVT) for displaced vertices; (2) better flavor tagging: Opposite Side Tag (OST) as well as Same Side⁴ Kaon Tag (SSKT); (3) improved proper time resolution: the “Layer 00” (L00) silicon placed right on the beampipe, at $\sim 1.5\text{ cm}$ from the beam. These innovations brought high hopes, but it is understandable that it took more time to get everything to work, as well as validated. Unfortunately, the performance turned out to be not as good as expected.⁵

Having used silicon vertex detectors already since Tevatron Run I, CDF implemented a two-track SVT trigger, capable of finding tracks in the silicon detector in $20\text{ }\mu\text{s}$ to determine displaced vertices. This was quite successful. However, the signal yield turned out smaller than originally expected (less than 1/5 for fully reconstructed events). Flavor tagging also turned out much harder than expected, especially for OST, where $\epsilon\mathcal{D}^2 \simeq 1.8\%$ was only $\sim 1/4$ of what was expected. Fortunately, the situation was saved by the SSKT performance, which was at expected levels. It was even slightly better than expected for semileptonic modes. But SSKT was difficult to understand and took time to incorporate into the analysis. Of critical importance is the combined PID of a special TOF, together with dE/dx . Though the discrimination power is not spectacular, but since the K^+/K^- from b quark fragmentation used to tag the B_s^0/\bar{B}_s^0 is relatively slow, both TOF and dE/dx gave the critical 1σ or slightly better discrimination. In the end, for hadronic and semileptonic SSKT, $\epsilon\mathcal{D}^2 \simeq 3.7$ and 4.8% , respectively, turned out to be more than a factor of 2 better than OST. For the L00, the purpose of which is to improve timing resolution, the single-sided layer of silicon placed at $\sim 1.5\text{ cm}$ from the beam, operating in a hadronic environment, is bound to be difficult. Noise problems reduced

⁴ Same side tagging [13–15] is based on flavor correlations from b quark fragmentation. Most naively, a \bar{B}_u^0 (B_u^-) would be accompanied by a π^- (π^+), while a \bar{B}_s^0 is accompanied by a K^- . For a \bar{B}_s^0 meson, the initial \bar{b} picks up an s quark from a nearby $s\bar{s}$ pair, while the \bar{s} ends up in a K^+ meson in the “vicinity”.

⁵ We take the time to discuss these, mainly to keep ourselves sober as we anticipate the new LHC era. With brand new—and colossal—accelerator and detectors in an unprecedentedly harsh environment, despite the innovations and diligence, one should be prepared for setbacks in the early days (years actually), and hopefully these may be overcome eventually with time.

the efficiency and resolution. Using a large sample of prompt D^+ candidates, the decay-time resolution for fully reconstructed hadronic events was found to be 87 fs, rather than the expected 45 fs.

Despite all these setbacks and disappointments, the investments of CDF finally paid off, even though 1 fb^{-1} rather than a few hundred pb^{-1} data were needed. The measurement of Δm_{B_s} in (3.13) is still a great achievement. Let us now present some highlight results of this analysis. We will not distinguish between the earlier work at 3σ evidence [7] versus the improvements that lead to observation [1] at over 5σ .

The secret of success is the fully reconstructed hadronic modes, where the two (displaced) track trigger was the major advantage that CDF had over DØ. In Fig. 3.6, we plot the invariant mass distribution for $\bar{B}_s^0 \rightarrow D_s^+ \pi^-$, with $D_s^+ \rightarrow \phi \pi^+$. These modes provide the best decay time resolution, since, unlike semileptonic decays where at least a neutrino is missing, full reconstruction means that the \bar{B}_s^0 momentum is directly measured. There are also partially reconstructed hadronic modes. We give the amplitude scan plot for the combined result in Fig. 3.7. The peak at $\Delta m_{B_s} = 17.77 \text{ ps}^{-1}$ gives an observed amplitude $\mathcal{A} = 1.21 \pm 0.20$ (stat) which is consistent with 1 and inconsistent with $\mathcal{A} = 0$ at $\mathcal{A}/\sigma_{\mathcal{A}} \simeq 6$, indicating that data are consistent with oscillations at this frequency. Using an unbinned maximum likelihood fit, fitting for Δm_{B_s} by fixing $\mathcal{A} = 1$, one finds the result in (3.13). The

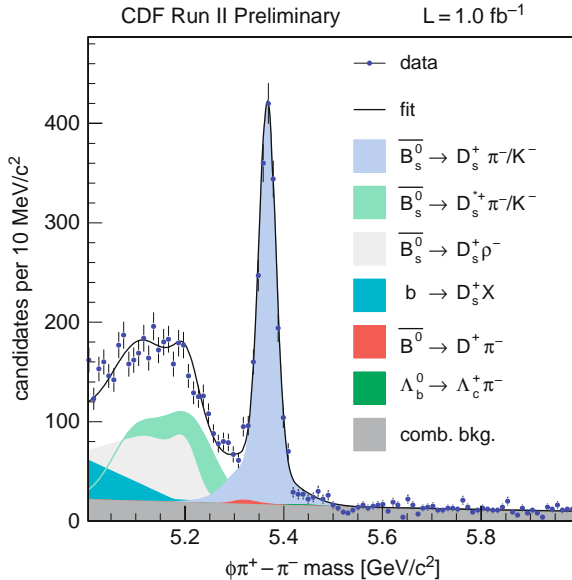


Fig. 3.6 The “golden” modes $\bar{B}_s^0 \rightarrow D_s^+ \pi^-$ (with $D_s^+ \rightarrow \phi \pi^+$) as well as $D_s^{*+} \pi^-$ and $D_s^+ \rho^-$, picked up by the two track SVT trigger of the CDF experiment. [Copyright (2006) by The American Physical Society]. Since the B_s is fully reconstructed, these modes offer the best proper time resolution for Δm_{B_s} determination (from [1])

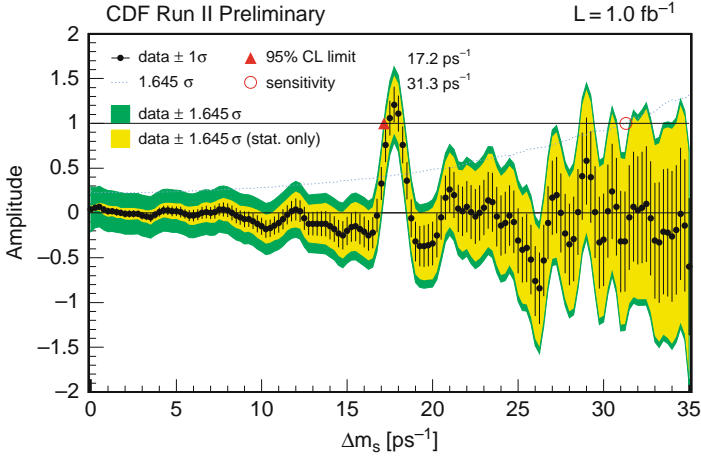


Fig. 3.7 “Amplitude” plot (all modes combined) versus Δm_{B_s} from CDF analysis with 1 fb^{-1} data [1], giving an apparent peak value at 17.77 ps^{-1} with amplitude consistent with 1. [Copyright (2006) by The American Physical Society.]

significance is over 5σ . Collecting the hadronic samples in five bins of proper decay time, one finds data to be consistent with $\cos \Delta m_{B_s} t$ with an amplitude of $\mathcal{A} = 1.28$.

Using Δm_{B_d} values from PDG and $\xi \simeq 1.2$ from lattice, a value of $|V_{td}/V_{ts}| \simeq 0.206$ is extracted, which goes into the “ Δm_s & Δm_d ” band in Fig. 1.6. We do not comment on this, as it is too early to relate to the presence or absence of New Physics, i.e., the violation of CKM unitarity. But we remark that, if one takes the current nominal values for f_{B_s} , e.g., from lattice studies, *the result of (3.13) seems a bit on the small side*. Recall from Fig. 3.3 that, before the experimental measurement precipitated, fitting to data and information other than Δm_{B_s} itself, the fitted values from the CKMfitter and UTfit groups tended to be of order 20 ps^{-1} . Our statement may be even more serious than epitomized by this figure, which has large fitter errors. CLEO [16] and Belle [17] have measured f_{D_s} by measuring $D_s^+ \rightarrow \ell^+ \nu$ decay rates, and the measured f_{D_s} values are considerably higher than current lattice results. If this carries over to f_{B_s} , the SM expectation for Δm_{B_s} would definitely be above 20 ps^{-1} , and one may need some “New Physics” to bring it down to the level of (3.13). Unfortunately, because of the large hadronic uncertainties in $f_{B_s}^2$, one cannot take this as a hint for New Physics. One has to turn to CPV that is less prone to hadronic physics.

3.2 Search for TCPV in B_s System

As stated, $\sin 2\Phi_{B_s}$ is expected to be very small if SM continues to hold sway. Although SM has withstood challenge after challenge without giving much ground, we have argued that the current frontier for New Physics search is $b \rightarrow s$ and $b \leftrightarrow s$

transitions. TCPV in B_s system holds the best hope, since $\sin 2\Phi_{B_s}$, once measured, does not suffer from hadronic uncertainties in its interpretation. The price to pay is to overcome the difficulty of very rapid oscillations, among other things, as we now elucidate.

3.2.1 $\Delta\Gamma_{B_s}$ Approach to $\phi_{B_s} : \cos 2\Phi_{B_s}$

Let us first briefly comment on the approach through width mixing, i.e., $\Delta\Gamma_{B_s}$ and ϕ_{B_s} from untagged $B_s^0 \rightarrow J/\psi\phi$ and other lifetime studies. With a large partial width for $b \rightarrow c\bar{c}s$ decay, the large fraction of common final states in $b\bar{s}$ vs. $\bar{b}s \rightarrow c\bar{c}s\bar{s}$ (i.e., the $c\bar{c}$ cut in the box diagram amplitude for $B_s^0-\bar{B}_s^0$ mixing) can generate a width difference. This enriches the possible CPV observables compared to the B_d system.

The DØ experiment has made a concerted effort on dimuon charge asymmetry A_{SL} , the untagged single muon charge asymmetry A_{SL}^s ,⁶ and the lifetime difference in untagged $B_s \rightarrow J/\psi\phi$ decay (hence does not involve oscillations) using a data set of 1.1 fb^{-1} . DØ holds the advantage in periodically flipping magnet polarity to reduce the systematic error on A_{SL} . Combining the three studies, they probe the CPV phase $\cos 2\Phi_{B_s}$ via

$$\Delta\Gamma_{B_s} = \Delta\Gamma_{B_s}^{\text{CP}} \cos 2\Phi_{B_s}, \quad (3.14)$$

where $\Delta\Gamma_{B_s}^{\text{CP}} \cong \Delta\Gamma_{B_s}^{\text{SM}}$. The main result of interest is given in Fig. 3.8, where $\phi_s = \Phi_{B_s}$ and $\Delta\Gamma_s = \Delta\Gamma_{B_s}^{\text{CP}}$. The fitted width difference of $0.13 \pm 0.09 \text{ ps}^{-1}$ is still larger than the SM expectation [10] of $\Delta\Gamma_{B_s}^{\text{SM}} = 0.096 \pm 0.039 \text{ ps}^{-1}$ (see (3.11)), but certainly not inconsistent. The extracted “first” measurement of $|\Phi_{B_s}| = 0.70^{+0.39}_{-0.47}$ is slightly off zero and with large central values. The sensitivity to both $\cos \Phi_{B_s}$ and $\sin \Phi_{B_s}$ is because of presence of interference terms between different angular amplitudes that arise through CPV. But given the large errors, the result is both consistent with SM expectation but certainly allows for NP.

The details on this somewhat technical subject, which is why we do not pursue it further, can be found in [20]. For a phenomenological digest, see [21]. A more recent CDF untagged, angular-resolved study [22] of $B_s \rightarrow J/\psi\phi$ using 1.7 fb^{-1} data finds $\Delta\Gamma_{B_s} = 0.076^{+0.059}_{-0.063} \pm 0.006 \text{ ps}^{-1}$, assuming CP conservation (i.e., setting $\Phi_{B_s} = 0$), which is consistent with the SM expectation of (3.11). Allowing for CPV, one is still consistent with $\Phi_{B_s} = 0$. However, sizable Φ_{B_s} values are allowed.

Overall, we find the $\cos 2\Phi_{B_s}$ approach a somewhat “blunt instrument.”

⁶ The same sign dilepton charge asymmetry and the single lepton charge asymmetry are familiar from kaon physics, where they are related to ε_K . The analogous $\varepsilon_{B_d^0}$ and $\varepsilon_{B_s^0}$ are also at the 0.1% level and very hard to measure, even at the B factories [18, 19]. At hadronic machines, this is further complicated by B_d^0 and B_s^0 production fractions. We do not go into any detailed discussion, as we are still far away from profitably probing these observables.

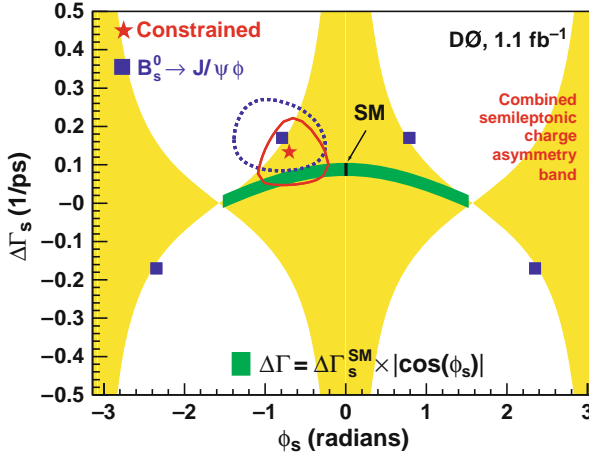


Fig. 3.8 Combined analysis of A_{SL} , A_{SL}^s , and lifetime difference in untagged $B_s \rightarrow J/\psi \phi$ by DØ [20] based on 1.1 fb^{-1} data. [Copyright (2007) by The American Physical Society.]

3.2.2 Prospects for $\sin 2\Phi_{B_s}$ Measurement

The more direct approach to measuring $\sin 2\Phi_{B_s}$ is via tagged TCPV study of $B_s \rightarrow J/\psi \phi$. Let us focus on the shorter term prospects for the competition for $\sin 2\Phi_{B_s}$ measurement between Tevatron and LHC experiments.

$B_s \rightarrow J/\psi \phi$ decay is analogous to $B_d \rightarrow J/\psi K_s$, except it is a VV final state. Thus, besides measuring the decay vertices, one also needs to perform an angular analysis to separate the CP even and odd components. As J/ψ is reconstructed in the dimuon final state, there are no triggering issues, and CDF and DØ should have comparable sensitivity. Assuming 8 fb^{-1} per experiment (which may be optimistic), the Tevatron could reach an ultimate sensitivity of [23]

$$\sigma(\sin 2\Phi_{B_s}) \sim 0.2/\sqrt{2} \quad (\text{Tevatron combined}). \quad (3.15)$$

Of course, as one continues improving techniques at the Tevatron, the gain may be more than simple luminosity.

However, the LHC has already achieved first beam in September 2008. But then, magnets quenched soon after! How fast can LHC turn on and produce physics results? We will have to wait and see, but some training period is expected, especially if one keeps in mind the slow start of Tevatron Run II. We will adopt a conservative estimate [25] for the “first year”—a floating concept in actual calendar terms—running of LHC: 2.5 fb^{-1} for ATLAS and CMS and 0.5 fb^{-1} for LHCb. Assuming this, the projection for ATLAS is $\sigma(\sin 2\Phi_{B_s}) \sim 0.16$, not better than the Tevatron, while for LHCb one has $\sigma(\sin 2\Phi_{B_s}) \sim 0.04$. The situation seems rather volatile, given that LHC accelerator and detector/analysis performance are yet unproven. We

Table 3.1 Rough sensitivity for $\sin 2\Phi_{B_s}$ measurement, ca. 2010–2011

	CDF/DØ	ATLAS/CMS	LHCb
$\sigma(\sin 2\Phi_{B_s})$	0.2/expt	0.16/expt	0.04
$\int \mathcal{L} dt$	(8 fb ⁻¹)	(2.5 fb ⁻¹)	(0.5 fb ⁻¹)

list these sensitivities side by side in Table 3.1, which should be viewed as reference values for 2010–2011, maybe even beyond.

If SM again holds sway, as we have witnessed in the past 30 years, then LHCb would clearly be the winner, since $\sigma(\sin 2\Phi_{B_s}) \sim 0.04$ starts to probe the SM expectation (3.8). This is not surprising, as the LHCb detector (see Fig. 3.9) has a forward design for the purpose of B physics. It takes advantage of the large collider cross section for $b\bar{b}$ production, while implementing a fixed target-like detector configuration, which allows more space for devices such as RICH detectors for PID and a better ECAL. We have seen how important a good PID system is for flavor tagging.

We stress, however, that 2009(–2010) *looks rather interesting*—Tevatron could get really lucky: it could glimpse the value of $\sin 2\Phi_{B_s}$ *only if* its strength is large; but *if* $|\sin 2\Phi_{B_s}|$ *is large*, it would definitely indicate New Physics. Thus,

The Tevatron could preempt LHCb and carry the glory of discovering physics beyond the Standard Model in $\sin 2\Phi_{B_s}$.

(publicly stressed [26, 27] since early 2007). Maybe the Tevatron should even run longer, especially if LHC dangles further. This adds to the existing competition on Higgs search between the Tevatron and the LHC and should not be overlooked.

So, now the question is ...

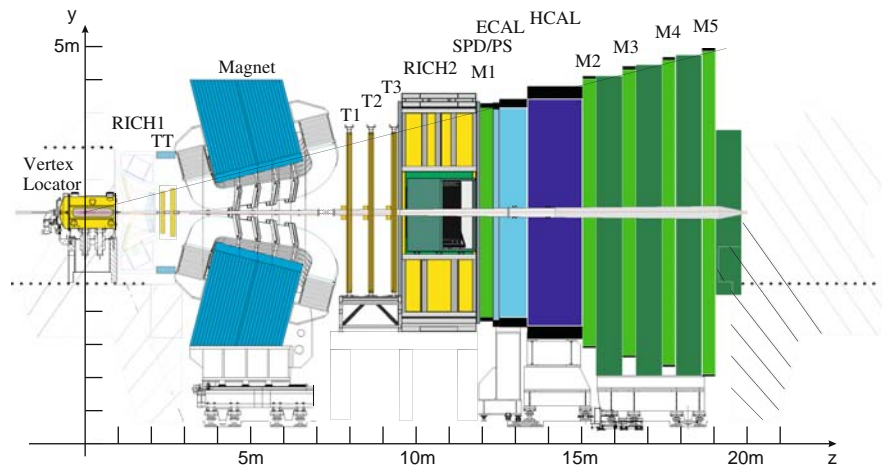


Fig. 3.9 The LHCb detector (adapted from Fig. 2.1 of [24], used with permission. [Copyright of Institute of Physics and IOP Publishing Limited 2008.]

3.2.3 Can $|\sin 2\Phi_{B_s}| > 0.5$?

The answer should clearly be in the positive, as it is a question to be answered by experiment. However, it is our observation in the past few years that there are very few believers—The SM has been too successful! In the following, we provide some phenomenological insight as *existence proof*. At the same time, we attempt to link with the hints for New Physics discussed in the previous chapter. That is, it is of interest to explore whether the New Physics hints in $\Delta B = 1$ ($b \rightarrow s$) processes of Chap. 2 have implications for the $\Delta B = 2$ ($b\bar{s} \rightarrow s\bar{b}$) processes. This subsection therefore has some phenomenology connotations.

One can of course resort to squark-gluino box diagrams, Fig. 3.2(b). Note, however, that squark-gluino loops, while possibly generating ΔS , cannot really move $\Delta\mathcal{A}_{K\pi}$ because their effects are decoupled in P_{EW} . If one wishes to have contact with both hints for NP in $b \rightarrow s$ transitions from the B factories, then one should pay attention to some common nature between $b \rightarrow s$ electroweak penguin diagrams and the box diagrams for B_s mixing. If there are new *nondecoupled* quarks in the loop, then both $\Delta\mathcal{A}_{K\pi}$ and ΔS could be touched. It also affects B_s mixing, as it is well known that the top quark effect in electroweak penguin and box diagrams are rather similar. Such new nondecoupled quarks are traditionally called the fourth-generation quarks,⁷ t' and b' .

The t' quark in the loop adds a term

$$V_{t's}^* V_{t'b} \equiv r_{sb} e^{i\phi_{sb}} \quad (3.16)$$

to (3.4). It is useful to visualize this,

$$V_{us}^* V_{ub} + V_{cs}^* V_{cb} + V_{ts}^* V_{tb} + V_{t's}^* V_{t'b} = 0 \quad (3.17)$$

$$\implies V_{ts}^* V_{tb} \simeq -V_{cb}^* V_{tb} - V_{t's}^* V_{t'b}, \quad (3.18)$$

where the last step again follows from $|V_{us}^* V_{ub}| \ll 1$. Note that $V_{cb}^* V_{tb}$ continues to be real by phase convention, but the t' contribution brings in the additional NP CPV phase $\arg(V_{t's}^* V_{t'b}) \equiv \phi_{sb}$ with even larger *Higgs affinity*, $\lambda_{t'} > \lambda_t \simeq 1$, since $m_{t'} > m_t$ by definition. The new weak phase enters the t quark contribution as

⁷ Traditionally [2, 3], there are two main problems with the fourth generation. One is the existence of only three light neutrinos, which has been known since 1989. The other problem is that the Electroweak Precision Tests (EWPT) seem to rule out the fourth generation with high confidence. We take the fourth generation just as an illustration, as it touches on many aspects of flavor physics and CPV (just like the top). But as an antidote, in regards neutrino counting in Z decay, we know that there is more to the neutral lepton sector since the observation of large neutrino mixing in 1998. The strict, minimal SM with “no right-handed neutrinos” is no more, and the neutrino sector carries a mass scale. As for EWPT, we cite the recent paper by Kribs et al. [28], as a challenge to the orthodox PDG view. These authors cite that the constraints by the LEP Electroweak Working Group (LEP EWWG) are more forgiving [29] for a fourth generation. The t' and b' should be heavy and close in mass (difference less than M_W), but not degenerate. We take these as limits on the parameter space, rather than strong discouragement.

well, through (four-generation) CKM unitarity. Dynamically speaking, these effects of t' are not different from what is already present in the three-generation SM (or SM3; we shall refer to the fourth-generation Standard Model as SM4), since both the presence of CPV, and large λ_t , are already verified by experiment.

It was shown [30] that the fourth generation could account for $\Delta\mathcal{A}_{K\pi}$, and $\Delta\mathcal{S}$ then moves in the right direction [31]. This was done in the PQCD approach up to Next-to-Leading Order (NLO), which is the state of the art. We note that PQCD is the only QCD-based factorization approach that *predicted* [32] both the strength and sign of $\mathcal{A}_{\text{CP}}(B^0 \rightarrow K^+\pi^-)$ in (2.7). At NLO in PQCD [33] factorization, an enhancement of C does relax a bit the $\Delta\mathcal{A}_{K\pi}$ problem discussed in Sect. 2.2.2 (see (2.9) and (2.10)), but it also demonstrates that a (perturbative) calculational approach could not generate $|C/T| > 1$. It is nontrivial, then, that incorporating the nondecoupled fourth generation t' quark to account for $\Delta\mathcal{A}_{K\pi}$, it can also move $\Delta\mathcal{S}$ (see Sect. 2.1.2) in the right direction.

The really exciting implication, however, is the impact on $\sin 2\Phi_{B_s}$: the t' effect in the box diagram also enjoys nondecoupling. As the difference of $\Delta\mathcal{A}_{K\pi}$ in (2.10) is large, both the strength and phase of $V_{t's}^* V_{t'b}$ are sizable [30], and the phase is not far from maximal. As we have mentioned, a near maximal phase from t' is precisely what allows the minimal impact on Δm_{B_s} , as it adds only in quadrature to the real contribution from top. But it makes the maximal impact on $\sin 2\Phi_{B_s}$. Furthermore, the t' effect can partially cancel against too large a t contribution in the real part, if the indication for large f_{D_s} from experiment is carried over to a larger f_{B_s} value than current lattice results.

Some Formalism for the Fourth Generation

At this point, it is illuminating to get a feeling of how these *nondecoupling t' effects* emerge. Ignoring $V_{us}^* V_{ub}$, i.e., taking (3.18) literally, the effective Hamiltonian for loop-induced $b \rightarrow s\bar{q}q$ transitions becomes

$$H_{\text{eff}}^{\text{loop}} \propto \sum_{i=3}^{10} (v_c C_i^t - v_{t'} \Delta C_i) O_i, \quad (3.19)$$

where C_i s are the effective Wilson coefficients of the (four-quark) operators O_i that arise from quantum loop effects and the CKM product

$$v_q \equiv V_{qs}^* V_{qb}. \quad (3.20)$$

The first $v_c C_i^t$ term is the usual SM, or SM3, effect, while

$$-v_{t'} \Delta C_i \equiv -v_{t'} (C_i^{t'} - C_i^t) \quad (3.21)$$

is the effect of the fourth generation. Note that the latter vanishes not only with $v_{t'} = V_{t's}^* V_{t'b}$ but also as $m_{t'} \rightarrow m_t$, which are the twin requirements of the GIM

mechanism [34]. This is a condition that quite a few calculations in the literature that involve the fourth generation do not respect ! We plot in Fig. 3.10(a) the functions ΔC_i for $i = 4, 6$ (strong penguin), 7 (electromagnetic penguin), and 9 (electroweak penguin). The functions for $i = 3, 5$ are similar to 4, 6 case, while for $i = 8$ (10), it is similar to 7 (9).

Let us understand the $m_{t'}$ dependence in Fig. 3.10(a). First, note that the different ΔC_i s converge to zero for $m_{t'} \rightarrow m_t$, as required by GIM. We have normalized $-\Delta C_i$ by $|C_4^t|$, the top contribution to the strong penguin coefficient. We see that $-\Delta C_{4(6)}$ has rather mild $m_{t'}$ dependence and is always small compared to the top contribution. This is because, as mentioned in Footnote 6 of Chap. 2, the strong penguin has less than logarithmic dependence on the heavy quark mass m_Q in the loop. Thus, when one subtracts $C_{4(6)}^{t'}$ from $C_{4(6)}^t$, not much is left [35].

The situation is rather different for the electroweak penguin coefficient ΔC_9 , which has linear $x_{t'} \equiv m_{t'}^2/M_W^2$ dependence arising from Z and box diagrams [36], as can be seen very clearly from Fig. 3.10(a). This is what we call nondecoupling of heavy t and t' effects through their large Higgs affinity, or Yukawa couplings, λ_t and $\lambda_{t'}$. For $m_{t'} > 350$ GeV, $|\Delta C_9|$ already exceeds $\frac{1}{2}|C_4^t|$. For the electromagnetic penguin coefficient ΔC_7 , the behavior is in between ΔC_4 and ΔC_9 . The m_t dependence of C_7 is roughly logarithmic, hence there is some difference between t' and t effect when they are not too close to being degenerate, but the difference is far less prominent than for C_9 . We note that the functional dependence of C_i s on heavy top mass can be traced to the so-called Inami–Lim functions [37] derived for kaons, while rediscovered [36], actually independently discovered, for electroweak-penguin-induced B decays.⁸

Adding a t' quark to the box diagram of Fig. 3.2(a), with obvious notation, one makes the following effective substitution [26, 27] in (3.1),

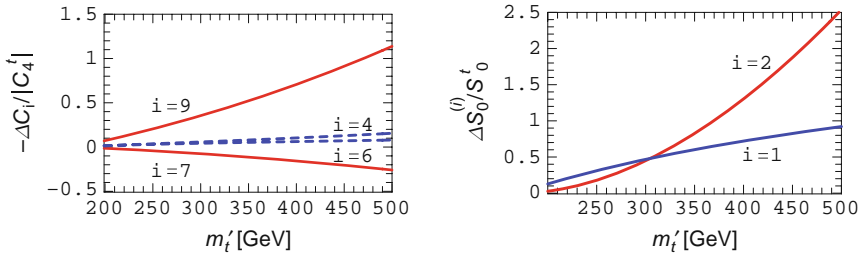


Fig. 3.10 The t' correction (a) $-\Delta C_i$ normalized to strength of strong penguin coefficient $|C_4^t|$ (both at m_b scale) and (b) $\Delta S_0^{(i)}$ normalized to S_0^t vs. $m_{t'}$, showing nondecoupling of t' effect (from [26, 27]). [Copyright (2007) by The American Physical Society.]

⁸ In paper [38], the predecessor paper to [36], the electroweak penguin contribution was simply dropped with respect to the electromagnetic contribution by G_F power counting arguments. So, nondecoupling is not intuitive.

$$v_t^2 S_0(t, t) \rightarrow v_c^2 S_0(t, t) - 2v_c v_{t'} \Delta S_0^{(1)} + v_{t'}^2 \Delta S_0^{(2)}, \quad (3.22)$$

where v_q is defined in (3.20) and (3.18) has been used. It is clear that the first term is just the SM3 effect, and is practically real, while

$$\Delta S_0^{(1)} \equiv S_0(t, t') - S_0(t, t), \quad (3.23)$$

$$\Delta S_0^{(2)} \equiv S_0(t', t') - 2S_0(t, t') + S_0(t, t). \quad (3.24)$$

These $\Delta S_0^{(i)}$ s respect GIM cancellation and vanish with $v_{t'}$, analogous to the ΔC_i terms in Eq. (3.19). Normalizing them to $S_0' = S_0(t, t)$, they are plotted vs. $m_{t'}$ in Fig. 3.10(b). Their behavior can be compared to ΔC_9 plotted in Fig. 3.10(a). The strong $m_{t'}$ dependence illustrates the nondecoupling of SM-like heavy quarks from box and EWP diagrams [36].

With large nondecoupling effects because of the heavy t' mass and bringing in a New Physics CPV phase into $b \rightarrow s$ transitions, the fourth generation is of particular interest for processes involving boxes and Z penguins.

Impact: Large and Negative $\sin 2\Phi_{B_s}$

We show in Fig. 3.11 the variation of Δm_{B_s} and $\sin 2\Phi_{B_s}$ with respect to the new CPV phase $\phi_{sb} \equiv \arg V_{t's}^* V_{t'b}$ in the fourth generation model, for the nominal $m_{t'} = 300$ GeV and $r_{sb} \equiv |V_{t's}^* V_{t'b}| = 0.02, 0.025$, and 0.03 , where stronger r_{sb} gives larger variation. Using the central value of $f_{B_s} \sqrt{B_{B_s}} = 295 \pm 32$ MeV, we get a nominal 3 generation value of $\Delta m_{B_s}|^{\text{SM}} \sim 24 \text{ ps}^{-1}$, which is the dashed line. The CDF measurement of (3.13) is the rather narrow solid band, attesting to the precision already reached by experiment, and that it is below the nominal SM value shown as the dashed line.

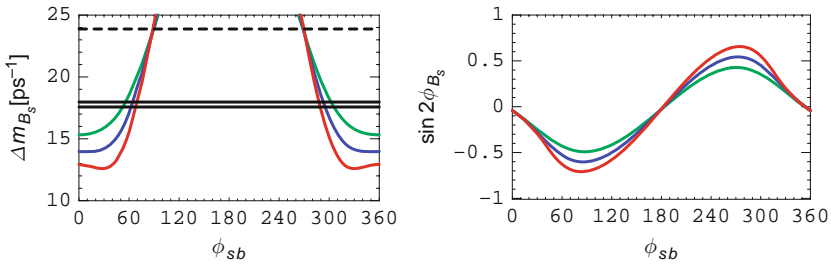


Fig. 3.11 Δm_{B_s} and $\sin 2\Phi_{B_s}$ vs. $\phi_{sb} \equiv \arg V_{t's}^* V_{t'b}$ for the fourth-generation extension of SM [26, 27], where $|V_{t's}^* V_{t'b}| = 0.02, 0.025, 0.03$ (larger value gives stronger variation) and $m_{t'} = 300$ GeV, which are for illustration. [Copyright (2007) by The American Physical Society.] Dashed horizontal line is the nominal three-generation SM expectation taking $f_{B_s} \sqrt{B_{B_s}} = 295$ MeV. Solid band is the experimental measurement by CDF [1]. The narrow range implied by Δm_{B_s} measurement projects out large values for $\sin 2\Phi_{B_s}$, where the right branch is excluded by the sign of $\Delta \mathcal{A}_{K\pi}$ (2.10)

Combining the information from $\Delta\mathcal{A}_{K\pi}$, Δm_{B_s} , and $\mathcal{B}(b \rightarrow s\ell^+\ell^-)$, the predicted value is [26, 27]

$$\sin 2\Phi_{B_s} = -0.5 \text{ to } -0.7 \quad (\text{fourth generation}), \quad (3.25)$$

where even the sign is predicted. Compared with the SM expectation in (3.8), the strength is enormous. Our motivation arose from the $\Delta\mathcal{A}_{K\pi}$ (and $\Delta\mathcal{S}$) problem. However, the range can be demonstrated by using the (stringent) Δm_{B_s} vs. (less stringent) $\mathcal{B}(b \rightarrow X_s\ell^+\ell^-)$ constraints alone, with $\Delta\mathcal{A}_{K\pi}$ selecting the minus sign in (3.25), as can be read off from Fig. 3.11. Note that for different $m_{t'}$, it maps into a different $\phi_{sb}-r_{sb}$ range, with minor changes in the predicted range for $\sin 2\Phi_{B_s}$.

We stress again that, because of the predicted enormous strength, (3.25) can be probed even before LHCb gets first data and should help motivate the Tevatron experiments. Inspection of Table 3.1, one sees that 2009–2010 *could be rather interesting indeed*. The Tevatron could well come out the winner.

3.2.4 Hints at Tevatron in 2008

From the time of the SUSY 2007 conference, when the writing of this monograph commenced, strides have been made at the Tevatron giving us a glimpse in 2008 of what may lie ahead.

Using 1.35 fb^{-1} data, CDF performed the first tagged and angular-resolved time-dependent CPV study of the $B_s \rightarrow J/\psi\phi$ decay process. The result [39], in terms of $\Delta\Gamma_{B_s}$ vs. $\beta_s = -\Phi_{B_s}$ is shown in Fig. 3.12. Using 2.8 fb^{-1} data, a similar analysis was conducted by DØ, assuming (3.13) for Δm_{B_s} as input. The result [40], in terms of $\phi_s = 2\Phi_{B_s}$, is also shown in Fig. 3.12. Up to a two-fold ambiguity in the CDF result,⁹ to the eye, one sees that both experiments find Φ_{B_s} to be negative, and with central values that are more consistent with the fourth-generation prediction of (3.25), than with the SM expectation given in (3.8).

Let us understand how Fig. 3.12 was reached. Both the $\cos 2\Phi_{B_s}$ approach, discussed in the previous section, and the $\sin 2\Phi_{B_s}$ approach study the B_s^0 decay to $J/\psi\phi$ final state, but the latter bears more similarities to the $\sin 2\phi_1/\beta$ ($\equiv \sin 2\Phi_{B_d}$) study at the B factories. One needs to resolve the time dependence of $B_s^0-\bar{B}_s^0$ oscillations. So, just like the measurement of Δm_{B_s} discussed in Sect. 3.1, one needs to tag the B_s^0 or \bar{B}_s^0 flavor at time of production, $t = 0$, and be able to resolve the time t of $B_s^0 \rightarrow J/\psi\phi$ decay. Furthermore, the study bears similarity to the $B_d^0 \rightarrow J/\psi K^{*0}$ analysis at B factories: the VV final state is not a CP eigenstate, and one needs to perform an angular analysis to separate the CP even (S - and D -wave) and odd (P -wave) final states to correct for the CP eigenvalue ξ_f in (A.9) for the given partial wave (note that J/ψ and ϕ are both CP even). Thus, this study is rather involved.

⁹ For the DØ result, this ambiguity is removed by assuming that the strong phases in $B_s^0 \rightarrow J/\psi\phi$ helicity amplitudes are the same as in $B \rightarrow J/\psi K^{*0}$.

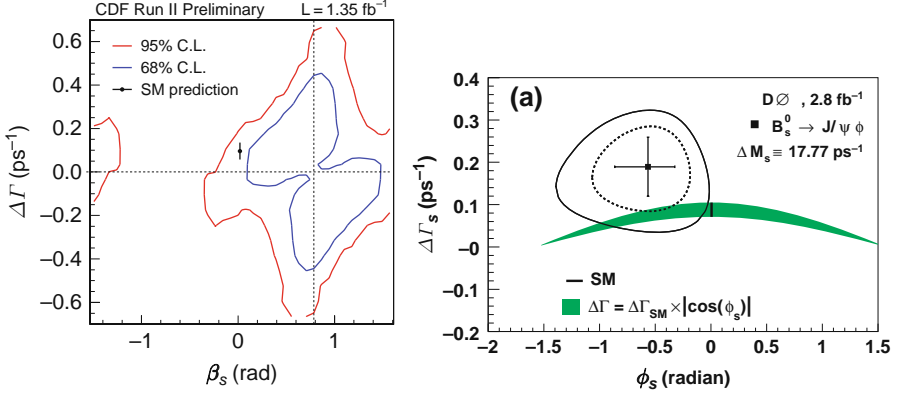


Fig. 3.12 $\Delta\Gamma_{B_s}$ vs. Φ_{B_s} from recent tagged time-dependent studies by CDF [39] using 1.35 fb^{-1} data, and DØ [40] using 2.8 fb^{-1} data [Copyright (2008) by The American Physical Society]. Note that $-\beta_s = \phi_s/2 = \Phi_{B_s}$.

Collection of Signal Events

Both CDF and DØ reconstruct $J/\psi\phi$ via $J/\psi \rightarrow \mu^+\mu^-$ and $\phi \rightarrow K^+K^-$ that emerge from a common vertex. The dimuon implies that, unlike the situation for Δm_{B_s} measurement, there is no problem for DØ with triggering the events, although the muon trigger threshold of $2.0 \text{ GeV}/c$ is higher than the $1.5 \text{ GeV}/c$ threshold for CDF. For CDF, as in their Δm_{B_s} study, an Artificial Neural Network (ANN) is employed to separate $B_s^0 \rightarrow J/\psi\phi$ signals from background. The ANN is trained with Monte Carlo (MC) data for the signal, and the background is taken from the sideband of actual data. In this way, with 1.35 fb^{-1} data, CDF observed ~ 2000 signal events with $S/B \sim 1$, which we plot in Fig. 3.13. Using similar method, ~ 7800 $B_d^0 \rightarrow J/\psi K^{*0}$ events were reconstructed as control sample. DØ also reconstructed ~ 2000 signal events, but with a larger 2.8 fb^{-1} data set. Since the study is statistics limited, maybe this could be improved with an ANN analysis in the future, and, if possible, lowering the muon trigger threshold.

Flavor Tagging

Turning to flavor tagging, for the CDF study, the mean effectiveness $Q \equiv \epsilon \mathcal{D}^2$ is only $\sim 1.2\%$ for Opposite Side Tagging (OST), lower than the 1.8% achieved for Δm_{B_s} measurement [1], while the mean Q for Same Side Kaon Tagging (SSKT) is $\sim 3.6\%$, also slightly lower than Δm_{B_s} measurement. This slightly lower Q for $B_s \rightarrow J/\psi\phi$ TCPV study, as compared to the B_s mixing study, is in part due to a lower average p_T . In contrast, for the DØ study, by incorporating same side tagging as well as OST, $\epsilon \mathcal{D}^2$ is improved significantly, from $\sim 2.5\%$ for the purely OST analysis of the Δm_{B_s} measurement [11] to $\sim 4.7\%$, becoming comparable to CDF.

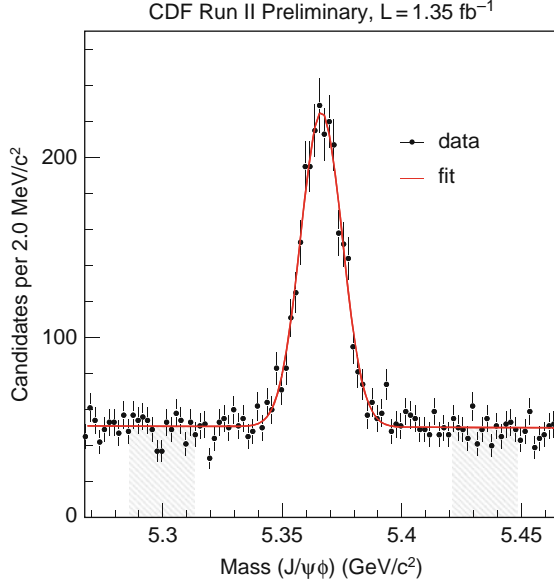


Fig. 3.13 $M(J/\psi \phi)$ distribution for $B_s^0 \rightarrow J/\psi \phi$ events reconstructed in $J/\psi \rightarrow \mu^+\mu^-$ and $\phi \rightarrow K^+K^-$ by CDF [39] with 1.35 fb^{-1} data. [Copyright (2008) by The American Physical Society.]

Angular-Resolved TCPV: Rich Interference

Although the need to perform angular analysis makes it much more involved, it provides considerably more analyzing power. The angular amplitudes are decomposed in the transversity basis [41]. There are three components A_0 , A_{\parallel} , and A_{\perp} , corresponding to linear polarization states of the vector mesons J/ψ and ϕ being either longitudinal (0) or transverse to their direction of motion and parallel (\parallel) or perpendicular (\perp) to each other. There are five variables: three amplitude strengths and two strong phase differences. The time evolution of the $|A_f(t)|^2$, beside the classic $\xi_f \sin 2\Phi_{B_s} \sin \Delta m_{B_s} t$ term (which is why we call this the $\sin 2\Phi_{B_s}$ approach), where ξ_f is the CP eigenvalue for amplitude f , there is also a $\xi_f \cos 2\Phi_{B_s} \sinh \Delta \Gamma_{B_s} t$ term from CP violation through width mixing. This enriches the simpler formula¹⁰ (A.9) for B_d^0 studies where width difference is negligible. The time evolution of the $\text{Re}(A_0^*(t)A_{\parallel}(t))$ interference term is likewise, except that it is modulated by $\cos \delta_{\parallel 0}$ of the strong phase difference $\delta_{\parallel 0} \equiv \delta_{\parallel} - \delta_0$.

The existence of CP violation itself, as well as difference in the final state strong phases, enriches further the interference between CP even and odd amplitudes,

¹⁰ In this discussion, direct CPV has been ignored for the $B_s^0 \rightarrow J/\psi \phi$ process. That is, $|\lambda_{B_s^0 \rightarrow J/\psi \phi}| = 1$ is assumed. Allowing for DCPV would further enrich the $B_s^0 \rightarrow J/\psi \phi$ study. However, considering our discussions in Sect. 2.3, ignoring DCPV here is a good approximation, as well as simplification, for discussing New Physics search.

namely $\text{Im}(A_0^*(t)A_\perp(t))$ and $\text{Im}(A_\parallel^*(t)A_\perp(t))$ terms. Take $\text{Im}(A_0^*(t)A_\perp(t))$ for example, one has a CPV term $\cos 2\Phi_{B_s} \sin \Delta\Gamma_{B_s} t$ modulo $\cos \delta_{\perp 0}$, but there is also a $\sin \delta_{\perp 0}$ final state interaction effect in the $\cos \Delta m_{B_s} t$ Fourier component that mimics CPV.

We can now try to understand the results in Fig. 3.12. The dotted cross lines in Fig. 3.12(a) show a reflection symmetry in the $\Phi_{B_s} - \Delta\Gamma_{B_s}$ plane, which is due to the presence of both CPV and CP conserving phases. This results in a two-fold ambiguity for Φ_{B_s} (but not for $\sin 2\Phi_{B_s}$). Note, however, that flavor tagging has reduced the four-fold ambiguity present in Fig. 3.8 to two-fold. The SM prediction of $\Phi_{B_s} \simeq -0.04$ and $\Delta\Gamma_{B_s} = 0.096 \text{ ps}^{-1}$ is also plotted in Fig. 3.12(a), which lies between the 68 and 95% C.L. curves. The deviation from SM is 1.5σ for CDF. For the DØ plot of Fig. 3.12(b), an input of $\Delta m_{B_s} = 17.77 \pm 0.12 \text{ ps}^{-1}$ was used, and a more aggressive assumption of fixing $\delta_{\perp 0} = 2.92 \text{ rad}$ and $\delta_{\parallel 0} = -0.46 \text{ rad}$, within a Gaussian width of $\pi/5$, which are the favored values from $B_d^0 \rightarrow J/\psi K^{*0}$ studies at the B factories [42]. Though questionable (a dubious “SU(3)” assumption), it removes the negative Δm_{B_s} solution. DØ then finds a 1.8σ deviation from SM. We should stress that, though the two-fold ambiguity involves a sign flip with Δm_{B_s} , it does not affect the value for $\sin 2\Phi_{B_s}$.

For sake of comparison, we choose to present the values for the 1σ ranges (caution: non-Gaussian) for $\sin 2\Phi_{B_s}$, assuming strong phase structure in $B_s^0 \rightarrow J/\psi \phi$ is similar to $B_d^0 \rightarrow J/\psi K^{*0}$ and constraining $\Delta\Gamma_{B_s} = \Delta\Gamma_{B_s}|^{\text{SM}} \cos 2\Phi_{B_s}$,

$$\begin{aligned} \sin 2\Phi_{B_s} &\in [-0.4, -0.9] \quad \text{CDF } 1.35 \text{ fb}^{-1}; \\ &[-0.2, -0.7] \quad \text{DØ } 2.8 \text{ fb}^{-1}. \end{aligned} \quad (3.26)$$

We have used only one digit of significance, and the CDF result also constrains the mean B_s width to the B_d width. (3.26) is not yet a demonstration that $\sin 2\Phi_{B_s}$ is nonzero and negative and deviating from SM prediction of -0.04 , but the comparison with (3.25) of the fourth-generation prediction is staggering. For DØ, we have used the value of $\sin 2\Phi_{B_s} = -0.46 \pm 0.28$, which is for 2.8 fb^{-1} . If DØ could improve signal event reconstruction efficiency, e.g., employ some ANN approach like that of CDF, together with at least doubling the data set, it seems that a smaller error than the estimation of 0.2 offered in Sect. 3.2.2 could be reached. Likewise, if we take the CDF result in (3.26) and assume Gaussian error, one has $\sin 2\Phi_{B_s} = -0.66 \pm 0.27$. Since this is for 1.35 fb^{-1} data, even though the current error may not be Gaussian, it seems that an error less than 0.2 can be reached with 6 fb^{-1} . (We note that extending to 1.7 fb^{-1} , the ANN signal yield [22] for $B_s^0 \rightarrow J/\psi \phi$ increased consistently from 2000 to 2500.) It remains to be seen whether the strong phase “nuisance” in $B_s^0 \rightarrow J/\psi \phi$ can be unravelled, but it looks like the prospects for measuring $\sin 2\Phi_{B_s}$ in the range of (3.25) is even more promising than what we presented in Table 1 of Sect. 3.2.2.

In fact, the UTfit group has made a strong claim, by boldly combining the results of Δm_{B_s} as well as Figs. 3.8 and 3.12. A *first evidence* (3.7σ) for New Physics in $b \leftrightarrow s$ transitions was claimed [43], with $\Phi_{B_s} = -19.9^\circ \pm 5.6^\circ$ or

$$\sin 2\Phi_{B_s} = -0.64^{+0.16}_{-0.14} \quad (\text{UTfit, Winter 2008}). \quad (3.27)$$

We will not go into what assumptions were made to reach this value, since it seems the significance is even better than our account above (subsequently, UTfit has dropped the significance to $\sim 2.5\sigma$), maybe in part because it contains information beyond $B_s \rightarrow J/\psi\phi$ TCPV analysis, e.g., those discussed in Sect. 3.2.1. While it is better to wait for an official Tevatron (or HFAG) average, we stress again that the value is tantalizingly consistent with (3.25), the prediction of the fourth-generation model! It is useful to remember, then, that the latter combines Δm_{B_s} and $\Delta\mathcal{A}_{K\pi}$ results. Thus, from current hints, we see that Nature may prefer linking $\Delta\mathcal{A}_{K\pi} > 0$ ($b \rightarrow s\bar{q}q$ transition) with large and negative $\sin 2\Phi_{B_s}$ in B_s^0 TCPV ($b\bar{s} \leftrightarrow s\bar{b}$ transition). And the link is most natural through nondecoupled chiral quarks.

Whether measurements with LHC data become available or not, much progress is expected in the coming year or two, so we will leave things as it is. We note that models like squark-gluino loops, or Z' models with specially chosen couplings, could also give large $\sin 2\Phi_{B_s}$, but they would be unable to link with $\Delta\mathcal{A}_{K\pi}$, and the two observables are not correlated in these scenarios.

Note Added

At ICHEP 2008 in Philadelphia, CDF updated [44] with 2.8 fb^{-1} data, but without flavor tagging, which makes the data set equivalent to 2 fb^{-1} . The result is consistent with the previous 1.35 fb^{-1} , with significance slightly improved. Thus, we have three measurements (two by CDF and one by $D\bar{0}$) of $\sin 2\Phi_{B_s}$, all large and negative in central value and consistent with each other (and the fourth-generation prediction). It looks like 2009 would be extremely interesting, which could extend into 2010. If the central value stays, observation at Tevatron with 2010 data seem likely [44]. It remains to be seen whether LHCb can produce physics results by Summer 2010.

References

1. Abulencia, A., et al. [CDF Collaboration]: Phys. Rev. Lett. **97**, 242003 (2006) 33, 40, 41, 42, 49, 51
2. Yao, W.M., et al. [Particle Data Group]: J. Phys. G **33**, 1 (2006) 34, 35, 36, 46
3. Amsler, C., et al.: Phys. Lett. B **667**, 1 (2008); and <http://pdg.lbl.gov/> 34, 35, 36, 46
4. See the webpage of the CKMfitter group. <http://ckmfitter.in2p3.fr> 35, 36
5. Charles, J., et al. [CKMfitter Group]: Eur. Phys. J. C **41**, 1 (2005) 35
6. Bona, M., et al. [UTfit Collaboration]: JHEP **07**, 028 (2005) 35
7. Gómez-Ceballos, G.: Talk at Flavor Physics and CP Violation Conference (FPCP2006), Vancouver, Canada, April 2006 35, 36, 40, 41
8. Dunietz, I., Fleischer, R., Nierste, U.: Phys. Rev. D **63**, 114015 (2001) 37, 38
9. Christenson, J.H., Cronin, J.W., Fitch, V.L., Turlay, R.: Phys. Rev. Lett. **13**, 138 (1964) 37
10. Lenz, A., Nierste, U.: JHEP **06**, 072 (2007) 38, 43
11. Abazov, V.M., et al. [$D\bar{0}$ Collaboration]: Phys. Rev. Lett. **97**, 021802 (2006) 38, 39, 51
12. Moser, H.G., Roussarie, A.: Nucl. Instrum. Meth. A **384**, 491 (1997) 39
13. Ali, A., Barreiro, F.: Z. Phys. C **30**, 635 (1986) 40

14. Gronau, M., Nippe, A., Rosner, J.L.: Phys. Rev. D **47**, 1988 (1993) 40
15. Gronau, M., Rosner, J.L.: Phys. Rev. D **49**, 254 (1994) 40
16. Artuso, M., et al. [CLEO Collaboration]: Phys. Rev. Lett. **99**, 071802 (2007) 42
17. Widhalm, L., et al. [Belle Collaboration]: Phys. Rev. Lett. **100**, 241801 (2008) 42
18. Aubert, B., et al. [BaBar Collaboration]: Phys. Rev. Lett. **96**, 251802 (2006) 43
19. Nakano, E., et al. [Belle Collaboration]: Phys. Rev. D **73**, 112002 (2006) 43
20. Abazov, V.M., et al. [DØ Collaboration]: Phys. Rev. D **76**, 057101 (2007) 43, 44
21. Hou, W.S., Mahajan, N.: Phys. Rev. D **75**, 077501 (2007) 43
22. Aaltonen, T., et al. [CDF Collaboration]: Phys. Rev. Lett. **100**, 121803 (2008) 43, 53
23. See, e.g. the last backup slide of talk by Bedeschi, F.: At the 4th Workshop on the CKM Unitarity Triangle (CKM2006), Nagoya, Japan, December 2006 44
24. Alves, A.A., et al. [LHCb Collaboration]: JINST **3**, S08005 (2008) 45
25. Nakada, T.: Talk at Flavour in the Era of the LHC Workshop, CERN, Geneva, Switzerland, March 2007 44
26. Hou, W.S., Nagashima, M., Soddu, A.: Phys. Rev. D **72**, 115007 (2005) 45, 48, 49, 50
27. Hou, W.S., Nagashima, M., Soddu, A.: Phys. Rev. D **76**, 016004 (2007) 45, 48, 49, 50
28. Kribs, G.D., Plehn, T., Spannowsky, M., Tait, T.M.P.: Phys. Rev. D **76**, 075016 (2007) 46
29. See <http://lepewwg.web.cern.ch/LEPEWWG/plots/summer2006/> 46
30. Hou, W.S., Nagashima, M., Soddu, A.: Phys. Rev. Lett. **95**, 141601 (2005) 47
31. Hou, W.S., Li, H.n., Mishima, S., Nagashima, M.: Phys. Rev. Lett. **98**, 131801 (2007) 47
32. Keum, Y.Y., Sanda, A.I.: Phys. Rev. D **67**, 054009 (2003) 47
33. Li, H.n., Mishima, S., Sanda, A.I.: Phys. Rev. D **72**, 114005 (2005) 47
34. Glashow, S.L., Iliopoulos, J., Maiani, L.: Phys. Rev. D **2**, 1285 (1970) 48
35. Hou, W.S.: Nucl. Phys. B **308**, 561 (1988) 48
36. Hou, W.S., Willey, R.S., Soni, A.: Phys. Rev. Lett. **58**, 1608 (1987) 48, 49
37. Inami, T., Lim, C.S.: Prog. Theor. Phys. **65**, 297 (1981) 48
38. Eilam, G., Soni, A., Kane, G.L., Deshpande, N.G.: Phys. Rev. Lett. **57**, 1106 (1986) 48
39. Aaltonen, T., et al. [CDF Collaboration]: Phys. Rev. Lett. **100**, 161802 (2008) 50, 51, 52
40. Abazov, V.M., et al. [DØ Collaboration]: Phys. Rev. Lett. **101**, 241801 (2008) 50, 51
41. Dighe, A.S., Duniety, I., Fleischer, R.: Eur. Phys. J. C **6**, 647 (1999) 52
42. Barberio, E., et al. [Heavy Flavor Averaging Group]: arXiv:0704.3575 [hep-ex] (unpublished) 53
43. Bona, M., et al. [UTfit Collaboration]: arXiv:0803.0659 [hep-ph] (unpublished) 53
44. See the parallel session talk by Tonelli, D., arXiv:0810.3229 [hep-ex], at the 34th International Conference on High Energy Physics (ICHEP2008), Philadelphia, USA, 29 July–5 August 2008; see also the plenary talk by Paulini, M 54

Chapter 4

H^+ Probes: $b \rightarrow s\gamma$ and $B \rightarrow \tau\nu$

When the observation of $b \rightarrow s\gamma$ was first announced by CLEO [1] in 1994 with 2 fb^{-1} data on the $\Upsilon(4S)$, it immediately became one of the most powerful constraints on many kinds of New Physics that enter the loop. In this chapter, we illustrate by the stringent bound it provides on the charged Higgs boson H^+ that automatically exists in minimal SUSY. A second probe of the H^+ boson is surprisingly a *tree-level* effect in $B^+ \rightarrow \tau^+\nu$, which became relevant only recently at the B factories.

4.1 $b \rightarrow s\gamma$

4.1.1 QCD Enhancement and the CLEO Observation

The $b \rightarrow s\gamma$ decay process is of great theoretical interest because of large QCD corrections [2, 3] that enhance the rate and because of its sensitivity [4, 5] to charged Higgs boson effects. We give the leading order SM diagram in Fig. 4.1(a). Dressing with QCD and dealing with resummation of large logarithms,¹ QCD enhances the $b \rightarrow s\gamma$ rate by a factor of 2–3 for heavy top quark (enhancement greater for low top mass). To extract information on possible underlying New Physics and also for its own sake, this marked the start of a major systematic QCD computation effort, moving from Next-to-Leading Order (NLO) to the current [6] Next-to-Next-to-Leading Order (NNLO). At order α_s^2 , one has hundreds (three-loop) and thousands (four-loop) of diagrams. A rather close dialogue between theory and experiment was developed as the experimental error improved.

The leading order diagram with the charged Higgs boson replacing the W is given in Fig. 4.1(b). Its effect can be readily accommodated in the QCD computation as

¹ These are of the form $(\alpha_s \log M_W^2/m_b^2)^n$, as was originally uncovered by the “large QCD corrections” for $n = 1$ [2, 3]. It represents the accumulation of QCD corrections over the large difference in scale between M_W (and m_t) and m_b . The detailed treatment involves effective theory renormalization group evolution and is rather technical. We remark that the “large” QCD correction is somewhat a misnomer. It is not a breakdown of perturbation theory but results from the $n = 0$ term being very strongly suppressed by the GIM mechanism.

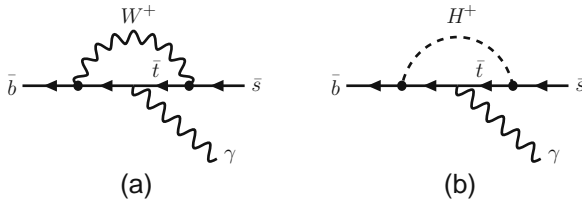


Fig. 4.1 (a) A diagram for $\bar{b} \rightarrow \bar{s}\gamma$ with a W boson loop, and (b) a diagram with W^+ replaced by H^+

a short distance correction. As the charged Higgs boson naturally occurs in supersymmetry and because of intriguing sensitivity of $b \rightarrow s\gamma$ rate to m_{H^+} , the process has been a focus of attention for both theorists and experimentalists.

After making a large investment on electromagnetic calorimetry based on CsI crystals for their detector upgrade to CLEO II, the CLEO experiment observed [7] the exclusive $B \rightarrow K^*\gamma$ decay in 1993. This is the first ever “penguin” process to be established in B physics and ushered in the golden age for CLEO. Unlike the inclusive $b \rightarrow s\gamma$ decay that is of higher theoretical interest, the exclusive process has large hadronic uncertainties, but it is certainly easier experimentally. To search for inclusive $b \rightarrow s\gamma$ decay, one requires an energetic photon, with π^0 and η veto. Since background control is critical and since a dominant type of background comes from the continuum (or non- $B\bar{B}$) $q\bar{q}$ background, one needs to take significant amount of data off the $\Upsilon(4S)$ resonance (typically 60 MeV) and make a subtraction. In the first CLEO observation of $b \rightarrow s\gamma$, the on- and off-resonance data were of order 2 fb^{-1} and 1 fb^{-1} , respectively. In the following, we will not quote off resonance data taking any further.

There are basically two approaches that one can take for inclusive measurement. The first approach, called the fully inclusive, uses all information available, combined in some discriminant to suppress background. The second approach is the technique called “partial reconstruction.” That is, identifying the experimentally defined $B \rightarrow X_s\gamma$ with the quark level $b \rightarrow s\gamma$ decay (called “duality”), one reconstructs only a subset of the recoil X_s system, i.e., in $K + n\pi$ modes [1] where K is either charged or as $K_S \rightarrow \pi^+\pi^-$, and $n\pi$ stands for 1–4 pions, with at most one π^0 . Admittedly, this may cause a bias compared to the fully inclusive $B \rightarrow X_s\gamma$, as duality is lost. However, in this way, CLEO managed to put background under control, observing 100 or so events. The fully inclusive approach had more events, but suffered from larger background. Combining the results of both approaches (taking correlations into account), CLEO gave

$$\mathcal{B}_{B \rightarrow X_s\gamma} = 2.32 \pm 0.57 \pm 0.35 \times 10^{-4} \quad (\text{CLEO 95}), \quad (4.1)$$

for $2.2 < E_\gamma < 2.7 \text{ GeV}$. The photon energy (in $\Upsilon(4S)$, or e^+e^- CM frame) is an additional parameter used for background control.

The measurement of (4.1) almost instantly became one of the most important probes of NP and is the best cited paper by CLEO. For instance, using calculations available at that time, CLEO gave the bound [1]

$$M_{H^+} > [244 + 63/(\tan \beta)^{1.3}] \text{ GeV} \quad (\text{CLEO 95}), \quad (4.2)$$

for the charged H^+ boson, where $\tan \beta = v_2/v_1$ is the ratio of vacuum expectation values of the two Higgs doublets that give a H^+ boson (not to be confused with the weak phase $\beta \equiv \phi_1$ of previous chapters).

Good electromagnetic calorimetry, so far based on CsI(Tl), i.e., Tl doped CsI crystals, became a standard subdetector for the B factories.

4.1.2 Measurement of $b \rightarrow s\gamma$ at the B Factories

CLEO updated with their full 10M $B\bar{B}$ data in 2001, using the fully inclusive approach and a photon energy cut of $E_\gamma > 2.0$ GeV. The early analysis of Belle with 6.5M $B\bar{B}$ data used the partial reconstruction approach, but Belle then switched to the fully inclusive analysis. BaBar, however, followed the partial reconstruction path, enlarging it to 38 modes in 2005, allowing for two π^0 's, η mesons, and three kaons. With the photon energy cut at $E_\gamma > 1.9$ GeV, the result is found to be [8] $\mathcal{B}_{B \rightarrow X_s \gamma} = 3.27 \pm 0.18^{+0.55+0.04}_{-0.40-0.09} \times 10^{-4}$, where the last error is due to theory.

At this point, we should remark on the photon energy cut. From $E_\gamma \simeq m_b/2$ at the parton level, the actual photon energy spectrum is smeared by Fermi motion inside the meson, as well as from gluon radiation. Thus, the photon “line” is Doppler broadened into a distribution. This distribution, or shape function, contains information on m_b and μ_π^2 , the parameters related to b quark mass and momentum inside the B meson. These parameters are independent of New Physics but relate to similar functions in other processes, e.g., in $b \rightarrow c\ell\nu$ decay. We will not get into this, because it becomes rather involved technically and it is farther removed from our quest for New Physics. The experimental study, however, typically requires a cut on photon energy to control background. To recover the full inclusive rate, correspondence with the theoretical spectral distribution is necessary, although this itself ought to be checked.

Actually, a photon energy cut on the full spectrum is also needed from the theory side to avoid nonperturbative effects at lower energies that are not under good control. Currently, theory sets an E_γ cut at 1.6 GeV, *in the B meson rest frame*, and extrapolation has to be made for proper comparison. For our purpose, suffice it to say that in the operator product expansion treatment of the E_γ distribution, the fraction of events with $E_\gamma > 2.0$, 1.9, and 1.8 GeV are roughly 89, 94, and 97%, respectively, of the full $E_\gamma > 1.6$ GeV spectrum.

With 152M $B\bar{B}$ pairs and the photon energy cut of $E_\gamma > 1.8$ GeV, Belle used [9] the fully inclusive approach. Besides π^0 and η veto and on-off resonance subtractions, the remaining backgrounds from $B\bar{B}$ events were subtracted using Monte Carlo distributions checked by data-controlled samples. The result is

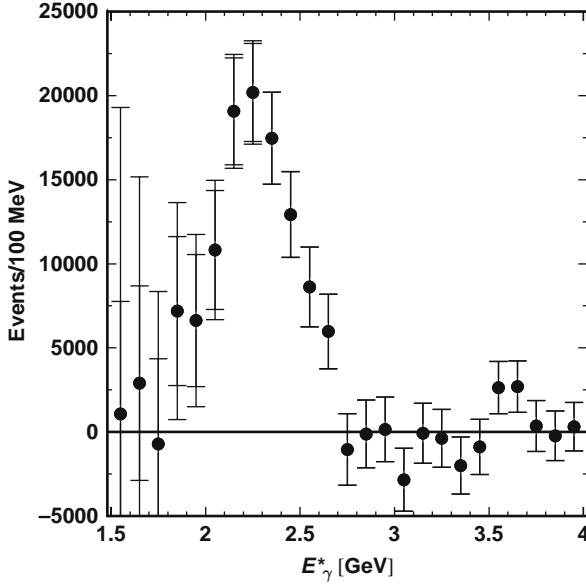


Fig. 4.2 The E_γ spectrum in $\Upsilon(4S)$ frame from fully inclusive $b \rightarrow s\gamma$ analysis by Belle [9], with a photon cut at 1.8 GeV for 152M $B\bar{B}$ pairs. [Copyright (2004) by The American Physical Society.]

$\mathcal{B}_{B \rightarrow X_s \gamma} = 3.55 \pm 0.32^{+0.30+0.11}_{-0.31-0.07} \times 10^{-4}$, where the last error is again due to theory. We plot the observed photon energy spectrum in Fig. 4.2. Noting the $E_\gamma > 1.8$ GeV cut, the Doppler-broadened (as well as due to gluon radiation) lineshape is apparent. To compare the various measurements and to compare with theory, one needs to subtract $b \rightarrow d\gamma$, correct for different E_γ range (including boosting to B rest frame), and extrapolate to 1.6 GeV (and B frame). The experimental average by HFAG in 2006 gives [10]

$$\mathcal{B}_{B \rightarrow X_s \gamma} = 3.55 \pm 0.26 \times 10^{-4} \quad (E_\gamma > 1.6 \text{ GeV}; \text{HFAG 06}), \quad (4.3)$$

where we have combined the various errors. The theoretical NLO result [11] at the start of the millennium is

$$\mathcal{B}_{B \rightarrow X_s \gamma}|^{\text{NLO}} = 3.57 \pm 0.30 \times 10^{-4} \quad (E_\gamma > 1.6 \text{ GeV}). \quad (4.4)$$

The agreement between (4.3) and (4.4) is excellent, both in central value and in error (experimental error is smaller!), leaving little space for New Physics, i.e., just in the error bars. This good agreement between experiment and NLO theory lasted until 2007.

The reduction in experimental error inspired a large theory effort at NNLO, i.e., to α_s^2 order, and is still not final. On the theory side, this is also to reduce the renormalization scale dependence at NLO. The outcome, however, resulted in a downward shift in the central value [6],

$$\mathcal{B}_{B \rightarrow X_s \gamma}^{\text{NNLO}} = 3.15 \pm 0.23 \times 10^{-4} \quad (E_\gamma > 1.6 \text{ GeV}). \quad (4.5)$$

With error now slightly lower than experiment, the central value is now more than 1σ below experiment, i.e., (4.3), in central value—another approach gives a number that is even lower [12]. This progress in theory puts the ball back in the court of the experiments.

With much more data to play with, Belle came out [13] in 2008 with a (still preliminary) new analysis with fully inclusive approach, using 657M $B\bar{B}$ pairs, while managing to lower the E_γ cut to 1.7 GeV. The result, for $E_\gamma > 1.7$ GeV, is $\mathcal{B}_{B \rightarrow X_s \gamma} = 3.31 \pm 0.19 \pm 0.37 \pm 0.01 \times 10^{-4}$, where the errors are statistical, systematic, and due to boost correction. Agreement with theory is slightly improved, in part because of a slight drop in central value. Note that the systematic error is now larger than the earlier published [9] result with E_γ cut at 1.8 GeV, because lowering the E_γ cut is at the cost of bringing in more background. With systematic error now dominant, it seems that relying on MC for subtraction of remaining $B\bar{B}$ background may not be easy to extend to larger data sets.

To confront the theoretical advancement, a fresher approach may eventually be needed. A promising new development, as the B factories increase in data, is the *full reconstruction of the tag side B meson* (for more discussion, see Sect. 4.2). With this approach, the signal side is then just an isolated energetic photon, without the need to specify or reconstruct the X_s system, and signal purity is improved. One also knows the charge, flavor, and momentum of the signal B , hence the photon energy spectrum is directly measured in the B frame. The systematics would be quite different from the previous approaches, be it partial reconstruction or fully inclusive. A first attempt has been performed by BaBar [14] recently, using 232M $B\bar{B}$ pairs. Roughly 0.68M pairs are tagged by one B decaying hadronically: the advantage of full reconstruction of tag side B comes at the cost of 3×10^{-3} in efficiency. BaBar set an E_γ cut at 1.9 GeV. Scaling by a factor of 0.936, the result is $\mathcal{B}_{B \rightarrow X_s \gamma} = 3.91 \pm 0.91 \pm 0.64 \times 10^{-4}$ for $E_\gamma > 1.6$ GeV. It should be stressed that the systematic errors can improve with a larger data set. Thus, this seems to be the path to follow in the long run, in particular at the future Super B Factory.

The NNLO theory development clearly demands a Super B Factory upgrade to continue the supreme dialogue between theory and experiment in $b \rightarrow s\gamma$.

4.1.3 Implications

This close dialogue allowed $b \rightarrow s\gamma$ to provide one of the most stringent bounds on New Physics models. The process is sensitive to all types of possible NP in the loop, such as stop-charginos, where a large literature exists. However, $b \rightarrow s\gamma$ is best known for its stringent constraint on the MSSM (Minimal SUSY SM) type of H^+ boson. Furthermore, the SUSY-related studies all need mechanisms to cancel against the large charged Higgs effect, which turns out to be constructive [4, 5] with SM. We therefore focus on the H^+ effect in the loop, which is illustrated in Fig. 4.1(b).

MSSM demands at least two Higgs doublets (2HDM), where one Higgs doublet couples to right-handed down type quarks and the other to up type. The physical H^+ is a cousin of the ϕ_{W^+} Goldstone boson in SM that gets eaten and becomes the longitudinal component of the W^+ boson. It is the ϕ_{W^+} that couples to mass, which is at the root of the nondecoupling phenomenon of the heavy top quark in the loop. In $bs\gamma$ coupling for heavy top,² however, the top is effectively decoupled (less than logarithmic dependence on m_t), i.e., the dependence on m_t is weak for large m_t . This arises by a subtlety of gauge invariance, or the demands of current conservation³ of the $bs\gamma$ vertex, and is the reason underlying why QCD corrections make such a large impact [2, 3] on this loop-induced decay. It is for the same reason that the process is sensitive to NP such as H^+ .

Replacing the W^+ by H^+ in the loop, in the MSSM type of 2HDM, the H^+ effect *always enhances the $b \rightarrow s\gamma$ rate, regardless of $\tan\beta$* , where $\tan\beta$ is the ratio of v.e.v.s between the two doublets. This effect was pointed out 20 years ago [4, 5]. Basically, the H^+ couples to $m_t \cot\beta$ at one end of the loop, and to $-m_b \tan\beta$ at the other end, making this contribution independent of $\tan\beta$, and the sign is fixed such that it is always constructive with the SM amplitude.

As stated, a main motivation for the large effort to push the QCD calculation to NNLO is to match the experimental error, to be able to better interpret the New Physics impact of the measurement. The effective field theory approach allows NP contributions at short distance to be readily incorporated. Without further ado, in Fig. 4.3 we show the plot [6] where the NNLO result of $\mathcal{B}(B \rightarrow X_s\gamma)$ vs. m_{H^+} is compared with the 2006 combined data [10] of (4.3). A nominal $\tan\beta = 2$ is taken. In Fig. 4.3, the solid lines give the H^+ effect, which approaches the dashed lines for m_{H^+} much greater than m_t (decoupling of heavy H^+). For lighter m_{H^+} , however, one has enhancement. One can compare with Fig. 1 of [5], where “Model 1” in this paper is the more popularly called Two Higgs Doublet Model II (2HDM-II), which automatically arises in MSSM. When H^+ is not much heavier than the top, its contribution can get even larger than SM effect!

Of course, experiment and NNLO theory are in reasonable agreement, therefore one can extract a bound on the m_{H^+} - $\tan\beta$ plane. We follow [6] and continue to use $\tan\beta = 2$ for illustration. By comparing the lower range of the NNLO result with the higher range of (4.3), shown as the dotted lines in Fig. 4.3, one has the bound

$$m_{H^+} > 295 \text{ GeV} \quad (\text{NNLO} + \text{HFAG06}), \quad (4.6)$$

² If the top quark turned out to be light compared to the W , one has m_t^2/M_W^2 power suppression [4, 5].

³ Basically, current conservation allows two conserved effective $bs\gamma$ couplings, of the form $\bar{s}q^2\gamma_\mu Lb$ and $\bar{s}\sigma_{\mu\nu}q_\nu m_b Rb$ (each contracted with a photon field A_μ). The latter can radiate a real photon, since the former vanishes with q^2 , where q_μ is the photon momentum. The form of the effective couplings demands an expansion in $q^2(< m_b^2)$ and $q_\nu m_b$ in the computation of the effective coefficients. In contrast, for the bsZ vertex, the current is not conserved (the conserved part is gauge related to $bs\gamma$), hence there is no need to make such expansions, and what replaces the previous q^2 and qm_b turns out to be m_t^2 .

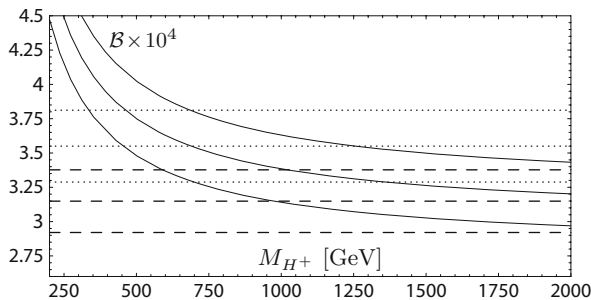


Fig. 4.3 $B(B \rightarrow X_s \gamma) (\times 10^4)$ vs. m_{H^+} (in GeV) in MSSM type two Higgs doublet model, with $\tan \beta = 2$ (taken from [6]). [Copyright (2007) by The American Physical Society.] For large m_{H^+} , one approaches SM (*dashed lines*), while for low m_{H^+} there is great enhancement. *Dotted lines* give the 1σ experimental range

at 90% C.L. This may seem to be barely an improvement over the first CLEO observation in 1995, i.e., (4.2), where one gets the bound of ~ 270 GeV using $\tan \beta = 2$. This is due to the tension between NNLO theory vs. experiment, i.e., theory is a bit on the low side.

If one takes the central value of both results seriously, one could say [6] that an H^+ boson with mass around 695 GeV (where the central values of theory and experiment meet) is needed to bring the NNLO rate up to the experimental central value of (4.3). This is because the H^+ effect in the MSSM type of 2HDM is always constructive [5] with the ϕ_{W^+} effect in SM, and again illustrates why the theory–experiment correspondence in $b \rightarrow s \gamma$ must go on.

We remark that, given that the NNLO result is lower than experiment, models that give a destructive effect to SM is constrained stronger. For example, in the other (non-MSSM) type of 2HDM, where both u and d quarks get mass from the same Higgs doublet (usually called 2HDM-I), the H^+ effect is destructive [5]. One would then need either a larger H^+ effect that overpowers the SM contribution or one would need *additional* New Physics to bring the rate up to experiment.

The ongoing saga should be watched. It would be interesting with LHC turn on, especially if a charged Higgs boson is discovered. Much more information could be extracted in the future with a Super B Factory. But will theorists be courageous enough to go beyond NNLO?

4.2 $B \rightarrow \tau \nu$ and $D^{(*)} \tau \nu$

As a cousin of the ϕ_{W^+} , the H^+ boson has an amazing tree-level effect that has only recently come to fore by the prowess of the B factories, namely the recent measurement of $B \rightarrow \tau \nu$ at 10^{-4} level, as well as the *subsequent* measurement of $B \rightarrow D^{(*)} \tau \nu$ at the percent level. Before going into these, let us first give some historic backdrop.

4.2.1 Enhanced H^+ Effect in $b \rightarrow c\tau\nu$ and $B^+ \rightarrow \tau^+\nu_\tau$

In the early CLEO and ARGUS (as well as CUSB) era of B physics studies, there was once a problem called the “semileptonic branching ratio” (or \mathcal{B}_{sl}) problem. The measured \mathcal{B}_{sl} at 10% or so, becoming more and more precise, was lower than the spectator model expectations of 12%. Most naively one would have guessed that \mathcal{B}_{sl} is roughly of order 16%, so the spectator model already incorporated many corrections. Although this \mathcal{B}_{sl} problem eventually dissipated and concerns us no more, a simple and potentially exciting possibility was that 10–20% of B meson decays went into New Physics-enhanced processes that were difficult to observe experimentally, hence had not been probed.

Enhanced $b \rightarrow sg$ or $b \rightarrow c\tau\nu$?

Two possibilities [16] could be provided by the charged Higgs boson in the Two Higgs Doublet Model context. One possibility is the non-MSSM type of model, i.e., 2HDM-I. In this model, the H^+ effect is destructive [5, 15] with SM, and $b \rightarrow s\gamma$ and $b \rightarrow sg$ (gluon is “on-shell”) rates could be easily enhanced (or suppressed). Since $b \rightarrow s\gamma$ was as yet unmeasured in 1990, it was proposed [16] that a rather enhanced $b \rightarrow sg$, at the 10–20% level, could be the cause of the \mathcal{B}_{sl} problem. This requires low $\tan\beta$ and would have been interesting also for the “charm deficit” problem (another problem of that time that has since dissipated), since $b \rightarrow sg$ has no charm in the final state and would suppress the charm count in B decays. Another corollary would be a suppressed $b \rightarrow s\gamma$, as the $\tan\beta$ - m_{H^+} parameter space falls in a region of destructive [15] effect in $b \rightarrow s\gamma$, while the H^+ effect overwhelms the SM. This fascinating possibility has been subsequently ruled out by the CLEO bound [17] of $\mathcal{B}_{b \rightarrow sg} < 6.8\%$ at the 90% C.L. Though the bound is by far not stringent,⁴ it excludes the possibility that $\mathcal{B}_{b \rightarrow sg}$ is above 10%.

The second possibility [16] is an enhanced $b \rightarrow c\tau\nu_\tau$, which could occur in 2HDM-II (i.e., SUSY-type) for large $\tan\beta$. The $b \rightarrow c\tau\nu_\tau$ decay, or $B \rightarrow \tau\nu_\tau + X$, is a fraction of $B \rightarrow c\ell\nu_\ell$ (for $\ell = e, \mu$) in rate because of phase space suppression by having two heavy particles in the final state. Compounded by the poor signature with two missing neutrinos, the mode had been basically ignored experimentally. It had been known that this mode could be enhanced if $\tan^2\beta m_b m_\tau / m_{H^+}^2$ is large [19]. With the \mathcal{B}_{sl} problem, this mechanism was invoked to enhance $b \rightarrow c\tau\nu_\tau$ to the 10–20% level, which aroused interests for search at LEP, where one has highly boosted B hadrons. By 1993, using the large missing energy associated with the two neutrinos as a tag for the $b \rightarrow \tau\bar{\nu}_\tau + X$ events, the ALEPH experiment measured [20] $\mathcal{B}_{B \rightarrow \tau\nu_\tau + X} = 4.08 \pm 0.76 \pm 0.62\%$, which ruled out the possibility of large enhancement of $b \rightarrow c\tau\nu_\tau$ rate. Subsequent measurements have settled at [21, 22]

⁴ The SM expectation for $b \rightarrow sg$ is at the 0.1% level [18], not particularly small. However, it remains a curiosity whether the rate is enhanced in Nature. We lack tools to isolate an “on-shell” gluon $b \rightarrow sg$ decay in the hadronic B decay environment. Had the b quark been at 20 GeV or heavier, the gluon and the s quark “jets” could possibly be distinguished. But m_b is too low.

$$\mathcal{B}_{B \rightarrow \tau \nu_\tau + X} = 2.41 \pm 0.23 \%, \quad (4.7)$$

which is still dominated by ALEPH measurements. The $B \rightarrow \tau \nu_\tau + X$ rate is 1/4 the rate of $B \rightarrow \ell \nu_\ell + X$ (where $\ell = e, \mu$), basically as expected in SM.

H^+ Effect on $B^+ \rightarrow \tau^+ \nu_\tau$

Soon after the first ALEPH measurement that ruled out large enhancement of the inclusive $B \rightarrow \tau \nu_\tau + X$ rate, it was pointed out [23] that the limit of $\mathcal{B}_{B^+ \rightarrow \mu^+ \nu_\mu} < 2 \times 10^{-5}$ by CLEO [24] at that time gave a limit on $\tan \beta$ that is slightly better than the ALEPH measurement. Both implied $\tan \beta < 0.5$ ($m_{H^+}/1 \text{ GeV}$) or so. Second, if one could improve the limit of $\mathcal{B}_{B^+ \rightarrow \tau^+ \nu_\tau} < 1.2\%$ by a factor of 2, the $B^+ \rightarrow \tau^+ \nu_\tau$ mode could surpass the previous two processes and hold the best long-term prospect.

Analogous to the π^+ and $K^+ \rightarrow \ell^+ \nu_\ell$ decay, the formula for $B^+ \rightarrow \tau^+ \nu_\tau$ decay in SM is well known,

$$\mathcal{B}_{B^+ \rightarrow \tau^+ \nu_\tau}^{\text{SM}} = \frac{G_F^2 m_B m_\tau^2}{8\pi} \left[1 - \frac{m_\tau^2}{m_B^2} \right] \tau_B f_B^2 |V_{ub}|^2, \quad (4.8)$$

where f_B is the B meson decay constant. Adding a SUSY-type (2HDM-II) charged Higgs H^+ boson, the formula is simply replaced by [23]

$$\mathcal{B}_{B^+ \rightarrow \tau^+ \nu_\tau}^{H^+} = r_H \mathcal{B}_{B^+ \rightarrow \tau^+ \nu_\tau}^{\text{SM}}, \quad r_H = \left[1 - \frac{m_{B^+}^2}{m_{H^+}^2} \tan^2 \beta \right]^2. \quad (4.9)$$

For light leptons $\ell = e, \mu$, one simply replaces τ by ℓ in both (4.8) and (4.9). Interestingly, the factor r_H depends only on $\tan \beta$ and m_{B^+}/m_{H^+} , and does not depend on m_τ , nor does it have hadronic uncertainties. All hadronic uncertainties are contained in the decay constant f_B , just like in SM itself.

Since the effect is at tree level and easy to understand (but not obvious), we give a little detail. The two processes, mediated by W^+ and H^+ , are illustrated in Fig. 4.4(a) and (b). The effective four-Fermi interaction is

$$\frac{G_F}{\sqrt{2}} V_{ub} \left\{ [\bar{u} \gamma_\mu L b][\bar{\tau} \gamma_\mu L \nu_\tau] - R_\tau [\bar{u} R b][\bar{\tau} L \nu_\tau] \right\} + \text{h.c.}, \quad (4.10)$$

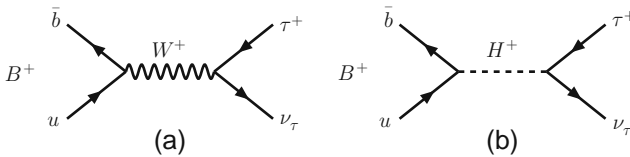


Fig. 4.4 (a) Diagram for $B^+ \rightarrow \tau^+ \nu$ via a W^+ boson, and (b) diagram with W^+ replaced by H^+

where h.c. stands for hermitian conjugate and

$$R_\tau = \frac{m_b m_\tau}{m_{H^+}^2} \tan^2 \beta. \quad (4.11)$$

The m_b and m_τ factors are due to the couplings of H^+ at each end of Fig. 4.4(b), where we have ignored m_u .

The SM axial-vector current and pseudoscalar density induce $B^\pm \rightarrow \tau^\pm \nu$ decay via the matrix elements,

$$\langle 0 | \bar{u} \gamma_\mu \gamma_5 b | B^- \rangle = i f_B p_{B\mu}, \quad \langle 0 | \bar{u} \gamma_5 b | B^- \rangle = -i f_B \frac{m_B^2}{m_b}. \quad (4.12)$$

which are simply related. Within SM, the W^+ gauge boson effect is helicity suppressed, hence the effect vanishes with the m_τ mass due to the need for helicity flip. This comes about because $p_{B\mu}$ of the axial-vector current matrix element contracts with $\bar{\tau} \gamma_\mu L \nu_\tau$. For the H^+ charged Higgs boson effect, there is no helicity suppression, but one has the aforementioned ‘‘Higgs affinity’’ factor, i.e., mass-dependent couplings. With m_u (and m_ν certainly) negligible, the H^+ couples as $m_\tau m_b \tan^2 \beta$, as in (4.11).

The absence of helicity suppression for the H^+ effect, but still having a dynamical coupling to the tau lepton mass, results in the R_H factor. The m_b in the $m_b m_\tau$ factor in (4.11) is cancelled by the $1/m_b$ in the density matrix element in (4.12), while m_τ factors out as a common factor (though of different origins) with the W^+ contribution and $m_b m_\tau$ gets replaced by the physical m_B^2 . Thus, r_H in (4.9) is independent of the quark mass m_b but depends only on the physical m_B mass. Note that the sign between the SM and H^+ contributions is always destructive [23], which is fixed by the relative sign in (4.10).

One also sees [23] that there are no interesting effects in 2HDM-I, since the $-\tan^2 \beta$ factor is replaced by $\cot \beta \tan \beta = 1$ and $m_{B^+}^2 / m_{H^+}^2$ would always be small.

4.2.2 $B \rightarrow \tau\nu$ and $B \rightarrow D^{(*)}\tau\nu$ Measurement

$B^+ \rightarrow \tau^+ \nu$ followed by τ^+ decay results in at least two neutrinos, which makes background very hard to suppress in the $B\bar{B}$ production environment. Thus, for a long time, the limit on $B^+ \rightarrow \tau^+ \nu$ was rather poor and not so interesting. This had allowed for the possibility that the effect of the H^+ could even dominate over SM, given that the SM expectation was only at 10^{-4} level. Even at the end of the CLEO era, the experimental limit was at the 10^{-3} level.

The change came with the enormous number of B mesons accumulated by the B factories, which allowed the full reconstruction method mentioned in Sect. 4.1.2 to finally become useful for rare and difficult decays. Fully reconstructing the tag side B meson, e.g., $B^- \rightarrow D^0 \pi^-$ decay, one has an efficiency of only 0.1–0.3%. At this cost, however, one effectively has a ‘‘B beam.’’ The situation is similar to Fig. 2.1, where the tag B is fully reconstructed, hence one knows the remaining event is an

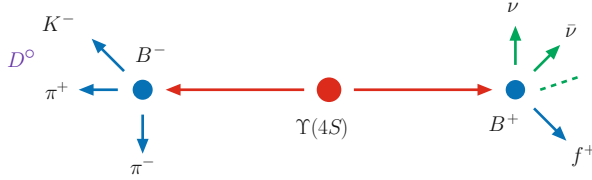


Fig. 4.5 Illustration of full reconstruction, for tag side B^- in $D^0\pi^- \rightarrow K^-\pi^+\pi^-$ final state, and signal B^+ decaying to $f^+\nu\bar{\nu}$, where f could be e, μ, π , or K . The dashed line indicates a possible third neutrino

opposite flavor B meson. It is useful to visualize the technique. We illustrate in Fig. 4.5 a full reconstruction event with the signal B decaying to $f^+\nu\bar{\nu}$, where f could be e or μ or π from τ decay, or a kaon, which will be discussed in Sect. 5.2.

As shown in Fig. 4.6, using full reconstruction in hadronic modes and with a data sample consisting of 449M $B\bar{B}$ pairs, in 2006 Belle reported $17.2^{+5.3}_{-4.7}$ events, where

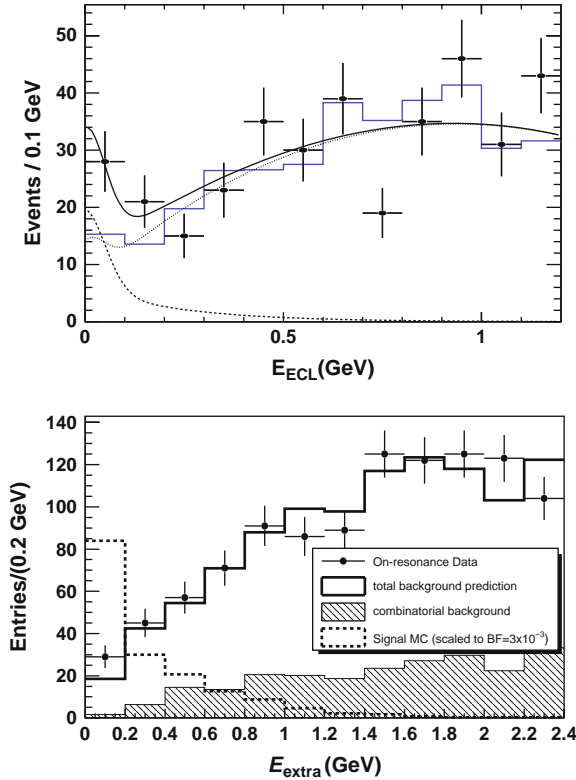


Fig. 4.6 Data showing evidence for $B \rightarrow \tau \nu$ (hadronic tag) search by Belle [25] and BaBar [26], plotted against extra energy in the EM calorimeter after full reconstruction of the other B . [Copyright (2006 and 2008) by The American Physical Society.]

the τ decay was searched for in decays to $e\nu\nu$, $\mu\nu\nu$, $\pi\nu$, and $\rho\nu$ channels. This constituted the first evidence, at 3.5σ significance, for $B^+ \rightarrow \tau^+\nu$, giving [25]

$$\mathcal{B}_{B \rightarrow \tau\nu} = 1.79_{-0.49-0.51}^{+0.56+0.46} \times 10^{-4} \quad (\text{Belle 449M}). \quad (4.13)$$

Besides full reconstruction tag of the other B , one needs to make sure that there really is just a single charged track (an extra π^0 for the ρ) and nothing else. The main tool used to suppress backgrounds is the remaining extra energy in the EM calorimeter, called E_{ECL} by Belle (and E_{Extra} by BaBar). As seen in Fig. 4.6(a), the peaking of events above background at $E_{\text{ECL}} \sim 0$ constituted evidence for $B \rightarrow \tau\nu$. This, of course, assumes that the studies have been careful enough such that there are no other types of peaking background.

With 320M $B\bar{B}$ pairs and $D\ell\nu$ reconstruction on tag side, however, in the same time frame BaBar saw no clear signal, giving $0.88_{-0.67}^{+0.68} \pm 0.11 \times 10^{-4}$, which is consistent with zero. Updating more recently to 383M, the $D\ell\nu$ tag result of $0.9 \pm 0.6 \pm 0.1 \times 10^{-4}$ is not different from the 320M result. However, with hadronic tag, BaBar also reported some evidence, at $(1.8_{-0.8}^{+0.9} \pm 0.4 \pm 0.2) \times 10^{-4}$ (second figure in Fig. 4.6), which is quite consistent with the Belle result of (4.13).

The combined result for BaBar is [26]

$$\mathcal{B}_{B \rightarrow \tau\nu} = 1.2 \pm 0.4 \pm 0.36 \times 10^{-4} \quad (\text{BaBar 383M}), \quad (4.14)$$

where we have followed HFAG to combine the background- and efficiency-related errors. The significance of (4.14) is 2.6σ , which is diluted by the semileptonic tag measurement, but it is basically consistent with the Belle result. Between (4.13) and (4.14), the existence of $B \rightarrow \tau\nu$ is now experimentally established.

Taking central values from lattice for f_B and $|V_{ub}|$ from semileptonic B decays, the nominal SM expectation is $1.6 \pm 0.4 \times 10^{-4}$. Thus, Belle and BaBar have reached SM sensitivity, and (4.13) and (4.14) now place a constraint on the $\tan\beta$ - m_{H^+} plane through $r_H \sim 1$. We illustrate the impact of $B \rightarrow \tau\nu$ in Fig. 4.7, together with the constraint from $b \rightarrow s\gamma$ of (4.6), as well as a few other processes. It is clear that $B \rightarrow \tau\nu$, which excludes a large region on the lower right, and $b \rightarrow s\gamma$, which excludes m_{H^+} below 300 GeV, provide the best constraints and are complementary to each other.

If one has a Super B Factory, together with development of lattice QCD, $B \rightarrow \tau\nu$ will become a superb probe of the H^+ boson, which would complement the direct H^+ searches at the LHC. Even if H^+ bosons are discovered, the $B \rightarrow \tau\nu$ process will provide us with useful information. Unlike the ever refined theory calculation that would be necessary for the $b \rightarrow s\gamma$ dialogue, the particularly nice feature for $B \rightarrow \tau\nu$ is its theoretical cleanliness, all hadronic effects being contained in f_B .

$B \rightarrow D^{(*)}\tau\nu$ Measurement

An analogous mode with larger branching ratio, $B \rightarrow D^{(*)}\tau\nu$, has recently emerged. In 2007, Belle announced the observation of [27]

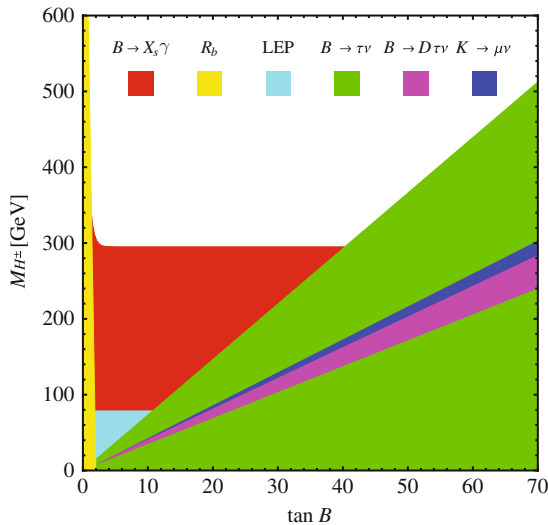


Fig. 4.7 Impact of $B \rightarrow \tau \nu$ on $\tan \beta$ - m_{H^+} plane, plotted together with constraint from $b \rightarrow s \gamma$ and other processes. (Taken from arXiv:0805.2141 [hep/ph], courtesy U. Haisch.)

$$\mathcal{B}_{D^{*-}\tau \nu} = 2.02^{+0.40}_{-0.37} \pm 0.37 \% \quad (\text{Belle 535M}), \quad (4.15)$$

based on 60^{+12}_{-11} reconstructed signal events, which is a 5.2σ effect. Subsequently, based on 232M $B\bar{B}$ pairs, BaBar announced the observation (over 6σ) of $D^{*0}\tau \nu$ and evidence (over 3σ) for $D^+\tau \nu$ [28]

$$\begin{aligned} \mathcal{B}_{D^{*0}\tau \nu} &= 1.81 \pm 0.33 \pm 0.11 \pm 0.06 \% \\ \mathcal{B}_{D^+\tau \nu} &= 0.90 \pm 0.26 \pm 0.11 \pm 0.06 \% \quad (\text{BaBar 232M}), \end{aligned} \quad (4.16)$$

where the last error is from normalization. Note that these values are somewhat on the larger side compared to the inclusive measurement of (4.7), even if $B \rightarrow D^*\tau \nu$ and $D\tau \nu$ saturate the inclusive rate.

At first sight, one may feel that $B \rightarrow D^{(*)}\tau \nu$ search should be easier than $B \rightarrow \tau \nu$ search, given the much larger branching ratio and the fact that one is resorting to full-reconstruction tag. The problem is that $B \rightarrow D^{(*)}\tau \nu$ suffers from an enormous peaking background from $B \rightarrow D^{(*)}\ell \nu$ for the leptonic τ decay modes. Belle used a modified missing mass to suppress this special peaking background.

The SM branching ratios, at 1.4% for $B \rightarrow D^*\tau \nu$, are poorly estimated. Furthermore, though the H^+ could hardly affect the $B \rightarrow D^*\tau \nu$ rate, it could leave its mark on the D^* polarization. The $B \rightarrow D\tau \nu$ rate, like $B \rightarrow \tau \nu$ itself, is more directly sensitive to H^+ effect [29], although $B \rightarrow \tau \nu$ has some advantage from our previous discussion. More theoretical work, as well as polarization information, would be needed for BSM (in particular, H^+ effect) interpretation. Note that $B \rightarrow \tau \nu$ decay probes the pseudoscalar coupling of H^+ , while $B \rightarrow D\tau \nu$ probes

the scalar coupling since $B \rightarrow D$ is a $0^- \rightarrow 0^-$ transition. In the long run (i.e., at Super B Factory), these two processes would provide complementary information. The effect of $B \rightarrow D\tau\nu$ measurement is also shown in Fig. 4.7, where one can see that its impact is weaker than $B \rightarrow \tau\nu$.

It is rather curious that, almost 25 years after the first B meson was reconstructed, we have newly measured modes with $\sim 1\text{--}2\%$ branching fractions!

Comment on New Physics in $D_s^+ \rightarrow \mu^+\nu, \tau^+\nu$

It is of interest to ask whether analogous effects to $B \rightarrow \tau\nu$ and $B \rightarrow D\tau\nu$ can be competitive in other systems. This could be so for the B_c system [16, 29], but this meson is difficult to produce and study. For lighter meson systems, we have pointed out that the charged Higgs effects are in general more subdued. Simply put, the m_B^2 in the r_H factor of (4.9) would be replaced by a much smaller mass. For example, replacing m_B^2 by m_K^2 for K mesons, the effect is much smaller, as one can see from Fig. 4.7. But since the measurements are rather precise and may improve further with kaon factory upgrades, it could still provide interesting constraints. However, to be competitive with $B \rightarrow \tau\nu$, usually further theoretical model assumptions need to be made.

The process $D_s^+ \rightarrow \ell^+\nu$, where $\ell = \mu, \tau$, proceeds via $c\bar{s}$ annihilation. Experimental measurement has made good progress recently. For this process, m_B^2 in (4.9) is replaced by $(m_s/m_c)m_{D_s}^2$, and the impact of H^+ on $D_s^+ \rightarrow \ell^+\nu_\ell$ decay is in general rather small [23]. Furthermore, this is a tree-level process proceeding without any CKM suppression, hence it seems rather hard for New Physics effects to compete with SM. The rate should measure $f_{D_s}|V_{cs}|$ in a rather clean way.

The experimental measurement has become rather precise [30, 31] recently,

$$f_{D_s}|\text{expt}| = 277 \pm 9 \text{ MeV}, \quad (4.17)$$

assuming $|V_{cs}| = 1$. Given confirmation between two experiments,⁵ there is little likelihood that the experimental number would change much. It should be noted that the CLEO and Belle measurements are sufficiently different, such that the systematic errors are not common.

The experimental result has been compared [33] recently with a *very precise* result from the lattice [34],

$$f_{D_s}|\text{latt}| = 241 \pm 3 \text{ MeV} \quad (\text{“rooting”}). \quad (4.18)$$

Note the % level errors for a nonperturbative lattice result! This precision arises in the “improved” staggered fermion approach in lattice QCD, with a big assumption to simplify the computation of the fermion determinant, called “rooting.” By taking

⁵ We note that the BaBar measurement [32] is not an absolute branching ratio measurement. But the result is similar in any case.

the fourth root of the quark determinant (a very complicated quantity that is in large part the gist of the lattice sea, or dynamical, quark effects), it drastically reduces the amount of computation needed. No other approach has been able to compete in the numerical precision reached by staggered fermions, although this is badly needed to check the systematic error of “rooting.” However, [33] claims that the precision of (4.18) can stand scrutiny. The authors then go on to claim that this discrepancy suggests New Physics.

It is not our purpose to comment on the intricacies of lattice QCD computations. In Sect. 3.1.3, we have in fact used the discrepancy of the above two equations to argue, in an intuitive way, that B_s mixing in SM is likely to be larger than the experimental measurement of (3.13). From that standpoint, we find the claim of [33] incredulous. The percent level numerical accuracy of a lattice calculation should be scrutinized thoroughly by the lattice QCD community before such a claim can be made. Afterall, unlike the experimental situation, (4.18) is so far a stand-alone result. Furthermore, the New Physics “models” proposed by [33], unlike our general arguments [23] for H^+ effects, are rather constructed and ad hoc, and not the ones that one would normally contemplate.

If the tree-dominant and Cabibbo-allowed $D_s^+ \rightarrow \ell^+ \nu$ is the chosen mode to reveal to us the first signs of New Physics, then, to paraphrase Einstein, “the Lord would be malicious.”

References

1. Alam, M.S. [CLEO Collaboration]: Phys. Rev. Lett. **74**, 2885 (1995) 57, 58, 59
2. Bertolini, S., Borzumati, F., Masiero, A.: Phys. Rev. Lett. **59**, 180 (1987) 57, 62
3. Deshpande, N.G., Lo, P., Trampetic, J., Eilam, G., Singer, P.: Phys. Rev. Lett. **59**, 183 (1987) 57, 62
4. Grinstein, B., Wise, M.: Phys. Lett. B **201**, 274 (1988) 57, 61, 62
5. Hou, W.S., Willey, R.S.: Phys. Lett. B **202**, 591 (1988) 57, 61, 62, 63, 64
6. Misiak, M., et al.: Phys. Rev. Lett. **98**, 022002 (2007) 57, 60, 62, 63
7. Ammar, R., et al. [CLEO Collaboration]: Phys. Rev. Lett. **71**, 674 (1993) 58
8. Aubert, B., et al. [BaBar Collaboration]: Phys. Rev. D **72**, 052004 (2005) 59
9. Koppenburg, P., et al. [Belle Collaboration]: Phys. Rev. Lett. **93**, 061803 (2004) 59, 60, 61
10. See the webpage of the Heavy Flavor Averaging Group (HFAG). <http://www.slac.stanford.edu/xorg/hfag>. We usually, but not always, take the Lepton-Photon 2007 (LP2007) numbers as reference 60, 62
11. Buras, A.J., Czarnecki, A., Misiak, M., Urban, J.: Nucl. Phys. B **631**, 219 (2002) 60
12. Becher, T., Neubert, M.: Phys. Rev. Lett. **98**, 022003 (2007) 61
13. Abe, K., et al. [Belle Collaboration]: arXiv:0804.1580 [hep-ex], Belle conference paper BELLE-CONF-0802 (unpublished) 61
14. Aubert, B., et al. [BaBar Collaboration]: Phys. Rev. D **77**, 051103 (2008) 61
15. Hou, W.S., Willey, R.S.: Nucl. Phys. B **326**, 54 (1989) 64
16. Grzadkowski, B., Hou, W.S.: Phys. Lett. B **272**, 383 (1991) 64, 70
17. Coan, T.E., et al. [CLEO Collaboration]: Phys. Rev. Lett. **80**, 1150 (1998) 64
18. Hou, W.S.: Nucl. Phys. B **308**, 561 (1988) 64
19. Krawczyk, P., Pokorski, S.: Phys. Rev. Lett. **60**, 182 (1988) 64
20. Buskulic, D., et al. [ALEPH Collaboration]: Phys. Lett. B **298**, 479 (1993) 64
21. Yao, W.M., et al. [Particle Data Group]: J. Phys. G **33**, 1 (2006) 64
22. Amsler, C., et al.: Phys. Lett. B **667**, 1 (2008); and <http://pdg.lbl.gov/> 64

23. Hou, W.S.: Phys. Rev. D **48**, 2342 (1993) 65, 66, 70, 71
24. The paper only appeared in 1995, Artuso, M., et al. [CLEO Collaboration]: Phys. Rev. Lett. **75**, 785 (1995) 65
25. Ikado, K., et al. [Belle Collaboration]: Phys. Rev. Lett. **97**, 251802 (2006) 67, 68
26. Aubert, B., et al. [BaBar Collaboration]: Phys. Rev. D **77**, 011107 (2008) 67, 68
27. Matyja, A., et al. [Belle Collaboration]: Phys. Rev. Lett. **99**, 191807 (2007) 68
28. Aubert, B., et al. [BaBar Collaboration]: Phys. Rev. Lett. **100**, 021801 (2008) 69
29. Grzadkowski, B., Hou, W.S.: Phys. Lett. B **283**, 427 (1992) 69, 70
30. Artuso, M., et al. [CLEO Collaboration]: Phys. Rev. Lett. **99**, 071802 (2007) 70
31. Widhalm, L., et al. [Belle Collaboration]: Phys. Rev. Lett. **100**, 241801 (2008) 70
32. Aubert, B., et al. [BaBar Collaboration]: Phys. Rev. Lett. **98**, 141801 (2007) 70
33. Dobrescu, B.A., Kronfeld, A.S., Phys. Rev. Lett. **100**, 241802 (2008) 70, 71
34. Follana, E., Davies, C.T.H., Lepage, G.P., Shigemitsu, J., Phys. Rev. Lett. **100**, 062002 (2008) 70

Chapter 5

Electroweak Penguin: bsZ Vertex, Z' , Dark Matter

In Sect. 2.2, we discussed the effects of the $b \rightarrow s\bar{q}q$ electroweak penguin interfering with the strong penguin and tree amplitudes. The quintessential electroweak penguin would be $b \rightarrow s\ell^+\ell^-$ decay or $b \rightarrow s\nu\nu$ that has no photonic contribution. We now discuss how the study of these processes, present already in SM, could help us probe New Physics as well. Besides presenting some background development, we will focus on the forward–backward asymmetry $A_{\text{FB}}(B \rightarrow K^*\ell^+\ell^-)$ as a probe of the bsZ vertex, comment briefly on a possible Z' boson as a source for generating effective $[\bar{s}b][\bar{\ell}\ell]$ and $[\bar{s}b][\bar{\nu}\nu]$ four-fermi interactions, and treat $b \rightarrow s\nu\nu$, which has the same signature as $b \rightarrow s + \text{nothing}$, as a probe of *light* Dark Matter (DM).

5.1 $A_{\text{FB}}(B \rightarrow K^*\ell^+\ell^-)$

5.1.1 Observation of m_t Enhancement of $b \rightarrow s\ell^+\ell^-$

The $B \rightarrow K^{(*)}\ell^+\ell^-$ process ($b \rightarrow s\ell^+\ell^-$ at inclusive level) arises from photonic penguin, Z penguin, and box diagrams, as shown in Fig. 5.1.

At first sight, one would think that the photonic penguin is at αG_F order (α from QED, G_F from one W), while the Z penguin and box diagrams, which have *two* heavy vector boson propagators, are effectively at G_F^2 order of weak interactions. Since G_F is small compared to the physical decay scale of m_b^2 , it seems intuitive to drop the Z penguin and box diagrams. This was in fact what was first [1] done historically. But it was soon pointed out [2] that the Z penguin (gauge related to both the photon penguin and box diagrams) would in fact dominate for large m_t ! We have already discussed this “nondecoupling” phenomenon of the SM heavy t quark in Sect. 3.2.3, but it is worthwhile to understand the origins of this.

A heuristic way to see Z penguin dominance of $b \rightarrow s\ell^+\ell^-$ is to observe that the above “ G_F power counting” has a loophole. Comparing αG_F of the photonic penguin with G_F^2 of the Z penguin, the two factors actually have different mass dimensions. To compensate, the latter should be written as $G_F^2 m^2$. This has been used in our simple power counting above, where we have used m_b^2 in a tacit way. However, from subtleties of the diagrams involved, and supported by a full calculation, one

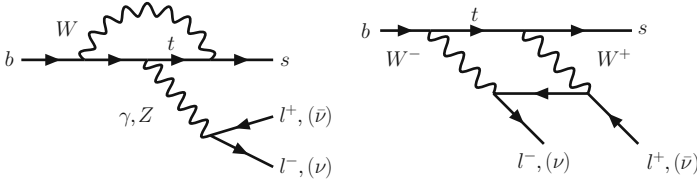


Fig. 5.1 Photonic penguin, Z penguin, and the box diagram for $b \rightarrow s \ell^+ \ell^-$, $s \nu \bar{\nu}$

finds m_t^2 instead of m_b^2 as the outcome. $G_F m_t^2$ is certainly not negligible compared to α for m_t above 100 GeV or so.

The source of this nondecoupling of SM heavy quarks is due to their large Yukawa couplings. Note that heavy particle propagators in general lead to decoupling, i.e., heavy mass effects are normally decoupled, with G_F power counting as a good example.¹ So, one would have thought that the effect of a heavy top would also be decoupled. In pure QED and QCD processes, this would indeed be the case. However, the weak interaction (or $SU(2) \times U(1)$) is more complicated:

$$\lambda_t \equiv \sqrt{2} \frac{m_t}{v} \quad (5.1)$$

is the dynamical Yukawa coupling, where v is the v.e.v. scale. The heaviness of m_t is a dynamical effect. It turns out that two powers of Yukawa couplings remain for the Z loop calculation, which results in *nondecoupling*. So why does this not happen for the photonic penguin?

It is not our purpose to present any diagrammatic calculations. However, it would be elucidating to give an account of the subtleties that distinguishes the γ and Z penguins, i.e., $\bar{s}b\gamma$ and $\bar{s}bZ$ couplings. So let us try to be as lucid as possible and explain in a language that hopefully even experimenters can grasp (see also Footnote 3 of Chap. 4). In attempting the calculations for the diagrams of Fig. 5.1, one would like to ignore all external masses and momenta as much as possible, since m_b^2/M_W^2 is small (i.e., $G_F m_b^2$ is negligible). In so doing, one then discovers that the $\bar{s}b\gamma$ vertex would vanish in the $m_b^2/M_W^2 \rightarrow 0$ limit. Hence, to extract the $\bar{s}b\gamma$ vertex, extra care needs to be taken, and one needs to make an expansion in small external masses and momenta, before setting them to zero. Alternatively, one recalls that the photon, even if off-shell, couples to conserved currents. This is a requirement of gauge invariance. A vanishing vertex is of course trivially conserved, but to have a nontrivially conserved $\bar{s}b\gamma$ vertex, the effective vertex would depend on the *external* momentum and mass(es). The point is that m_b and m_s are of unequal mass, so $\bar{s}\gamma_\mu b$ is not a conserved current.

In the notation of Inami and Lim [3], we write the effective $\bar{s}b\gamma$ vertex as

$$\bar{s} \left[(q^2 \gamma_\mu - q_\mu \not{q}) \mathcal{F}_1 + i \sigma_{\mu\nu} q^\nu (m_b R + m_s L) \mathcal{F}_2 \right] b, \quad (5.2)$$

¹ Technically, this statement is actually not true. For low energy tree-level effects, it is the process mass scale vs M_W scale that provides suppression. See below.

where q is the four-momentum carried off by the photon. It is clear that (5.2) is explicitly conserved, i.e., contracting with q^μ , both terms vanish. Note that the q_μ term, when contracting with another conserved current (e.g., $\bar{\ell}\gamma_\mu\ell$ in our case, or an external photon polarization vector), would vanish. Furthermore, the contribution of the \mathcal{F}_1 “form factor” would vanish for on-shell ($q^2 = 0$) photons. So, it is the \mathcal{F}_2 term that contributes to physical $b \rightarrow s\gamma$ decay, but both \mathcal{F}_1 and \mathcal{F}_2 contribute to $b \rightarrow s\ell^+\ell^-$.

We see now what must be collected in expanding the $\bar{s}b\gamma$ vertex of Fig. 5.1: we must collect $q^2\gamma_\mu$ and $q_\mu q_\nu$, as well as $\sigma_{\mu\nu}q^\nu m_{b,s}$ terms. That they come together to give the form of (5.2) is a check on the calculation. In contrast, the $\bar{s}bZ$ vertex is not conserved, because the electroweak gauge invariance is spontaneously broken down to electromagnetism. Thus, in computing the $\bar{s}bZ$ vertex of Fig. 5.1, one does not need to put the vertex in the form of (5.2), and in fact one could set m_b^2/M_W^2 to zero from the outset. It is this subtlety, that the electromagnetic current is conserved, but the charge and neutral current is not, that sets apart the behavior (in m_t dependence) of the $\bar{s}b\gamma$ and $\bar{s}bZ$ couplings.

The result above is of course gauge invariant. In the physical gauge, the longitudinal components of the W^+ boson lead to m_t in the numerator in the $\bar{t}bW^+$ coupling. In gauges where one has unphysical scalars ϕ_W^+ , these are the would-be Goldstone bosons that got “eaten” by the W^+ boson to make it heavy, and, as a partner to the SM neutral Higgs boson, it couples to top via (5.1). The whole picture works consistently for the $\bar{s}bZ$ vertex, which is not conserved, but for the $\bar{s}b\gamma$ vertex, the requirement of (5.2) by current conservation replaces the possible m_t^2 factors by q^2 and $m_{b(s)}q$, and the m_t effect for $\bar{s}b\gamma$ is closer to the decoupling kind,² as already commented on in Sect. 3.2.3.

We have thus given arguments for why the m_t dependence of photonic and Z penguins are so different, and how the latter could dominate for large enough m_t . It is intricately related to spontaneous symmetry breaking and mass generation in the electroweak theory. A full calculation of course bears all this out. We plot in Fig. 5.2 the more than 20 years old result from the original observation [2] of large m_t enhancement of the decay rates of $b \rightarrow s\ell^+\ell^-$, $s\nu\bar{\nu}$. Note that $b \rightarrow s\mu^+\mu^-$ is slightly smaller than $b \rightarrow se^+e^-$, because the latter has a low q^2 enhancement from the photonic penguin. The strong, almost m_t^2 dependence is most apparent for $b \rightarrow s\nu\bar{\nu}$, which has no photon contribution, and we have summed over three neutrinos. Of course, much progress has been made in sophisticated calculations of the rates of $b \rightarrow s\ell^+\ell^-$, $s\nu\bar{\nu}$. However, the results of Fig. 5.2 captures the main effect, and all subsequent calculations are corrections.

Although $b \rightarrow s\gamma$ was already observed by CLEO in the 1990s, the first observation of an electroweak penguin decay was only made by Belle in 2001. With 31.3M $B\bar{B}$ pairs, combining $B \rightarrow Ke^+e^-$ and $K\mu^+\mu^-$ events (K stands for both charged and neutral kaons), Belle observed [4] ~ 14 events with a combined statistical

² For the $\bar{s}b\gamma$ vertex, the photon can also radiate off the W^+ (not shown in Fig. 5.1). But for the $\bar{s}bg$ vertex, the gluon can only radiate off the top. With always two top propagators, the $\bar{s}bg$ vertex has even weaker m_t dependence.

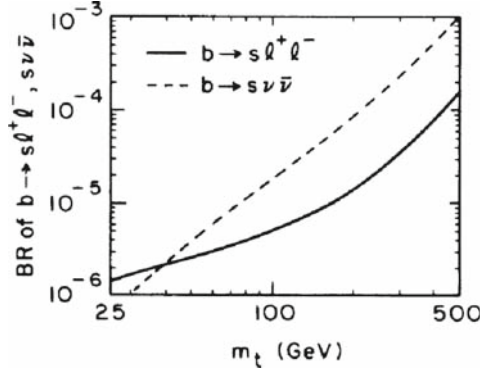


Fig. 5.2 Large m_t enhancement [2] of $b \rightarrow s\ell^+\ell^-$, $s\nu\bar{\nu}$ rates. [Copyright (1987) by The American Physical Society.]

significance of 5.3σ for $B \rightarrow K\ell^+\ell^-$. The result was consistent with SM, but subject to $B \rightarrow K$ form factors, so the interpretation is less interesting. Observation of $B \rightarrow K^*\ell^+\ell^-$ [5, 6] soon followed. Repeating the $b \rightarrow s\gamma$ history, the inclusive $b \rightarrow s\ell^+\ell^-$ measurement ($B \rightarrow X_s\ell^+\ell^-$ experimentally) was subsequently observed a year or so later, by Belle in summer 2002. With 65.4M $B\bar{B}$ pairs and again combining e^+e^- and $\mu^+\mu^-$, a total of ~ 60 events were observed [7] with 5.4σ statistical significance, and $b \rightarrow s\ell^+\ell^-$ became experimentally established.

Many modes, including the exclusive $B \rightarrow \pi\ell\ell$, $\rho\ell\ell$ modes (replacing s by d in Fig. 5.2), have now been searched for. A new study, based on 657M $B\bar{B}$ pairs by Belle [8], has pushed the limit on $B^+ \rightarrow \pi^+\ell^+\ell^-$ down to the 5×10^{-8} level, which is only a factor of 1.5 above SM expectations [9]. Put differently, it seems that the measurement of $B \rightarrow \pi\ell\ell$ and $b \rightarrow d\ell\ell$ is a Super B Factory subject.

In the experimental studies, one cuts out the J/ψ and ψ' resonance regions in q^2 , as these produce the same final states and are in fact much larger. These charmonium regions actually provide a large control sample to test the fit models for the electroweak penguin study. The results on electroweak penguins as of 2008 are summarized in Fig. 5.3. The inclusive rate is consistent with SM expectations (see, e.g., [10]), hence confirming the large m_t enhancement [2]. Note that the latter observation was made in 1986, prior to the ARGUS discovery [11] of large B_d mixing, which led to the change in mindset that the top quark is uniquely heavy.

Given that the top is a v.e.v. scale fermion, we could say that TeV scale physics influenced the $b \rightarrow s\ell\ell$ rate, as a prime example of the flavor–TeV link. Since electroweak symmetry breaking is the main theme for the LHC as a machine to probe, to go above the v.e.v. scale, the complementary nature of $b \rightarrow s\ell\ell$ with the high energy approach again resonates with the cartoon of Fig. 1.1. Our special interest in the fourth generation can also be seen from this perspective [2]. The t' quark, being a SM-type chiral quark with mass generated through the analog of (5.1) can also affect the bsZ coupling, so $b \rightarrow s\ell\ell$ is also a sensitive probe of t' , as we shall soon see.

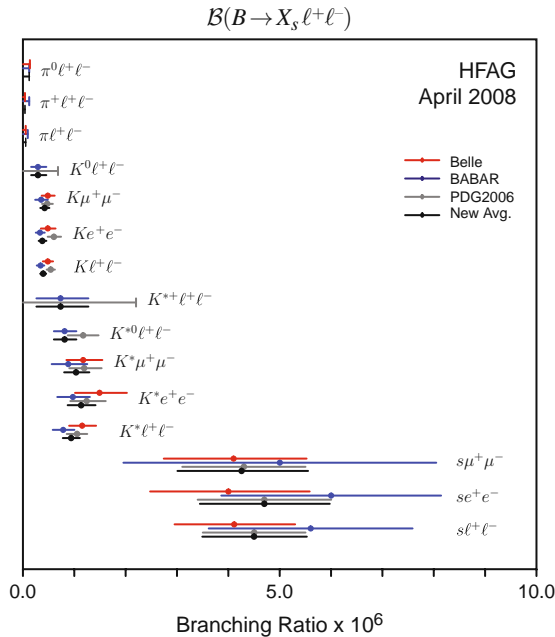


Fig. 5.3 HFAG plot for various $B \rightarrow X \ell^+ \ell^-$ measurements

5.1.2 B Factory Measurements of $A_{\text{FB}}(B \rightarrow K^* \ell^+ \ell^-)$

The top quark exhibits nondecoupling in the Z penguin and box diagrams, which is analogous to the electroweak penguin effect in $B^+ \rightarrow K^+ \pi^0$ and the box diagrams for $B_s^0 - \bar{B}_s^0$ mixing. We have elucidated that, due to this nondecoupling effect of the top quark, the Z penguin dominates the $b \rightarrow s \ell^+ \ell^-$ decay amplitude [2].

Not long after the large m_t enhancement was pointed out, it was soon noted that interference between the vector (γ and Z) and axial vector (Z only, box as an appendage) contributions in $b \rightarrow s \ell^+ \ell^-$ production gives rise to an interesting forward–backward asymmetry [12]. This is akin to the familiar \mathcal{A}_{FB} in $e^+ e^- \rightarrow f \bar{f}$, but the *enhancement of the bsZ effective coupling compared with the $bs\gamma$ effective coupling brings the Z from M_Z down to below the B mass, much closer to the γ* . Furthermore, *one now probes potential New Physics in the $b \rightarrow s$ loop*. Since interference between amplitudes is the essence of quantum physics, thus, \mathcal{A}_{FB} is of great interest. In particular, for the differential $d\mathcal{A}_{\text{FB}}(q^2)/dq^2$ asymmetry, the variation over $q^2 \equiv m_{\ell\ell}^2$ probes different regions of interference between $bs\gamma$ and bsZ .

It is more than a figure of speech to say that the $\ell^+ \ell^-$ pair in the final state, much like an electron microscope that scatters an electron wave off the material being probed, actually provides us with a “microscope” to look back at what is happening inside the loop-induced $bs\gamma$ and bsZ vertices.

With both the inclusive $B \rightarrow X_s \ell^+ \ell^-$ and exclusive $B \rightarrow K^{(*)} \ell^+ \ell^-$ decays measured [5, 6, 13] (see Fig. 5.3), experimental interest turned to \mathcal{A}_{FB} for $B \rightarrow K^* \ell^+ \ell^-$. The study for inclusive \mathcal{A}_{FB} , though desirable, is more challenging because of background issues and largely impossible in a hadronic environment. The experimentally defined forward–backward asymmetry is

$$\frac{d\mathcal{A}_{\text{FB}}(q^2)}{dq^2} \equiv \frac{d\mathcal{B}/dq^2|^{+} - d\mathcal{B}/dq^2|^{-}}{d\mathcal{B}/dq^2|^{+} + d\mathcal{B}/dq^2|^{-}}, \quad (5.3)$$

where $d\mathcal{B}/dq^2$ is the differential rate, and the \pm superscript indicates forward and backward moving ℓ^+ versus the B meson direction in the $\ell^+ \ell^-$ frame.

Since the process is quite easy to visualize, let us give the quark level decay amplitude [9],

$$\begin{aligned} \mathcal{M}_{b \rightarrow s \ell^+ \ell^-} \propto V_{cs}^* V_{cb} \left\{ -2 \frac{m_b m_B}{q^2} C_7^{\text{eff}} [\bar{s} i \sigma_{\mu\nu} \hat{q}^\nu R b] [\bar{\ell} \gamma^\mu \ell] \right. \\ \left. + C_9^{\text{eff}} [\bar{s} \gamma_\mu L b] [\bar{\ell} \gamma^\mu \ell] + C_{10} [\bar{s} \gamma_\mu L b] [\bar{\ell} \gamma^\mu \gamma_5 \ell] \right\}, \quad (5.4) \end{aligned}$$

which is of the same form as 20 years ago [2], with short distance physics, including within SM, isolated in the Wilson coefficients C_7^{eff} , C_9^{eff} , and C_{10} , which can be systematically computed. The $1/q^2$ term clearly carries the C_7 effective photon contribution, which comes from the $\sigma_{\mu\nu}$ term in (5.2), while C_9^{eff} and C_{10} are from the Z penguin (as well as the $q^2 \gamma_\mu$ term of (5.2) and the box diagram). We have factored out $V_{cs}^* V_{cb}$ instead of the usual $V_{ts}^* V_{tb}$. This has the advantage of being the product of CKM elements that are already measured and real by standard convention [5, 6].

A commonly used formula for the differential \mathcal{A}_{FB} is

$$\frac{d\mathcal{A}_{\text{FB}}(q^2)}{dq^2} \propto C_{10} \xi(q^2) \left[\text{Re}(C_9^{\text{eff}}) F_1 + \frac{1}{q^2} C_7^{\text{eff}} F_2 \right]. \quad (5.5)$$

The formulas for $\xi(q^2)$ and the form factor-related functions F_1 and F_2 can be found in [9]. Within SM, the Wilson coefficients are practically real, as has been ingrained into the formula. This form has somehow influenced the development of the subject, as we will discuss. Actually, C_9^{eff} receives some long distance $c\bar{c}$ effect that can be absorptive [2], hence the real part is taken since this is not a CPV observable.

As shown in Fig. 5.4, the study of forward–backward asymmetry in $B \rightarrow K^* \ell^+ \ell^-$ by Belle with 386M $B\bar{B}$ pairs [14] is consistent with SM and rules out the possibility of flipping the sign of C_9 or C_{10} separately from SM value (the two lower curves). But having both C_9 or C_{10} flipped in sign, equivalent to flipping sign of C_7 , is not ruled out. BaBar took the more conservative approach of giving \mathcal{A}_{FB} in just two q^2 bins, below and above $m_{J/\psi}^2$. With 229M $B\bar{B}$, the higher q^2 bin is consistent [15] with SM and disfavors BSM scenarios. Interestingly, in the lower q^2

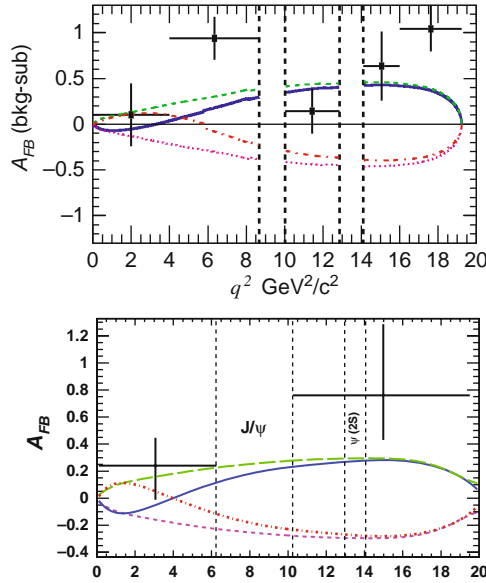


Fig. 5.4 Measurements of $A_{\text{FB}}(B \rightarrow K^* \ell^+ \ell^-)$ by Belle [14] [Copyright (2006) by The American Physical Society] and BaBar [16]. The two lower curves are for flipping the sign of either C_9 or C_{10} with respect to SM (solid curve), while the upper curve is for C_9 and C_{10} both flipping sign

bin, while sign-flipped BSMs are less favored, the measurement is $\sim 2\sigma$ away from SM. This is not inconsistent with the Belle result.

BaBar has updated with 384M $B\bar{B}$ pairs [16], which is shown in the second plot in Fig. 5.4. For the high q^2 bin, the results are qualitatively the same as before. For the low q^2 bin ($4m_\mu^2$ to $6.25 \text{ GeV}^2/c^4$), BaBar has improved its measurement to $A_{\text{FB}}|_{\text{low } q^2} = 0.24^{+0.18}_{-0.23} \pm 0.05$. The SM expectation in this region is $A_{\text{FB}}|_{\text{low } q^2}^{\text{SM}} = -0.03 \pm 0.01$. Though not excluded, viewed together with the Belle result, it seems that the low q^2 behavior is not quite SM-like.³

5.1.3 Interpretation and Future Prospects

While the above is interesting, it should be clear that the B Factory statistics is still rather limited and cannot be much improved without a Super B Factory. But LHCb can do very well in this regard within a couple of years of LHC turn-on.

³ Note added: Belle announced their 657M $B\bar{B}$ pair result at ICHEP2008 [17], improving on the published result. All q^2 bins (six in all) turn out positive, and the deviation from SM becomes even more acute. It would be desirable to give a combined experimental significance on the deviation from SM expectations.

Wilson Coefficients with Finite Weak Phase

In view of the LHCb prospects, we recently noticed [18] that, in (5.5), there is no reason a priori why the Wilson coefficients should be kept real when probing BSM physics! This can be seen most easily by inspection of (5.4): the Wilson coefficients are effective couplings of four-fermi interactions, and in a theory that allows for CPV, in general they should be complex from CPV phases. If one keeps an open mind (rather than, for example, taking the oftentimes tacitly assumed Minimal Flavor Violation, or MFV [19], mindset), (5.5) should be restored to its proper form,

$$\frac{dA_{\text{FB}}(q^2)}{dq^2} \propto \text{Re}(C_9^{\text{eff}} C_{10}^*) F_1' + \frac{1}{q^2} \text{Re}(C_7^{\text{eff}} C_{10}^*) F_2', \quad (5.6)$$

where we have absorbed $\xi(q^2)$ into the F_i' form factor combinations. In pointing this out, we stress that we are not concerned with CP conserving long distance effects such as in C_9^{eff} , but the possibility that the C_i s may pick up BSM weak (CP violating) phases. If present, they could enrich the interference pattern through (5.6), in contrast to the usual form of (5.5), which basically takes the short distance Wilson coefficients as real *by fiat*. After all, if P_{EW} is the culprit for the $\Delta A_{K\pi}$ problem discussed in Sect. 2.2, the equivalent C_9 and C_{10} for $B^+ \rightarrow K^+\pi^0$ decay seem to carry *large* weak phases. Let Nature speak through $B \rightarrow K^*\ell^+\ell^-$ data!

Taking the sign convention of LHCb, which is opposite to Belle and BaBar, we illustrate [18] in Fig. 5.5 the situation where New Physics enters through effective bsZ and $bs\gamma$ couplings. In this case, with $\ell^+\ell^-$ produced from the virtual Z^* , C_9 , and C_{10} cannot differ by much at short distance, which is the reason for the “degenerate tail” for larger $\hat{s} \equiv q^2/m_B^2$ (when the effect of C_7 becomes unimportant) in the $dA_{\text{FB}}/d\hat{s}$ plot. We allow the Wilson coefficients to be only constrained by the measured radiative ($b \rightarrow s\gamma$) and electroweak ($b \rightarrow s\ell\ell$) penguin rates, hence $dB/d\hat{s}$ may vary in the shaded area in Fig. 5.5, then dA_{FB}/dq^2 could in fact vary in the corresponding shaded region, where the variation is more prominent for $q^2 < m_{J/\psi}^2$. Conventional wisdom suggest that it is the precise position of the

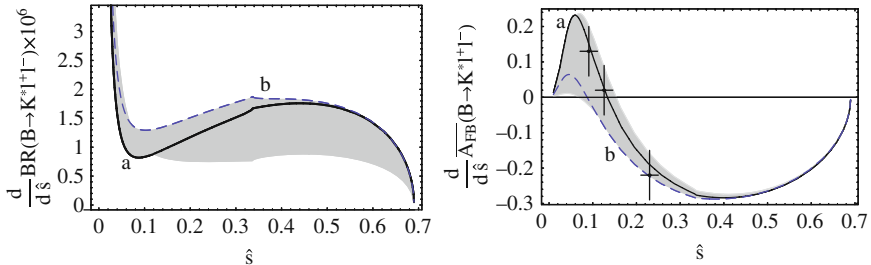


Fig. 5.5 Possible dA_{FB}/dq^2 in $B \rightarrow K^*\ell^+\ell^-$ allowed by complex Wilson coefficients [18], (5.6) [Copyright (2008) by The American Physical Society]. The three data points are taken from 2 fb^{-1} LHCb Monte Carlo for illustration, which has the power to distinguish between SM (solid curve) vs e.g. fourth generation model (dashed curve). The sign convention is opposite that of Belle and BaBar

zero that is of interest, in part because it is less form factor dependent. We see that, allowing for sizable weak phases for the Wilson coefficients, the position of the zero can be anywhere around or below the SM expectation.

The fourth generation with parameters as determined from Δm_{B_s} , $\mathcal{B}(B \rightarrow X_s \ell^+ \ell^-)$ and $\Delta \mathcal{A}_{K\pi}$ belongs to the class of BSM models of Fig. 5.5 and gives rise to [18] the dashed line, which is close to the lower boundary of the shaded region for $d\mathcal{A}_{\text{FB}}/d\hat{s}$. The SM result is close to the upper boundary. Note that for the differential decay rate, the fourth generation is at the upper boundary and could run into trouble if the measured rate drops further. However, this would be a form factor-dependent issue. To get a feeling for the future, we take the MC study [20, 21] for 2 fb^{-1} data by LHCb (achievable in a couple years of running, once LHC reaches productive luminosity) and plot three sample data points for $d\mathcal{A}_{\text{FB}}/d\hat{s}$ to illustrate expected data quality. These data points are based on MC studies of events generated from the SM (solid line). It is clear that LHCb can distinguish between SM and the fourth generation, or other New Physics models in the shaded region.

Back to the present (closing) period of the B Factory era. From Fig. 5.5, we could also compare with Belle and BaBar data [14–16] shown in Fig. 5.4 and see that the current data are already probing the difference between SM and the fourth-generation model⁴ or the more general statement that Wilson coefficients C_i could be complex, i.e., carry weak phase. As stated, the SM expectation is $\mathcal{A}_{\text{FB}} \sim -0.03$ (*note the B Factory sign convention*) for the region $q^2 \in (4m_\mu^2, 6.25 \text{ GeV}^2/c^4)$. This can be understood from the solid curve in Fig. 5.5(b), where the corresponding region is $\hat{s} < 0.22$. Since there is a crossing over zero, and since the region below the zero is slightly larger than above, we see that the SM expectation is slightly negative. But Belle and BaBar data both indicate that $\mathcal{A}_{\text{FB}} > 0$ is preferred. This is sometimes phrased as “ $C_7 = -C_7^{\text{SM}}$ seems preferred from \mathcal{A}_{FB} data,” but it should be viewed as just a way of expression, since it has been pointed out [22] that $C_7 = -C_7^{\text{SM}}$, i.e., flipping the sign of the photonic penguin, would lead to too large a $B \rightarrow X_s \ell^+ \ell^-$ rate as compared with experiment.

This actually illustrates our point to use (5.6) rather than (5.5) in fitting data. In fact, we could even claim that Belle and BaBar data favor somewhat the fourth-generation curve in Fig. 5.5. Compared with the solid curve, the zero for the dashed curve has moved to much lower q^2 , with a drop in peak value as well. Therefore, in the fourth-generation model which is motivated by $\Delta \mathcal{A}_{K\pi}$ (Sect. 2.2.2), and maybe now the hint for large and negative $\sin 2\Phi_{B_s}$ as well (Sect. 3.2), we have $\mathcal{A}_{\text{FB}} > 0$ for the low q^2 bin, which is in better agreement with data. This offers a third hint that maybe the fourth-generation model where sizable $b \rightarrow s$ CPV phase should be taken seriously !

⁴ It is gratifying that in their recent update, the BaBar experiment [16] has adopted our argument and now uses (5.6) as the reference formula.

Prognosis

It should be clear that the LHCb experiment has good discovery potential using \mathcal{A}_{FB} to probe the presence of weak phases in short distance Wilson coefficients, *without measuring CPV*. It is interesting to note that, once again the Tevatron could possibly make earlier impact. With 1 fb^{-1} data, CDF has demonstrated [23] branching ratio measurement capability in $B^0 \rightarrow K^{*0} \mu^+ \mu^-$, comparable to that of Belle and BaBar. However, CDF and DØ seem more interested in studying $B_s \rightarrow \phi \mu^+ \mu^-$, which is certainly of interest, but has not made any further update on $B^0 \rightarrow K^{*0} \mu^+ \mu^-$. But given that CDF and DØ expect to accumulate of order $6\text{--}8 \text{ fb}^{-1}$ data per experiment by 2009–2010, if the studies of $B^0 \rightarrow K^{*0} \mu^+ \mu^-$ could continue toward \mathcal{A}_{FB} measurement, there is good potential for Tevatron to improve on Belle and BaBar results for \mathcal{A}_{FB} , which would also be updated with the full data set. *A more definite statement on whether SM is disfavored could come forth before LHCb data arrives.*

If there is New Physics that affects the $[\bar{s}b][\bar{\ell}\ell]$ four-quark operator, for example in Z' models with FCNC couplings, the allowed range for \mathcal{A}_{FB} is practically unlimited [18]. But the Z' model is quite arbitrary as a low energy effective theory. Unlike the fourth-generation model which links many processes through CKM unitarity, the Z' model has too much freedom in “U(1)” charges, hence not predictive. It would be better to discuss the Z' model once an extra Z' is discovered at the LHC, and then check its flavor properties.

Finally, if large deviations from SM are uncovered for \mathcal{A}_{FB} and one infers the presence of new CPV phases through bsZ and $bs\gamma$ interference, one would then expect sizable direct CPV in $b \rightarrow s\gamma$ [18]. For example, in our fourth-generation model, $\mathcal{A}_{\text{CP}}(b \rightarrow s\gamma) \sim 2\%$ is predicted, while much larger DCPV is possible for wilder possibilities. $\mathcal{A}_{\text{CP}}(b \rightarrow s\gamma)$ measurement is another major goal for the Super B Factory upgrade, but probably only to % level precision. There are other measurables for $B \rightarrow K^* \ell \ell$ as well, such as K^* longitudinal polarization fraction F_L and the transverse asymmetries $A_T^{(1)}$ and $A_T^{(2)}$. These are akin to similar quantities in $B \rightarrow \phi K^*$ angular analysis [24] and would be interesting in the long run. Preliminary results from BaBar [16] indicate that F_L is low compared to SM expectation in the low q^2 bin, which also seems to prefer “ $C_7 = -C_7^{\text{SM}}$ ” over SM.

5.2 $B \rightarrow K^{(*)} \nu \nu$

We will be somewhat cursory in this section, because the subject is still at its infancy and the SM sensitivity is not yet reached.

The $B \rightarrow K^* \nu \nu$ (and $b \rightarrow s \nu \nu$) decay mode is attractive from the theory point of view, since the photonic penguin does not contribute, nor do J/ψ or ψ' decay to $\bar{\nu} \nu$. It can arise only from short distance physics, such as Z penguin and box diagram contributions [2] in Fig. 5.1, hence the decay rates are better predicted. Note that the SM expectation for $B^+ \rightarrow K^+ \nu \bar{\nu}$, at 4×10^{-6} level [25], is about an order of magnitude larger than $B^+ \rightarrow K^+ \ell^+ \ell^-$. Of course, a rough factor of 6 comes from [2] counting three neutrinos, and Z charge of e vs. ν .

The search for these processes allows us to probe, in principle, what happens in the bsZ loop in a clean way. Since the neutrinos go undetected, what is of special interest is that the process also allows us to probe light Dark Matter (DM), which is complementary to the DAMA/CDMS type of direct search. This is because the latter type of experiments rely on detecting special electronic signals arising from a nucleus displaced by a DM particle. But this means that the approach loses sensitivity for light DM particles. Such DM pairs could arise from exotic Higgs couplings to the $b \rightarrow s$ loop.

5.2.1 Experimental Search

Though clean theoretically, with two missing neutrinos, the experimental signal is rather poor, and hence has not been widely searched for. In fact, it is complementary with $B^+ \rightarrow \tau^+ \nu$ search for semileptonic τ decays. A simple estimate shows that $B^+ \rightarrow \tau^+ \nu \rightarrow K^+ \nu \nu$ is subdominant to the direct $B^+ \rightarrow K^+ \nu \nu$ electroweak penguin decay, while the CKM suppressed $B^+ \rightarrow \pi^+ \nu \nu$ electroweak penguin decay is subdominant compared to $B^+ \rightarrow \tau^+ \nu \rightarrow \pi^+ \nu \nu$. As we have seen in Sect. 4.2, compounded with a larger $B^+ \rightarrow \tau^+ \nu \rightarrow \pi^+ \nu \nu$ rate, with the addition of the leptonic τ decay modes, it is $B^+ \rightarrow \tau^+ \nu$ that is already measured (Sect. 4.2).

At the B factories, BaBar pioneered $B^+ \rightarrow K^+ \nu \nu$ search, using the approach of full reconstruction of the other charged B meson (see Fig. 4.5). With 89M $B\bar{B}$ pairs, the 90% C.L. limit of 5.2×10^{-5} was obtained [26] for $B^+ \rightarrow K^+ \nu \nu$, which is more than an order of magnitude above SM. More recently, as a companion study to $B \rightarrow \tau \nu$ search, Belle has searched in many modes with a large data set of 535M $B\bar{B}$ pairs [27], again using the aforementioned method of full reconstruction of the other B . No signal was found, and the most stringent limit is 1.4×10^{-5} in $B^+ \rightarrow K^+ \nu \nu$. This is still more than a factor of 3 above the SM expectation of $\sim 4 \times 10^{-6}$ for this mode.⁵ However, it strengthens the bound on light DM production in $b \rightarrow s$ transitions [28]. A complementary approach for search of light DM, as well as light exotic Higgs bosons, is discussed in Chap. 7.

It seems that to measure the theoretically clean $B \rightarrow K^* \nu \nu$ modes, one again requires a Super B Factory. Furthermore, here one really needs to improve on background suppression, which seems challenging. After all, $B \rightarrow \tau \nu$ has just very recently been discovered through the technique of full reconstruction of the other B . The issues for improving the measurements are common between $B \rightarrow \tau \nu$ and $B \rightarrow K^* \nu \nu$, i.e., the challenge of modes with missing mass. Even with full reconstruction of the other B , one probably needs to improve on detector hermeticity. We note that there is no resort to LHCb for this mode. Thus, it should be an emphasis for the Super B Factory effort.

⁵ BaBar has recently updated $B \rightarrow K^+ \nu \nu$ and $K^* \nu \nu$ search with 454M $B\bar{B}$ s, using semileptonic $B \rightarrow D^{(*)} \ell \nu$ to tag the other B . The $K^* \nu \nu$ limits are slightly better than Belle's. However, whether one sets the best limit here or there depends on fluctuations.

5.2.2 Constraint on Light Dark Matter

From the fact that $b \rightarrow s\ell\ell$ measurement is in good agreement with SM expectations, one would infer that $B \rightarrow K\nu\nu$ cannot deviate from SM expectation. However, besides sheer experimental prowess and for sake of confirmation, a bigger motivation for studying $B \rightarrow K + \text{nothing}$ is to search for light Dark Matter (DM). As Dark Matter is demanded by astrophysical and cosmological evidence, this highlights the importance of the search for the $B \rightarrow K + \text{nothing}$ signature.

There are several aspects as to why *light* DM is important. By “light”, we mean GeV or even sub-GeV scale, rather than the more typical weak scale DM, as the quintessential particle physics candidate for DM would be WIMPs (Weakly Interacting *Massive* Particles, which is one of the biggest motivations for SUSY). As a motivation for light DM, there are puzzling 0.511 MeV lines from the galactic bulge [29], and suggestions have been made that annihilation of sub-GeV WIMPs near galactic center could lead to positron abundance. Second, for typical underground experiments for DM search, such as DAMA or CDMS, one detects the electronic signals from DM–nucleus collisions. Denoting the DM particle as S , because the energy transfer to the nucleus scales as m_S^2/m_{Nuc}^2 , there is little sensitivity to m_S below a few GeV. On the other hand, if light DM does exist, they could be the predominant end products of Higgs decay, $h \rightarrow SS$, where h is the SM-like Higgs boson. If this happens, Higgs search at the LHC would be affected drastically. Thus, it is imperative to gain access to the possibility of light DM.

So how does light DM become relevant in $b \rightarrow s$ transitions? If one had a light Higgs boson h^0 , then $b \rightarrow sh^0$ would be rather sizable [30], again because of the Higgs affinity (now with direct Higgs boson emission) of the top quark in the loop and being a two-body decay process. This possibility is now ruled out.⁶ The simplest light DM arises from having a singlet Higgs boson. In these models, the singlet Higgs can have both a bare mass and a component generated by a Higgs coupling λ to the v.e.v. scale. If it so happens that the singlet Higgs mass m_S is light, though fine-tuned, its coupling to the SM-like Higgs boson could still be large. Combining $b \rightarrow sh^*$ production, where h^* is a virtual SM-like Higgs boson, followed by

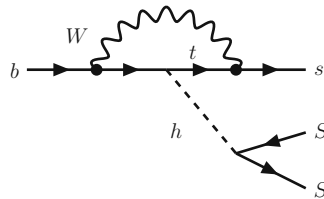


Fig. 5.6 Diagram for $b \rightarrow sh^{0*} \rightarrow sSS$, where h^0 is the SM-like Higgs boson and S is a light singlet Higgs boson that is a Dark Matter candidate

⁶ There is still a possibility that the HyperCP events [31] are due to a very light Higgs boson in an exotic model.

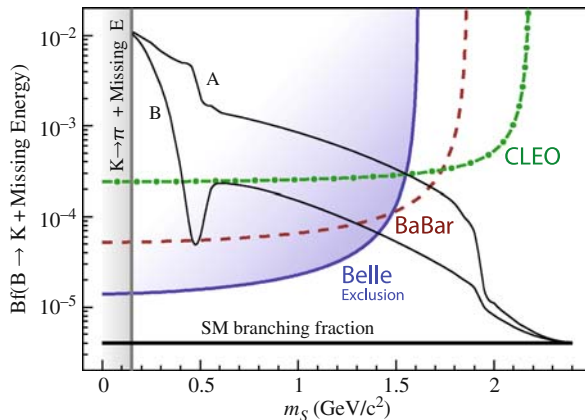


Fig. 5.7 Experimental bound on singlet Higgs scenario for light Dark Matter from $B^+ \rightarrow K^+ + \text{nothing}$ (courtesy K.F. Chen). See text for further explanation

$h^* \rightarrow SS$, because of the aforementioned coupling, one has $b \rightarrow sSS$ (see Fig. 5.6), which leads to $B \rightarrow KSS$ and gives a $B \rightarrow K + \text{nothing}$ signature, because the decay of S is inhibited. The point is that, with m_t enhancement of htt coupling (common with Ztt) and with λ enhancement of hSS coupling, the $b \rightarrow sSS$ process in general dominates over $b \rightarrow s\nu\nu$, so long that it is kinematically allowed.

Without going into further detail, we plot in Fig. 5.7 the bound on m_S from $B^+ \rightarrow K^+ + \text{nothing}$ search vs. the singlet scalar mass m_S . The curves A and B [28] can be viewed as reflecting a range of possible but generous assumptions on strong interaction uncertainties that affect the DM annihilation cross section, in the assessment of consistency with cosmological abundance requirements. The vertical straight line to the left comes from a similar kaon decay constraint, while the straight line near the bottom is the expected $B^+ \rightarrow K^+ \nu \nu$ “SM background” rate. The other three curves correspond to experimental search limits.

It is instructive to understand the behavior of the latter curves. The horizontal part of these curves reflects the reach of the experimental limit on $B^+ \rightarrow K^+ \nu \nu$, which is dictated more by data size. The lines turn vertical for heavier m_S , which reflects the p_K cut employed by the experimental study to reject $b \rightarrow c$ background (in fact there are also upper bound cuts on p_K to reject background events such as coming from $B \rightarrow K^* \gamma$). The stiffer the p_K cut, the earlier one loses sensitivity to heavier m_S because of phase space for the KSS final state. The dot-dash curve is the bound from CLEO [5, 6], which has the lowest p_K cut. We then progress through the more and more stringent BaBar [26] and Belle [27] curves. Note, however, that these studies aim at more stringent bound on $B^+ \rightarrow K^+ \nu \nu$, and a larger p_K cut is needed to suppress background. If one targets singlet Higgs DM search, then the p_K and other cuts should be re-optimized for different m_S assumptions. There is thus room for improvement even with the same data set.

It is safe to state that $m_S < 1.5$ GeV or so is excluded by $B^+ \rightarrow K^+ + \text{nothing}$ studies for the singlet Higgs model. Note that the singlet Higgs scenario is the

simplest for light DM. One can certainly enlarge the model with further assumptions, and there is no lack of other, more elaborate models. Our discussion is only meant as an illustration. In any case, a Super B Factory, with much more data, could have more say on this important subject, *especially if LHC data suggest that the Higgs may be decaying differently than expected.*

References

1. Eilam, G., Soni, A., Kane, G.L., Deshpande, N.G.: Phys. Rev. Lett. **57**, 1106 (1986) 73
2. Hou, W.S., Willey, R.S., Soni, A.: Phys. Rev. Lett. **58**, 1608 (1987) 73, 75, 76, 77, 78, 82
3. Inami, T., Lim, C.S.: Prog. Theor. Phys. **65**, 297 (1981) 74
4. Abe, K., et al. [Belle Collaboration]: Phys. Rev. Lett. **88**, 021801 (2002) 75
5. Yao, W.M., et al. [Particle Data Group]: J. Phys. G **33**, 1 (2006) 76, 78, 85
6. Amsler, C., et al.: Phys. Lett. B **667**, 1 (2008); and <http://pdg.lbl.gov/> 76, 78, 85
7. Kaneko, J., et al. [Belle Collaboration]: Phys. Rev. Lett. **90**, 021801 (2003) 76
8. Wei, J.T., et al. [Belle Collaboration]: Phys. Rev. D **78**, 011101 (2008) 76
9. Ali, A., Ball, P., Handoko, L.T., Hiller, G.: Phys. Rev. D **61**, 074024 (2000) 76, 78
10. Ali, A., Lunghi, E., Greub, C., Hiller, G.: Phys. Rev. D **66**, 034002 (2002) 76
11. Albrecht, H., et al. [ARGUS Collaboration]: Phys. Lett. B **192**, 245 (1987) 76
12. Ali, A., Mannel, T., Morozumi, T.: Phys. Lett. B **273**, 505 (1991) 77
13. See the webpage of the Heavy Flavor Averaging Group (HFAG). <http://www.slac.stanford.edu/xorg/hfag>. We usually, but not always, take the Lepton-Photon 2007 (LP2007) numbers as reference 78
14. Ishikawa, A., et al. [Belle Collaboration]: Phys. Rev. Lett. **96**, 251801 (2006) 78, 79, 81
15. Aubert, B., et al. [BaBar Collaboration]: Phys. Rev. D **73**, 092001 (2006) 78, 81
16. Aubert, B., et al. [BaBar Collaboration]: Phys. Rev. D **79**, 031102 (2009) 79, 81, 82
17. Talk by Wei, J.T. [for the Belle Collaboration]: At the 34th International Conference on High Energy Physics (ICHEP2008), Philadelphia, USA, 29 July–5 August; the result is written up in arXiv:0810.0335 [hep-ex] 79
18. Hou, W.S., Hovhannisyan, A., Mahajan, N.: Phys. Rev. D **77**, 014016 (2008) 80, 81, 82
19. D'Ambrosio, G., Giudice, G.F., Isidori, G., Strumia, A.: Phys. Rev. B **645**, 155 (2002) 80
20. Dickens, J. [LHCb Collaboration]: Talk at the 4th Workshop on the CKM Unitarity Triangle (CKM2006), Nagoya, Japan, December 2006 81
21. Dickens, J., Gibson, V., Lazzeroni, C., Patel, M.: LHCb Note CERN-LHCB-2007-039 81
22. Gambino, P., Haisch, U., Misiak, M.: Phys. Rev. Lett. **94**, 061803 (2005) 81
23. Preliminary result from CDF Collaboration, shown in talk by Rescigno, M.: At the 4th Workshop on the CKM Unitarity Triangle (CKM2006), Nagoya, Japan, December 2006 82
24. Chen, K.F., et al. [Belle Collaboration]: Phys. Rev. Lett. **94**, 221804 (2005) 82
25. Buchalla, G., Hiller, G., Isidori, G.: Phys. Rev. D **63**, 014015 (2001) 82
26. Aubert, B., et al. [BaBar Collaboration]: Phys. Rev. Lett. **94**, 101801 (2005) 83, 85
27. Chen, K.F., et al. [Belle Collaboration]: Phys. Rev. Lett. **99**, 221802 (2007) 83, 85
28. Bird, C., et al.: Phys. Rev. Lett. **93**, 201803 (2004) 83, 85
29. Jean, P., et al.: Astron. Astrophys. **407**, L55 (2003) 84
30. Willey, R.S., Yu, H.L.: Phys. Rev. D **26**, 3086 (1982) 84
31. Park, H., et al. [HyperCP Collaboration]: Phys. Rev. Lett. **94**, 021801 (2005) 84

Chapter 6

Right-Handed Currents and Scalar Interactions

It should be clear from the previous chapters that loop-induced $b \rightarrow s$ transitions offer many good probes of New Physics at the TeV scale, and it is the current frontier of flavor physics. As last examples of their usefulness, we discuss probing for Right-Handed (RH) interactions via time-dependent CP violation in $B^0 \rightarrow K_S^0 \pi^0 \gamma$ decay and searching for enhancement of $B_s \rightarrow \mu^+ \mu^-$ as probe of BSM Higgs boson effects. Combining signature versus the raw cross sections, the former is best done at a (Super) B Factory, while the latter is the domain of hadron colliders, where great strides have already been made.

The question of right-handed interactions has been with us since the establishment of left-handedness of the weak interactions. The TCPV probe of $B^0 \rightarrow K_S^0 \pi^0 \gamma$ decay, or more generally $B^0 \rightarrow X^0 \gamma$, utilizes a beautiful refinement of the TCPV discussed in Chap. 2, which allows us to probe RH interactions involving b to s flavor conversion. It also utilizes a special experimental environment that is rather unique to the asymmetric energy B factories. For $B_s \rightarrow \mu^+ \mu^-$, though the signature is straightforward, the actual effect that occurs at large $\tan \beta$ (the ratio of vacuum expectation values of multi-Higgs models) is rather subtle compared with the straightforward charged Higgs effect of $B^+ \rightarrow \tau^+ \nu$.

6.1 TCPV in $B \rightarrow K_S^0 \pi^0 \gamma, X^0 \gamma$

With large QCD enhancement [1, 2], the $b \rightarrow s \gamma$ rate is dominated by the SM. The left-handedness of the weak interaction dictates that the γ emitted in $\bar{B}^0 \rightarrow \bar{K}^{*0} \gamma$ decay has left-handed helicity (defined somewhat loosely), where the emission of right-handed (RH) photons is suppressed by $\sim m_s/m_b$, as can be read off from (5.2). This reflects the need for a mass insertion for helicity flip and the fact that a power of m_b is required for the $b \rightarrow s \gamma$ vertex by gauge invariance (or current conservation). For $B^0 \rightarrow K^{*0} \gamma$ decay that involves $\bar{b} \rightarrow \bar{s} \gamma$, the opposite is true, and the emitted photon is dominantly of RH kind.

The fact that photon helicities do not match for $\bar{B}^0 \rightarrow \bar{K}^{*0} \gamma$ vs. $B^0 \rightarrow K^{*0} \gamma$ has implications for a conceptually very interesting probe [3]. Mixing-dependent CPV, i.e., TCPV, involves the interference of \bar{B}^0 and $\bar{B}^0 \xrightarrow{\text{mix}} B^0$ decays to a common

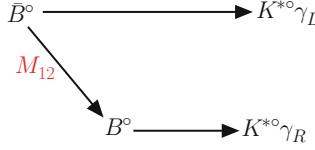


Fig. 6.1 Mismatch in photon helicity for $\bar{B}^0 \rightarrow \bar{K}^{*0}\gamma$ decay vs. $\bar{B}^0 \xrightarrow{\text{mix}} B^0 \rightarrow K^{*0}\gamma$ decay in the SM. To have TCPV in the $K^{*0}\gamma$ final state ($K^{*0} \rightarrow K_S^0\pi^0$), Nature needs to provide a sizable right-handed photon component for $\bar{B}^0 \rightarrow \bar{K}^{*0}\gamma$ decay

final state that is not flavor-specific (i.e., no definite flavor). For radiative $\bar{B}^0 \rightarrow \bar{K}^{*0}\gamma$ decay vs. $\bar{B}^0 \xrightarrow{\text{mix}} B^0 \rightarrow K^{*0}\gamma$ decay, the common final state is $K_S^0\pi^0$. As illustrated in Fig. 6.1, since within the SM the $\bar{B}^0 \rightarrow \bar{K}^{*0}\gamma$ process leads to γ_L , while the $B^0 \rightarrow K^{*0}\gamma$ process gives rise to γ_R , these two processes cannot interfere as the final states are orthogonal to each other! This is in contrast to, say, TCPV in the common CP eigenstate of ϕK_S from \bar{B}^0 decay and $\bar{B}^0 \xrightarrow{\text{mix}} B^0$ decays. The interference requires RH photons from $\bar{B}^0 \rightarrow \bar{K}^{*0}\gamma$ decay, which is suppressed by the helicity flip factor of $m_s/m_b \sim \text{few } \%$ within SM.

However, if there are RH interactions that also induce $b \rightarrow s\gamma$ transition, then $\bar{B}^0 \rightarrow \bar{K}^{*0}\gamma$ would acquire a γ_R component to interfere with the $\bar{B}^0 \xrightarrow{\text{mix}} B^0 \rightarrow K^{*0}\gamma$ amplitude [3]. Thus, *TCPV in $B^0 \rightarrow K^{*0}\gamma$ decay mode probes RH interactions!* This does not require the RH interaction, which is necessarily New Physics, to carry extra CPV phase, since there is already the measured SM phase $\Phi_{B_d} = \phi_1/\beta$ in $B_d^0\text{--}\bar{B}_d^0$ mixing.

A formula at this point may help us grasp the physics. Analogous to the TCPV S parameter discussed in Chap. 2, we have [3, 4]

$$\mathcal{S}_{X^0\gamma} = \xi_{X^0} \frac{2|C_{11}C'_{11}|}{|C_{11}|^2 + |C'_{11}|^2} \sin(2\Phi_{B_d} - \phi_{11} - \phi'_{11}), \quad (6.1)$$

where ξ_{X^0} is the CP eigenvalue of the state X^0 , and $|C_{11}|$ and ϕ_{11} are the strength and CPV phase of the left-handed $b \rightarrow s\gamma$ Wilson coefficient (11 rather than 7, because one has counted 7–10 for the electroweak penguin four-quark operators, where here one refers to the term that can radiate an on-shell photon), with a prime indicating the right-handed counterpart. Equation (6.1) makes clear that TCPV would vanish with $|C'_{11}|$ and that the CPV phase of the decay amplitudes can affect the measured value. It should be noted that a RH component in $\bar{B}^0 \rightarrow \bar{K}^{*0}\gamma$ decay is rather easy to hide in $b \rightarrow s\gamma$ inclusive rate, since the LH and RH components add in quadrature. In fact, if one takes the deficit of the NNLO prediction seriously, i.e., (4.5) vs. the experimental measurement (4.3), one could even say that data call for some extra contribution to the inclusive $b \rightarrow s\gamma$ rate.

Alas, Nature plays a trick on us for the search of TCPV in $B^0 \rightarrow K^{*0}\gamma$ decay. As mentioned, $K^{*0}\gamma$ has to be in a CP eigenstate, such as $K^{*0} \rightarrow K_S^0\pi^0$, so the final state is $K_S^0\pi^0\gamma$. The π^0 and γ certainly do not give rise to vertices. For the K_S^0 ,

though “short-lived,” it is produced with high momentum such that it typically decays at the outer layers of the silicon detector, and one has poor vertex information. Since one needs Δz to convert to Δt for a TCPV measurement, it seems impossible to study TCPV in the $K_S^0 \pi^0 \gamma$ final state. The intriguing suggestion of [3], beautiful as it is, appeared to be just an impossible dream. Such was the impression from (at least some of us on) the Belle side.

Fortunately, with a larger silicon vertex detector and with an extra silicon layer compared to Belle, BaBar was not deterred and pushed forward a technique called “ K_S vertexing.” It was demonstrated [5] that, though degraded, the $K_S \rightarrow \pi^+ \pi^-$ decay does give some vertex information. The key point is the availability of the beam direction information because of the boost (thanks to the asymmetric beam energies of the B factories), providing a “beam profile” for the somewhat rudimentary K_S momentum vector to point back to. The closeness of m_B to half the $\Upsilon(4S)$ mass implies that the transverse motion is small. The method, illustrated in Fig. 6.2, was validated with gold-plated modes like $B^0 \rightarrow J/\psi K_S$, by removing the $J/\psi \rightarrow \ell^+ \ell^-$ tracks. Using 124M $B \bar{B}$ events, the first measurement [5] gave $\mathcal{S}_{K_S^0 \pi^0} = 0.48_{-0.47}^{+0.38} \pm 0.06$. Though errors are large, this was the proof of principle for K_S vertexing. BaBar then demonstrated [6] that the technique could be applied to $B^0 \rightarrow K^{*0} \gamma$ decay, finding $\mathcal{S}_{K^{*0}[K_S^0 \pi^0] \gamma} = 0.25 \pm 0.63 \pm 0.14$. The method has been extended to other TCPV studies such as in $B^0 \rightarrow K_S K_S K_S$.

The current status of TCPV in $B^0 \rightarrow K^{*0} \gamma$ decay is as follows. Using 535M $B \bar{B}$ pairs, the result from Belle [7] is $\mathcal{S}_{K^{*0}[K_S^0 \pi^0] \gamma} = -0.32_{-0.33}^{+0.36} \pm 0.05$, while the BaBar update with 431M gives [8] $\mathcal{S}_{K_S \pi^0 \gamma} = -0.08 \pm 0.31 \pm 0.05$, combining to give [9]

$$\mathcal{S}_{K^{*0}[K_S^0 \pi^0] \gamma} = -0.19 \pm 0.23 \quad (\text{HFAG 2008}), \quad (6.2)$$

which is consistent with zero, hence with the SM as well. Since Ref. [8] is yet unpublished, if one combines the Belle result with the published 232M result from BaBar [10], the average is $\mathcal{S}_{K^{*0}[K_S^0 \pi^0] \gamma} = -0.28 \pm 0.26$, again consistent with zero. Recent measurements have also been made in $B^0 \rightarrow K_S \pi^0 \gamma$ mode without requiring the $K_S \pi^0$ to reconstruct to a K^{*0} , as well as in the $B^0 \rightarrow \eta K_S \gamma$ mode.

This is a very interesting direction to explore, but again one needs a Super B Factory to seriously probe for RH interactions. At the LHCb, one lacks the “beam profile” technique for K_S vertexing, since one does not know the original B -direction.



Fig. 6.2 Figure illustrating K_S vertexing. The B^0 – \bar{B}^0 system is boosted in the z -direction, leading to an elongated “IP profile,” where IP stands for Interaction Point. Although the decay lifetime of K_S from B decay is not optimal for the silicon vertex detector, intersecting the K_S momentum with the IP profile gives some information of the B meson decay vertex

The $B_s \rightarrow \phi\gamma$ mode may be used, although the ϕ is also not so good in providing a vertex, since the K^+K^- pair is rather colinear because of $2m_K \sim m_\phi$. Probably, the LHCb upgrade would be needed to be competitive with a Super B Factory. Other ideas to probe RH currents in $b \rightarrow s\gamma$ are $\gamma \rightarrow e^+e^-$ conversion in detector [11], Λ polarization in $\Lambda_b \rightarrow \Lambda\gamma$ decay [12], and angular F_L and A_T measurables in $B \rightarrow K^*\ell^+\ell^-$ decay mentioned in the Chap. 5. If an observation is made, one would need multiple measurables to clarify, since one can see from (6.2) that $\mathcal{S}_{K^{*0}[K_S^0\pi^0]\gamma}$ involves not only the strength but also the phase of C'_{11} .

We have not gone into possible New Physics models that could generate TCPV in $B^0 \rightarrow K^{*0}\gamma$ since this is an existence proof by experiment, and current data are still far away from giving any hint. One particular model we are fond of, an interesting case that combines SUSY and flavor, is with maximal $\tilde{s}_R\text{--}\tilde{b}_R$ RH squark mixing [13]. It is motivated in approximate Abelian flavor symmetry models [14] together with SUSY, which provides also the strong dynamics. In this model, the flavor-mixed light $\tilde{s}\tilde{b}_{1R}$ squark could be driven light by the large flavor mixing, even if SUSY is above the TeV scale. If a “solo \tilde{b} ” squark is discovered at the LHC, while little else is seen as far as SUSY is concerned, one should test whether this new \tilde{b} squark also has a large \tilde{s} component.

6.2 $B_s \rightarrow \mu^+\mu^-$

Because of the possibility of rather large $\tan\beta$ enhancement and because of its straightforward signature, the $B_s \rightarrow \mu^+\mu^-$ decay mode has been a favorite mode for probing exotic Higgs sector effects in MSSM at hadron colliders.

The process proceeds in SM just like $b \rightarrow s\ell^+\ell^-$, except s is now in the initial state as the \bar{s} spectator quark that annihilates with the b quark. Since B_s is a pseudoscalar, the photonic penguin does not contribute. The SM expectation is only $\sim 3.4 \times 10^{-9}$ [15], because of f_{B_s} and helicity suppression. Much like $B^+ \rightarrow \tau^+\nu$, the process is basically sensitive to (pseudo)scalar operators. In MSSM, one has both neutral scalar and pseudoscalar bosons arising from a 2HDM-II framework. But these bosons are flavor-conserving at tree level, and naively they cannot mediate $\bar{s}b \rightarrow \bar{\mu}\mu$. However, at the loop level, and for large $\tan\beta$, one can “no longer diagonalize the masses of the quarks in the same basis as their Yukawa couplings” [16–18]. We illustrate this in Fig. 6.3 with a diagram involving the sb self-energy. A second diagram is shown where a $t\text{--}W\text{--}H^+$ loop emits exotic neutral Higgs bosons that turn into muon pairs. It is argued that both type of diagrams lead to amplitudes $\propto \tan^3\beta$ [16–18] for large $\tan\beta$, hence an *enhancement of $\tan^6\beta$ in rate!* Showing two diagrams also serves the purpose to illustrate that the effective $bs\mu\mu$ coupling depends on how SUSY is broken and can differ substantially between different scenarios. This is in contrast with the simple clarity of the $\tan\beta$ dependence of the charged H^+ boson effect in $B^+ \rightarrow \tau^+\nu_\tau$, (4.10) and (4.11), which arises at the tree level. Of course, there could be more drastic theories for $B_s \rightarrow \mu^+\mu^-$, such as R -parity violating SUSY, which we do not go into.

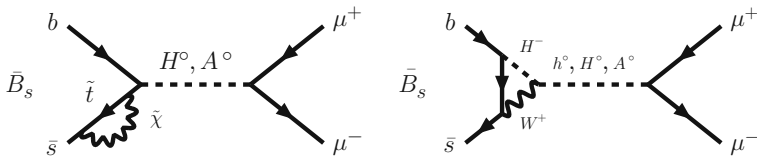


Fig. 6.3 Diagrams illustrating neutral Higgs-mediated FCNC for $B_s \rightarrow \mu^+ \mu^-$

For experiment, however, it is straightforward enough, and one need not be concerned with model details. With the ease for trigger and the large number of B mesons produced, this is the subject vigorously pursued at hadron facilities, and there is enormous range for search. There is much at stake, since prior to observing the Higgs, the bound on $B_s \rightarrow \mu^+ \mu^-$ put stringent constraints on SUSY models. If exotic Higgs are observed in the future, $B_s \rightarrow \mu^+ \mu^-$ measurement would still be rather invaluable.

The two-track nature makes the search relatively straightforward, although the issue is background control. One has to be careful with muon identification, checking for fakes, e.g., from K^\pm penetrating to the muon system. DØ employs a likelihood ratio cut, while CDF uses a neural network for separation of signal vs. background. To avoid bias, a blind analysis is done by both experiments, i.e., event selection is optimized prior to unveiling the signal region. For the estimate of branching fraction, a well-known mode such as $B^+ \rightarrow J/\psi K^+$ (where $J/\psi \rightarrow \mu^+ \mu^-$) is used as normalization mode.

With Run-II data now taking good shape, the Tevatron experiments have improved the limits on this mode considerably since 2006. The recent 2 fb^{-1} limits from CDF and DØ are 4.7×10^{-8} [19] and 7.5×10^{-8} [20], respectively, at 90% C.L., combining to give

$$\mathcal{B}(B_s \rightarrow \mu^+ \mu^-) < 4.7 \times 10^{-8} \quad (\text{HFAG Winter 2008}), \quad (6.3)$$

at 90% C.L. This is still an order of magnitude away from SM, but the CDF limit is an improvement of about factor of 2 over the previous limit.

The expected reach for the Tevatron is about 2×10^{-8} at $\sim 7 \text{ pb}^{-1}$ per experiment, assuming improvements in the 2010 run. This is still more than a factor of 6 above SM. Further improvement would have to come from LHCb. LHCb claims [21] that, with just 0.05 fb^{-1} data, it would overtake the Tevatron in this mode. It would attain 3σ evidence for SM signal with 2 fb^{-1} and 5σ observation with 10 fb^{-1} . To follow our suggested modest 0.5 fb^{-1} expectation for the first year of LHCb data taking, we expect LHCb to exclude branching ratio values down to SM expectation by 2010 or so. Before that, the race between Tevatron and LHC for discovery is yet unfinished.

Clearly, much progress will come with the turning on of LHC, where direct search for Higgs particles and charginos would also be vigorously pursued. Hopefully, we are in for some excitement soon.

References

1. Bertolini, S., Borzumati, F., Masiero, A.: Phys. Rev. Lett. **59**, 180 (1987) 87
2. Deshpande, N.G., Lo, P., Trampetic, J., Eilam, G., Singer, P.: Phys. Rev. Lett. **59**, 183 (1987) 87
3. Atwood, D., Gronau, M., Soni, A.: Phys. Rev. Lett. **79**, 185 (1997) 87, 88, 89
4. Chua, C.K., He, X.G., Hou, W.S.: Phys. Rev. D **60**, 014003 (1999) 88
5. Aubert, B., et al. [BaBar Collaboration]: Phys. Rev. Lett. **93**, 131805 (2004) 89
6. Aubert, B., et al. [BaBar Collaboration]: Phys. Rev. Lett. **93**, 201801 (2004) 89
7. Ushiroda, Y., et al. [Belle Collaboration]: Phys. Rev. D **74**, 111104(R) (2006) 89
8. Aubert, B., et al. [BaBar Collaboration]: arXiv:0708.1614 [hep-ex], contributed to 23rd Lepton-Photon Symposium, August 2007, Daegu, Korea 89
9. See the webpage of the Heavy Flavor Averaging Group (HFAG). <http://www.slac.stanford.edu/xorg/hfag>. We usually, but not always, take the Lepton-Photon 2007 (LP2007) numbers as reference 89
10. Aubert, B., et al. [BaBar Collaboration]: Phys. Rev. D **72**, 051103(R) (2005) 89
11. Grossman, Y., Pirjol, D.: JHEP. **0006**, 029 (2000) 90
12. Mannel, T., Recksiegel, S.: J. Phys. G **24**, 979 (1998) 90
13. Chua, C.K., Hou, W.S., Nagashima, M.: Phys. Rev. Lett. **92**, 201803 (2004) 90
14. Leurer, M., Nir, Y., Seiberg, N.: Nucl. Phys. B **420**, 468 (1994) 90
15. Buras, A.J.: Phys. Lett. B **566**, 115 (2003) 90
16. Huang, C.S., Liao, W., Yan, Q.S.: Phys. Rev. D **59**, 011701 (1999) 90
17. Choudhury, S.R., Gaur, N.: Phys. Lett. B **451**, 86 (1999) 90
18. Babu, K.S., Kolda, C.: Phys. Rev. Lett. **84**, 228 (2000) 90
19. Aaltonen, T., et al. [CDF Collaboration]: Phys. Rev. Lett. **100**, 101802 (2008) 91
20. Abazov, V.M., et al. [DØ Collaboration]: Dzero Note 5344-CONF (unpublished) 91
21. Eisenhardt, S.: Talk at 2007 Europhysics Conference on High Energy Physics, Manchester, England, July 2007 91

Chapter 7

Bottomonium Decay and New Physics

Before we turn to non-B physics probes, we make a detour from our main theme of $b \rightarrow s$ loop probes of New Physics and give some account of a special arena in the decays of bottomonium, namely $\Upsilon(nS)$, $n = 1 - 3$. As we have mentioned in Sect. 5.2, the CDMS/DAMA type of approaches for Dark Matter (DM) search are not sensitive to light DM. The bottomonium system offers to (partially) cover such a window. At the same time, the related exotic Higgs sector can also be probed. These suggestions have led the Belle and BaBar experiments to make dedicated data runs on $\Upsilon(nS)$ resonances below the $\Upsilon(4S)$.

7.1 $\Upsilon(3S) \rightarrow \pi^+\pi^-\Upsilon(1S) \rightarrow \pi^+\pi^- + \text{Nothing}$

As we have discussed briefly in Sect. 5.2, Dark Matter (DM) particles could be as light as the GeV order. Part of the motivation is the 0.511 MeV γ rays [1] coming from the galactic center that indicate slow positrons, which suggest a particle lighter than 100 MeV if the source is DM annihilation. Combined with the insensitivity of DAMA/CDMS experiments to low mass DM,¹ as we have argued in Sect. 5.2, it is imperative for us to gain probes of light DM. Such low-mass DM may not be so easy to see at the LHC.

Assuming light DM χ , the pair annihilation cross section of dark matter particles, $\sigma(\chi\chi \rightarrow q\bar{q})$, is estimated [2] from cosmological data. Assuming time-reversal invariance, this is applied to $b\bar{b} \rightarrow \chi\chi$, and the estimate is that $\mathcal{B}(\Upsilon(1S) \rightarrow \chi\chi) \sim 0.6\%$. The mass of χ , of course, has to be lighter than m_b , and the details depend on whether the “mediator,” or nature of coupling, is of scalar, pseudoscalar, or vector type. The suggestion from theory was to use radiative return (or ISR), i.e., $\Upsilon(4S) \rightarrow \gamma_{\text{ISR}}\Upsilon(nS)$, followed by meticulous studies of many decay channels of $\Upsilon(nS)$ down to $\Upsilon(1S)$, to tag and search for $\Upsilon(1S) \rightarrow \text{nothing}$. It was argued that, with 400 fb^{-1} on the $\Upsilon(4S)$, a bound of 0.1% could be attained [2].

¹ In fact, since DAMA uses NaI crystals, it has better sensitivities to lower mass than CDMS. Combined with possibility of DM flow patterns, it is not impossible that the DAMA indication for, and CDMS limit on, DM could be compatible.

Here, the Belle experiment proved their prowess. Rather than doing a meticulous $\Upsilon(4S)$ radiative return study, by assessing the situation and studying tagging efficiencies to optimize the trigger, the Belle experiment instead took a dedicated 4-day run *directly* on the $\Upsilon(3S)$ in 2006, collecting 2.9 fb^{-1} , corresponding to 11M $\Upsilon(3S)$ events. The idea [3] bears some similarity to the full reconstruction tag method for getting a “ B beam.” That is, using kinematics of $\Upsilon(3S) \rightarrow \Upsilon(1S)\pi^+\pi^-$ decay, where one knows the energy of the initial state (in CM frame), by reconstructing the $\pi^+\pi^-$ system, one looks for a peak in the recoil mass distribution at the $\Upsilon(1S)$, *but observing no signal in the detector* ($\Upsilon(1S) \rightarrow \text{nothing}$). Combining cross section versus pion efficiency, Belle concluded that a $\Upsilon(3S)$ run is the best.

Of course, as always, it is a matter of control of signal over background, and optimization of the two-track trigger was crucial. Since the pions are on the soft side, both need to be able to reach an appreciable portion of the tracker (CDC). The trigger was studied further and verified with the control sample of $\Upsilon(3S) \rightarrow \Upsilon(1S)\pi^+\pi^-$, where $\Upsilon(1S) \rightarrow \mu^+\mu^-$. The main background comes from two-photon events, i.e., $e^+e^- \rightarrow e^+e^-\pi^+\pi^-$, where the e^+ and e^- escape detection. To suppress these, one uses the fact that for these events, the two pions tend to have balanced p_T , and the $\pi\pi$ system would be rather boosted, in contrast to signal events. Peaking background arise from $\Upsilon(3S) \rightarrow \Upsilon(1S)\pi^+\pi^-$ events where $\Upsilon(1S) \rightarrow \ell^+\ell^-$ and the leptons go outside of detector acceptance. These backgrounds can be remedied only when “cracks” or holes of the detector are plugged. For the combinatoric, two-photon background, a very forward photon tagger might help.

The result of the Belle study is shown in Fig. 7.1. Fitting with combinatoric and peaking backgrounds as described, Belle extracted 38 ± 39 signal events, which is consistent with no signal. The expected number of events with $\mathcal{B}(\Upsilon(1S) \rightarrow \chi\chi) = 0.6\%$ is 244. The limit of

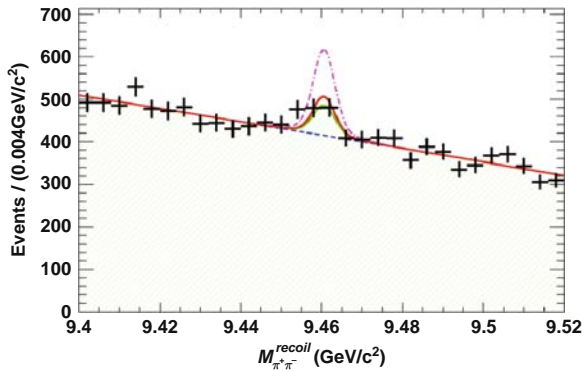


Fig. 7.1 Recoil mass $M_{\pi^+\pi^-}^{\text{recoil}}$ against the $\pi^+\pi^-$ tag in the Belle search [3] for dark matter via $\Upsilon(3S) \rightarrow \Upsilon(1S)[\rightarrow \text{nothing}]\pi^+\pi^-$. [Copyright (2004) by The American Physical Society.] Dashed (lower solid) line is the combinatoric (peaking) background; see text for description. The other solid line fits to data, while the dot-dash line is the expectation from $\mathcal{B}(\Upsilon(1S) \rightarrow \chi\chi) = 0.6\%$

$$\mathcal{B}(\Upsilon(1S) \rightarrow \text{invisible}) < 0.25\%, \quad (\text{Belle } 2.9 \text{ fb}^{-1} \Upsilon(3S) \text{ run}), \quad (7.1)$$

at 90% C.L. rules out the original theory expectation [2]. But of course, the case should not be viewed as closed, both because of the importance but also because the theory could certainly be refined.

The Belle study was followed by a search by CLEO [4], using 1.2 fb^{-1} on the $\Upsilon(2S)$ for $\pi^+\pi^-\Upsilon(1S)$ decay where the $\Upsilon(1S)$ decays invisibly. A limit slightly poorer than that of Belle's is set. This is because of the softer pions from $\Upsilon(2S)$ decay as compared to $\Upsilon(3S)$, and though CLEO has better understanding of their detector because of long and steady experience, trigger efficiency that drove Belle to study $\Upsilon(3S)$ does matter. In a different mass domain, the BES experiment also searched for the invisible decay of J/ψ [2] in $\psi(2S) \rightarrow \pi^+\pi^- J/\psi$ transitions [5], again turning out a null result.

When the PEP-II accelerator had to be terminated earlier than scheduled because of the US funding situation, the BaBar experiment decided to take 30 fb^{-1} on the $\Upsilon(3S)$ (10 times Belle data) in early 2008, followed by 15 fb^{-1} on $\Upsilon(2S)$ (12 times CLEO data). The purpose is at least three-fold. The first is for bottomonium spectroscopy, in particular the η_b , which BaBar has recently announced discovery [6] in the inclusive γ data in $\Upsilon(1S) \rightarrow \gamma\eta_b$. This is quite some triumph, since the η_b has been hiding ever since the Υ discovery, for the past 30 years. A second motivation is for the potential to search for the exotic pseudoscalar Higgs boson a_1 via $\Upsilon(1S) \rightarrow \gamma a_1$, followed by $a_1 \rightarrow \tau^+\tau^-$. The light a_1 could even be behind the 214.3 MeV $\mu^+\mu^-$ events observed [7] by the HyperCP experiment in $\Sigma^+ \rightarrow p\mu^+\mu^-$, which provides further motivation. This we will cover in the next section. A third motivation is to push down on the bound of (7.1). Having 10 times Belle data certainly helps. But inspection of Fig. 7.1 suggests that one may need to reduce the background. Something like an Extreme Forward Calorimeter (EFC, see Fig. 2.2) of Belle needs to be active for MIPs (Minimum Ionizing Particle) and electron rejection.

Forward Detector Improvement

The EFC [8] was an integral part of the Belle detector, precisely plugging the forward (and backward) holes caused by the QCS final focusing magnet. It was designed for three purposes: (i) a (relative) luminosity monitor; (ii) a photon tagger for two-photon events when one photon is off-shell; (iii) improve hermeticity. For the first role, it gave important contributions to KEKB collider commissioning, and the EFC is still a useful instrument for the KEKB accelerator. The design with radiation-hard BGO [9, 10] was in part for the second role of tagging the γ^* with e^-/e^+ . For the third role, a major motivation was to help the pursuit of $B \rightarrow \tau\nu$ because of the difficult missing-mass signature. A proof of principle was conducted [11] to show that MIP detection was possible with the radiation-hard BGO crystal design.

However, an early study [12] found that the Belle detector has too many holes already. Furthermore, the service and cabling of SVD and inner CDC detectors not

only took up space in the forward and backward cones, they also give rise to material in front of the EFC. The power of the EFC to improve hermeticity, though providing a factor of two improvement in S/B , was by far insufficient for the $B \rightarrow \tau \nu$ cause, and this direction was not actively pursued. As we have seen, the B factories took the punishment of 10^{-3} in efficiency to finally use the full reconstruction tag approach to measure the $B \rightarrow \tau \nu$ mode.

With interest gaining in missing-energy and especially missing-mass events, one needs to renew the 10-year-old design of the EFC for the Super B Factory, using LHC/ILC technology such as pixel detectors. With much improved coverage in the forward-backward directions, with both calorimetry and muon detection capabilities, it is estimated that a limit of $\mathcal{B}(\Upsilon(1S) \rightarrow \text{invisible}) < 2 \times 10^{-4}$ can be reached with 500 fb^{-1} running on the $\Upsilon(3S)$. But the SM expectation of $\mathcal{B}(\Upsilon(1S) \rightarrow \nu \bar{\nu}) \sim 10^{-5}$ remains out of reach. Whether such a “Super Forward Detector” should be built may depend on the confluence of LHC and DM studies, i.e., whether one definitely has rather light DM.

For the BaBar run on the $\Upsilon(3S)$, given that BaBar has a difficult IR (interaction region), it remains to be seen how much improvement on (7.1) can be achieved with 30 fb^{-1} . BaBar may have an advantage in triggering on soft pions because of a larger silicon detector.

7.2 $\Upsilon(1S) \rightarrow \gamma a_1^0$ Search

Let us turn to elucidate the physics of a light a_1^0 pseudoscalar as follows.

The popular Minimal Super Symmetric Standard Model (MSSM) has been under stress lately, mainly from the Higgs mass limit, $m_H > 114.4 \text{ GeV}$ [13, 14]. A Higgs boson, or SM-like Higgs boson h^0 , around 100 GeV would be most natural. In general, some fine-tuning of parameters needs to be done to accommodate this. It has been suggested that a natural way to avoid fine-tuning of parameters is to go to NMSSM, N standing for “Next (to).” Besides the Higgs sector of 2HDM-II, one adds an additional singlet Higgs field. Assuming CP invariance in the Higgs sector, the Higgs particle spectrum consists of three neutral scalars, two neutral pseudoscalars, and a pair of charged Higgs. That is, an extra scalar and pseudoscalar compared to a 2HDM. To make a long story short, one of the pseudoscalars, called the a_1^0 , is light, and the region of parameter space reduces much of the fine-tuning of MSSM, by allowing the SM-like Higgs boson to evade the LEP-II bound. The a_1^0 should have enough nonsinglet content, i.e., fraction $\cos \theta_A$ of the pseudoscalar A^0 of MSSM, such that the $h^0 \rightarrow a_1^0 a_1^0$ width is large, thereby suppressing the $h^0 \rightarrow b\bar{b}$ decay and evade the bound from $e^+e^- \rightarrow Zb\bar{b}$. Since the latter bound extends to $Z4b$, one further needs $m_{a_1^0} < 2m_b$ such that $a_1^0 \rightarrow b\bar{b}$ decay is itself forbidden.

To sum it up, let us take $\tan \beta = 10$ as example. One needs $\cos \theta_A > 0.05$ to give $\mathcal{B}(h^0 \rightarrow a_1^0 a_1^0) > 0.7$ and $m_{a_1^0} < 2m_b$. By evading the $Zh^0 \rightarrow Zb\bar{b}$ bound on h^0 with $a_1^0 \rightarrow \tau^+ \tau^-$, one notes that the signature of $Za_1^0 \rightarrow Z\tau^+ \tau^-$ and $Zh^0 \rightarrow Z4\tau$ have not been well studied at LEP. It has been suggested [15] that a subdued

$h^0 \rightarrow b\bar{b}$ (at $\sim 10\%$) could in fact account for an excess of $Zb\bar{b}$ events just below 100 GeV.

So why are we going into this theory detail? Even if NMSSM softens the fine-tuning of MSSM, it seems to be quite contrived in itself. The answer is several fold. Chiefly for our concern is that, with $m_{a_1^0} < 2m_b$, the a_1^0 can be accessed in $\Upsilon(nS)$ decay. There are two other concerns that heighten the importance for the search of a light a_1^0 . The scenario outlined in the previous paragraph [15] may be difficult, perhaps even impossible, to unravel at a hadronic collider. However, the light a_1 can precisely be searched for in $\Upsilon \rightarrow \gamma a_1$ decay, where a lower bound on this rate is argued [15]. This search could turn out to be of utmost importance if the SM-like Higgs does not show up at the LHC. Note that even $h^0 \rightarrow \gamma\gamma$ might get diluted away by the $h^0 \rightarrow a_1^0 a_1^0$ mode. If this is what is realized in Nature, then even with an ILC (International Linear Collider), which could observe $h^0 \rightarrow a_1^0 a_1^0$, information from $\mathcal{B}(\Upsilon \rightarrow \gamma a_1)$ would still be valuable and complementary.

A second data-based motivation is for an a_1^0 lighter than $2m_s$, which would be rather light indeed. If this is the case, then $a_1 \rightarrow \mu^+ \mu^-$ would dominate.² It has been suggested that the $3 \mu^+ \mu^-$ events at 214.3 MeV as seen by the HyperCP experiment at Fermilab, in the $\Sigma^+ \rightarrow p \mu^+ \mu^-$ process, could be [16] such a light pseudoscalar. Admittedly, having three events in a narrow mass region just above threshold, and appearing only in the $\Sigma^+ \rightarrow p \mu^+ \mu^-$ mode in these latter days rather than much earlier, seem to challenge our senses. However, it is claimed that *this is possible in the NMSSM*, while all K and B constraints are satisfied. Let us not go into the detailed theoretical intricacies [16], but to note that the HyperCP events must be followed up experimentally. One suggestion [17] is $\Upsilon(1S) \rightarrow \gamma a_1^0 \rightarrow \gamma \mu^+ \mu^-$ search.

Besides η_b and DM search, the possibility for a_1^0 search was one of the major motivations for BaBar's end run on the $\Upsilon(3S)$ and $\Upsilon(2S)$ just before shutting down. Besides direct radiative decay of $\Upsilon(3S)$ and $\Upsilon(2S)$ to a_1^0 , the stronger recommendation [15], maybe influenced by the Belle special run on $\Upsilon(3S)$ for DM search discussed already, was to use $\Upsilon(3S)$, $\Upsilon(2S) \rightarrow \pi^+ \pi^- \Upsilon(1S)$, followed by $\Upsilon(1S) \rightarrow \gamma a_1^0$, using the $\pi^+ \pi^-$ as tag for the $\Upsilon(1S)$. But the CLEO experiment had already collected 1.1 fb^{-1} on the $\Upsilon(1S)$ (and 1.2 fb^{-1} each on the $\Upsilon(2S)$ and $\Upsilon(3S)$) with the CLEO III detector, before scaling down the energy to CLEO-c. With the 21.5M $\Upsilon(1S)$ events at hand, an analysis by CLEO claimed [18] very recently that much of the parameter space for $2m_\tau < m_{a_1^0} < 7.5 \text{ GeV}$ and for light $a_1 \rightarrow \mu^+ \mu^-$ ($m_{a_1} < 2m_s$) are ruled out.

$\Upsilon(1S) \rightarrow \gamma a_1^0$ decay is nothing but the Wilczek process [19] for a pseudoscalar Higgs particle, with the $a_1^0 b\bar{b}$ coupling modulated by $\tan \beta \cos \theta_A$, where $\tan \beta$ is the usual enhancement factor for down-type quarks (and charged leptons) in 2HDM-II, and $\cos \theta_A$ expresses the 2HDM-II fraction of a_1^0 . Thus,

² Between $2m_s$ and $2m_\tau$, the a_1^0 would decay hadronically and would be a rather difficult object to study at the LHC. However, it seems hard for this case to survive B decay bound, since most likely $b \rightarrow s a_1^0$ would be too large.

$$\mathcal{B}_{\Upsilon(1S) \rightarrow \gamma a_1^0} = \tan^2 \beta \cos^2 \theta_A \times \mathcal{B}_{\Upsilon(1S) \rightarrow \gamma A^0}^{\text{Wilczek}}, \quad (7.2)$$

where $\mathcal{B}_{\Upsilon(1S) \rightarrow \gamma A^0}^{\text{Wilczek}}$ includes kinematics and all corrections. For both $a_1^0 \rightarrow \tau^+ \tau^-$ and $\mu^+ \mu^-$ search, CLEO [18] selected two tracks with opposite charge, with at least one γ , but applying a π^0 veto.

For $a_1^0 \rightarrow \tau^+ \tau^-$ candidates, a missing energy between 2 and 7 GeV was required. The two tracks were demanded to be $e^\pm \mu^\mp$ or $\mu^\pm \mu^\mp$. Events with $e^+ e^-$ are discarded because of severe Bhabha background. The signal is then a near monochromatic peak in E_γ over the background. The background comes mainly from continuum $e^+ e^- \rightarrow (\gamma) \tau^+ \tau^-$, where possibly one photon from a π^0 daughter of a τ lepton was not constructed. The continuum background was estimated by scaling from data collected at, or near, the $\Upsilon(4S)$, which described the $\Upsilon(1S)$ data rather well. No significant peak was observed. Plotting with the NMSSM results of [15], the CLEO limits on $\Upsilon(1S) \rightarrow \gamma a_1^0 \rightarrow \gamma \tau^+ \tau^-$ are given in Fig. 7.2. For the medium grey region of $2m_\tau < m_{a_1^0} < 7.5$ GeV, most models are ruled out, except when the nonsinglet fraction $|\cos \theta_A|$ is small. For the light grey region, corresponding to $7.5 \text{ GeV} < m_{a_1^0} < 8.8$ GeV, some models, or parameter space, are allowed, as CLEO is losing sensitivity. For the models marked in black, corresponding to $8.8 \text{ GeV} < m_{a_1^0} < 9.2$ GeV, CLEO has little sensitivity.

For $a_1^0 \rightarrow \mu^+ \mu^-$ search [18], both tracks must pass muon ID and the total observed energy of the $\gamma \mu^+ \mu^-$ should be consistent with the $\Upsilon(1S)$. One searches for peaks in $m_{\mu^+ \mu^-}$, as it has better resolution than E_γ . The background arises from radiative (ISR) $e^+ e^- \rightarrow \gamma \mu^+ \mu^-$ with a rather hard photon, with $e^+ e^- \rightarrow \gamma J/\psi \rightarrow \gamma \mu^+ \mu^-$ providing a control mode to check things such as resolution. The $\Upsilon(1S)$ data are well described by scaling from $\Upsilon(4S)$ data (adjusting for J/ψ position). The

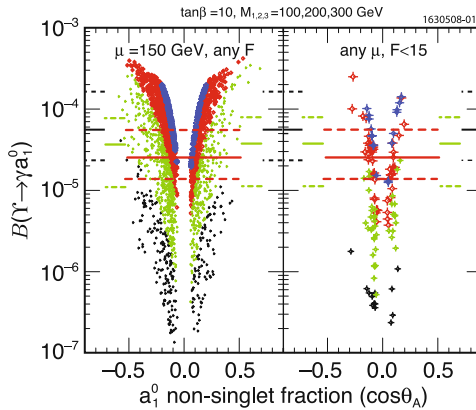


Fig. 7.2 CLEO upper limits (solid line) on $\Upsilon(1S) \rightarrow \gamma a_1^0 \rightarrow \gamma \tau^+ \tau^-$, based on 21.5M $\Upsilon(1S)$ events [18]. The underlying theory plot is from [15], which corresponds to NMSSM model parameters, where the figure on the right with fewer models is for “less fine-tuning (F).” Different grey shades correspond to different a_1^0 mass, with the black points corresponding to the heaviest a_1^0 , where CLEO loses sensitivity. The CLEO bounds have respective shading

special interest is for $m_{a_1^0} = 214.3 \text{ MeV}$, i.e., the region of HyperCP events. A fit in this region gives $7.5^{+5.3}_{-4.5}$ events, giving the bound of $\mathcal{B}(\Upsilon(1S) \rightarrow \gamma a_1^0) < 2.3 \times 10^{-6}$ at 90% C.L. Translated to $\tan \beta \cos \theta_A$, the bound disfavors the claim by [16], and CLEO “calls for a reevaluation of the a_1^0 hypothesis for the HyperCP events.” The situation is volatile indeed!

We remark that a_1^0 – η_b mixing [20] has been considered for the heavy mass $m_{a_1^0} > 9.2 \text{ GeV}$ case. But with BaBar observation [6] of η_b in the recoil photon from $\Upsilon(3S) \rightarrow \gamma \eta_b$, based on 109M $\Upsilon(3S)$ events, the likelihood for a_1^0 – η_b mixing effect is not a high one. BaBar finds $m_{\eta_b} \simeq 9389 \text{ MeV}$, with $\Upsilon(1S)$ – $\eta_b(1S)$ hyperfine splitting at 71 MeV. The latter is not much higher than expected from QCD.

Prognosis

It seems that, besides the interests in spectroscopy, the bottomonium system also provides a window on New Physics. With 28 fb^{-1} on the $\Upsilon(3S)$ collected in the 2008 end-run by BaBar, it remains to be seen how much improvement on DM search limit can be achieved beyond the Belle result [3]. The question is background control. The same data can be used for $\Upsilon(1S) \rightarrow \gamma a_1^0$ search, using $\Upsilon(3S) \rightarrow \pi^+ \pi^- \Upsilon(1S)$. But here CLEO has preempted with 1.1 fb^{-1} data directly on the $\Upsilon(1S)$ [18]. For that matter, Belle has collected $5 \times$ the data on the $\Upsilon(1S)$ compared to CLEO in June 2008. We await the Belle analysis on a_1^0 search with this data, as well as BaBar’s results from their large data sample on the $\Upsilon(3S)$ and $\Upsilon(2S)$. It is interesting that $\Upsilon(1S)$, $\Upsilon(2S)$, $\Upsilon(3S)$ studies have turned into a new arena on New Physics and plugs a potential weak spot for LHC.

A future Super B Factory could probe this arena with ease, if flexible enough in its C.M.S. energy. Depending on how the LHC physics unfolds, it may turn out to be rather important. Because of this, the Super B Factory design should improve on hermeticity.

References

1. Jean, P., et al.: Astron. Astrophys. **407**, L55 (2003) 93
2. McElrath, B.: Phys. Rev. D **72**, 103508 (2005) 93, 95
3. Tajima, O., et al. [Belle Collaboration]: Phys. Rev. Lett. **98**, 132001 (2006) 94, 99
4. Rubin, P., et al. [CLEO Collaboration]: Phys. Rev. D **75**, 031104 (2007) 95
5. Ablikim, M., et al. [BES Collaboration]: Phys. Rev. Lett. **100**, 1920011 (2008) 95
6. Aubert, B., et al. [BaBar Collaboration]: Phys. Rev. Lett. **101**, 071801 (2008) 95, 99
7. Park, H., et al. [HyperCP Collaboration]: Phys. Rev. Lett. **94**, 021801 (2005) 95
8. Wang, M.Z., et al.: Nucl. Instrum. Meth. A **455**, 319 (2000) 95
9. Sahu, S.K., et al.: Nucl. Instrum. Meth. A **388**, 144 (1997) 95
10. Akhmetshin, R., et al.: Nucl. Instrum. Meth. A **455**, 324 (2000) 95
11. Ueno, K., et al.: Nucl. Instrum. Meth. A **396**, 103 (1997) 95
12. Wang, C.H., et al.: A Study of $B \rightarrow \tau \nu$ Search at BELLE, Belle (internal) Note 180, (1997) 95
13. Yao, W.M., et al. [Particle Data Group]: J. Phys. G **33**, 1 (2006) 96
14. Amsler, C., et al.: Phys. Lett. B **667**, 1 (2008); and <http://pdg.lbl.gov/> 96
15. Dermisek, R., Gunion, J.F., McElrath, B.: Phys. Rev. D **76**, 051105 (2007) 96, 97, 98

16. He, X.G., Tandean, J., Valencia, G.: Phys. Rev. Lett. **98**, 081802 (2007) 97, 99
17. Mangano, M.L., Nason, P.: Mod. Phys. Lett. A **19**, 1373 (2007) 97
18. Love, W., et al. [CLEO Collaboration]: Phys. Rev. Lett. **101**, 151802 (2008) 97, 98, 99
19. Wilczek, F.: Phys. Rev. Lett. **39**, 1304 (1977) 97
20. Fullana, E., Sanchis-Lozano, M.A.: Phys. Lett. B **653**, 67 (2007) 99

Chapter 8

D and *K* Systems: Box and EWP Redux

We shall cover only D^0 mixing and rare $K \rightarrow \pi \nu \bar{\nu}$ decays.

D^0 mixing was observed in 2007, 31 years after the observation of D mesons (see Table 8.1). Being the smallest in (relative) strength and the last one to be observed, one has come full circle from the original insight by Gell-Mann and Pais [1], on possible quantum-mechanical mixing in the neutral kaon–anti-kaon system. It also demonstrates that the B factories are charm factories at the same time (the ~ 1.3 nb cross section for $e^+e^- \rightarrow c\bar{c}$ production is larger than ~ 1.1 nb for $e^+e^- \rightarrow B\bar{B}$ production), while the study of charm at $D\bar{D}$ threshold would still play a key role. Though veiled by hadronic effects, the observation of D^0 mixing opens a new avenue for probing New Physics, especially in the future pursuit of CPV at a Super B (rather, Flavor) Factory.

On the other hand, being the forebear of FCNC and CPV studies, limits in the kaon system have been pushed down to the extreme. However, facilities have dwindled. We shall use the $K_L \rightarrow \pi^0 \nu \bar{\nu}$ (CPV) and $K^+ \rightarrow \pi^+ \nu \bar{\nu}$ modes to illustrate a renewed plan to reach down to SM sensitivities and hopefully discover New Physics along the way.

Table 8.1 Current values of measurements of meson mixing in mass and lifetime, ordered in first year of measurement, where $x = \Delta m/\Gamma$, $y = \Delta\Gamma/2\Gamma$. The number in parenthesis in the last column is the year the meson was discovered

	x	y	Date
K^0	0.474	0.997	1956 (1950)
B_d^0	0.776	< 0.009	1987 (1983)
B_s^0	26.9	0.067 ± 0.038	2006 (1992)
D^0	$0.0089^{+0.0026}_{-0.0027}$	$0.0075^{+0.0017}_{-0.0018}$	2007 (1976)

8.1 D^0 Mixing

Thirty-one years after the D^0 meson was first observed, between the Belle and BaBar experiments, and with quite some feat of experimental effort, D^0 – \bar{D}^0 mixing was finally observed in 2007. This is the last neutral meson mixing to be measured.

While the measurements of mixing for $K^0-\bar{K}^0$ and $B_d^0-\bar{B}_d^0$ systems were rather soon after the mesons were discovered, measurement of meson mixings was much more challenging for the $B_s^0-\bar{B}_s^0$ and $D^0-\bar{D}^0$ systems. For B_s , the challenge was the ultrafast oscillations, while to date the mixing in lifetime (width mixing), or lifetime difference, is not yet established. For D^0 , the challenge was the sheer smallness of x_D and y_D , i.e., the smallness of mass and lifetime differences. To date, we are not firmly sure which one is the larger. Curiously, the observation of $B_s^0-\bar{B}_s^0$ and $D^0-\bar{D}^0$ mixings came in such close succession, in 2006 and 2007, respectively. It reflects the maturity of the Tevatron and the B factories, as well as the complementary nature, and some level of competition, between them. Furthermore, the measurement of meson mixing is the prelude to the even more interesting CPV studies. The epic has just started for these two relative newborns.

8.1.1 SM Expectations and Observation at B Factories

Just like the K^0 , B_d^0 , and B_s^0 meson systems, the box diagrams shown in Fig. 8.1 govern the short distance contributions to D^0 mixing. But this is the only case¹ where one has the down-type quarks in the loop.

From our previous discussions of box diagrams, because the d and s quark masses are so small, their contribution is negligible at short distance, so only the b quark contribution matters in the box diagram. But even m_b is tiny compared to m_t (or M_W), which leads to suppression factors of m_b^2/M_W^2 . In addition, $V_{ub}V_{cb}^*$ is extremely small compared to the leading $V_{ud}V_{cd}^* \simeq -V_{us}V_{cs}^* \cong -0.22$ in the CKM triangle relation

$$V_{ud}V_{cd}^* + V_{us}V_{cs}^* + V_{ub}V_{cb}^* = 0. \quad (8.1)$$

Thus, in the SM, because of lack of “Higgs affinity” in the loop, D^0 mixing receives very tiny Short Distance (SD) contributions. Normally, this implies that it is an excellent probe of New Physics. But the smallness of SD effects makes it susceptible to Long Distance (LD) contributions of hadronic origins.

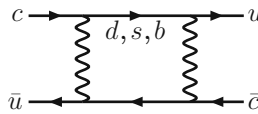


Fig. 8.1 A SM box diagram for $D^0-\bar{D}^0$ mixing. The $q'\bar{q}$ contributions (where $q^{(\prime)} = d, s$), though negligible at short distance, could generate Γ_{12}^D at hadron level, since $c \rightarrow q'u\bar{q}$ and $c\bar{u} \rightarrow q'\bar{q}$ generate D^0 decays

¹ For the unaware, the top decay width is of order 1.4 GeV, so the top lifetime is much shorter than the strong interaction time scale of 10^{-23} s for it to pair with light quarks to form bound states. There are no T mesons, charged or neutral.

Cutting across the light s and d quark lines in the box diagram, the resulting diagram is the squared amplitudes of $c \rightarrow su\bar{d}, su\bar{s}, du\bar{d}, du\bar{s}$, as well as $c\bar{u} \rightarrow s\bar{d}, s\bar{s}, d\bar{d}, d\bar{s}$ processes. Note that the annihilation type of diagrams are not suppressed compared to spectator diagrams, because the charm mass is not too far above the hadronic scale. These squared amplitudes correspond to, for example, Right-Sign (RS) or Cabibbo-Favored (CF) $D^0 \rightarrow K^-\pi^+$, Cabibbo-Suppressed (CS) $D^0 \rightarrow K^-K^+, \pi^-\pi^+$, and “wrong-sign” (WS) or Doubly Cabibbo-Suppressed (DCS) $D^0 \rightarrow K^+\pi^-$ hadronic processes. Put another way, D^0 and \bar{D}^0 decay to common final states can interfere and generate the absorptive part of the hadronic level box amplitude, or a *width difference*, much like in $K^0-\bar{K}^0$ and $B_s^0-\bar{B}_s^0$ systems.

It has been argued [2] that SU(3) breaking effects in PP and $4P$ (where P stands for K or π) final states can generate a percent level $y_D \equiv \Delta\Gamma_D/2\Gamma_D$, the parameter usually used in place of the width difference $\Delta\Gamma_D$. It was further shown that a y_D at the percent level can generate, via a dispersion relation, the dispersive mass mixing $x_D = \Delta m_D/\Gamma_D$ that is comparable in size to y_D . Unfortunately, the hadronic uncertainties are uncontrollable. These estimates concur with earlier arguments [3] that $x_D \sim y_D \sim 1\%$ is possible from long distance SM, or hadronic, effects. With the observation of $D^0-\bar{D}^0$ mixing in 2007, so far $x_D \sim y_D \sim 1\%$ seems to be the case, i.e., consistent with long distance effects.

Observation at B Factories

The 2007 observation of D^0 mixing is the combined result of

1. Belle analysis of 540 fb^{-1} data for $D^0 \rightarrow K^+K^-, \pi^+\pi^-$ (CP eigenstates) vs. $K^-\pi^+$ to extract y_{CP} [4];
2. both Belle [5] and BaBar [6] analyzed $D^0 \rightarrow K^\mp\pi^\pm$ (Cabibbo-favored vs. doubly Cabibbo-suppressed), with 400 fb^{-1} and 384 fb^{-1} data respectively, to extract x'_D and y'_D , where (x'_D, y'_D) is a rotation from (x_D, y_D) by a strong phase δ between the Cabibbo allowed and suppressed $D^0 \rightarrow K^\mp\pi^\pm$ decays;
3. a time-dependent Dalitz analysis of $D^0 \rightarrow K_S\pi^+\pi^-$ by Belle [13] with 540 fb^{-1} , which allows one to extract x_D and y_D directly.

The main progress, almost concurrent, was the evidence shown separately in Refs. [4] and [6]. These analyses are rather complicated and technical. We highlight only very briefly the key points.

Let us first mention three general aspects for conducting D^0 mixing studies. To tag the flavor of D^0 , one uses the slow pion (denoted as π_s^+) in $D^{*+} \rightarrow D^0\pi^+$. A slow π_s^- that forms a D^{*-} would tag a \bar{D}^0 (analogous to same side tagging). Second, the intersection of the reconstructed D^0 track and the beam profile gives vertex information, similar to “ K_S vertexing.” Finally, almost every B decay has D mesons in the final state, but the B lifetime would severely smear the timing information. To cut out $B\bar{B}$ background, one typically requires $p_{D^0} > 2.5 \text{ GeV}$ in the e^+e^- c.m. frame. Thus, in the language of B_d and B_s mixing studies at hadronic machines, at B factories one uses prompt D^{*+} production with “same side tagging.” Indeed, as

we shall see, after the evidence of D^0 mixing was announced separately by Belle [4] and BaBar [6], CDF has also measured [7] D^0 mixing.

$y_{CP}: D^0 \rightarrow K^- K^+, \pi^- \pi^+ \text{ vs. } K^- \pi^+$

The $K^- K^+$ and $\pi^- \pi^+$ are CP even final states. In the limit of no CPV, which is a good approximation² since there is no evidence of CPV yet in D^0 system, τ_{P-P^+} gives the lifetime of the CP even D^0 and \bar{D}^0 meson eigenstate. One can measure the difference between the “flavor-specific” lifetime vs. the lifetime in CP eigenstate,

$$y_{CP} \equiv \frac{\tau_{K^- \pi^+}}{\tau_{K^- K^+}} - 1 \cong y_D \cos \phi \cong y_D. \quad (8.2)$$

The first approximation in (8.2) is analogous to (3.10) for B_s system, where we have dropped a term related to CPV in mixing. That is, setting $|q/p| \cong 1$ in

$$|D_{1,2}\rangle = p|D^0\rangle \pm q|\bar{D}^0\rangle, \quad (8.3)$$

which is defined similarly to (A.11). The second, or last, step follows from absence of CPV, which is borne out by data so far. The measurement of y_{CP} probes D^0 meson width mixing, or Γ_{12} .

The FOCUS experiment reported a y_{CP} at several percent level in 2000 [9, 10], which aroused much interest at the B factories. The FOCUS value was soon put to rest by Belle, BaBar, and CLEO [9, 10]. To measure a smaller value, one needs much more data. By early 2007, using 540 fb^{-1} data collected on the $\Upsilon(4S)$ resonance, Belle found 111K, 1.22M, and 49K events in the $K^- K^+$, $K^- \pi^+$, and $\pi^- \pi^+$ final states, respectively, with high purity. Fitting both the $\pi^- \pi^+$ and $K^- K^+$ modes vs. $K^- \pi^+$ mode, Belle found [4] $y_{CP} = 1.31 \pm 0.32 \pm 0.25 \%$, which constitutes 3.2σ (4.1σ statistical) evidence. The effect is visible to the eye from the ratio of decay-time distributions, that the CP even mixture of D^0 and \bar{D}^0 meson state decays slightly faster, just like the case of K_S^0 . Of course, unlike the striking difference in lifetime for K_S^0 and K_L^0 , the small % level lifetime difference is due to many more open channels for both the CP even and odd states in the D^0 – \bar{D}^0 system.

The Belle y_{CP} result was subsequently confirmed by BaBar using 384 fb^{-1} data, with slightly lower significance. Combined together, y_{CP} is currently the most precisely measured D^0 mixing parameter [9–11]. At the same level of precision, there is currently no indication for t -dependent nor time-integrated CPV in the lifetime of D^0 vs $\bar{D}^0 \rightarrow K^+ K^-$. Because of the smallness of x_D and y_D themselves, it would require even higher statistics for CPV phases to be profitably probed.

² For a more complete treatment considering CPV in D mixing, we refer to [8]. The formalism bears much similarity with our limited discussion of the B_s system. Although unequivocal indication for New Physics has to come with observation of TCPV in D^0 system, so far we are not yet there.

$y'_D: D^0 \rightarrow K^-\pi^+$ vs. $K^+\pi^-$

$D^0 \rightarrow K^-\pi^+$ is a CF (Cabibbo-favored) decay, hence it is called the Right-Sign (RS) decay when associated with a π_s^+ tag. For the $K^+\pi^-$ final state (called WS) with a π_s^+ tag, it could either come from DCS decay, or through $D^0 \rightarrow \bar{D}^0$ oscillation, then the $\bar{D}^0 \rightarrow K^+\pi^-$ decay. Thus, this is nothing but TCPV, except that, like the B_s system, width mixing is possibly present. In addition, since the CF vs. DCS $D^0 \rightarrow K^\mp\pi^\pm$ amplitudes could have a strong phase difference $\delta_{K\pi}$ (i.e., they mix via final state rescattering) between them, one actually measures

$$x'_D = x_D \cos \delta_{K\pi} + y_D \sin \delta_{K\pi}, \quad y'_D = -x_D \sin \delta_{K\pi} + y_D \cos \delta_{K\pi}. \quad (8.4)$$

Because x_D and y_D are so small, the exponential time dependence of mass and width mixing can be approximated linearly in amplitude, hence are up to quadratic terms when comparing rates. That is, the probability for a π_s^+ tagged $D^0(t=0) \equiv D^0$ at time zero to be detected at time t in the WS final state $K^+\pi^-$ is

$$|\langle K^+\pi^- | D^0(t) \rangle|^2 e^{\hat{t}} \propto R_D + \sqrt{R_D} y'_D \hat{t} + \frac{1}{4} (x_D'^2 + y_D'^2) \hat{t}^2, \quad (8.5)$$

where $\hat{t} \equiv t/\tau$ is normalized by the mean lifetime τ of D^0/\bar{D}^0 mesons, and once again we have ignored CPV. In (8.5), R_D is the ratio of the DCS to CF decay rates, the $x_D'^2 + y_D'^2$ term arises from mixing alone, while the term linear in t is due to interference between the DCS and mixing amplitudes, which is the main term of interest. In the limit that x'_D and y'_D are small, it is this interference term that has the best sensitivity.

With 400 fb^{-1} data, the Belle study [5] gave approximately 2σ exclusion from zero in the $(x_D'^2, y_D')$ plane, with R_D consistent with SM expectation. Subsequently, and almost concurrent with the Belle evidence [4] for y_{CP} , the BaBar experiment announced 3.9σ evidence [6] for D^0 mixing with a data of 384 fb^{-1} . Identifying about 4000 WS events vs. 1.14M RS events, the best fit value assuming no CPV (again with R_D consistent with SM) was $(x_D'^2, y_D') \times 10^3 = (-0.22 \pm 0.30 \pm 0.21, +9.7 \pm 4.4 \pm 3.1)$. The negative $x_D'^2$ value is unphysical, but still consistent with zero, while y_D' is at the % level. The sensitivity is clearly in y_D' , as the $x_D'^2$ measurement does not translate too well into x'_D .

The BaBar result for y_D' was later confirmed by CDF [7] with 1.5 fb^{-1} data, finding $(x_D'^2, y_D') \times 10^3 = (-0.12 \pm 0.35, +8.5 \pm 7.6)$, claiming 3.8σ deviation from zero in $(x_D'^2, y_D')$ plane. In principle, this could have been achieved in the same time frame as the BaBar study, but in any case it demonstrates clearly that D^0 mixing can be pursued in a hadronic environment.

 $x_D, y_D: t\text{-dep. } D^0 \rightarrow K_S\pi^+\pi^- \text{ Dalitz Analysis}$

The unique feature of time-dependent Dalitz analysis in D^0/\bar{D}^0 decay to the self-conjugate $K_S\pi^+\pi^-$ final state is its ability to *probe both x_D and y_D directly, including the sign of x_D* . At the starting point, it is like extending the y_p program

to $D^0/\bar{D}^0 \rightarrow K^{*\pm}\pi^\mp$ in the $K_S\pi^+\pi^-$ final state. But the self-conjugate nature of the final state means the CF and DCS decays populate the same Dalitz plot, with a flip of $m_{K_S\pi^-}^2 \leftrightarrow m_{K_S\pi^+}^2$, allowing them to interfere. Combining with the time evolution (i.e., x_D and y_D) of the D^0 vs. \bar{D}^0 tagged states, there is such prowess in the t -dependent Dalitz analysis method that one can in principle extract much information, including information on q/p and CPV in the long run. There is considerable similarity with the formalism for study of mixing-dependent CPV in B_s system, where one also has $\Delta\Gamma_{B_s} \neq 0$. The difference is, of course, $\Delta m_{B_s}/\bar{\Gamma}_{B_s}$, which is so large, while $\Delta m_D/\bar{\Gamma}_{D^0}$ and $\Delta\Gamma_D/2\bar{\Gamma}_{D^0}$ are so tiny.

Note that the $D^0 \rightarrow \rho^0 K_S$ decay to CP eigenstate, just like the CF $D^0 \rightarrow K^{*-}\pi^+$ decay and DCS $D^0 \rightarrow K^{*+}\pi^-$ decay, also populates different bands in the $K_S\pi^+\pi^-$ Dalitz plot. In fact, one currently models the quasi-two-body as well as nonresonant contributions (treated as a complex constant term), and these bring in many fitting parameters, including strong phases. But one has a large number of events in the Dalitz plot signal region. The methodology is quite similar to the “ DK Dalitz” program [12] for ϕ_3/γ extraction, where one utilizes the analyzing power of interference of $D^0/\bar{D}^0 \rightarrow K_S\pi^+\pi^-$ in the $K_S\pi^+\pi^-$ Dalitz plot. Although in principle (limit of infinite statistics) the approach is model independent, in practice, one also models resonant and nonresonant D decay to $K_S\pi\pi$.

Using the t -dep. Dalitz analysis approach in $K_S\pi^+\pi^-$, in Spring 2007, Belle came out with the result [13] using a data set of 540 fb^{-1} . With $\sim 0.5\text{M}$ signal events in the $K_S\pi^+\pi^-$ Dalitz plot and assuming negligible CPV, the fitted numbers were $x_D = 0.80 \pm 0.29_{-0.07-0.14}^{+0.09+0.10} \%$ and $y_D = 0.33 \pm 0.24_{-0.12-0.08}^{+0.08+0.06} \%$, where the last error is the systematic error due to the Dalitz decay model. The result disfavors $(x_D, y_D) = (0, 0)$ by 2.2σ , which may seem less significant than the y_{CP} and y'_D results. But this is the first result with real significance for x_D , indicating that x_D is positive and of similar strength to y_D .

This method is by far the most sophisticated, hence most complicated of all approaches to D^0 mixing. But it also means that a detailed exposition is beyond the scope of this book. In any case, one does not have any indication for New Physics at present.

Combined Result: Observation of D^0 Mixing in 2007

By late Spring 2007, the pursuit of the above three methods had produced measurements that, when combined, excluded $(x_D, y_D) = (0, 0)$ at the 5σ level (see Fig. 8.2), thereby D^0 mixing became established. This does not include the BaBar confirmation of y_{CP} , nor the CDF confirmation of y'_D . The best fit, assuming CP invariance, gives,

$$x_D = 0.87_{-0.34}^{+0.30} \%, \quad y_D = 0.66_{-0.20}^{+0.21} \% \quad (\text{May 2007}), \quad (8.6)$$

with $\delta_{K\pi} = 0.33_{-0.29}^{+0.26} \text{ rad}$, or $(18.9_{-16.6}^{+14.9})^\circ$. While y_D is more solid, a finite $\%$ level x_D is indicated.

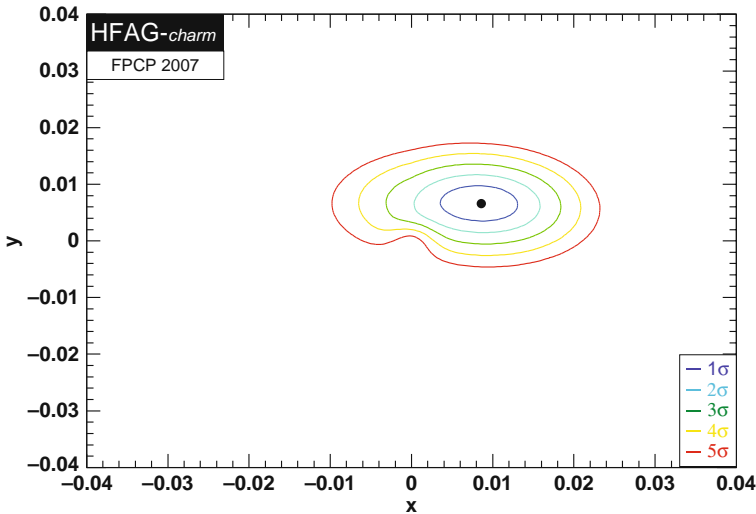


Fig. 8.2 Observation of D^0 mixing in Spring 2007: HFAG 2007 plot (used with permission) of combined fit to data, with (8.6) as best fit result, together with $\delta_{K\pi} = 0.33^{+0.26}_{-0.29}$ rad, and assuming CP invariance

Further progress has been made after summer 2007, which we have partly discussed. Rather than going into any further detail, we just quote the FPCP2008 results from HFAG [11]. Although data are consistent with no CPV, as significance has been further improved, we quote the fit that allows for CPV,

$$x_D = 0.89^{+0.26}_{-0.27} \%, \quad y_D = 0.75^{+0.17}_{-0.18} \% \quad (\text{May 2008}), \quad (8.7)$$

with $\delta_D = (21.9^{+11.3}_{-12.4})^\circ$. There is no drastic change from 2007, except some gain in significance.

8.1.2 Interpretation and Prospects

As we have already discussed, $|x_D| \sim y_D \sim 1\%$ can arise in the SM by hadronic final state effects. This is precisely what is observed by experiment. Note that the short distance effect for x_D is negligible. It is of some interest to note that, if the $4P$ final state dominates the long distance contribution, which is consistent with $y_D \sim 1\%$, then x_D^{LD} and y_D (necessarily long distance) should be of the opposite sign [16], while data show the same sign. Although it has been checked [2] that changing hadronic parameters does not change this conclusion, unfortunately the hadronic effects are not well under control for one to make a definite statement. In any case, one should remember the Δm_K enterprise of 20–30 years ago. That is, although the observed strength could arise from charm and even long distance

effects, comparable BSM at even twice the observed Δm_K is always allowed. The same can be applied to Δm_D .

We have spent some time covering what it took to bring forth the observation of D^0 mixing, but what we are really interested in is the New Physics impact, rather than hadronic physics. Although one has made great experimental stride, for the moment, however, one cannot say that there is indication for New Physics in D^0 mixing. A rather comprehensive study for New Physics implications can be found in [17]. Ultimately it seems, one would need to measure CPV, expected to be tiny within SM (with or without long distance dominance), to find unequivocal evidence for BSM. We stress again that CPV effects in D^0 mixing appear to be small [11] at present. Put another way, had CPV effects been observed with present sensitivities, we would have found convincing BSM physics.

As a special New Physics case, we plot the result [15] for a fourth generation in Fig. 8.3. This is along the line where one can account for $\Delta\mathcal{A}_{K\pi}$ (Sect. 2.2), predict $\sin 2\Phi_{B_s} = -0.5$ to -0.7 (Sect. 3.2.3), and predict positive A_{FB} in the low q^2 bins (Sect. 5.1, in particular Sect. 5.1.2 and 5.1.3) for $B \rightarrow K^*\ell^+\ell^-$. As can be seen from Fig. 8.3, which is consistent with Fig. 2 of [17], the expectation for Δm_D is basically consistent with (slightly above) experimental measurement. This should be of considerable interest, not only because it is being probed experimentally, but because one could have found a much larger result in contradiction with data.

Let us see how this result emerged. It is advantageous to use a 4×4 parametrization [18] that follows SM3 to put one weak phase in V_{ub} , but the other two phases in $V_{t's}$ and $V_{t'd}$, respectively. For the rotation angles, one keeps the SM3 definition utilizing the $|V_{us}|$, $|V_{cb}|$, and $|V_{ub}|$ elements, as they are now well measured. For the three new angles, we choose $|V_{t'b}|$, $|V_{t's}|$, and $|V_{t'd}|$, which are accessible through loop effects, rather than $|V_{ub'}|$, $|V_{cb'}|$, $|V_{tb'}|$, which are less accessible so far. One thus has a convenient parametrization that fully implements 4×4 unitarity.

Taking $m_{t'} = 300$ GeV as bench mark, with $V_{t's}^* V_{t'b}$ fixed by $\Delta\mathcal{A}_{K\pi}$ (which constrains the product $V_{t's}^* V_{t'b} m_{t'}^2$), we used [14, 15] $V_{t'b} \sim -0.22$ to saturate the $Z \rightarrow b\bar{b}$ constraint, hence $V_{t's} \sim -0.114 e^{-i70^\circ}$. The kaon constraints then fixes

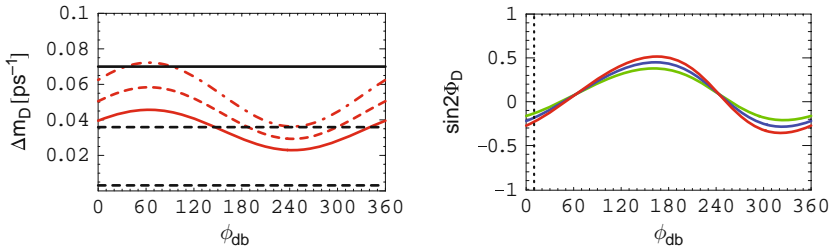


Fig. 8.3 Defining $V_{t'd} V_{t'b}^* \equiv r_{db} e^{-i\phi_{db}}$: **(a)** Δm_D^{SD} vs. ϕ_{db} for $m_{b'} = 230$ (solid), 270 (dash), and 310 (dotdash) GeV and $r_{db} = 10^{-3}$, where the solid horizontal line is the PDG2006 bound, while the dashed band is 2σ range for $x_D = 0.80 \pm 0.34\%$, the situation at Moriond 2007; **(b)** $\sin 2\Phi_D$ vs. ϕ_{db} for $m_{b'} = 270$ GeV and $r_{db} \sim (0.8, 1, 1.2) \times 10^{-3}$ [from [15], copyright (2007) by The American Physical Society]

$V_{t'd} \sim 0.0044 e^{-i10^\circ}$. It is nontrivial that $b \rightarrow d$ observables such as $\sin 2\phi_1$ become SM-like (see Fig. 1(b) of [15]),³ as measured by experiment, while $b \rightarrow s$ transitions have large CPV effect.

Besides continued progress, there are two things to watch in regards D^0 mixing. While other measurements have seen steady progress for several years, it is for the first time that the Dalitz analysis of Belle [13] sees an indication for x_D . Second, to unravel some of the hadronic physics in the decay final state, one needs to gain independent access to the strong phases. Employing quantum coherence just like in TCPV studies in $Y(4S) \rightarrow B^0 \bar{B}^0$ decays, by a tagged Dalitz analysis in $\psi(3770) \rightarrow D^0 \bar{D}^0$ decays, one can [19] extract the strong phase δ_D , which would in turn feedback on x_D and y_D extraction. Unfortunately, CLEO-c ended up not taking enough data on the $\psi(3770)$ resonance before shutdown. However, BES-III has started data taking in 2008, so in the near future, this and other possible threshold charm factories could aid the D^0 mixing program considerably through this type of studies. Basically, the Dalitz type of analysis, with the help of quantum coherence, holds the power for the future.

This is an area where a Super B Factory can compete well with LHCb because of its diversity. However, LHCb can also play a role, as evidenced by the CDF study [7] of D^0 mixing with $D^0 \rightarrow K^\pm \pi^\mp$ mode using 1.5 fb^{-1} data, which yield a result that is complementary to Belle and BaBar in this mode.

8.2 $K \rightarrow \pi \nu \bar{\nu}$ Decays

Kaon physics is the wellspring from which the SM flavor structure sprang out, giving forth ideas of GIM cancellation (hence charm), box diagrams, strong and electroweak penguins, as well as the experimental discovery of CPV, which lead to the KM postulate of three generations, before two generations were even complete. But despite its years, kaon physics is not yet a spent force. For New Physics, the focus is on the electroweak penguin processes $K^+ \rightarrow \pi^+ \nu \bar{\nu}$ and $K_L \rightarrow \pi^0 \nu \bar{\nu}$, where the latter is CP violating. As depicted in Fig. 8.4, these are the original electroweak penguins where strong heavy quark mass dependence was uncovered by Inami and Lim [20]. The advantage of pursuing this program is the rather small theoretical uncertainties, thanks to the long history of kaon physics. Unlike D^0 mixing of the previous section, these processes are short distance dominated, the main hadronic dependence is in the transition form factors, which can be extracted from similar charged current decays. Theoretical uncertainties are only at the few % level [21] and smaller for $K_L \rightarrow \pi^0 \nu \bar{\nu}$. The other useful measurement, again because of short distance dominance, is the venerable and well-measured ε_K parameter, which depends on $f_K^2 B_K$ and is a focus of lattice studies.

³ In fact, as Fig. 1(b) of [15] shows, the four-generation $b \rightarrow d$ quadrangle cannot be easily distinguished from the three-generation $b \rightarrow d$ triangle. This explains why we did not observe indications for New Physics in Fig. 1.6.

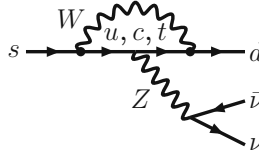


Fig. 8.4 SM Z penguin diagram for $s \rightarrow d\bar{\nu}\nu$ decay, which generates $K^+ \rightarrow \pi^+\nu\bar{\nu}$ and $K_L \rightarrow \pi^0\nu\bar{\nu}$ transitions

If 10% measurement of the SM prediction for the $K^+ \rightarrow \pi^+\nu\bar{\nu}$ and $K_L \rightarrow \pi^0\nu\bar{\nu}$ modes can be achieved, then whether these two measurements would meet together with ε_K on the $\bar{\rho}-\bar{\eta}$ plane is both a test of (three generation) CKM structure and a probe of BSM. For $K_L \rightarrow \pi^0\nu\bar{\nu}$ mode, the path would be longer, but there is also more reach for New Physics discovery.

8.2.1 Current Status

This field saw its last hurrah in ε'/ε a decade ago [9, 10]. Despite the top effect through the electroweak penguin, which allowed ε'/ε to nearly vanish, unfortunately, the interpretation of ε'/ε is almost completely clouded by long distance effects. For New Physics probes, we concentrate only on modes that are not marred by hadronic effects.

$K^+ \rightarrow \pi^+\nu\bar{\nu}$

There has been a long standing hint of three events for $K^+ \rightarrow \pi^+\nu\bar{\nu}$ decay at BNL by the E787/949 experiments (an effort extending 20 years). But very recently, E949 gave their final results.

The previous three events were based on a sample of 7.7×10^{12} (!) stopped K^+ s at the BNL AGS proton accelerator, with pion momentum in the range $211 < p_{\pi^+} < 229$ MeV/c, which is above the $K^+ \rightarrow \pi^+\pi^0$ peak. With background estimated at 0.44 ± 0.05 events, the measured branching ratio is $B(K^+ \rightarrow \pi^+\nu\bar{\nu}) = 1.47^{+1.30}_{-0.89} \times 10^{-10}$ [9, 10], which should be compared with the SM prediction of $\sim 0.82 \times 10^{-10}$.

E949 extended the search to $140 < p_{\pi^+} < 195$ MeV/c, which is *below* the $K^+ \rightarrow \pi^+\pi^0$ peak, using a smaller sample of 1.7×10^{12} stopped K^+ decays. Similar to the previous study above $K^+ \rightarrow \pi^+\pi^0$ peak, one detects the incoming charged kaon, its decay at rest, together with an outgoing charged pion with no other detector activity in coincidence.

Active degraders were used for the final stage slow down of the incoming kaon, which gives coincidence with the decay in the target. For the emitted π^+ , besides measuring its momentum, it is further brought to rest in a “range stack,” for sake of both positive identification as well as measurement of the energy. It is important to veto all other activity, especially photons, e.g., from the π^0 in $K^+ \rightarrow \pi^+\pi^0$ decay, which is the dominant background. Another background to deal with is π^+

rescattering in the target. The extended study to below the $K^+ \rightarrow \pi^+ \pi^0$ peak was possible by improvements made in background rejection via the active degrader and the range stack. A blind analysis was used, i.e., the “signal box” was opened only after the signal selection criteria, acceptance, and background estimates were all completed.

The pion energy vs. range plot [22] of the final E949 analysis is given in Fig. 8.5. Although the signal region is smaller for the previously published analysis above the $K^+ \rightarrow \pi^+ \pi^0$ peak, it carries 4.2 times the sensitivity than the new analysis below the $K^+ \rightarrow \pi^+ \pi^0$ peak. This is due both to lower S/B as well as statistics for the new, lower momentum analysis. From the three events in the lower box of Fig. 8.5 alone, one gets $\mathcal{B}(K^+ \rightarrow \pi^+ \nu \bar{\nu}) = 7.89^{+9.26}_{-5.10} \times 10^{-10}$. Combining with the earlier result of E787/949 using the upper box, the final result is

$$\mathcal{B}(K^+ \rightarrow \pi^+ \nu \bar{\nu}) = 1.73^{+1.15}_{-1.05} \times 10^{-10} \quad (2008), \quad (8.8)$$

which has central value higher than, but still consistent with, SM prediction of $\sim 0.82 \times 10^{-10}$. One cannot say there is a strong indication for New Physics.

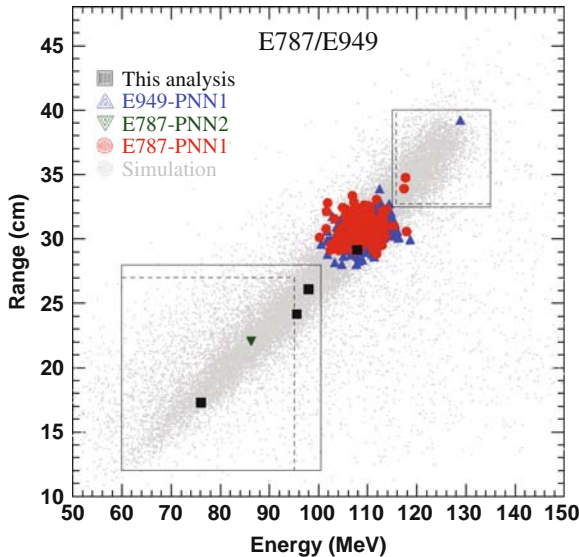


Fig. 8.5 Measured energy vs. range plot for all events passing $K^+ \rightarrow \pi^+ \nu \bar{\nu}$ cuts of final E787/E949 analysis [22]. The three events in the smaller box for larger E_π are from the higher momentum π^+ study, and the lower E_π box is for the update study below $K^+ \rightarrow \pi^+ \pi^0$ peak (the downward-pointing triangle is from earlier E787 data). The latter gives rise to the cluster of events around $E_\pi \simeq 108$ MeV. The grey dots are simulated $K^+ \rightarrow \pi^+ \nu \bar{\nu}$ events (from [22], [Copyright (2008) of American Physical Society])

$K_L \rightarrow \pi^0 \nu \bar{\nu}$

The E391a experiment, which ran at KEK PS, is the first dedicated experiment on $K_L \rightarrow \pi^0 \nu \bar{\nu}$. It has recently produced the new limit [23] of

$$\mathcal{B}(K_L \rightarrow \pi^0 \nu \bar{\nu}) < 6.7 \times 10^{-8} \quad (2008), \quad (8.9)$$

at 90% C.L., which improves its own previous limit by a factor of 3. Another data set equivalent in size is being analyzed. The limit is of course very far away from the SM expectation of $\sim 2.8 \times 10^{-11}$. But this also means that there is great potential for discovery of BSM physics. Note that this decay is intrinsically CP violating, since the decay amplitude is the *difference* between K^0 and \bar{K}^0 decay because of the K_L wavefunction. This adds to the interest in this mode as a probe of New Physics.

$K_L \rightarrow \pi^0 \nu \bar{\nu}$ search is considerably more challenging than $K^+ \rightarrow \pi^+ \nu \bar{\nu}$. The beam is more difficult, while the signal is just two photons (from π^0) *and nothing else*. Besides measuring these two photons well and demanding $m_{\gamma\gamma} = m_{\pi^0}$ while vetoing everything else, one needs to reconstruct the K_L decay vertex along the beam direction. This requires a “pencil” beam. The discriminant is then missing p_T (carried away by $\nu \bar{\nu}$) vs. Z_{vertex} , which forms the fiducial region that must be studied very carefully.

To reduce backgrounds from beam–gas interaction, the K_L decay region is maintained at the high vacuum of 10^{-5} Pa, while separated from the detector region by a thin membrane. The main background is from $K_L \rightarrow \pi^0 \pi^0 (\pi^0)$, where two (four) photons escape detection, and neutron halo of the beam that interact with the detector and produce π^0 and η mesons. The latter turned out to dominate for E391a. In fact, for the three run periods at the 12 GeV PS, the first period suffered from serious neutron-induced backgrounds that were caused by the drooping of the membrane. Having fixed this, for the second run period, the $K_L \rightarrow \pi^0 \pi^0$ background was estimated by MC simulation and verified with reconstructed 4γ events. To understand neutron halo background, a dedicated run with an inserted aluminum plate was undertaken.

The signal box was opened only after all the selection criteria and background estimates were determined. No events were seen in the neutral pion p_T vs. Z_{vertex} signal region. The number of K_L decays were estimated at 5.1×10^9 (note that this is considerably smaller than $N_{K^+} \sim 10^{13}$ of the previous section) by measuring the number of $K_L \rightarrow \pi^0 \pi^0$ events. Together with signal acceptance estimated at 0.67% and background estimate of 0.41 ± 0.11 events (neutron dominant), the single event sensitivity is found to be $\sim 2.9 \times 10^{-8}$. With no events in the signal box, the limit of (8.9) was extracted. The limit will improve when analysis of the third run, equivalent in statistics of the second, is completed.

8.2.2 Future Prospects

With the cancellation of the CKM project at Fermilab (not to mention the earlier KAMI effort) and the KOPIO project at BNL, the kaon program in the USA has

withered. Can the USA revamp its kaon program with Project-X at Fermilab? Let us wait and see.

At CERN, the NA62 [24] experiment is under review during 2008. Assuming the SM branching ratio of $\sim 10^{-10}$, it aims at reaching $\mathcal{O}(80)$ $K^+ \rightarrow \pi^+ \nu \bar{\nu}$ events with 2 years of running at the SPS. Unlike the E787/949 experiment at BNL, to provide better kinematic constraints, 75 GeV/c K^+ mesons decaying in flight would be used. One could use, and modify, the existing beam-line as well as the NA48 detector. For background rejection, the kaon momentum would be measured by pixel detectors to provide kinematic constraint, photons (from π^0) need to be vetoed, and the π^+ momentum needs to be measured with positive particle identification. Once approved, data taking could start in 2012. If successful, the hope [25] is to upgrade the CERN proton complex toward “EUREKA” (European Rare-Decays Experiments with Kaons) to reach ~ 1000 K^+ events, then ~ 100 K_L events, by upgrading the CERN proton complex.

For $K_L \rightarrow \pi^0 \nu \bar{\nu}$ search, E391a should really be viewed as the pilot study for the more ambitious E14 proposal [26] at the J-PARC (Japan Proton Accelerator Research Complex) facility, where the 30 GeV (50 GeV capable) Main Ring is being commissioned in 2008. Due to budget limitation, the K_L beam line is deferred to 2009. The E14 experiment (now named KOTO) would start with a modified E391a detector. The K_L yield will gain a factor of 40 from KEK PS, and with 2–3 years of running, the run period would gain a factor of 10, again from KEK PS run. By upgrading the detector, one could gain in acceptance by a factor of 3. One key upgrade is the reuse of the KTeV CsI calorimeter, which is longer and finer segmented than the E391a calorimeter detector. Together with new readout (waveform digitization), better resolution can be achieved. The beam-line would be newly designed based on experience gained from E391a to reduce beam halo and in fact allows further improvement in the future. The vetoes are also improved. Overall, the aim for E14 is to reach a sensitivity of three events in three Snowmass years (1×10^7 s) with $S/B \sim 1.5$, assuming SM rate of $\sim 3 \times 10^{-11}$. The earliest start date is 2011. If there is New Physics enhancement, then discovery could come earlier, but if SM persists, then a 10% measurement requires $\mathcal{O}(100)$ events, and it would probably take a decade to reach, in J-PARC Phase 2.

What New Physics can there be? Inspecting Fig. 8.4, we see that $K \rightarrow \pi \nu \bar{\nu}$ decay arises from the electroweak penguin, which has strong m_t dependence for the three-generation Standard Model. This allows great sensitivity to the effect of the fourth-generation, because the t' effect exhibits nondecoupling. Of special interest is the CPV decay process $K_L \rightarrow \pi^0 \nu \bar{\nu}$, which is proportional to $\text{Im}(V_{td}^* V_{ts})$ in amplitude. The latter should in general be finite. Again, along the line where one can account for $\Delta\mathcal{A}_{K\pi}$ (Sect. 2.2), predict $\sin 2\Phi_{B_s} = -0.5$ to -0.7 (Sect. 3.2.3) and predict positive A_{FB} in the low q^2 bins (Sect. 5.1, in particular Sect. 5.1.2 and 5.1.3) for $B \rightarrow K^* \ell^+ \ell^-$, rather large enhancements of $K_L \rightarrow \pi^0 \nu \bar{\nu}$ decay is predicted [14, 15]. The rates could be even enhanced by two orders of magnitude to the 10^{-9} level, close to the Grossman–Nir bound of $\mathcal{B}(K_L \rightarrow \pi^0 \nu \bar{\nu}) < 1.5 \times 10^{-9}$, which is inferred from $\mathcal{B}(K_L \rightarrow \pi^0 \nu \bar{\nu}) < 4.4 \mathcal{B}(K^+ \rightarrow \pi^+ \nu \bar{\nu})$ [27] and the K^+ rate.

Regardless of the actual source of New Physics, this large enhancement range illustrates the importance of $K_L \rightarrow \pi^0 \nu \bar{\nu}$ measurement. The allowed enhancement

is not just a reflection of the uncertainty in New Physics from other constraints, but because constraints such as ε'/ε suffer from very large hadronic uncertainties. But $K_L \rightarrow \pi^0 \nu \bar{\nu}$ is dominated by short distance physics, so a precise measurement in the future would be rather important in pinning down the parameter space of possible New Physics, whatever it is that enter $K_L \rightarrow \pi^0 \nu \bar{\nu}$ in a significant way. In contrast, despite early E787 indications, the combined E787/949 result of (8.8) is already consistent with SM (only 1σ higher) expectation for $K^+ \rightarrow \pi^+ \nu \bar{\nu}$.

In any rate, the $K^+ \rightarrow \pi^+ \nu \nu$ and $K_L \rightarrow \pi^0 \nu \nu$ decays are clean modes theoretically, and especially the latter holds big room for discovering BSM physics. The challenge is to get the experiment done, but these are still some years away.

References

1. Gell-Mann, M., Pais, A.: Phys. Rev. **97**, 1387 (1955) 101
2. Falk, A.F., et al.: Phys. Rev. D **69**, 114021 (2004) 103, 107
3. Bigi, I.L., Uraltsev, N.: Nucl. Phys. B **592**, 92 (2001) 103
4. M. Starič, M., et al. [Belle Collaboration]: Phys. Rev. Lett. **98**, 211803 (2007) 103, 104, 105
5. Zhang, L.M., et al. [Belle Collaboration]: Phys. Rev. Lett. **96**, 151801 (2006) 103, 105
6. Aubert, B., et al. [BaBar Collaboration]: Phys. Rev. Lett. **98**, 211802 (2007) 103, 104, 105
7. Aaltonen, T., et al. [CDF Collaboration]: Phys. Rev. Lett. **100**, 121802 (2008) 104, 105, 109
8. Bergmann, S., et al.: Phys. Lett. B **486**, 418 (2000) 104
9. Yao, W.M., et al. [Particle Data Group]: J. Phys. G **33**, 1 (2006) 104, 110
10. Amsler, C., et al.: Phys. Lett. B **667**, 1 (2008); and <http://pdg.lbl.gov/> 104, 110
11. See the webpage of the Heavy Flavor Averaging Group (HFAG). <http://www.slac.stanford.edu/xorg/hfag>. We usually, but not always, take the Lepton-Photon 2007 (LP2007) numbers as reference 104, 107, 108
12. Poluektov, A., et al. [Belle Collaboration]: Phys. Rev. Lett. **70**, 072003 (2004) 106
13. Zhang, L.M., et al. [Belle Collaboration]: Phys. Rev. Lett. **99**, 131803 (2007) 103, 106, 109
14. Hou, W.S., Nagashima, M., Soddu, A.: Phys. Rev. D **72**, 115007 (2005) 108, 113
15. Hou, W.S., Nagashima, M., Soddu, A.: Phys. Rev. D **76**, 016004 (2007) 108, 109, 113
16. Falk, A.F., Grossman, Y., Ligeti, Z., Petrov, A.A.: Phys. Rev. D **64**, 054034 (2002) 107
17. Golowich, E., Hewett, J., Pakvasa, S., Petrov, A.A.: Phys. Rev. D **76**, 095009 (2007) 108
18. Hou, W.S., Soni, A., Steger, H.: Phys. Lett. B **192**, 441 (1987) 108
19. Asner, D.M., Sun, W.M.: Phys. Rev. D **73**, 034024 (2006) 109
20. Inami, T., Lim, C.S.: Prog. Theor. Phys. **65**, 297 (1981) 109
21. Buras, A.J., Schwab, F., Uhlig, S.: Rev. Mod. Phys. **80**, 965 (2008) 109
22. Artamonov, A.V., et al. [E949 Collaboration]: Phys. Rev. Lett. **101**, 191802 (2008) 111
23. Ahn, J.K., et al. [E391a Collaboration]: Phys. Rev. Lett. **100**, 201802 (2008) 112
24. See the webpage <http://test-na62.web.cern.ch/test-NA62/> 113
25. Sozzi, M.S.: Talk at the 5th Workshop on the CKM Unitarity Triangle (CKM2008), Rome, Italy, September 2008 113
26. Nomura, T.: Talk at Flavor Physics and CP Violation Conference (FPCP2008), Taipei, Taiwan, May 2008 113
27. Grossman, Y., Nir, Y.: Phys. Lett. B **398**, 163 (1997) 113

Chapter 9

Lepton Number Violating μ and τ Decay

Before concluding, we touch upon exciting developments in rare τ decays: radiative decays which have $b \rightarrow s$ echoes and the enigmatic (if found) baryon number violating decays. There should be no doubt that we would have uncovered Beyond the Standard Model physics if any of these are observed. Again, it is the B factories that have pushed the frontier recently. Compared to the 1.1 nb cross section for $e^+e^- \rightarrow B\bar{B}$ and 1.3 nb for $e^+e^- \rightarrow c\bar{c}$, the $e^+e^- \rightarrow \tau^+\tau^-$ cross section of 0.9 nb is not far behind. Thus, B factories are also tau and charm factories!

Of course, Lepton Flavor Violation (LFV) is already observed in neutrino oscillations, a great subject of its own which we have not covered, despite the extreme apparent smallness of neutrino masses. The study of mixing in the neutrino sector has enjoyed a golden 10 years since 1998. Two unexpectedly large mixing angles were uncovered, which are in strong contrast to the hierarchical angles seen in the quark sector. The current drive to measure θ_{13} mixing angle, to hopefully open the chapter on CPV in neutrino sector, goes hand in hand with lofty ideas such as leptogenesis, the proposal that the baryon asymmetry of the Universe came through some lepton asymmetry in the early Universe at an earlier step.

What we consider in this chapter is LFV in the charged lepton sector, which is something we have never observed yet. If they exist, the source has to lie outside of the SM. Before discussing the relative new field of LFV τ decay search at the B factories, we briefly discuss the promising MEG experiment for $\mu \rightarrow e\gamma$ search, which is the current leading edge of a history as long as particle physics itself.

9.1 $\mu \rightarrow e\gamma$

The muon was discovered in $\mu \rightarrow e\bar{\nu}_e\nu_\mu$ decay, which occurs practically 100% of the time. The fact that the kinematically allowed $\mu \rightarrow e\gamma$ seemed completely absent was the first indication that the electron and the muon numbers are separately conserved.

With the observation of neutrino oscillations, hence neutrinos have mass, $\mu \rightarrow e\gamma$ is then in principle generated, through diagrams similar to Fig. 4.1(a), but with neutrinos in the loop and the photon radiating off the W boson. However, because

of the extreme smallness of neutrino masses, the rate vanishes as $|\Delta m_\nu^2|^2/M_W^4$, and the generated rate is less than 10^{-40} ! In the limit of strictly massless neutrinos, the original definition of SM, then separate lepton numbers are automatically conserved. Turning this around, this means that *any* measurement of $\mu \rightarrow e\gamma$ would constitute discovery of BSM physics.

The first phase of experiments was conducted in the 1950s. By the mid-1960s, limits on $\mu \rightarrow e\gamma$ had already reached down to 10^{-8} . A second round of experiments in the 1970s reached 10^{-10} , after which the design and construction of $\mu \rightarrow e\gamma$ experiments (like most other particle physics experiments) became stretched in time. The latest result, from the MEGA experiment done at LAMPF, gives the limit [1]

$$\mathcal{B}(\mu \rightarrow e\gamma) < 1.2 \times 10^{-11} \quad (1999, \text{MEGA}), \quad (9.1)$$

at 90% C.L.¹ The MEGA result came out around the exciting time of the 1998 observation of ν_μ to ν_τ (“atmospheric”) neutrino oscillations. Together with the near completion of B factories, they inspired many theoretical studies on $\mu \rightarrow e\gamma$ and $\tau \rightarrow \ell\gamma$ (see [4] as an example). Not surprisingly, these BSM theories suggest, in the SUSY-GUT context, that $\mu \rightarrow e\gamma$ could occur in the 10^{-15} – 10^{-11} range. Diagrammatically, these processes occur through loop processes similar to Fig. 9.1(a) shown for $\tau \rightarrow \mu\gamma$ transitions in the next section, through slepton mixing effects in the loop. A new experiment capable of probing this range is called for, and the MEG experiment at PSI, aimed at reaching below 10^{-13} , rose to this challenge. It is exciting that physics runs have already started in late 2008.

As the extremely impressive limit of (9.1) suggests, MEG needs to push hard on background reduction. The signal consists of a 52.8-MeV positron back-to-back with a 52.8-MeV photon in time coincidence and coming from a common origin. With the muon stopped to decay at rest, positive charge is selected to avoid muon capture by nucleus. Accidental overlap of events (an e^+ from $\mu^+ \rightarrow e^+\nu_e\bar{\nu}_\mu$ and a γ from $\mu^+ \rightarrow e^+\gamma\nu_e\bar{\nu}_\mu$) is the dominant background. Thus, a DC muon beam, rather than a pulsed one, is used. The 590 MeV cyclotron at PSI is the world’s most powerful proton cyclotron for this purpose.

Several special detector designs are worthy of note. For e^+ detection at the low energy of 52.8 MeV, sensitive but very low mass drift chambers were designed and constructed, together with a timing counter that is the world’s best in performance ($\sigma_t \sim 40$ ps). A special COBRA (COnstant Bending RAdius) magnet was designed with graded, rather than uniform B field, to provide constant e^+ bending radius, independent of the e^+ emission angle. For a uniform field, a low energy e^+ tends to be swept out too quickly. For photon detection and measurement, liquid xenon as scintillator was chosen. The light yield is comparable (80%) to NaI, but with fast response (4.2 ns) and short decay time. Because of the narrow temperature

¹ A different type of LFV probe, e.g., that of $K \rightarrow \pi\mu^\pm e^\mp$, also has limits reaching below 10^{-10} level [2, 3].

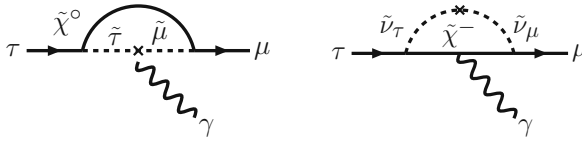


Fig. 9.1 Diagrams illustrating $\tau \rightarrow \mu\gamma$ transition induced by SUSY particles in the loop. Lepton flavor violation is indicated by the *cross*, or mixing, of different flavored sleptons

range between liquid and solid Xe phases, care must be taken for reliable and stable temperature control. A liquid Xe detector prototype was therefore constructed and tested.

With these specially designed subdetectors, including the DAQ readout system, MEG went through an engineering run in 2007 to establish calibration procedures. After correcting for problems that were encountered and going through another engineering run in 2008, one expects 20 weeks of physics data taking in the remainder of 2008. Based on the 2007 engineering run and improvements, the expected background is 0.4 events, with single event sensitivity expected at 2.6×10^{-13} , or

$$\mathcal{B}(\mu \rightarrow e\gamma) < 7.2 \times 10^{-13} \quad (\text{expectation, MEG 2008 data}) \quad (9.2)$$

is expected at 90% C.L., with further improvements depending on run time. One may reach 10^{-13} with two years of running in the so-called Phase I of MEG. With a possible upgrade to Phase II, 10^{-14} can be contemplated. The potential for discovery is exciting.

There are further versions of LFV probes using muons, such as $\mu \rightarrow eee$ and $\mu \rightarrow e$ conversion on nuclei. These probe different effective interactions, but we refrain from going further into these subjects.

9.2 $\tau \rightarrow \ell\gamma, \ell\ell\ell'$

Just like $\mu \rightarrow e\gamma$ decay, the $\tau \rightarrow \ell\gamma$ decays are extremely suppressed in SM by the very light neutrino masses. The great progress in neutrino physics of the past decade, in particular the observed near maximal ν_μ - ν_τ mixing, has stimulated a lot of interest in LFV $\tau \rightarrow \mu$ transitions, as they echo the $b \rightarrow s$ transitions that have been the dominant theme of our interest. In the context of Grand Unified Theories (GUTs), which in general needs SUSY to make the unification of couplings work, there is clearly $\tau \rightarrow \mu$ and $b \rightarrow s$ correspondence. For further discussion, see [5]. In exploring $\tau \rightarrow \mu$ transitions, once (if) they are observed, there is great potential to check the link with $b \rightarrow s$ loop transitions in a given model. This shows the utility of flavor physics in a broad framework.

With SUSY, the favorite underlying physics models range from sneutrino-chargino or charged slepton-neutralino loops (Fig. 9.1), exotic Higgs, R -parity violation, to ν_R in SO(10) or large extra dimensions (LED). Predictions for $\tau \rightarrow \ell\gamma, \ell\ell\ell, \ell\ell\ell'$,

ℓM^0 (where M^0 is a neutral meson) could reach the 10^{-7} level, and generally populate 10^{-8} to 10^{-10} , which should be compared to the more suppressed range for $\mu \rightarrow e\gamma$. These models are often well motivated from observed near maximal $\nu_\mu - \nu_\tau$ mixing, or from interesting ideas such as seesaw mechanism in SUSY-GUT context, or baryogenesis through leptogenesis. We refrain from getting into details of theory, as the body of literature is rather large, but comment that there may also be a link to another subject that we have not covered. There is a long existing discrepancy between experiment and theory for $g - 2$ of the muon, where SUSY with large $\tan \beta$ is a favored contender as the source [6]. The muon $g - 2$ is a flavor diagonal effect.

On the experimental side, the stars are once again the B factories: With $\sigma_{\tau^+\tau^-} \sim 0.9 \text{ nb}$ comparable to $\sigma_{b\bar{b}} \sim 1.1 \text{ nb}$, B factories are also τ (and charm) factories! In the CLEO era of the 1990s, where $\mathcal{O}(10^7)$ τ s were collected, the limit on $\tau \rightarrow \mu\gamma$ reached 10^{-6} . With the advent of the B factories, and as data accumulated steadily, the limits are approaching the 10^{-8} level, entering the interesting region of potential discovery for the neutrino-SUSY/GUT-inspired models. Many modes have been studied. We will only discuss $\tau \rightarrow \ell\gamma$ and $\tau \rightarrow \ell\ell\ell'$.

The study of τ LFV is in some sense simpler than the study of Standard Model tau decays: the signal side has low multiplicity, such as $\tau \rightarrow \mu\gamma$, and is *fully reconstructed*, with E_{sig} equal the beam energy ($E_{\text{beam}}^{\text{CM}}$) and $M_{\mu\gamma}$ equal the tau mass. The main effort is again the control of backgrounds. To pick up a genuine $e^+e^- \rightarrow \tau^+\tau^-$ event, one tags the other τ by one-prong (maybe three-prong also) decays, where missing neutrinos imply that the reconstructed $E_{\text{tag}} < E_{\text{beam}}^{\text{CM}}$ and $M_{\text{tag}} < m_\tau$ for tag side. The two τ s are well separated, providing another discriminant. For $\tau \rightarrow \mu\gamma$ search, to suppress $e^+e^- \rightarrow \mu^+\mu^-\gamma$ background, the tag side track should not be a muon.

Track energy, p_T , angular, total CM energy, and other cuts are employed to suppress Bhabha, $\mu^+\mu^-$, two photon, and $q\bar{q}$ backgrounds. One utilizes further the kinematics of an $e^+e^- \rightarrow \tau(\rightarrow \mu\gamma)\tau(\rightarrow \text{track} + \nu(\nu))$ event to suppress the remaining $\tau^+\tau^-$ and $\mu^+\mu^-$ backgrounds, for example, γ from π^0 s, μ misidentified as π , or an $m_{\nu(\nu)}^2$ cut that utilizes the fact that it should be no more than the parent τ mass. One then models the final background distributions with the side band in $M_{\mu\gamma}$ vs. $\Delta E \equiv E_{\mu\gamma}^{\text{CM}} - E_{\text{beam}}^{\text{CM}}$, with the signal region blinded. The result is found to be consistent with MC. With a data set of 535 fb^{-1} (477M $\tau^+\tau^-$ pairs), Belle found no events in the signal box, setting the limit of [7]

$$\mathcal{B}(\tau \rightarrow \mu\gamma) < 4.5 \times 10^{-8}, \quad (\text{Belle } 535 \text{ fb}^{-1}) \quad (9.3)$$

at 90% C.L., the current best limit on radiative τ decays. A similar study, with higher background because of the e^+e^- production environment, gives $\mathcal{B}(\tau \rightarrow e\gamma) < 12 \times 10^{-8}$ at 90% C.L.

For $\tau \rightarrow \ell\ell\ell$ and $\ell\ell\ell'$ modes, six charged lepton combinations ($e^-e^+e^-$, $\mu^-\mu^+\mu^-$, $e^-\mu^+\mu^-$, $\mu^-e^+e^-$, $\mu^+e^-e^-$, and $e^+\mu^-\mu^-$) have been studied, each with their own special background considerations. The event consists of four charged tracks with zero net charge, with one track on the tag-side hemisphere, and three

tracks on the signal side. In special mode-dependent background studies, for example, one has to reject the large $\gamma \rightarrow e^+e^-$ conversion background for $\tau \rightarrow \ell e^+e^-$ modes. Because of having like sign muon or electron pairs, the $\tau^- \rightarrow \mu^+e^-e^-$ and $e^+\mu^-\mu^-$ modes have the lowest background, hence the best limits were reached for these two modes. With 535 fb^{-1} ($492\text{M } \tau^+\tau^-$ pairs²) data, Belle set the limit of [8]

$$\mathcal{B}(\tau^- \rightarrow \mu^+e^-e^- (e^+\mu^-\mu^-)) < 2.0 (2.3) \times 10^{-8} \quad (\text{Belle } 535 \text{ fb}^{-1}) \quad (9.4)$$

at 90% C.L., the current best limit for LFV τ decays. The limit for $\tau^- \rightarrow e^-\mu^+\mu^-$ is at 4.1×10^{-8} . Limits from BaBar (using 376 fb^{-1}) are not far behind [9].

Dozens of LFV $\tau \rightarrow \ell M^0$ decays have been studied, where M^0 is a neutral hadron, be it pseudoscalar, vector, or scalar. The limits have reached below 10^{-7} . Based on a recent suggestion [10] that $\tau \rightarrow \mu f_0$ could be more than twice the size of $\tau \rightarrow \mu\mu\mu$ (a scalar couples to $s\bar{s}$ vs $\mu^+\mu^-$), a preliminary result from Belle using 671 fb^{-1} data sets a limit of 3.3×10^{-8} .

Evidently, the search program at B factories is still ongoing, and some models, or part of their parameter space, are already ruled out. With BaBar closed, and with Belle at best giving results at 1 ab^{-1} , however, one would just scratch the 10^{-8} boundary. *To probe deeper into the parameter space of various LFV rare τ decays that are of great interest, a Super B Factory would be called for.*

At a Super B Factory, limits for $\tau \rightarrow \ell\ell\ell'$ can reach 10^{-9} , but $\tau \rightarrow \ell\gamma$ suffers from a irreducible background of $e^+e^- \rightarrow \tau^+\tau^-\gamma$, and may not reach far below 10^{-8} . Nevertheless, the LFV search program at the Super B factories is quite unique and complementary to direct search programs at the LHC. The LHCb experiment can compete in the all charged track modes, but modes with neutrals would be difficult. However, unlike the B factories, the main source of τ leptons are in fact B and D mesons, so background considerations are quite different and nontrivial.

9.3 $\tau \rightarrow \bar{\Lambda}\pi, \bar{p}\pi^0$

A somewhat wild idea is to search for Baryon Number Violation (BNV) in τ decay. The search was started by the ARGUS experiment [11] and followed by CLEO [12] in the 1990s, which searched for $\tau^- \rightarrow \bar{p}\pi^0, \bar{p}\eta, \bar{p}\pi^0\pi^0, \bar{p}\pi^0\eta, \bar{p}\gamma$ modes. However, before the CLEO paper was published, Marciano pointed out [13] in 1995 that, by using proton decay constraints, the estimated BNV τ decay branching ratios are too small to be observed. This, however, did not deter the B Factory experiments, and Belle [15] searched for both $B-L$ conserving $\tau^- \rightarrow \bar{\Lambda}\pi^-$, as well as $B-L$ violating $\tau^- \rightarrow \Lambda\pi^-$ decays, which was extended by BaBar [16] to $\bar{\Lambda}K^-$ and ΛK^- . So far, no signal was found, as expected. However, the observation of Marciano was extended [14] to BNV decays involving higher generations (i.e., including c, b, t as

² The number of $\tau^+\tau^-$ pairs is higher than in [7], because an updated calculation of the $e^+e^- \rightarrow \tau^+\tau^-$ cross section is used; thus, (9.3) should be modified slightly.

well as τ), with the pessimistic conclusion that proton decay bounds preclude the possibility of observing any of these decays in any current or future experiments. This seemed to have had a dampening effect on experimental activity.

The experimental signature is, however, rather tantalizing, so let us still explore it. After all, Belle and BaBar have accumulated unprecedented numbers of $\tau^+\tau^-$ pairs in the clean e^+e^- production environment. Also, baryon number violation has never been observed so far, while we know it is definitely needed for the early Universe, so all search avenues should be explored.

The Belle study [15] used a data set of 154 fb^{-1} , corresponding to 137M $\tau^+\tau^-$ pairs, while BaBar used [16] 237 fb^{-1} , or 50% more. The limits reached are around 10^{-7} . Whether it is slightly above or below this depends on whether a random event turns up in the signal box. The event signature is $\bar{p}\pi^+(p\pi^-)\pi^-(K^-)$ on signal side, with $\bar{p}\pi^+$ reconstructing to a $\bar{\Lambda}$ and $\bar{\Lambda} + \text{track}$ reconstructing to tau mass, where PID is used to separate π^- from K^- track. The $\bar{\Lambda}$ or Λ pairing with the π^- just determines whether there is $B - L$ conservation or not. For the tag side one uses the one-prong τ decays as before. So, the signature is four charged tracks with zero net charge and missing energy, similar to $\tau \rightarrow \ell\ell\ell'$ search. The hadronic track nature means that the major remaining background after the usual event selection procedure would be generic $\tau^+\tau^-$ or continuum $q\bar{q}$ events. One can compare MC with side band close to the signal box, which is kept blind until all selections and background rejection procedures are made. The analysis is very similar to LFV searches of the previous section, except one uses proton and Λ identification, instead of electron or muon identification. The limit can in principle improve by at least a factor of two with the data at hand.

So why is the proton lifetime setting such a strong bound on τ BNV? To elucidate Marciano's argument, we plot in Fig. 9.2 a diagram [14] for proton decay mediated by a virtual τ . On the middle-left side of the diagram, the blob illustrates the BNV $uud\bar{\tau}$ effective coupling. The virtual tau then decays in some standard way. If the $uud\bar{\tau}$ coupling exists, it can then induce proton decay. In turn, one can use the proton lifetime to set a bound on τ BNV. In this way, one finds that $\mathcal{B}(\tau \rightarrow \bar{p}\pi^0) < \text{few} \times 10^{-39}$. For strange baryons, one further involves the weak interaction, and the limit is weakened to

$$\mathcal{B}(\tau \rightarrow \bar{\Lambda}\pi^-) < \text{few} \times 10^{-30}, \quad (9.5)$$

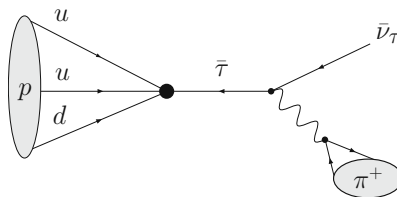


Fig. 9.2 Diagram [14] illustrating virtual τ mediating proton decay. [Copyright (2006) by The American Physical Society.]

which is depressingly small. In the same vein, for any BNV effective four-fermi interaction, one can always [14] link with some nucleon decay process, sometimes by invoking weak interaction loops as one goes to top and beauty quarks. The limits never appear more promising than (9.5), which is surprising, but discouraging.

In the study of [14], however, some really fascinating decay signatures are uncovered, that may be worth contemplating. To name a few: $D^+ \rightarrow \bar{\Lambda} \ell^+$, $D^0 \rightarrow \bar{\Sigma}^- \ell^+$, $\bar{p} \ell^+$; $B^{0,+} \rightarrow \Xi_{cc}^{+,++} \ell^-$ (probably not suppressed by $B \rightarrow \Xi_{cc}$ form factor!) and inclusive $\bar{b} \rightarrow c u \ell^-$ (wrong charge combination); $t \rightarrow \bar{b} \bar{c} \ell^+$. Experimentalists should be quite attracted to these astounding signatures. But if the argument of Marciano is correct, all these modes cannot exist at an observable level, even if BNV exists!

Our view is, *whenever an experimental search can be conducted, it should be done*, regardless of what the theoretical expectation is. After all, there could be some symmetry and/or cancellation among diagrams, or other wilder ideas, as we know that Nature is more ingenious than we are.

References

1. Brooks, M.L., et al. [MEGA Collaboration]: Phys. Rev. Lett. **83**, 1521 (1999) 116
2. Yao, W.M., et al. [Particle Data Group]: J. Phys. G **33**, 1 (2006) 116
3. Amsler, C., et al.: Phys. Lett. B **667**, 1 (2008); and <http://pdg.lbl.gov/> 116
4. Hisano, J., Nomura, D.: Phys. Rev. D **59**, 116005 (1999) 116
5. Chang, D., Masiero, A., Murayama, H.: Phys. Rev. D **67**, 075013 (2003) 117
6. For a recent review, see Stöckinger, D.: J. Phys. G **34**, R45 (2007) 118
7. Hayasaka, K., et al. [Belle Collaboration]: Phys. Lett. B **666**, 16 (2008) 118, 119
8. Miyazaki, Y., et al. [Belle Collaboration]: Phys. Lett. B **660**, 154 (2008) 119
9. Aubert, B., et al. [BaBar Collaboration]: Phys. Rev. Lett. **99**, 251803 (2007) 119
10. Chen, C.H., Geng, C.Q.: Phys. Rev. D **74**, 035010 (2006) 119
11. Albrecht, H., et al. [ARGUS Collaboration]: Z. Phys. C **55**, 539 (1992) 119
12. Godang, R., et al. [CLEO Collaboration]: Phys. Rev. D **59**, 091303 (1999) 119
13. Marciano, W.J.: Nucl. Phys. B Proc. Suppl. **40**, 3 (1995) 119
14. Hou, W.S., Nagashima, M., Soddu, A.: Phys. Rev. D **72**, 095001 (2006) 119, 120, 121
15. Miyazaki, Y., et al. [Belle Collaboration]: Phys. Lett. B **632**, 51 (2006) 119, 120
16. Aubert, B., et al. [BaBar Collaboration]: hep-ex/0607040, contributed to 33rd International Conference on High Energy Physics (ICHEP 06), July 2006, Moscow, Russia 119, 120

Chapter 10

Discussion and Conclusion

The last subsection brings us to wilder speculations that we have stayed away from throughout our discourse. In the SUSY conference, the context from which this book originally arose, ideas range widely, if not wildly. There are now a wide range of ideas regarding how electroweak symmetry breaking and its protection could occur in Nature. Some of these frameworks could touch upon flavor. To this author, from an experimental point of view, however, the question is identifying the smoking gun, or else it is better to stick to the simplest (rather than elaborate) explanation of an effect that requires New Physics. That has been our guiding principle. Most of the new(er) ideas related to EWSB are best tested by direct search at the LHC, rather than in flavor physics, since the problem of electroweak symmetry breaking and the problem of flavor are largely orthogonal issues.

10.1 From Unparticles to Extending the Standard Model

Perhaps the wildest idea in 2007, and probably the one bringing out the most insight, is “unparticle physics” [1]. Unfortunately, this suggestion seems difficult to pinpoint or rule out experimentally. We do not discuss what this is all about, but note that it has clearly stimulated much theoretical interest. On the flavor and CPV front, for example, there is the suggestion that unparticles could generate DCPV in unexpected places [2], such as $B^0 \rightarrow D^- D^+$ or $B^+ \rightarrow \tau^+ \nu$. This suggestion may well have been stimulated by the 3.2σ indication [3] of DCPV in $B^0 \rightarrow D^- D^+$ by the Belle experiment that is otherwise very difficult to explain. It should be stressed that the concurrent BaBar result is consistent with zero [4], while further studies of other $B^0 \rightarrow D^{(*)} \bar{D}^{(*)}$ modes have *not* revealed anything to support the evidence for DCPV in $B^0 \rightarrow D^- D^+$. So, the Belle result needs to be revisited with more data. But searching for DCPV in the $B^+ \rightarrow \tau^+ \nu$ mode is also suggested [2], which is interesting. If I may speculate, maybe unparticles could generate BNV in the modes of the previous subsection, including charm and beauty decays [5]. In this sense, new ideas such as unparticles can stimulate search efforts in otherwise unmotivated places, hence they are very valuable.

To be conservative on where New Physics may emerge on the flavor front, one has to look where the SM can be extended.¹ Extensions can be in the following sectors:

- The gauge sector

As an example, we have briefly touched upon the Z' in Chap. 5, but remarked that Z' with FCNC is quite arbitrary as a model.

Another possibility is $SU_R(2)$, or restoration of parity at high energy. Though not touched upon specifically, probes of right-handed interactions were discussed in Chaps. 5 and 6. In general, the new gauge interaction must be broken, with scale considerably higher than the weak scale.

- The Higgs sector

We discussed charged Higgs boson effects in Chap. 4, using two Higgs doublet models as example. Effect of exotic neutral scalar and pseudoscalars were covered in Chaps. 5, 6, and 7. We have not explored CPV induced purely from enlarging the Higgs sector, since these tend to be orthogonal to flavor physics and are preferably probed at colliders.

Beyond the Higgs sector, the general question is how EWSB is actually induced and how to treat the hierarchy problem. We have not gone into these directions, as we have viewed the motivation as again orthogonal to the flavor physics sector. Ideas of large, even warped, extra dimensions [6] have been a popular approach. However, the main signature of Kaluza-Klein excitations are best searched for at high-energy colliders, such as the LHC. Once they are established, one can then ask how they are related to flavor.

- The neutrino sector

Here we refer to the presence of right-handed neutrinos, where the possibility of Majorana masses is an intriguing possibility, bringing in physics ideas with rich impact, such as the seesaw mechanism and leptogenesis [7]. We have seen clear evidence for neutrino mass since 1998 [8, 9], which definitely goes beyond the original minimal SM. But we have barely touched upon neutrino physics, since it has a life of its own, separate from flavor physics. The closest link is our Chap. 9.

- The fermion sector (or matter fields)

All matter fields, except the right-handed neutrino, have some SM gauge charge(s), the extension of which should impact on observables of interest. We have (perhaps strangely) always used the sequential fourth-quark generation as our prime example. This is in part because the extension from CKM3 to CKM4, bringing in new mixing angles as well as CPV phases, is bound to touch upon all experimental measurables of interest, such as those presented in Chaps. 2, 3, 5, and 8. After all, it is through the study of similar processes that the SM itself got established.

¹ The SUSY extension is not conservative from the flavor point of view. Not only it is a large extension—doubling number of all fields, hence introducing a very large number of parameters—but the extension is motivated from EWSB, or the protection thereof, not from flavor physics. In fact, flavor and CPV cause major problems for having TeV scale SUSY, since it runs easily into conflict with flavor physics measurements, and there is a question of naturalness.

In the next section, we will finally give our reason why we seem so fond of the fourth generation.

It is certainly possible to extend the matter fields to exotic quantum numbers. An example is vector-like quarks, which could arise from Little Higgs models [10], which again is about EWSB physics. We remark that new fields such as vector-like quarks tend to bring in another scale parameter, which in general has to be higher than the v.e.v. scale. Thus, the impact of such new matter fields on low(er) energy flavor observables would be less pronounced than the fourth-generation case.

10.2 Fourth Generation—CPV for Heaven and Earth ?

The three-generation structure of SM was predicted by Kobayashi and Maskawa [11], before the second quark generation was even complete! The textbook argument is that, even with two quark generations, one has enough phase freedom in the quark fields to remove CPV phases in the 2×2 CKM matrix that governs the $\bar{u}_i \gamma_\mu L d_j W^\mu$ weak coupling. Only by having three generations of quarks would the weak interactions break CP invariance, and the CPV phase turns out to be *unique*, which is another attractive feature. Inspecting Fig. 1.6 once again, one can only admire the success of the KM model that, after three and a half decades of extensive experimental effort, not only the third-generation fermions were discovered one after the other, but also three-generation unitarity of (1.4) holds, with all data meeting consistently in the same parameter region.

But our goal is on probing beyond SM, on flavor and the link to TeV scale physics. Although KM as the dominant source of CPV in the laboratory seems proven so far, it predicts that the $b \rightarrow s$ unitarity triangle represented by (3.4) should have the same area as the $b \rightarrow d$ unitarity triangle represented by (1.4), as shown pictorially in Fig. 3.4 (or Fig. A.2). The usual convention of taking $V_{cs} V_{cb}^*$ real is implied (though not necessary), and the extremely small phase of $V_{ts} V_{tb}^*$ (see also (A.6)) then gives the SM prediction that the analogous CPV phase in tagged $B_s \rightarrow J/\psi \phi$ study would be much, much smaller than for $B_d \rightarrow J/\psi K_S$. If true, then only the LHCb experiment would have the capability to probe the minuscule SM value of $\sin 2\Phi_{B_s} \simeq -0.04$ given in (3.8). However, we have advocated that it is precisely here where New Physics effects may be unfolding before us, and a common thread could be the fourth generation, since all hints involve electroweak penguin or box diagrams.

10.2.1 New Physics CPV on Earth: from $\Delta\mathcal{A}_{K\pi}$ to $\sin 2\Phi_{B_s}$

Let us recapitulate the points, scattered about in Chaps. 2, 3, 5, and 8, on the impact of the fourth generation on CPV and FCNC observables, from the B factory hint of $\Delta\mathcal{A}_{K\pi} \neq 0$ to the emerging possibility that $|\sin 2\Phi_{B_s}| \gg -\sin 2\Phi_{B_s}|^{\text{SM}}$.

No one predicted it, so it came as a surprise that the intuitive expectation of $\mathcal{A}_{B^0 \rightarrow K^+ \pi^-} \simeq \mathcal{A}_{B^+ \rightarrow K^+ \pi^0}$ is not realized in Nature. As seen from (2.7), (2.8), and (2.9), even the sign seems different between $\mathcal{A}_{B^0 \rightarrow K^+ \pi^-}$ and $\mathcal{A}_{B^+ \rightarrow K^+ \pi^0}$, and the difference between the two DCPV asymmetries is larger than the well-measured $\mathcal{A}_{B^0 \rightarrow K^+ \pi^-}$. Stimulated by this, already in 2005, we proposed [12] that this could be due to the effect of the fourth generation. The insight came from noting the nondecoupling nature of the heavy chiral t' quark in the electroweak penguin, that the effect grows with $m_{t'}^2$, just like the top, and that it brings in the CKM factor $V_{t's} V_{t'b}^*$, carrying with it a new CPV phase. Having shown that this is feasible in detailed PQCD factorization model calculations [13], we also showed that $\Delta\mathcal{S}$ dips by -0.1 , which is in the right direction, and by a tolerable amount, given that the $\Delta\mathcal{S}$ problem had technically disappeared in summer 2008.

Of course, the doubt was raised [14, 15] that a rather enhanced color-suppressed amplitude C , if it has very different strong phase than the tree amplitude T , could also generate $\Delta\mathcal{A}_{K\pi}$. Although the hadronic “smearing” is by far not as severe as in kaon physics, such as in ε'/ε , this nagging doubt caused many people to not take this potential hint of New Physics seriously. See Sect. 2.2 for further discussion.

However, by noting that the $m_{t'}$ dependence of the box diagram, which governs $B_s - \bar{B}_s$ mixing, is rather similar to the electroweak penguin diagram, we made the prediction already in 2005 [16, 17], that TCPV in tagged $B_s \rightarrow J/\psi\phi$, i.e., $\sin 2\Phi_{B_s}$ is *large and negative*. This was refined [16, 17] in 2006 with the precise measurement of Δm_{B_s} by CDF [18] to $\sin 2\Phi_{B_s} = -0.5$ to -0.7 , i.e., (3.25). The prediction is based on assuming that the large effect in $\Delta\mathcal{A}_{K\pi}$ receives a major contribution from New Physics in P_{EW} , where the negative sign of $\sin 2\Phi_{B_s}$ is correlated with the sign of $\Delta\mathcal{A}_{K\pi}$. Since $\sin 2\Phi_{B_s}$ is the CPV phase of M_{12}^s , the $B_s - \bar{B}_s$ mixing amplitude which is dominated by short distance physics, it does not suffer from hadronic uncertainties [19], just like $\sin 2\Phi_{B_d} \equiv \sin 2\phi_1/\beta$ that was measured by Belle and BaBar. This was discussed at some length in Sect. 3.2.3. We then discussed in Sect. 3.2.4 the exciting development since late 2007, that data at the Tevatron seem to support (3.25). If this holds true, then it seems that the Tevatron could *discover* New Physics CPV in tagged $B_s \rightarrow J/\psi\phi$, which would then be quickly confirmed by LHCb, once the latter takes real data.

As discussed in Sect. 5.1, there is also an indication of deviation from SM in $A_{FB}(B \rightarrow K^* \ell^+ \ell^-)$. As seen from Belle and BaBar data, there seems to be better agreement with SM4 rather than SM3. This again can be checked soon with precision by the LHCb experiment. As further corollaries, one could find support from, the following:

1. A percent level $\mathcal{A}_{B^+ \rightarrow J/\psi K^+}$, which could show up in Tevatron data and likely LHCb data.
2. Normal looking $\mathcal{B}(b \rightarrow s\gamma)$, but eventually direct CPV in $\mathcal{A}(b \rightarrow s\gamma)$ at percent level, while absence of $\mathcal{S}_{B^0 \rightarrow K_S \pi^0 \gamma}$ because of absence of RH currents.
3. D^0 meson mass mixing $x_D \sim 1\text{--}2\%$ (already observed but marred by long distance physics) and small but finite TCPV in D^0 -mixing.

4. Spectacularly enhanced $K_L \rightarrow \pi^0 \bar{\nu} \nu$ from SM expectations, the measurement of which would help pinpoint the relevant CKM product $V_{t'd} V_{t's}^*$.

Items 3 and 4 above are consequences of asking the following question: If there are fourth-generation effects lurking in $b \rightarrow s$ transitions, why do the $b \rightarrow d$ processes indicate a triangle, rather than a quadrangle? That is, why the CKM unitarity fit of Fig. 1.6 shows no sign of deviation from the triangle relation of (1.4)? This question was dealt with in [16]. With large $V_{t's} V_{t'b}^*$ (including CPV phase) as implied by sizable $\Delta\mathcal{A}_{K\pi}$ (which fixes $V_{t's} V_{t'b}^*$ for given $m_{t'}$), after taking into account the $Z \rightarrow b\bar{b}$ and rare kaon constraints (which fixes $|V_{t'b} V_{t'b'}^*|$ and $V_{t'd} V_{t's}^*$, including phase), the actual $b \rightarrow d$ quadrangle mimics the SM3 triangle (see Fig. 1(b) of [16]), within experimental resolution at the B factories.

That $b \rightarrow d$ transitions are SM-like is a *nontrivial test*. Indeed, another possible solution is rejected by this experimental requirement. With refined analysis and precision measurements in the future Super B Factory era, in principle one could distinguish the quadrangle

$$V_{ud} V_{ub}^* + V_{cd} V_{cb}^* + V_{td} V_{tb}^* + V_{t'd} V_{t'b}^* = 0 \quad (10.1)$$

from the triangle of (1.4), but this is beyond our present scope. It is better to confirm (3.25), the prediction of large and negative $\sin 2\Phi_{B_s}$, by refining the measurement of (3.26) first.

An outcome of the study incorporating $Z \rightarrow b\bar{b}$ and rare kaon constraints, with the help of 4×4 unitarity, is fixing the SM4 unitarity quadrangle,

$$V_{us} V_{ub}^* + V_{cs} V_{cb}^* + V_{ts} V_{tb}^* + V_{t's} V_{t'b}^* = 0. \quad (10.2)$$

We plot in Fig. 10.1 the $b \rightarrow s$ quadrangle corresponding to the SM4 unitarity relation (10.2), together with the SM3 $b \rightarrow d$ triangle of (1.4). The latter is from the current three-generation fit to all data, Fig. 1.6, the success of which led to Kobayashi and Maskawa receiving the 2008 Nobel Prize.

We note that, if one draws the line linking S and O in Fig. 10.1, one recovers the rather squashed and elongated triangle corresponding to $V_{us} V_{ub}^* + V_{cs} V_{cb}^* + V_{ts} V_{tb}^* = 0$ (or (3.4)) for SM3, the three-generation SM. This triangle, given already in Figs. 3.4 and A.2, has the same area as the $b \rightarrow d$ triangle. It is the very tiny phase angle of the $b \rightarrow s$ triangle in SM3 at the vertex S that gives rise to the very small value of $\sin 2\Phi_{B_s}^{\text{SM3}}$. The sign, which is opposite to $\sin 2\Phi_{B_d}^{\text{SM3}} \equiv \sin 2\phi_1/\beta$, is due to the “orientation” being opposite to the SM3 $b \rightarrow d$ triangle. The large phase angle in SM4 at vertex S leads to the large area of the quadrangle, which is about 30 times the area of the $b \rightarrow d$ triangle. We caution that Fig. 10.1 is for purpose of illustration. The length of $V_{ts} V_{tb}^*$ (and in part its phase angle) depends on the value of $m_{t'}$. A larger $m_{t'}$ than our nominal 300 GeV would result in a smaller $|V_{ts} V_{tb}^*|$. If one assumes the central value of the experimental measurement of (3.26), then for $m_{t'} \sim 600$ GeV, the length $|V_{ts} V_{tb}^*|$ will reduce roughly by half.

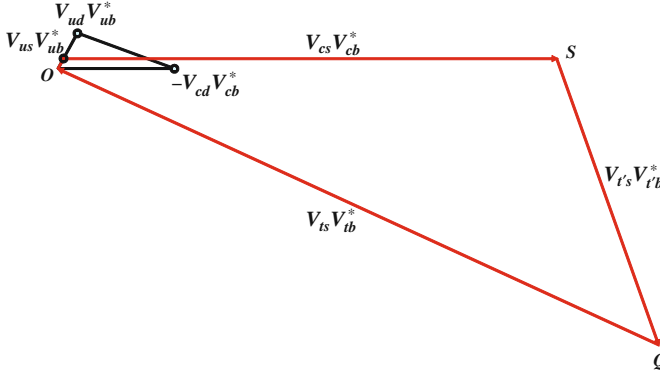


Fig. 10.1 The small SM-like $b \rightarrow d$ triangle (gives area $A/2$ in (10.4)), and SM4 $b \rightarrow s$ quadrangle (gives area $A_{234}^{sb}/2$ in (10.5)). The large area, and the size and orientation of phase angle at S , leads to the prediction that $\sin 2\Phi_{B_s}$ is large and negative. The actual $b \rightarrow d$ quadrangle cannot be distinguished from the triangle (which is taken from Fig. 1.6) within experimental resolutions at the B factories

We stress again that SM3 itself arose from the study of FCNC kaon physics, which lead to predictions for D and B systems. If there is a fourth generation, it would touch upon all these heavy flavor sectors: K , B , and D as well. Thus, as shown above, we would have a lot to check here on Earth, for the correlated (by CKM unitarity) footprints of the fourth generation.

10.2.2 Jarlskog Invariant for Three Generations

There has always been a very strong motivation for the search of New Physics CP violation: the starry heavens. Why the current Universe has only matter, but no antimatter? We expect them to be produced equally in the Big Bang. But we see no antibaryons in our Universe, i.e., $n_{\bar{B}}/n_{\gamma} = 0$, while [20]

$$\frac{n_{\bar{B}}}{n_{\gamma}} = (6.1 \pm 0.2) \times 10^{-10} \quad (\text{WMAP}), \quad (10.3)$$

so BAU is 100%. But the folklore is that CP violation in SM falls short by 10^{-10} . How to account for the matter predominance of our Universe is a fundamental issue at the core of our very existence.

Let us now explain how this 10^{-10} arises, and then offer our insight, or the way out with the existence of the 4th generation.

It is truly remarkable that the SM possesses [21] all the necessary ingredients for baryogenesis, i.e., the Sakharov [22] conditions of (1) baryon number violation, (2) CP violation, and (3) departure from equilibrium (in the very hot early Universe). But then the agony is the insufficiency in the latter two conditions: CPV is way too small, while the electroweak phase transition (EWPhT) seems only a crossover, rather than the needed first-order transition.

The relevant source of CPV is the Jarlskog invariant [23],

$$J = (m_t^2 - m_u^2)(m_t^2 - m_c^2)(m_c^2 - m_u^2)(m_b^2 - m_d^2)(m_b^2 - m_s^2)(m_s^2 - m_d^2) A, \quad (10.4)$$

where A is twice the area of any unitarity triangle. Equation (10.4) incorporates all requirements for CPV to be nonvanishing, i.e., a nontrivial A (nondegenerate unitarity triangle) and nondegeneracy of any pair of like charge quarks. While A is dimensionless, note that the nondegenerate quark mass condition (related to GIM mechanism) implies that J has 12 mass dimensions. To compare with n_B/n_γ , a dimensionless quantity, one typically normalizes by the EWPhT temperature $T \sim 100 \text{ GeV}$ (or roughly the v.e.v. scale). Putting in quark masses, and our knowledge that [8, 9] $A \simeq 3 \times 10^{-5}$, one immediately finds $J/T^{12} \sim 10^{-20}$, which falls short of (10.3) by 10^{-10} . The main source of suppression is the smallness of light quark masses. The actual situation is even worse, since there are additional coupling constant factors as well [24].

The KM model seems depressingly deficient in supplying enough CPV for baryogenesis. Although BAU does provide an extremely strong motivation to continue our search for New Physics CPV, there is a sense of futility: Whatever we find in the laboratory, how can it be relevant for the Heavens? How can it bridge, or jump, the abyss of over 10^{-10} !?

10.2.3 New Physics CPV for the Heavens: Fourth Generation for BAU !?

Some time in late summer 2007, it occurred to me one day that the fourth generation actually provided a simple way out. *By the simple extension from three to four quark generations, one can enhance (10.4) by over 10^{13} !*

Before we proceed to elucidate this point, let me confess that this simple observation came after working on fourth-generation topics for over 20 years, with full knowledge of the Jarlskog invariant. Further, it came after 3 years of intense work that was stimulated by $\Delta\mathcal{A}_{K\pi} \neq 0$, together with the insight of nondecoupling of t' quark in $b \rightarrow s$ electroweak penguin and $b\bar{s} \leftrightarrow s\bar{b}$ box diagram loops. The key, or eureka moment, was to link large Yukawa couplings to the Jarlskog invariant, that the small mass suppression of (10.4) is a dynamical effect, the same as in P_{EW} and box diagrams. That is, large Yukawa couplings can modify (10.4) !

If one shifts by one generation with fourth-generation SM (SM4), from 1–2–3 generations in (10.4) to 2–3–4 generation, then (10.4) becomes [25]

$$\begin{aligned} J_{(2,3,4)}^{sb} &\simeq (m_{t'}^2 - m_c^2)(m_{t'}^2 - m_t^2)(m_t^2 - m_c^2) \\ &\quad (m_{b'}^2 - m_s^2)(m_{b'}^2 - m_b^2)(m_b^2 - m_s^2) A_{234}^{sb} \\ &\sim \frac{m_{t'}^2}{m_c^2} \left(\frac{m_{t'}^2}{m_t^2} - 1 \right) \frac{m_{b'}^4}{m_b^2 m_s^2} \frac{A_{234}^{sb}}{A} J > 10^{13} J. \end{aligned} \quad (10.5)$$

The difference of light quark mass pairs, $(m_s^2 - m_d^2)$, $(m_c^2 - m_u^2)$, and $(m_b^2 - m_t^2)$, now all drop out. Assuming $m_{b',t'} \sim 300$ GeV, one gains in the mass factors by 10^{13} , while one can see from Fig. 8.3 that the gain in CPV phase area is by a factor of $A_{234}^{sb}/A \sim 30$ (we will discuss the ambiguity shortly). For $m_{b',t'} \sim 600$ GeV, the gain in mass factors jumps to 10^{15} , while the gain in phase area is still an order of magnitude. Beyond this mass range, i.e., above the unitarity bound [26], one has entered the nonperturbative, strong Yukawa coupling limit.² Note that even if $A_{234}^{sb}/A \sim 1$, i.e., no spectacular enhancement for $\sin 2\Phi_{B_s}$, the gain is still more than a factor of 10^{13} . Not only the 10^{-10} deficiency of KM3 can be overcome, the additional gauge coupling suppression factors can be accommodate as well.

It was further shown [25], using the degeneracy limits (in this case, d and s , even u and c , on the v.e.v. scale) studied by Jarlskog [29] for $n > 3$ generations, that the four-generation world effectively becomes the three-generation world of 2–3–4 generation quarks. One then sees why (10.5) would turn out to be by far the dominant, and why J in (10.4), which could be written as³ $J(1, 2, 3)$, would be so tiny (the 10^{-10} gap!).

There are three independent phases [8, 9] in SM4. One is the already measured $b \rightarrow d$ transition phase, where it is miraculous that the three- and four-generation world cannot be distinguished [16, 17] at present. The second CPV phase could be emerging in a spectacular way in $b \rightarrow s$ transitions, as we have stressed. A third subdominant phase can be glimpsed from Fig. 10.1. Since $V_{us}V_{ub}^*$ is small, the triangle that results from shrinking $|V_{us}V_{ub}^*| \rightarrow 0$ is not much different from the quadrangle itself. This small difference is at the root of the small CPV in D^0 mixing (Fig. 8.3(b)). We may have been a little cavalier in the notation of A_{234}^{sb} , but again there is no doubt that $J_{(2,3,4)}^{sb}$ of (10.5) is the predominant CPV effect in SM4, and the relevant one for BAU.

Actually, the discussion above is not a proof that SM4 is necessarily the source of CPV for BAU. Further issues such as order of electroweak phase transition linger, while ideas for baryogenesis abound. But it is remarkable that SM4, unlike SM3, seems to provide *enough CPV for the very profound problem of generating BAU*. That this is the same KM model, except extended from three to four generations, utilizing the fact that the t' and b' quarks are v.e.v. scale objects with large Yukawa couplings, can be used as argument for their existence.

10.2.4 Litmus Test on Earth: Search for t' and b'

We must have often appeared to the reader to be running the gauntlet, when in chapter 8 after chapter we used the fourth generation as prime example for New

² It is curious whether this regime could be [27] the source of EWSB itself, à la the Nambu–Jona-Lasinio model [28]. If so, the Higgs boson becomes composite, analogous to the σ particle in hadron physics.

³ We have modified the more general notation of $J(2, 3, 4)$ of Jarlskog [29].

Physics effects. The justification in earlier chapters were the insight that nondecoupling allowed easy entry of heavy fourth-generation t' and b' effects into electroweak (Z) penguin and box diagrams. So, they were used as existence proofs for having large effects on experimental observables of interest. But our statement above that the fourth generation may provide sufficient CPV for the baryon asymmetry of the Universe provides important justification for our usage, in the context of our theme of Flavor and TeV link.

Admittedly, the fourth generation has long been viewed by many as ruled out already: by neutrino counting and by ElectroWeak Precision Tests (EWPT). However, if we take strictly an experimental view and look only at hard facts rather than perceptions, we would comment that these two venerated results are just that, venerated experimental results. But to claim the fourth generation is therefore ruled out is very much a projection from common perceptions.

Neutrino counting states that there are only three light active neutrino species, nothing more. But we have learned since 1998 that neutrinos mix, hence they have mass. The existence of extra mass scale(s) calls for New Physics. The common misconception is from the old tradition that the neutrino is massless for a standard generation, hence having three generations is the end of the story. From direct experimental search, however, limits [8, 9] on heavy charged and neutral leptons come largely from LEP, rather than the Tevatron, while the new era of LHC would provide more information on quark physics rather than lepton physics. Why the new neutral lepton, necessarily rather heavy, is so different from the first three nearly massless neutrinos, would need data from future high-energy leptonic machines, such as the ILC, to clarify. It is an experimental question.

For electroweak precision tests, the strong statement from Particle Data Group that a fourth generation is ruled out with high confidence [8, 9] comes with the fine print that it applies to the case of degenerate t' and b' . Unfortunately, the strong statement seems to stick in the minds of many people, with the fine print forgotten. As stressed recently [30], however, the fourth generation is not in such great conflict with EWPT, especially the high-energy data from LEP and the Tevatron. The t' and b' must be split in mass, but not by too much. One may then object and ask why the fourth generation needs to be split (to satisfy S parameter), but split not more than M_W (to satisfy ρ , or T parameter)? Is that natural? Again, from the experimental view, this is what data tell us at present.

Armed with motivation from “New Physics CPV on Earth” and “New Physics CPV for the Heavens,” which strongly motivate the existence of the fourth generation, we wish to stress that we are entering an unprecedented era: the LHC. Note that, despite the negatives of neutrino counting and EWPT, every high-energy collider has pursued the search [8, 9] for t' and b' . But all suffer from falling cross sections and energy reach.⁴ This is not the case for the LHC. With 14 TeV

⁴ The current best limit from CDF using 2.8 fb^{-1} data gives [31] $m_{t'} > 311 \text{ GeV}$ at 90% C.L. There are some hints of activity, but probably one cannot be conclusive with Tevatron data, because of signal vs. background issues.

center-of-mass energy, the LHC can cover the full range of SM chiral quarks. Even beyond the unitarity bound [26] of 600 GeV or so, experimental study is not a problem. *At the LHC, we can discover, or rule out, the existence of a fourth generation once and for all* [32]. Serious efforts have started at the ATLAS and CMS experiments [33], and in several years, depending on LHC turn on schedule, we would know.

This is the true litmus test for (10.5) as the possible source of CPV for BAU. Once t' and b' are discovered, then the sufficient CPV source is there. If we find rather enhanced $\sin 2\Phi_{B_s}$, then so much the better. But even if the current Tevatron central value of (3.26) evaporates, so long that A_{234}^{sb}/A is not of order 10^{-10} (which would be unnatural and impossible to verify experimentally), the possibility of a fourth-generation CPV source for BAU would be established.

As a final remark, we comment that the discovery of t' and b' would extend flavor physics directly into the TeV regime. We would start to explore *really heavy* flavor physics, just like heavy flavor physics itself started with the discovery of the D and B meson systems. Flavor physics *at* the TeV scale, however, is left for the future.

10.3 Summary and Conclusion

To summarize, I have covered a rather wide range of probes of TeV scale physics via heavy flavor processes. At the moment, we have several hints for New Physics:

- $\Delta\mathcal{S}$: a long-standing, but slowly diminishing, difference between TCPV in $B \rightarrow J/\psi K^0$ vs. penguin-dominant $b \rightarrow s\bar{q}q$ modes, which turned circumstantial in 2008;
- $\Delta\mathcal{A}_{K\pi}$: difference in DCPV between $B^+ \rightarrow K^+\pi^0$ and $B^0 \rightarrow K^+\pi^-$ modes, which is experimentally established;
- $A_{\text{FB}}(B \rightarrow K^*\ell^+\ell^-)$: hint of discrepancy with SM expectation in lower q^2 bins, seen by both Belle and BaBar;
- $\sin 2\Phi_{B_s}$: Both CDF and DØ see a hint for *large and negative* mixing-dependent CPV in tagged $B_s \rightarrow J/\psi\phi$.

The first three hints are from the B factories, while the last is from the Tevatron.

With $\Delta\mathcal{S}$ reduced to a problem at best to be tested at the Super B Factory, we note that the large CPV effect in $\Delta\mathcal{A}_{K\pi}$ is not unequivocal in its interpretation. For the CP conserving measurement of $A_{\text{FB}}(B \rightarrow K^*\ell^+\ell^-)$, one has form factor dependence, although at present there is no indication of crossing of zero (which is supposedly less form factor dependent within SM) at all. It would be good if Belle and BaBar can come up with the significance of the deviation from SM. Once LHCb takes data, whether there is a genuine discrepancy with SM would be quickly clarified.

The thing to watch in 2009–2010, in my opinion, is whether the Tevatron could *observe* large mixing-dependent CPV in tagged $B_s \rightarrow J/\psi\phi$, i.e., $\sin 2\Phi_{B_s}$. If so, it would be unequivocal evidence for BSM. Though still too early to conclude,

it should be clear that the Tevatron can get several times the data than has been analyzed, and *the hint could turn into evidence, even observation, before LHCb physics arrives*. The longer it takes for LHCb to take real data, the better the case for prolonging the Tevatron run. In any case, if the hint for sizable $\sin 2\Phi_{B_s}$ is true, it can be quickly confirmed by LHCb once data arrive. If the hint for large $\sin 2\Phi_{B_s}$ from the Tevatron fades away, LHCb can probe down to the SM expectation with still a lot of range for New Physics discovery. But it would be a great disappointment if we again confirm the Standard Model.

Taking the present hint of $\sin 2\Phi_{B_s}$ seriously, together with the insight that a fourth generation could provide the source of CPV for the baryon asymmetry of the Universe, we have stressed that a new era of very heavy flavor physics could emerge from the LHC. The search for t' and b' should be taken seriously, since it links to all the flavor physics hints for BSM from the B factories and the Tevatron. If these new heavy quarks are discovered at the LHC directly, then an LHC vs. Super B Factory dialogue would be even more interesting.

Other processes that have good potential for New Physics search in the not too distant future are (in sequence of our coverage) direct CPV in $B^+ \rightarrow J/\psi K^+$; $b \rightarrow s\gamma$; $B \rightarrow \tau\nu$; $B_s \rightarrow \mu\mu$; Υ decay; D^0 mass mixing and CPV; $K_L \rightarrow \pi^0\nu\nu$; $\mu \rightarrow e\gamma$; and $\tau \rightarrow \ell\gamma, \ell\ell\ell'$. Most of these probes involve flavor loops and probe Beyond SM New Physics in a way that is complementary to direct search at the LHC. For example, $B \rightarrow \tau\nu$ and $b \rightarrow s\gamma$ rate measurements would provide stringent constraints that complement direct studies of H^+ production at the LHC, whether it is found or not.

Though no unequivocal indication for New Physics has emerged so far, the B factories have not yet exhausted their bag of surprises. With such a diverse search platform, I hope I have made it clear that a Super B Factory would be superb to probe deeper into all the above D , B , and τ subjects (except $\sin 2\Phi_{B_s}$ and maybe $B_s \rightarrow \mu\mu$). Before a Super B Factory arrives, we will attain some new heights with LHCb. If New Physics emerges in $\sin 2\Phi_{B_s}$ in the next few years, its impact would be dramatic.

With Kobayashi and Maskawa (source of CP symmetry breaking) and Nambu (insight into spontaneous symmetry breaking) receiving the 2008 Nobel Prize, it symbolizes the transition from the B factory to the LHC era. But flavor physics would stay as a strong element of our effort to unravel TeV scale physics. We are entering exciting times.

References

1. Georgi, H.: Phys. Rev. Lett. **98**, 221601 (2007) 123
2. Zwicky, R.: Phys. Rev. D **77**, 036004 (2008) 123
3. Fratina, S., et al. [Belle Collaboration]: Phys. Rev. Lett. **98**, 221802 (2007) 123
4. Aubert, B., et al. [BaBar Collaboration]: Phys. Rev. Lett. **99**, 071801 (2007) 123
5. Hou, W.S., Nagashima, M., Soddu, A.: Phys. Rev. D **72**, 095001 (2006) 123
6. See, e.g. the brief review by Randall, L.: Science **296**, 1422 (2002) 124
7. Fukugita, M., Yanagida, T.: Phys. Lett. B **174**, 45 (1986) 124

8. Yao, W.M., et al. [Particle Data Group]: J. Phys. G **33**, 1 (2006) 124, 129, 130, 131
9. Amsler, C., et al.: Phys. Lett. B **667**, 1 (2008); and <http://pdg.lbl.gov/> 124, 129, 130, 131
10. For a review, see Schmaltz, M., Tucker-Smith, D.: Ann. Rev. Nucl. Part. Sci. **55**, 229 (2005) 125
11. Kobayashi, M., Maskawa, T.: Prog. Theor. Phys. **49**, 652 (1973) 125
12. Hou, W.S., Nagashima, M., Soddu, A.: Phys. Rev. Lett. **95**, 141601 (2005) 126
13. Hou, W.S., Li, H.n., Mishima, S., Nagashima, M.: Phys. Rev. Lett. **98**, 131801 (2007) 126
14. Peskin, M.E.: Nature **452**, 293 (2008), companion paper to Ref. [17] of Chap. 2. 126
15. See, e.g., Gronau, M.: Talk at Flavour Physics and CP Violation Conference (FPCP2007), Bled, Solvenia, May 2007 126
16. Hou, W.S., Nagashima, M., Soddu, A.: Phys. Rev. D **72**, 115007 (2005) 126, 127, 130
17. Hou, W.S., Nagashima, M., Soddu, A.: Phys. Rev. D **76**, 016004 (2007) 126, 130
18. Abulencia, A., et al. [CDF Collaboration]: Phys. Rev. Lett. **97**, 242003 (2006) 126
19. Bigi, I.I.Y., Sanda, A.I.: Nucl. Phys. B **193**, 85 (1981) 126
20. Bennett, C.L., et al. [WMAP Collaboration]: Astrophys. J. Suppl. **148**, 1 (2003) 128
21. Kuzmin, V.A., Rubakov, V.A., Shaposhnikov, M.E.: Phys. Lett. B **155**, 36 (1985) 128
22. Sakharov, A.D.: Pisma Zh. Eksp. Teor. Fiz. **5**, 32 (1967) [JETP Lett. **5**, 24 (1967)] 128
23. Jarlskog, C.: Z. Phys. C **29**, 491 (1985) 129
24. For a recent review, see the lectures by Cline, J.M.: hep-ph/0609145, given at Les Houches, France, summer 2006 129
25. Hou, W.S.: arXiv:0803.1234 [hep-ph] (unpublished) 129, 130
26. Chanowitz, M.S., Furman, M.A., Hinchliffe, I.: Phys. Lett. B **78**, 285 (1978) 130, 132
27. Holdom, B.: JHEP **0608**, 076 (2006) 130
28. Nambu, Y., Jona-Lasinio, G.: Phys. Rev. **122**, (1961) 345 130
29. Jarlskog, C.: Phys. Rev. D **36**, 2128 (1987) 130
30. Kribs, G.D., Plehn, T., Spannowsky, M., Tait, T.M.P.: Phys. Rev. D **76**, 075016 (2007) 131
31. See public note 9234 of the CDF Collaboration. <http://www-cdf.fnal.gov/> 131
32. Arhrib, A., Hou, W.S.: JHEP **0607**, 009 (2006) 132
33. See the webpage, <http://indico.cern.ch/conferenceProgram.py?confId=33285>, for ATLAS and CMS talks at the initiation workshop Beyond the 3rd SM generation at the LHC era, held at CERN, Geneva, Switzerland, September 2008 132

Appendix A

A CP Violation Primer

A.1 Generalities

CP violation is defined as a difference in probability between a particle process from the antiparticle process, e.g., between $B \rightarrow f$ and $\bar{B} \rightarrow \bar{f}$. As is typical in quantum phenomena, it requires the presence of two interfering amplitudes. However, besides the familiar i from quantum mechanics, it needs *complex dynamics* as well.¹ That is, the interference involves the presence of two different kinds of phases. Let us elucidate how CPV occurs.

Consider the amplitude $A = A_1 + A_2$ for the particle process, which is a sum of two terms, where amplitude A_j has both a CP -invariant phase δ_j (quantum mechanical i) and a CPV phase ϕ_j (i from CPV *dynamics*). Absorbing an overall phase by defining $A_1 = a_1$ to be real, one has

$$\begin{aligned} A &= A_1 + A_2 = a_1 + a_2 e^{i\delta} e^{+i\phi} \\ \bar{A} &= \bar{A}_1 + \bar{A}_2 = a_1 + a_2 e^{i\delta} e^{-i\phi}, \end{aligned} \quad (\text{A.1})$$

where $a_2 \equiv |A_2|$. The δ and ϕ are called the “strong” and “weak” phases, respectively. The strong phase δ arises from (re)scattering or quantum time evolution and does not distinguish between particle and antiparticle, hence the sign is unchanged between A and \bar{A} . However, the dynamical or weak phase ϕ changes sign for the antiparticle process \bar{A} . This enrichment of quantum interference leads to a possible asymmetry between particle and antiparticle probabilities, for example, involving \bar{B}^0 vs. B^0 . From (A.1), one finds

$$\mathcal{A}_{\text{CP}} \equiv \frac{\Gamma_{\bar{B}^0 \rightarrow \bar{f}} - \Gamma_{B^0 \rightarrow f}}{\Gamma_{\bar{B}^0 \rightarrow \bar{f}} + \Gamma_{B^0 \rightarrow f}} = \frac{2a_1 a_2 \sin \delta \sin \phi}{a_1^2 + a_2^2 + 2a_1 a_2 \cos \delta \cos \phi}, \quad (\text{A.2})$$

¹ Imagine e of electrodynamics is complex. This is not possible as it is a gauge coupling.

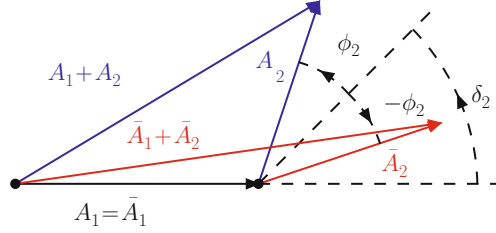


Fig. A.1 Mechanism for CPV, the geometric picture for (A.2)

defined with respect to quarks (e.g., \bar{B}^0 contains a b quark). As \mathcal{A}_{CP} vanishes with either δ or $\phi \rightarrow 0$, CPV requires the presence of *both* CP conserving and CPV phases.

Equation (A.1) is illustrated in Fig. A.1, which shows geometrically how the \mathcal{A}_{CP} of (A.2) materializes. By a phase choice, we place $A_1 = \bar{A}_1$ on the real axis. Then A_2 and \bar{A}_2 , which are of the same length $|A_2| = |\bar{A}_2| = a_2$, are as depicted, where A_2 (\bar{A}_2) is rotated by $+\phi$ ($-\phi$) from the common δ phase angle. We see that, if $\delta = 0$, then $A_1 + A_2$ and $\bar{A}_1 + \bar{A}_2$ are at an angle ϕ above or below the real axis and are of equal length. If, however, $\phi = 0$, then $A_1 + A_2$ and $\bar{A}_1 + \bar{A}_2$ coalesce into the same vector, hence are necessarily of equal length. Only when *both* $\delta \neq 0$ and $\phi \neq 0$, do we have $|A_1 + A_2| \neq |\bar{A}_1 + \bar{A}_2|$, as one can see from the asymmetry formula (A.2).

CP Violation in Standard Model with Three Generations

In the KM model with three generations, one needs the presence of all three generations in a process to make CPV occur [1]. In the standard phase convention [2, 3] of keeping V_{us} and V_{cb} real, the unique CPV phase is placed in the 13 element V_{ub} and hence the 31 element V_{td} as well by unitarity of V . We give the CKM matrix V in Wolfenstein form [2–4],

$$V = \begin{pmatrix} V_{ud} & V_{us} & V_{ub} \\ V_{cd} & V_{cs} & V_{cb} \\ V_{td} & V_{ts} & V_{tb} \end{pmatrix} \simeq \begin{pmatrix} 1 - \lambda^2/2 & \lambda & A\lambda^3(\rho - i\eta) \\ -\lambda & 1 - \lambda^2/2 & A\lambda^2 \\ A\lambda^3(1 - \rho - i\eta) & -A\lambda^2 & 1 \end{pmatrix}, \quad (\text{A.3})$$

where,

$$\lambda \equiv V_{us} \cong 0.22, \quad A\lambda^2 \equiv V_{cb} \simeq 0.04, \quad A\lambda^3\sqrt{\rho^2 + \eta^2} \equiv |V_{ub}| \sim 0.003. \quad (\text{A.4})$$

For those with any interest in flavor and CPV physics, it is useful to memorize (A.3) and the orders of magnitude in (A.4). The current measured strength of the CPV phases $\phi_3 \equiv \arg V_{ub}^*$ and $\phi_1 \equiv \arg V_{td}$ (Belle notation for phases) can be found in Chap. 1.

The matrix V is unitary, i.e.,

$$V^\dagger V = V V^\dagger = I. \quad (\text{A.5})$$

It can be readily checked that this relation holds for the Wolfenstein form of V in (A.3) to λ^3 order. At this order, V_{ts} is real and negative, but it picks up a tiny imaginary part at λ^4 order (see below). Note that $\sqrt{\rho^2 + \eta^2} \sim 1/3$ compared with $\lambda \cong 0.22 \sim 1/4.5$. Thus, together with $A \sim 0.8$, $|V_{ub}|$ is actually closer to λ^4 rather than λ^3 order, while $|V_{td}|$ is of order λ^3 .

Since we highlight CPV in $b \rightarrow s$ and $b \leftrightarrow s$ ($B_s^0 - \bar{B}_s^0$ oscillations) transitions as the current frontier for probing physics beyond SM, we extend (A.3) to λ^5 order,

$$V \cong \begin{pmatrix} 1 - \frac{1}{2}\lambda^2 - \frac{1}{8}\lambda^4 & \lambda & A\lambda^3(\rho - i\eta) \\ -\lambda + A^2\lambda^5(\frac{1}{2} - \rho - i\eta) & 1 - \frac{1}{2}\lambda^2 - (\frac{1}{8} + \frac{1}{2}A^2)\lambda^4 & A\lambda^2 \\ A\lambda^3(1 - \bar{\rho} - i\bar{\eta}) & -A\lambda^2 + A\lambda^4(\frac{1}{2} - \rho - i\eta) & 1 - \frac{1}{2}A^2\lambda^4 \end{pmatrix}, \quad (\text{A.6})$$

where the definitions of (A.4) for the three upper-right off-diagonal elements, namely V_{us} , V_{cb} , and V_{ub} , remain the same and $[2, 3] \bar{\rho}/\rho = \bar{\eta}/\eta = 1 - \frac{1}{2}\lambda^2$. We see that $V_{ts}^* V_{tb}$ picks up a CPV phase at λ^4 order, while the real part is at λ^2 order. This implies a rather small phase angle, as compared with the phase in $V_{td}^* V_{tb}$, where the imaginary and real parts are not drastically different in strength.

It is useful to visualize the so-called unitarity triangles that arise from the unitarity relation (A.5). Take the db element of $V V^\dagger = I$, for example, one has

$$V_{ud} V_{ub}^* + V_{cd} V_{cb}^* + V_{td} V_{tb}^* = 0. \quad (\text{A.7})$$

The usual convention is to normalize by $A\lambda^3$, then $V_{cd} V_{cb}^*/A\lambda^3 \cong -1$, and $V_{ud} V_{ub}^*/A\lambda^3 \cong \rho + i\eta$ (for our purpose, let us not distinguish between $\bar{\rho} + i\bar{\eta}$ and $\rho + i\eta$), and $V_{td} V_{tb}^*/A\lambda^3$ follows by unitarity. Equation (A.7) is represented by the regular triangle to the left in Fig. A.2.

For the sb element of $V V^\dagger = I$, one has

$$V_{us} V_{ub}^* + V_{cs} V_{cb}^* + V_{ts} V_{tb}^* = 0. \quad (\text{A.8})$$

If one represents this in the same plot as (A.7), one notes that $V_{ud} V_{ub}^*/A\lambda^3 \cong \rho + i\eta$ is replaced by $V_{us} V_{ub}^*/A\lambda^3 \cong \lambda(\rho + i\eta)$ or the corresponding side has shrunk by

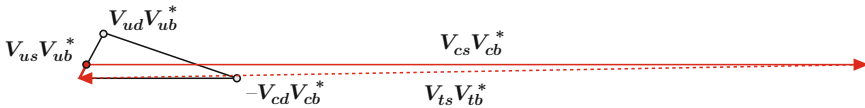


Fig. A.2 Geometric representations of (A.7) and (A.8), the latter being the long, *squashed triangle*. It is common to take the lower left point as the origin

$\lambda \cong 0.22$ in length. At the same time, $V_{cd}V_{cb}^*/A\lambda^3 \cong -1$ becomes $V_{cs}V_{cb}^*/A\lambda^3 \cong +1/\lambda$, which is now extended by $1/\lambda$ times and positive. It is represented by the long horizontal solid line extending to the right. Again, $V_{ts}V_{tb}^*/A\lambda^3$ follows by unitarity, which is represented by the slightly slanted dotted line pointing left (back to the “origin”). Thus, (A.8) is represented by the rather squashed and elongated triangle in Fig. A.2.

A.2 Illustration: Direct CP Violation

Direct CPV (DCPV), which has recently been established in $B^0 \rightarrow K^+\pi^-$ decay, gives the most intuitive illustration of Sect. A.1. That is, we have $f = K^+\pi^-$ in (A.2). Experimentally, the measurement of DCPV in $B^0 \rightarrow K^+\pi^-$ decay is the most straightforward, being just a counting experiment. One simply counts the difference between the number of events in $K^-\pi^+$ and $K^+\pi^-$ final states, with $m_{K\pi}$ reconstructing to m_{B^0} and with background under control. It is a matter of waiting for enough statistics. This is also a so-called self-tagged mode, since the charge of the K^\pm points back to the decaying particle being a B^0 or a \bar{B}^0 .

In Fig. A.3, we show the leading tree (T) and penguin (P) diagrams for $B^0 \rightarrow K^+\pi^-$ decay. Reading off from (A.3), one can readily see that the tree $b \rightarrow u\bar{s}u$ diagram carries a weak phase $\phi_3 = \arg V_{us}V_{ub}^*$, while P is dominated by $V_{cs}V_{cb}^* \cong -V_{ts}V_{tb}^*$, which is practically real. If the T and P amplitudes develop a relative strong phase δ (some absorptive part in the amplitudes), the interference between T and P would lead to *direct* (i.e., in decay amplitude itself) CPV. Indeed, this was observed in 2004 [5, 6], and $\mathcal{A}_{B^0 \rightarrow K^+\pi^-} \equiv \mathcal{A}_{CP}(B^0 \rightarrow K^+\pi^-) \sim -10\%$ is not small, recalling that $|\varepsilon'/\varepsilon|$ is at the 10^{-6} level in the kaon system. This illustrates rather clearly (A.1) and (A.2), where, to good approximation, $a_1 = |P|$ and $a_2 = |T|$. Unfortunately, the strong phase difference δ is of hadronic nature, the computation of which is rather challenging, and theorists do not generally agree with each other.

The whimsical name of the “penguin” diagram is attributed to a bet by John Ellis 30 years ago. Let us not get deeper into the historical anecdote, but note that if one complains that Fig. A.3(b) bears no resemblance to a “penguin,” then neither

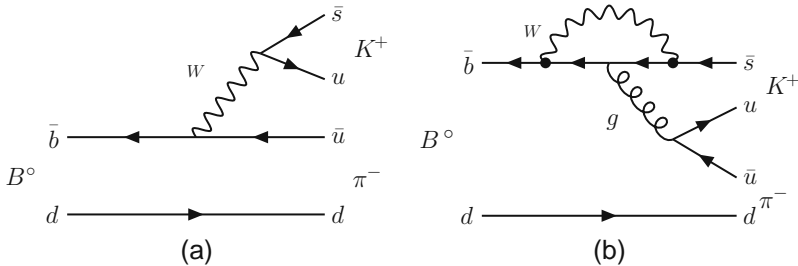


Fig. A.3 Tree and Penguin diagrams for $B^0 \rightarrow K^+\pi^-$ decay

does a Feynman diagram bear any resemblance to Feynman (although unlike the “penguin,” Feynman did pen it) !

A.3 Time-Dependent CP Violation

The idea for mixing- or time-dependent CP violation (TCPV) study at B factories is a beautiful one. Rather than derive the TCPV formalism [7], where we may get lost in the details, we give the formula and elucidate its content, thereby hopefully getting to appreciate some part of its beauty. In this way, we also prepare for the discussion of actual experimental studies in Chap. 2.

The TCPV asymmetry for $B^0 \rightarrow f$ decay, where f is a CP eigenstate, is

$$\begin{aligned} A_{CP}(\Delta t) &\equiv \frac{\Gamma(\bar{B}^0(\Delta t) \rightarrow f) - \Gamma(B^0(\Delta t) \rightarrow f)}{\Gamma(\bar{B}^0(\Delta t) \rightarrow f) + \Gamma(B^0(\Delta t) \rightarrow f)} \\ &= -\xi_f (\mathcal{S}_f \sin \Delta m \Delta t + \mathcal{A}_f \cos \Delta m \Delta t). \end{aligned} \quad (\text{A.9})$$

The first part of (A.9) is defined quite analogous to (A.2), except that it is a little more delicate: $B^0(\Delta t)$ denotes the state at time Δt that evolved from a B^0 state at $\Delta t = 0$ and likewise for $\bar{B}^0(\Delta t)$. To avoid clutter and to compare better with (A.2) in a more transparent way, we have used a looser notation for what are actually differential decay rates (when conducting the analysis). Let us understand the second half of (A.9), where ξ_f is the CP eigenvalue of f , $\Delta m \equiv \Delta m_{B_d}$ and (BaBar uses $\mathcal{C}_f \equiv -\mathcal{A}_f$, i.e., picking up the initials for sine and cosine)

$$\mathcal{S}_f = \frac{2 \operatorname{Im} \lambda_f}{|\lambda_f|^2 + 1}, \quad \mathcal{A}_f = \frac{|\lambda_f|^2 - 1}{|\lambda_f|^2 + 1}, \quad (\text{A.10})$$

are CPV coefficients, where λ_f is defined as

$$\lambda_f = \frac{q}{p} \frac{\langle f | S | \bar{B}^0 \rangle}{\langle f | S | B^0 \rangle}. \quad (\text{A.11})$$

We see that λ_f depends on both B^0 – \bar{B}^0 mixing, i.e., $B_{H,L} = p B^0 \mp q \bar{B}^0$ (where H, L stands for the nominally “heavy” and “light” states) and decay to final state f . This is why TCPV is also called CPV in mixing–decay interference. The lifetime difference between the two neutral B mesons have been ignored to yield the simpler form of (A.9). This is a very good approximation for the B_d^0 – \bar{B}_d^0 system (but not so good for B_s^0 – \bar{B}_s^0 system, as will be touched upon in Chap. 2), so $q/p \cong e^{-2i\phi_1}$, hence $|q/p| \cong 1$. Using this last point, one can easily check that \mathcal{A}_f is nothing but the DCPV asymmetry in B^0 decay, hence this notation is more transparent than BaBar’s usage of \mathcal{C}_f .

For the golden $J/\psi K_S$ mode, the decay amplitude is real in the standard phase convention of (A.3), since it is dominated by the (color-suppressed) $b \rightarrow c\bar{c}s$ tree diagram, where $V_{cs}^* V_{cb}$ carries practically no weak phase. Thus,

$$\mathcal{S}_{J/\psi K_S} \cong \sin 2\phi_1, \quad \mathcal{A}_{J/\psi K_S} \cong 0, \quad (\text{A.12})$$

to very good accuracy. This is explained in Chap. 2. Many other $b \rightarrow (c\bar{c})_{\text{charmonium}} s$ modes are also studied and correcting for ξ_f adds to the statistics.

Inspecting (A.2), (A.9), (A.10), and (A.12) altogether, one can now interpret (A.9) and gain some insight into the beauty and power of TCPV measurement, especially in the $J/\psi K^0$ mode (both $J/\psi K_S^0$ and $J/\psi K_L^0$). As stated, the $B^0 \rightarrow J/\psi K^0$ mode is dominated by a single decay amplitude, the color-suppressed $b \rightarrow c\bar{c}s$ tree diagram, with practically no weak phase in the decay amplitude. But there are two paths from an initial B^0 (i.e., B^0 at time $\Delta t = 0$) to decay to the $J/\psi K^0$ final state: a direct $B^0 \rightarrow J/\psi K^0$ decay or via B^0 oscillating to \bar{B}^0 , then $\bar{B}^0 \rightarrow J/\psi K^0$ decay. This corresponds to A_1 and A_2 of (A.2). As there is no CPV phase in either B^0 or \bar{B}^0 decay to $J/\psi K^0$, one is measuring the CPV phase in the B^0 to \bar{B}^0 oscillation amplitude. Here, the CP conserving phase is just the quantum mechanical time evolution phase $e^{i\Delta m \Delta t}$, which is *measured* experimentally. Thus, we measure the CPV phase factors \mathcal{S}_f and \mathcal{A}_f in the $\sin \Delta m \Delta t$ and $\cos \Delta m \Delta t$ oscillation coefficients when measuring the t -dependent asymmetries as defined in the first part of (A.9). The \mathcal{S}_f and \mathcal{A}_f corresponds to $\sin \phi$ in (A.2). With B^0 – \bar{B}^0 mixing dominated by the top quark, $S_{J/\psi K^0}$ measures a pure weak phase, and there is no “hadronic” or other ambiguity.

We stress that with ϕ_1 a fundamental, unique phase in the three-generation CKM matrix V , its measurement is as fundamental as determining the electromagnetic coupling constant α , the strong coupling constant α_s , or the Weinberg angle $\sin \theta_W$.

References

1. Kobayashi, M., Maskawa, T.: Prog. Theor. Phys. **49**, 652 (1973) 136
2. Yao, W.M., et al. [Particle Data Group]: J. Phys. G **33**, 1 (2006) 136, 137
3. Amsler, C., et al.: Phys. Lett. B **667**, 1 (2008); and <http://pdg.lbl.gov/> 136, 137
4. Wolfenstein, L.: Phys. Rev. Lett. **51**, 1945 (1983) 136
5. Aubert, B., et al. [BaBar Collaboration]: Phys. Rev. Lett. **93**, 131801 (2004) 138
6. Chao, Y., Chang, P., et al. [Belle Collaboration]: Phys. Rev. Lett. **93**, 191802 (2004) 138
7. Bigi, I.I.Y., Sanda, A.I.: Nucl. Phys. B **193**, 85 (1981) 139

Index

- $\mathcal{A}_{\text{CP}}(B^+ \rightarrow J/\psi K^+)$, 26, 126
- $\mathcal{A}_{\text{CP}}(b \rightarrow s\gamma)$, 82, 127
- Abelian flavor symmetry, 90
- $A_{\text{FB}}(B \rightarrow K^* \ell^+ \ell^-)$, 77–82, 126, 132
- Amplitude scan method, 39, 41
- Angular analysis, 50, 52, 82
- Artificial neural network (ANN), 51, 53
- Asymmetric beam energies, 8, 11, 12, 14, 87, 89
- $B^+ \rightarrow \tau^+ \nu_\tau$, 65–70, 83, 90, 96
- $B_s \rightarrow \mu^+ \mu^-$, 87, 90, 91
- $B_s \rightarrow \phi \mu^+ \mu^-$, 82
- Bag parameter, 7, 35
- Baryogenesis, 115, 129, 130
- Baryon Asymmetry of the Universe (BAU), 11, 115, 127–133
- Baryon number violation (BNV), 115, 119, 120, 123, 128
- $b \rightarrow c \tau \nu_\tau$ ($B \rightarrow \tau \nu_\tau + X$), 64, 65
- B_d^0 – \bar{B}_d^0 mixing, 5, 7, 12, 76, 101, 139, 140
- B_s^0 – \bar{B}_s^0 mixing, 33–43, 50, 54, 81, 101, 126, 137
- $B \rightarrow D^{(*)} \tau \nu_\tau$, 68–70
- Beam-constrained mass M_{bc} , 19
- Belle detector, 14
- Beyond the Standard Model (BSM), 3, 4, 29, 33, 37, 45, 69, 78–81, 108, 109, 112–116, 123–125, 133, 137
- B factory, 3, 4, 7, 8, 12, 20, 27, 39, 58, 59, 61, 66–69, 76, 78, 79, 81, 83, 93, 95, 99, 101, 102, 104–106, 115, 118–121, 126, 127, 132, 133
- $b \rightarrow sg$, 64
- $b \rightarrow s\gamma$ ($B \rightarrow X_s \gamma$), 57–64, 68, 88, 126
- Big Bang, 128
- $B \rightarrow K + \text{nothing}$, 84, 85
- $B \rightarrow K^* \gamma$, 58, 87–90
- $B \rightarrow K^{(*)} \ell^+ \ell^-$, 73–82
- $B \rightarrow K^{(*)} \nu \nu$, 82–85
- $B^+ \rightarrow J/\psi K^+$, 26–29, 91
- $B^0 \rightarrow \eta' K_S$, 16–18
- $B^0 \rightarrow \phi K_S$, 15–18
- $B^0 \rightarrow K_S^0 \pi^0 \gamma$, 87–90
- B–L conservation (violation), 120
- Box diagram, 6, 7, 25, 34, 35, 37, 43–49, 73, 74, 77, 82, 102, 109, 126, 129, 131
- $b \rightarrow s \ell^+ \ell^-$, 73–78, 81
- $b \rightarrow s \nu \bar{\nu}$, 74, 75, 82
- BSM Higgs boson, 82–85, 87, 90, 91, 93, 95–99, 124
- Cabibbo-favored (CF), 103–105
- Cabibbo-suppressed (CS), 103
- Charged Higgs boson, 57–59, 90, 124
- CKM, 6–8, 11, 15, 25, 26, 29, 35–38, 42, 47, 68, 70, 78, 82, 102, 110, 124–128, 136, 140
- Color-suppressed tree (C), 24, 26, 28, 33, 126, 139
- Complex dynamics, 80, 135
- $\cos 2\Phi_{B_s}$, 43, 52
- CP violation (CPV), 2–7, 125, 126, 128–133, 135–140
- current conservation, 62, 75, 87
- $D_s^+ \rightarrow \ell^+ \nu_\ell$, 70, 71
- Dalitz analysis, 105, 106, 109
- Dark matter (DM), 82–85, 93, 96, 97, 99
- D^0 – \bar{D}^0 mixing, 101–109, 130
- Decay constant, 7, 35, 42, 65, 68, 70, 90
- $\Delta \Gamma_{B_s}$, 43, 52, 53
- $\Delta \mathcal{A}_{K\pi}$ problem, 21–26, 29, 33, 46, 47, 49, 54, 80, 81, 125–127, 129, 132
- $\Delta \mathcal{S}$ problem, 11, 16–18, 26, 29, 33, 46, 47, 126, 132
- Direct CPV (DCPV), 11, 18–29, 82, 123, 126, 132, 138, 139
- DORIS, 8

- Doubly Cabibbo-suppressed (DCS), 103, 105, 106
- Electromagnetic calorimetry, 58, 67, 68, 113
- Electroweak penguin (P_{EW}), 24–26, 46, 48, 49, 73, 78, 82, 110, 113, 126, 129, 131
- Electroweak phase transition (EWPhT), 128, 129
- Electroweak precision tests (EWPT), 46, 131
- Electroweak symmetry breaking (EWSB), 1, 4, 75, 76, 123–125, 130
- Energy difference ΔE , 19
- Energy frontier, 4
- EPR coherence, 12
- ε_K , 110
- ε'/ε , 110, 114, 138
- Extra Dimensions, 117, 124
- Flavor changing neutral current (FCNC), 16, 29, 82, 91, 101, 124, 125, 128
- Flavor tagging, 13, 39, 40, 45, 51–53, 103, 109, 118
- Forward Detector, 95, 96
- Forward-backward asymmetry (A_{FB}), 73, 77–82, 126, 132
- Fourth generation, 25, 26, 28, 29, 46–50, 53, 54, 76, 81, 108, 113, 124–132
- Full reconstruction, 61, 66–69, 83, 93, 96
- GIM mechanism, 7, 48, 49, 57, 109, 129
- Grand Unified Theory (GUT), 116, 117
- Grossman–Nir bound, 113
- Hermeticity, 83, 95, 96, 99
- Hierarchy problem, 124
- Higgs affinity, Yukawa coupling, 6, 46, 48, 66, 74, 84, 102, 129, 130
- Higgs boson, 1, 84, 85, 96, 97, 130
- HyperCP events, 84, 95, 97, 99
- Inami–Lim functions, 48, 109
- International Linear Collider (ILC), 1, 4, 97, 131
- IP (beam) profile, 89, 103
- J-PARC, 113
- Jarlskog Invariant, 128–130
- $K^+ \rightarrow \pi^+ \nu \bar{\nu}$, 109–114
- $K_L \rightarrow \pi^0 \nu \bar{\nu}$, 112–114, 127
- K-short (K_S) vertexing, 89, 103
- $K \rightarrow \pi \mu^\pm e^\mp$, 116, 117
- Kaluza–Klein excitations, 124
- KEKB, 12–15, 95
- Kobayashi and Maskawa (KM), 5, 7, 8, 125, 127–130, 133, 136
- K^0 – \bar{K}^0 mixing, 7, 101
- Large fluctuations, 16
- Large Hadron Collider (LHC), 1–4, 33, 37, 40, 44, 45, 49, 63, 68, 76, 79, 81, 82, 84, 85, 87, 89–91, 93, 96, 97, 99, 109, 119, 123, 126, 131–133
- LEP, 34, 46, 64, 96, 131
- Leptogenesis, 115, 118, 124
- Lepton charge asymmetry A_{SL} , 43
- Lepton flavor violation (LFV), 115–119
- Lepton number conservation, 116
- Little Higgs, 125
- Loops, 1, 6, 7, 16, 37, 46–48, 54, 57, 62, 73–78, 83, 84, 93, 102, 108, 115–117, 121, 129, 133
- Luminosity frontier, 3
- Minimal Flavor Violation (MFV), 79
- Minimum ionizing particle (MIP), 95, 96
- Mixing-decay interference, 139
- $\mu \rightarrow e \gamma$, 115–117
- Muon $g - 2$, 118
- Nambu–Jona-Lasinio model, 130
- Neutrino counting, 46, 131
- Neutrino mixing (oscillation), 115, 116, 124
- New Physics (NP), 4, 8, 11, 16, 17, 21, 23–26, 33, 39, 43, 49, 58, 59, 61, 62, 64–66, 70, 77, 79, 81, 87, 88, 93, 99, 101, 102, 108, 109, 112, 113, 123, 124, 126, 127, 129, 131–133
- Next-to-next-to-leading order (NNLO), 57, 60–63, 88
- Nondecoupling, 6–8, 25, 46–49, 54, 61, 73, 74, 76, 77, 113, 126, 129, 131
- ν_μ – ν_τ mixing, 117
- Opposite side tagging (OST), 39, 40, 51
- Oscillation probability, 38
- Partial reconstruction, 58
- Particle identification (PID), 13, 19–21, 40, 45
- PEP-II, 3, 7, 12–15, 95
- Perturbative QCD factorization (PQCD), 19, 24, 25, 47, 126
- Photon energy cut, 59–61
- Photonic penguin, 73–75, 77
- Polarization in $B \rightarrow V V$, 29
- PSI, 12, 116
- QCD factorization (QCDF), 20, 24

- R-parity violating SUSY, 90
- Radiative return (ISR), 93
- Rare B reconstruction, 19
- Right-handed (RH) interactions, 87–89, 124
- Sakharov conditions, 11, 128
- Same side tagging (SST), 40, 51, 103
- Self-tagging, 19, 138
- Semileptonic B_s^0 decay, 38–40
- $\mathcal{S}_f, \mathcal{A}_f$, 12, 15–17, 139, 140
- $\Sigma^+ \rightarrow p\mu^+\mu^-$, 97
- $\sin 2\beta/\phi_1$, 4, 5, 7, 13, 15, 16, 33, 37, 50, 136, 139, 140
- $\sin 2\Phi_{B_s}$, 33, 37, 38, 43–54, 81, 125–127, 130, 132, 133
- Slepton mixing, 116–118
- Soft Collinear Effective Theory (SCET), 25
- Spontaneous symmetry breaking, 6, 75, 133
- Squark mixing, 15, 16, 35, 37, 90
- Standard Model (SM), 1, 5, 136
- Strong penguin amplitude (P), 15, 21–25, 48, 73, 138
- Strong phase, 21–29, 50, 52, 53, 105, 106, 109, 135, 138
- Super B factory, 3, 4, 18, 61, 63, 68, 70, 76, 79, 82, 83, 86, 87, 89, 96, 99, 109, 119, 127, 132, 133
- Supersymmetry (SUSY), 16, 25, 34, 46, 54, 57, 61–63, 65, 89–91, 96–98, 116–118, 123, 124
- Systematic error, 21, 27, 28, 61, 70, 71
- Tagged $B_s^0 \rightarrow J/\psi\phi$, 44, 50–54, 125, 126, 132, 133
- $\tan \beta$, 59, 62–69, 87, 90, 118
- Tau/charm factory, 101, 115, 118
- $\tau \rightarrow \bar{p}\pi^0$, 119, 120
- $\tau \rightarrow \ell\ell\ell^{(\prime)}$, 118, 119
- $\tau \rightarrow \ell\gamma$, 117–119
- $\tau^\pm \rightarrow \Lambda\pi^\pm$, 119, 120
- Tevatron, 3, 5, 20, 27–29, 33, 34, 36, 38, 40, 44, 45, 50, 54, 82, 91, 102, 104, 126, 131–133
- Time-dependent CPV (TCPV), 11, 13, 15, 23, 26, 50–54, 87–89, 104–106, 126, 127, 132, 139, 140
- Tree amplitude (T), 21, 23, 71, 126, 138
- Two track vertex trigger, 40, 41
- Unitarity bound, 130, 132
- Unitarity quadrangle, 109, 127, 128, 130
- Unitarity triangle, 8, 29, 36, 37, 109, 125, 127–129, 137, 138
- Unparticle physics, 123
- Untagged $B_s^0 \rightarrow J/\psi\phi$, 43, 44
- $\Upsilon(1S) \rightarrow \gamma a_1^0$, 96–99
- $\Upsilon(nS)$ probes, 93–99
- $\Upsilon(1S) \rightarrow \text{nothing}$, 93–96
- Vacuum expectation value (v.e.v.), 1, 5, 7, 59, 62, 74, 76, 84, 87, 125, 129, 130
- Vector-like quark, 125
- Weak phases, 2, 11, 21, 24, 25, 28, 46, 59, 80–82, 108, 135, 138–140
- Weakly Interacting Massive Particle (WIMP), 84
- Width mixing, 37, 43, 52, 53, 101–109
- Wilczek process, 98
- Wilson coefficients, 47, 48, 78–82, 88
- Wolfenstein form, 36, 136, 137
- x_D , 103, 105–109, 126
- Z penguin, 73–78, 80, 82
- Z' model, 29, 54, 81, 82, 124
- $Z \rightarrow b\bar{b}$, 127